

MSFC MPR-SAT-FE-73-1



g4

SATURN

MPR-SAT-FE-73-1

FEBRUARY 28, 1973

N73-33822

(NASA-TM-X-69534) SATURN V LAUNCH
VEHICLE FLIGHT EVALUATION REPORT-AS-512
APOLLO 17 MISSION (NASA) 295 P BC
16.75

CSCL 22C

Unclassified
G3/30 19845

SATURN V LAUNCH VEHICLE FLIGHT EVALUATION REPORT-AS-512 APOLLO 17 MISSION

PROPERTY OF
MARSHALL SPACE FLIGHT CENTER
A&TS-MS-IL

PREPARED BY
SATURN FLIGHT EVALUATION WORKING GROUP



NATIONAL AERONAUTICS AND SPACE ADMINISTRATION

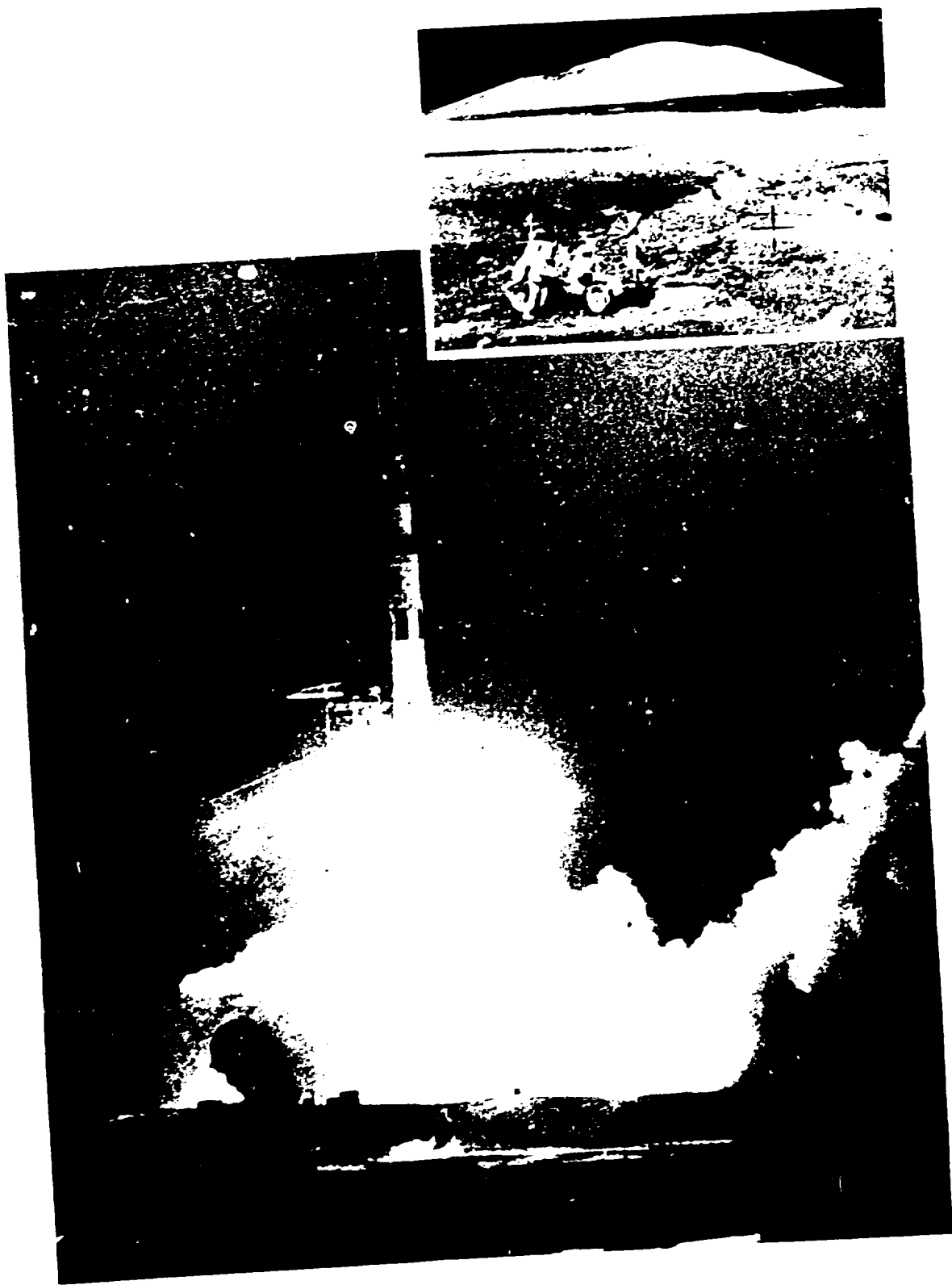
GEORGE C. MARSHALL SPACE FLIGHT CENTER

FEBRUARY 28, 1973

MPR-SAT-FE-73-1

SATURN V LAUNCH VEHICLE
FLIGHT EVALUATION REPORT - AS-512
APOLLO 17 MISSION

PREPARED BY
SATURN FLIGHT EVALUATION WORKING GROUP



MPR-SAT-FE-73-1

SATURN V LAUNCH VEHICLE FLIGHT EVALUATION REPORT - AS-512
APOLLO 17 MISSION

BY

Saturn Flight Evaluation Working Group
George C. Marshall Space Flight Center

ABSTRACT

Saturn V AS-512 (Apollo 17 Mission) was launched at 00:33:00 Eastern Standard Time (EST) on December 7, 1972, from Kennedy Space Center, Complex 39, Pad A. The vehicle lifted off on a launch azimuth of 90 degrees east of north and rolled to a flight azimuth of 91.504 degrees east of north. The launch vehicle successfully placed the manned spacecraft in the planned translunar coast mode. The S-IVB/IU impacted the lunar surface within the planned target area.

This was the third Apollo Mission to employ the Lunar Roving Vehicle (LRV) during Extravehicular Activity (EVA). The performance of the LRV was satisfactory and, as on Apollo 15 and 16 Missions, resulted in a significant increase in lunar exploration capability relative to the lunar exploration missions made without the LRV. The average distance traversed with the LRV on the last three Apollo Missions was approximately 30 kilometers, where the average distance traversed on the three Missions without the LRV was approximately 3 kilometers. The total distance traveled on the lunar surface with the LRV on this Mission was 35.7 kilometers (17 miles).

All launch vehicle Mandatory and Desirable Objectives were accomplished except the precise determination of the lunar impact point. It is expected that this will be accomplished at a later date. No failures or anomalies occurred that seriously affected the mission.

Any questions or comments pertaining to the information contained in this report are invited and should be directed to:

Director, George C. Marshall Space Flight Center
Huntsville, Alabama 35812
Attention: Chairman, Saturn Flight Evaluation Working Group, SAT-E (Phone 205-453-1030)

PRECEDING PAGE BLANK NOT FILMED

TABLE OF CONTENTS

	Page		Page
TABLE OF CONTENTS	iii	4.2.2	4-2
LIST OF ILLUSTRATIONS	vii	4.2.3	4-2
LIST OF TABLES	xi	4.2.4	4-9
ACKNOWLEDGEMENT	xiii		
ABBREVIATIONS	xiv		
MISSION PLAN	xviii		
FLIGHT SUMMARY	xxi		
MISSION OBJECTIVES ACCOMPLISHMENT	xxviii		
FAILURES AND ANOMALIES	xxvix		
SECTION 1 - INTRODUCTION			
1.1 Purpose	1-1	5.1	5-1
1.2 Scope	1-1	5.2	5-1
SECTION 2 - EVENT TIMES			
2.1 Summary of Events	2-1	5.3	5-4
2.2 Variable Time and Commanded Switch Selector Events	2-2	5.4	5-7
SECTION 3 - LAUNCH OPERATIONS			
3.1 Summary	3-1	5.5	5-7
3.2 Prelaunch Milestones	3-1	5.6	5-7
3.2.1 S-IC Stage	3-3	5.6.1	5-7
3.2.2 S-II Stage	3-3	5.6.2	5-8
3.2.3 S-IVB Stage	3-4	5.7	5-9
3.2.4 IU Stage	3-4	5.8	5-9
3.3 Terminal Countdown	3-8	5.9	5-10
3.4 Propellant Loading	3-8	5.10	5-11
3.4.1 RP-1 Loading	3-8		
3.4.2 LOX Loading	3-8		
3.4.3 LH ₂ Loading	3-9		
3.5 Ground Support Equipment	3-9		
3.5.1 Ground/Vehicle Interface	3-9		
3.5.2 MSFC Furnished Ground Support Equipment	3-10		
SECTION 4 - TRAJECTORY			
4.1 Summary	4-1		
4.2 Trajectory Evaluation	4-1	6.1	6-1
4.2.1 Ascent Phase	4-1	6.2	6-1
		6.3	6-8
		6.4	6-10
		6.5	6-11
		6.6	6-13
		6.6.1	6-13
		6.6.2	6-16
		6.7	6-17

TABLE OF CONTENTS (CONTINUED)

	Page		Page
6.8 S-II Helium Injection System	6-17	8.2.2 Bending Moments	8-3
6.9 POGO Suppression System	6-19	8.2.3 Vehicle Dynamic Characteristics	8-3
6.10 S-II Hydraulic System	6-19	8.2.3.1 Longitudinal Dynamic Characteristics	8-3
		8.2.4 Vibration	8-8
		8.3 S-II POGO Limiting Backup Cutoff System	8-8
SECTION 7 - S-IVB PROPULSION		SECTION 9 - GUIDANCE AND NAVIGATION	
7.1 Summary	7-1	9.1 Summary	9-1
7.2 S-IVB Chilldown and Buildup Transient Performance for First Burn	7-2	9.2 Guidance Comparisons	9-1
7.3 S-IVB Mainstage Performance for First Burn	7-2	9.3 Navigation and Guidance Scheme Evaluation	9-7
7.4 S-IVB Shutdown Transient Performance for First Burn	7-6	9.3.1 Variable Launch Azimuth	9-7
7.5 S-IVB Parking Orbit Coast Phase Conditioning	7-8	9.3.2 First Boost Period	9-12
7.6 S-IVB Chilldown and Buildup Transient Performance for Second Burn	7-9	9.3.3 Earth Parking Orbit	9-14
7.7 S-IVB Mainstage Performance for Second Burn	7-12	9.3.4 Second Boost Period	9-16
7.8 S-IVB Shutdown Transient Performance for Second Burn	7-12	9.3.5 Post-TLI Period	9-16
7.9 S-IVB Stage Propellant Management	7-12	9.4 Navigation and Guidance System Components	9-16
7.10 S-IVB Pressurization System	7-15	9.4.1 ST-124M Stabilized Platform System	9-16
7.10.1 S-IVB Fuel Pressurization System	7-15	9.4.2 Guidance Computer	9-17
7.10.2 S-IVB LOX Pressurization System	7-16		
7.11 S-IVB Pneumatic Control Pressure System	7-19	SECTION 10 - CONTROL AND SEPARATION	
7.12 S-IVB Auxiliary Propulsion System	7-19	10.1 Summary	10-1
7.13 S-IVB Orbital Safing Operations	7-23	10.2 S-IC Control System Evaluation	10-1
7.13.1 Fuel Tank Safing	7-23	10.2.1 Liftoff	10-1
7.13.2 LOX Tank Dumping and Safing	7-26	10.2.2 Inflight Dynamics	10-1
7.13.3 Cold Helium Dump	7-26	10.3 S-II Control System Evaluation	10-6
7.13.4 Ambient Helium Dump	7-27	10.4 S-IVB Control System Evaluation	10-7
7.13.5 Stage Pneumatic Control Sphere Safing	7-27	10.4.1 During First Burn	10-7
7.13.6 Engine Start Tank Safing	7-28	10.4.2 During Parking Orbit	10-11
7.13.7 Engine Control Sphere Safing	7-28	10.4.3 During Second Burn	10-11
7.14 S-IVB Hydraulic System	7-28	10.4.4 Control System Evaluation After S-IVB Second Burn	10-14
7.14.1 Boost and First Burn	7-28		
7.14.2 Parking Orbit and Second Burn	7-28	10.5 Instrument Unit Control Components Evaluation	10-22
SECTION 8 - STRUCTURES		10.5.1 Gimbal Angle Resolvers	10-22
8.1 Summary	8-1	10.5.2 ST-124M Power Supplies	10-22
8.2 Total Vehicle Structures Evaluation	8-1	10.6 Separation	10-22
8.2.1 Longitudinal Loads	8-1	10.6.1 S-IC/S-II Separation	10-22
		10.6.2 S-II Second Plane Separation	10-22
		10.6.3 S-II/S-IVB Separation	10-23
		10.6.4 CSM Separation	10-23
SECTION 11 - ELECTRICAL NETWORKS AND EMERGENCY DETECTION SYSTEM			
11.1 Summary	11-1		
11.2 S-IC Stage Electrical System	11-1		
11.3 S-II Stage Electrical System	11-2		
11.4 S-IVB Stage Electrical System	11-3		

TABLE OF CONTENTS (CONTINUED)

	Page		Page
11.4.1 Summary	11-3	17.3.2 Trajectory Effects	17-5
11.4.2 S-IVB Aft Battery No. 1, Unit No. 1, Temperature Increase	11-3	17.3.3 Perturbing Mechanisms	17-6
11.5 Instrument Unit Electrical System	11-9	17.3.4 Tentative Conclusions	17-8
11.6 Saturn V Emergency Detection System (EDS)	11-15	17.4 Trajectory Evaluation	17-9
SECTION 12 - SUMMARY		17.5 Impact Conditions	17-13
12.1 Summary	12-1	17.6 Tracking Data	17-13
12.2 Base Pressures	12-1	SECTION 18 - SPACECRAFT SUMMARY	18-1
12.2.1 S-IC Base Pressures	12-1	SECTION 19 - MSFC INFLIGHT DEMONSTRATION	19-1
12.2.2 S-II Base Pressures	12-1	SECTION 20 - LUNAR ROVING VEHICLE	
12.3 S-IC/S-II Separation Pressures	12-3	20.1 Summary	20-1
SECTION 13 - VEHICLE THERMAL ENVIRONMENT		20.2 Deployment	20-2
13.1 Summary	13-1	20.3 LRV to Stowed Payload Interface	20-2
13.2 S-IC Base Heating	13-1	20.4 Lunar Tractorability Environment	20-2
13.3 S-II Base Heating	13-2	20.5 Wheel Soil Interaction	20-2
13.4 Vehicle Fercheating Thermal Environment	13-3	20.6 Locomotion Performance	20-4
13.5 S-IC/S-II Separation Thermal Environment	13-3	20.7 Mechanical Systems	20-4
SECTION 14 - ENVIRONMENTAL CONTROL SYSTEM		20.7.1 Harmonic Drive	20-4
14.1 Summary	14-1	20.7.2 Wheels and Suspension	20-5
14.2 S-IC Environmental Control	14-1	20.7.3 Brakes	20-5
14.3 S-II Environmental Control	14-2	20.7.4 Stability	20-5
14.4 IU Environmental Control	14-2	20.7.5 Hand Controller	20-6
14.4.1 Thermal Conditioning System (TCS)	14-2	20.7.6 Loads	20-6
14.4.2 Gas Bearing System Performance	14-5	20.8 Electrical Systems	20-6
SECTION 15 - DATA SYSTEMS		20.8.1 Batteries	20-6
15.1 Summary	15-1	20.8.2 Traction Drive System	20-6
15.2 Vehicle Measurement Evaluation	15-1	20.8.3 Distribution System	20-6
15.3 Airborne VHF Telemetry Systems Evaluation	15-1	20.8.4 Steering	20-7
15.4 C-Band Radar System Evaluation	15-5	20.8.5 Amp-Hour Integrator	20-7
15.5 Secure Range Safety Command System Evaluation	15-5	20.9 Control and Display Console	20-7
15.6 Command and Communications System Evaluation	15-8	20.10 Navigation System	20-7
15.6.1 Summary of Performance	15-8	20.11 Crew Station	20-7
15.6.2 Performance Analysis	15-8	20.12 Thermal	20-8
15.7 Ground Engineering Cameras	15-12	20.13 Structural	20-10
SECTION 16 - MASS CHARACTERISTICS		20.14 Lunar Roving Vehicle Configuration	20-10
16.1 Summary	16-1	APPENDIX A - ATMOSPHERE	
16.2 Mass Evaluation	16-1	A.1 Summary	A-1
SECTION 17 - LUNAR IMPACT		A.2 General Atmospheric Con- ditions at Launch Time	A-1
17.1 Summary	17-1	A.3 Surface Observations at Launch Time	A-1
17.2 Translunar Coast Maneuvers	17-1	A.4 Upper Air Measurements	A-1
17.3 Trajectory Perturbations	17-3	A.4.1 Wind Speed	A-1
17.3.1 Introduction	17-3	A.4.2 Wind Direction	A-1
		A.4.3 Pitch Wind Component	A-1
		A.4.4 Yaw Wind Component	A-1
		A.4.5 Component Wind Shears	A-1
		A.4.6 Extreme Wind Data in the High Dynamic Region	A-1

TABLE OF CONTENTS (CONTINUED)

	Page
A.5 Thermodynamic Data	A-6
A.5.1 Atmospheric Temperature	A-14
A.5.2 Atmospheric Pressure	A-14
A.5.3 Atmospheric Density	A-14
A.5.4 Optical Index of Refraction	A-14
A.6 Comparison of Selected Atmospheric Data for Saturn V Launches	A-14
APPENDIX B - AS-512 SIGNIFICANT CONFIGURATION CHANGES	
B.1 Introduction	B-1

LIST OF ILLUSTRATIONS

Figure	Page	Figure	Page
2-1 AS-512 Telemetry Time Difference	2-3	6-7 S-II Steady State Operation	6-9
3-1 Electrical Support Equipment Partial Schematic	3-5	6-8 S-II Fuel Tank Ullage Pressure	6-14
3-2 Diode Chip Detail	3-7	6-9 S-II Fuel Pump Inlet Conditions	6-15
4-1 Ascent Trajectory Position Comparison	4-3	6-10 S-II LOX Tank Ullage Pressure	6-16
4-2 Ascent Trajectory Space-Fixed Velocity and Flight Path Angle Comparisons	4-3	6-11 S-II LOX Pump Inlet Conditions	6-18
4-3 Ascent Trajectory Acceleration Comparison	4-4	6-12 S-II Center Engine LOX Feedline Accumulator Bleed System Performance	6-20
4-4 Dynamic Pressure and Mach Number Comparisons	4-4	6-13 S-II Center Engine LOX Feedline Accumulator Fill Transient	6-20
4-5 Launch Vehicle Groundtrack	4-8	6-14 S-II Center Engine LOX Feedline Accumulator Helium Supply System Performance	6-21
4-6 Injection Phase Space-Fixed Velocity and Flight Path Angle Comparisons	4-10	7-1 S-IVB Start Box and Run Requirements - First Burn	7-3
4-7 Injection Phase Acceleration Comparison	4-10	7-2 S-IVB Thrust Buildup Transient for First Burn	7-4
5-1 S-IC LOX Start Box Requirements	5-2	7-3 S-IVB Steady-State Performance	7-5
5-2 S-IC Engines Thrust Buildup	5-3	7-4 S-IVB Thrust Decay	7-7
5-3 S-IC Stage Propulsion Performance	5-5	7-5 S-IVB CVS Performance - Coast Phase	7-8
5-4 S-IC Fuel Tank Ullage Pressure	5-9	7-6 S-IVB Ullage Conditions During Repressurization Using O ₂ /H ₂ Burner	7-10
5-5 S-IC LOX Tank Ullage Pressure	5-10	7-7 S-IVB O ₂ /H ₂ Burner Thrust and Pressurant Flowrate	7-10
6-1 S-II Engine Start Tank Performance	6-3	7-8 S-IVB Start Box and Run Requirements - Second Burn	7-11
6-2 S-II Engine Helium Tank Pressures	6-4	7-9 S-IVB Steady-State Performance - Second Burn	7-13
6-3 S-II Typical Start Tank Conditions During Hold Operations	6-4	7-10 S-IVB LH ₂ Ullage Pressure - First Burn, Parking Orbit and Second Burn	7-16
6-4 Comparison of S-II Start Tank Conditions During CDT and Launch	6-5	7-11 S-IVB Fuel Pump Inlet Conditions - First Burn	7-17
6-5 S-II Start Tank Rechill Sequence (Engine 1, Typical)	6-6	7-12 S-IVB Fuel Pump Inlet Conditions - Second Burn	7-17
6-6 S-II Engine Pump Inlet Start Requirements	6-7	7-13 S-IVB LOX Tank Ullage Pressure - First Burn, Earth Parking Orbit, and Second Burn	7-18

LIST OF ILLUSTRATIONS (CONTINUED)

Figure	Page	Figure	Page
7-14 S-IVB LOX Pump Inlet Conditions - First Burn	7-20	8-9 AS-512 Dynamic Responses During S-II Accumulator Fill (1-110 Hz Filter)	8-10
7-15 S-IVB LOX Pump Inlet Conditions - Second Burn	7-20	8-10 AS-512 S-IVB Gimbal Block Acceleration During S-II Burn - Longitudinal (8 to 20 Hz Filter)	8-10
7-16 S-IVB Cold Helium Supply History	7-21	8-11 S-IVB Gimbal Block Acceleration and S-II Center Engine Thrust Pad Acceleration Spectra at $T + 185$ to 190 Seconds	8-11
7-17 S-IVB LOX Dump and Orbital Safing Sequence	7-24	8-12 Noise on S-IVB Gimbal Block During S-II Burn	8-12
7-18 S-IVB LH ₂ Ullage Pressure - Translunar Coast	7-24	8-13 AS-512 S-IVB LOX Pump Inlet Pressure Spectra	8-13
7-19 S-IVB LOX Dump Parameter Histories	7-25	9-1 Trajectory and ST-124M Platform Velocity Comparisons, Boost-to-EPO (Trajectory Minus LVDC)	9-2
7-20 S-IVB LOX Tank Ullage Pressure - Translunar Coast	7-27	9-2 Trajectory and ST-124M Platform Velocity Comparisons, Boost-to-TLI (Trajectory Minus LVDC)	9-4
8-1 AS-512 Longitudinal Acceleration at IU and CM During Thrust Build-up and Launch	8-2	9-3 Comparison of LVDC and Postflight Trajectory During EPO	9-8
8-2 Longitudinal Load Distribution at Time of Maximum Bending Moment, CECO and OECO	8-3	9-4 Continuous Vent System (CVS) Thrust and Acceleration During EPO	9-9
8-3 Bending Moment and Load Factor Distribution at Time of Maximum Bending Moment	8-4	9-5 Steering Commands, First Boost	9-10
8-4 AS-512 Envelope of Combined Loads Producing Minimum Safety Margins for S-IC Flights	8-5	9-6 Steering Commands, Second Burn	9-15
8-5 IU Vibration During S-IC Burn (Longitudinal)	8-6	10-1 Pitch Plane Dynamics During S-IC Burn	10-3
8-6 AS-512 Longitudinal Acceleration at IU and CM During Center Engine Cutoff	8-7	10-2 Yaw Plane Dynamics During S-IC Burn	10-4
8-7 AS-512 Longitudinal Acceleration at IU and CM During Outboard Engine Cutoff	8-8	10-3 Pitch and Yaw Plane Free Stream Angle of Attack During S-IC Burn	10-5
8-8 AS-512 Center Engine Chamber Pressure and Gimbal Pad Acceleration During S-II Burn (8 to 20 Hz Filter) Compared to AS-511	8-9	10-4 Pitch Plane Dynamics During S-II Burn	10-8
		10-5 Yaw Plane Dynamics During S-II Burn	10-9
		10-6 Pitch Plane Dynamics During S-IVB First Burn	10-10

LIST OF ILLUSTRATIONS (CONTINUED)

Figure	Page	Figure	Page
10-7 Yaw Plane Dynamics During S-IVB First Burn	10-10	13-5 S-II Heat Shield Aft Radiation Heat Rate	13-6
10-8 Pitch Plane Dynamics During Parking Orbit	10-12	14-1 IU TCS Coolant Control Parameters	14-3
10-9 Pitch Plane Dynamics During S-IVB Second	10-13	14-2 IU Sublimator Performance During Ascent	14-4
10-10 Yaw Plane Dynamics During S-IVB Second Burn	10-13	14-3 Selected IU Component Temperatures	14-6
10-11 Pitch Plane Dynamics During Translunar Coast (Sheet 1 of 6)	10-15	14-4 IU TCS Hydraulic Performance	14-7
10-12 AS-312 S-IC-S-II Separation Distance	10-23	14-5 IU TCS Sphere Pressure	14-8
11-1 S-IVB Stage Forward No. 1 Battery Voltage and Current	11-4	14-6 IU Inertial Platform GN ₂ Pressure	14-9
11-2 S-IVB Stage Forward No. 2 Battery Voltage and Current	11-5	14-7 IU GRS GN ₂ Sphere Pressures	14-9
11-3 S-IVB Stage Aft No. 1 Battery Voltage and Current	11-6	15-1 VHF Telemetry Acquisition and Loss Times	15-6
11-4 S-IVB Stage Aft No. 2 Battery Voltage and Current	11-7	15-2 C-Band Acquisition and Loss Times	15-7
11-5 S-IVB Aft Battery No. 1 Data	11-8	15-3 CCS Downlink Phase Lock Times (Liftoff to TLI)	15-9
11-6 S-IVB Aft Battery No. 1 Heater Control Circuit	11-10	15-4 CCS Coverage (TLI to Lunar Impact)	15-10
11-7 IU 6010 Battery Parameters	11-11	17-1 Translunar Coast Maneuvers Overview	17-4
11-8 IU 6020 Battery Parameters	11-12	17-2 Modeled Translunar Coast Maneuvers	17-4
11-9 IU 6030 Battery Parameters	11-13	17-3 Gravity-Only Lunar Impact Trajectory Residuals	17-7
11-10 IU 6040 Battery Parameters	11-14	17-4 Lunar Impact Trajectory Residuals with Perturbing Influences Modeled	17-7
12-1 S-II Heat Shield Forward Face Pressure	12-2	17-5 Early PTC Tumble Residuals	17-10
12-2 S-II Thrust Cone Pressure	12-2	17-6 Late PTC Tumble Residuals	17-11
12-3 S-II Heat Shield Aft Face Pressure	12-3	17-7 Lunar Landmarks	17-14
13-1 S-IC Base Region Total Heating Rate	13-4	17-8 Tracking Data Availability	17-15
13-2 S-IC Ambient Gas Temperature Under Engine Cocoon	13-4	20-1 Apollo 17 LRV EVA-3 Traverse	20-3
13-3 S-II Heat Shield Aft Heat Rate	13-5	20-2 LRV Power Usage	20-4
13-4 S-II Heat Shield Recovery Temperature	13-6	20-3 LRV Fender Fix	20-9
		20-4 LRV Battery No. 1 (Left) Temperature	20-11

LIST OF ILLUSTRATIONS (CONTINUED)

Figure	Page
20-3 LRV Battery No. 2 (Right) Temperature	20-11
A-1 Surface Weather Map Approximately 6 1/2 Hours After Launch of AS-512	A-2
A-2 500 Millibar Map Approximately 6 1/2 Hours After Launch of AS-512	A-4
A-3 Scalar Wind Speed at Launch Time of AS-512	A-7
A-4 Wind Direction at Launch Time of AS-512	A-8
A-5 Pitch Wind Velocity Component (W_x) at Launch Time of AS-512	A-9
A-6 Yaw Wind Velocity Component (W_y) at Launch Time of AS-512	A-10
A-7 Pitch (S_x) and Yaw (S_y) Component Wind Shears at Launch Time of AS-512	A-11
A-8 Relative Deviation of Temperature and Pressure from the PRA-63 Reference Atmosphere, AS-512	A-15
A-9 Relative Deviation of Density and Absolute Deviation of the Index of Refraction from the PRA-63 Reference Atmosphere, AS-512	A-16

LIST OF TABLES

Table		Page	Table		Page
1	Mission Objectives Accomplishment		9-1	Inertial Platform Velocity Comparisons (PACSS-12 Coordinate System)	9-5
2	Summary of Significant Anomalies		9-2	Navigation Comparisons (PACSS-13)	9-6
3	Summary of Anomalies		9-3	State Vector Differences at Translunar Injection	9-11
2-1	Time Base Summary	2-1	9-4	AS-512 End Conditions	9-12
2-2	Significant Event Times Summary	2-4	9-5	Coast Phase Guidance Steering Commands at Major Events	9-13
2-3	Variable Time and Commanded Switch Selector Events	2-10	10-1	AS-512 Misalignment and Liftoff Conditions Summary	10-2
3-1	AS-512/Apollo 17 Pre-launch Milestones	3-2	10-2	Maximum Control Parameters During S-IC Burn	10-6
4-1	Comparison of Significant Trajectory Events	4-5	10-3	Maximum Control Parameters During S-IC Burn	10-7
4-2	Comparison of Cutoff Events	4-6	10-4	Maximum Control Parameters During S-IVB First Burn	10-11
4-3	Comparison of Separation Events	4-7	11-1	S-IC Stage Battery Power Consumption	11-1
4-4	Parking Orbit Insertion Conditions	4-8	11-2	S-II Stage Battery Power Consumption	11-2
4-5	Translunar Injection Condition	4-8	11-3	S-IVB Stage Battery Power Consumption	11-9
5-1	F-1 Engine Systems Buildup Times	5-2	11-4	IU Battery Power Consumption	11-10
5-2	S-IC Individual Standard Sea Level Engine Performance	5-6	15-1	AS-512 Measurement Summary	15-2
5-3	S-IC Propellant Mass History	5-8	15-2	AS-512 Flight Measurements Waived Prior to Flight	15-2
6-1	S-II Engine Performance	5-11	15-3	AS-512 Measurement Malfunctions	15-3
6-2	AS-512 Flight S-II Propellant Mass History	6-13	15-4	AS-512 Launch Vehicle Telemetry Links	15-4
7-1	S-IVB Steady State Performance - First Burn (STDV Open +135-Second Time Slice at Standard Altitude Conditions)	7-6	15-5	Command and Communication System Command History, AS-512	15-11
7-2	S-IVB Steady State Performance - Second Burn (STDV Open +172-Second Time Slice at Standard Altitude Conditions)	7-14	16-1	Total Vehicle Mass - S-IC Burn Phase - Kilograms	16-3
7-3	S-IVB Stage Propellant Mass History	7-14	16-2	Total Vehicle Mass - S-IC Burn Phase - Pounds	16-4
7-4	S-IVB APS Propellant Consumption	7-22	16-3	Total Vehicle Mass - S-II Burn Phase - Kilograms	16-5
			16-4	Total Vehicle Mass - S-II Burn Phase - Pounds	16-6

LIST OF TABLES (CONTINUED)

Table		Page	Table		Page
16-5	Total Vehicle Mass - S-IVB First Burn Phase - Kilograms	16-7	A-6	Selected Atmospheric Observations for Apollo/Saturn 501 through Apollo/Saturn 512 Vehicle Launches at Kennedy Space Center, Florida	A-17
16-6	Total Vehicle Mass - S-IVB First Burn Phase - Pounds Mass	16-8	B-1	S-IC Significant Configuration Changes	B-1
16-7	Total Vehicle Mass - S-IVB Second Burn Phase - Kilograms	16-9	B-2	S-II Significant Configuration Changes	B-1
16-8	Total Vehicle Mass - S-IVB Second Burn Phase - Pounds Mass	16-10	B-3	S-IVB Significant Configuration Changes	B-1
16-9	Flight Sequence Mass Summary	16-11	B-4	IU Significant Configuration Changes	B-2
16-10	Mass Characteristics Comparison	16-13			
17-1	Translunar Coast Maneuvers	17-2			
17-2	Trajectory Parameters After APS-2 Burn	17-9			
17-3	Lunar Impact Conditions	17-12			
17-4	Lunar Impact Times	17-13			
17-5	S-IVB/IU Tracking Stations	17-15			
20-1	Apollo 17 LRV Performance Summary	20-5			
20-2	Apollo Lunar EVA Summary	20-5			
20-3	LRV Significant Configuration Changes	20-12			
A-1	Surface Observations at AS-512 Launch Time	A-3			
A-2	Solar Radiation at AS-512 Launch Time, Launch Pad 39A	A-5			
A-3	Systems Used to Measure Upper Air Wind Data for AS-512	A-5			
A-4	Maximum Wind Speed in High Dynamic Pressure Region for Apollo/Saturn 501 through Apollo/Saturn 512 Vehicles	A-12			
A-5	Extreme Wind Shear Values in the High Dynamic Pressure Region for Apollo/Saturn 501 through Apollo/Saturn 512 Vehicles	A-13			

ACKNOWLEDGEMENT

This report is published by the Saturn Flight Evaluation Working Group, composed of representatives of Marshall Space Flight Center, John F. Kennedy Space Center, and MSFC's prime contractors, and in cooperation with the Manned Spacecraft Center. Significant contributions to the evaluation have been made by.

George C. Marshall Space Flight Center

Science and Engineering

Aero-Astroynamics Laboratory
Astrionics Laboratory
Computation Laboratory
Aeronautics Laboratory
Space Sciences Laboratory

Saturn Program Office

John F. Kennedy Space Center

Manned Spacecraft Center

The Boeing Company

McDonnell Douglas Astronautics Company

International Business Machines Corporation

North American Rockwell/Space Division

North American Rockwell/Rocketdyne Division

General Electric Company

ABBREVIATIONS

ACN	Ascension Island	CT4	Cape Telemetry 4
ACS	Alternating Current Power Supply	CVS	Continuous Vent System
ALSEP	Apollo Lunar Surface Experiments Package	CYI	Grand Canary Island
ANT	Antigua	DAC	Data Acquisition Camera
AOS	Acquisition of Signal	DDAS	Digital Data Acquisition System
APS	Auxiliary Propulsion System	DEE	Digital Events Evaluator
ARIA	Apollo Range Instrument Aircraft	DGU	Directional Gyro Unit
ASC	Accelerometer Signal Conditioner	DO	Desirable Objective
ASI	Augmented Spark Igniter	DOM	Data Output Multiplexer
AVP	Address Verification Pulse	DTS	Data Transmission System
BDA	Bermuda	EBW	Exploding Bridge Wire
BST	Boost	ECO	Engine Cutoff
CCS	Command and Communications System	ECP	Engineering Change Proposal
C&DC	Control and Display Console	ECS	Environmental Control System
CDDT	Countdown Demonstration Test	EDS	Emergency Detection System
CDR	Commander	EMR	Engine Mixture Ratio
CECO	Center Engine Cutoff	EMU	Extra-Vehicular Mobility Unit
CIF	Central Instrumentation Facility	EPO	Earth Parking Orbit
CG	Center of Gravity	ESC	Engine Start Command
CM	Command Module	EST	Eastern Standard Time
CNV	Cape Kennedy	ETC	Goddard Experimental Test Center
CRO	Carnarvon	ETW	Error Time Word
CRP	Computer Reset Pulse	EVA	Extra-Vehicular Activity
CSM	Command and Service Module	FCC	Flight Control Computer
		FM/FM	Frequency Modulation/ Frequency Modulation

ABBREVIATIONS (CONTINUED)

FMR	Flight Mission Rule	LMP	Lunar Module Pilot
FRT	Flight Readiness Test	LMR	Launch Mission Rule
GBI	Grand Bahama Island	LOI	Lunar Orbit Insertion
GBS	Gas Bearing System	LOS	Loss of Signal
GDS	Goldstone	LOX	Liquid Oxygen
GDSW	Goldstone Wing	LRV	Lunar Roving Vehicle
GG	Gas Generator	LSS	Lunar Soil Simulant
GOX	Gaseous Oxygen	LUT	Launch Umbilical Tower
GRR	Guidance Reference Release	LV	Launch Vehicle
GSE	Ground Support Equipment	LVDA	Launch Vehicle Data Adapter
GSFC	Goddard Space Flight Center	LVDC	Launch Vehicle Digital Computer
GTK	Grand Turk Island	LVGSE	Launch Vehicle Ground Support Equipment
GWM	Guam	MAD	Madrid
HAW	Hawaii	MADW	Madrid Wing
HDA	Holddown Arm	MAP	Message Acceptance Pulse
HE	Helium	MCC-H	Mission Control Center - Houston
HFCV	Helium Flow Control Valve	MESA	Modularized Equipment Storage Assembly
HSK	Honeysuckle Creek	MFV	Main Fuel Valve
ICD	Interface Control Document	MILA	Merritt Island Launch Area
IGM	Iterative Guidance Mode	ML	Mobile Launcher
IMU	Inertial Measurement Unit	MO	Mandatory Objective
IU	Instrument Unit	MOV	Main Oxidizer Valve
KSC	Kennedy Space Center	MR	Mixture Ratio
LCRU	Lunar Communication Relay Unit	MRCV	Mixture Ratio Control Valve
LET	Launch Escape Tower	MSC	Manned Spacecraft Center
LH ₂	Liquid Hydrogen		
LIT	Lunar Impact Team		
LM	Lunar Module		

ABBREVIATIONS (CONTINUED)

MSFC	Marshall Space Flight Center	PRA	Patrick Reference Atmosphere
MSFN	Manned Space Flight Network	PTCS	Propellant Tanking Computer System
MSS	Mobile Service Structure	PTC	Passive Thermal Control
MTF	Mississippi Test Facility	PU	Propellant Utilization
NASA	National Aeronautics and Space Administration	PWM	Pulse Width Modulator
NPSP	Net Positive Suction Pressure	RACS	Remote Automatic Calibration System
NPV	Nonpropulsive Vent	RF	Radio Frequency
OAT	Overall Test	RFI	Radio Frequency Interference
OCP	Orbital Correction Program	RMS	Root Mean Square
OECO	Outboard Engine Cutoff	RP-1	S-IC Stage Fuel
OFSO	Overfill Shutoff Sensor	SA	Service Arm
OMPT	Observed Mass Point Trajectory	SC	Spacecraft
OT	Operational Trajectory	SCFM	Standard Cubic Feet per Minute
OTBV	Oxidizer Turbine Bypass Valve	SCIM	Standard Cubic Inch per Minute
PACSS	Project Apollo Coordinate System Standards	SIM	Scientific Instrument Module
PAFB	Patrick Air Force Base	SLA	Spacecraft/LM Adapter
PCA	Point of Closest Approach	SM	Service Module
PCM	Pulse Code Modulation	SPS	Service Propulsion System
PCM/FM	Pulse Code Modulation/ Frequency Modulation	SPS	Stabilized Platform Subsystem
PEA	Platform Electronics Assembly	SPU	Signal Processing Unit
PIO	Process Input/Output	SRSCS	Secure Range Safety Command System
PLSS	Portable Life Support System	SSDO	Switch Selector and Discrete Output Register
POI	Parking Orbit Insertion	STDV	Start Tank Discharge Valve
PMR	Programmed Mixture Ratio		

ABBREVIATIONS (CONTINUED)

SV	Space Vehicle
TCS	Thermal Conditioning System
TCS	Terminal Countdown Sequencer
TD&E	Transportation, Docking and Ejection
TEI	Transearth Injection
TEX	Corpus Christi (Texas)
TLC	Translunar Coast
TLI	Translunar Injection
TM	Telemetry
TMR	Triple Module Redundant
TSM	Tail Service Mast
TVC	Thrust Vector Control
UCR	Unsatisfactory Condition Report
USAЕ	U. S. Army Engineer
USB	Unified S-Band
UT	Universal Time
VA	Volt Amperes
VAN	Vanguard (ship)
VHF	Very High Frequency
WES	Waterways Experimental Station
Z	Zulu Time (equivalent to UT)

MISSION PLAN

The AS-512 flight (Apollo 17 mission) to the Taurus-Littrow site is the twelfth flight in the Apollo/Saturn V flight program, the seventh mission planned for lunar landing, and the third mission planned for the Lunar Roving Vehicle. The Apollo 17 mission is the first Apollo flight planned for night launch and for translunar injection over the Atlantic Ocean. The primary mission objectives are: a) perform selenological inspection, survey, and sampling of materials and surface features in a preselected area of the Taurus-Littrow region; b) deploy and activate surface experiments; and c) conduct inflight experiments and photographic tasks. The crew consists of E. A. Cernan (Mission Commander), R. E. Evans (Command Module Pilot), and H. H. Schmitt (Lunar Module Pilot).

The AS-512 Launch Vehicle (LV) is composed of the S-IC-12, S-II-i2, S-IVB-512, and Instrument Unit (IU)-512 stages. The Spacecraft (SC) consists of SC/Lunar Module Adapter (SLA)-21, Command Module (CM)-114, Service Module (SM)-114, and Lunar Module (LM)-12. The LM has been modified to carry the Lunar Roving Vehicle (LRV)-3.

Vehicle launch from Complex 39A at Kennedy Space Center (KSC) is planned along a 90 degree azimuth followed by a roll to a flight azimuth of approximately 72 degrees measured east of true north. Vehicle mass at ignition is nominally 6,530,819 lbm.

The S-IC stage powered flight lasts approximately 162 seconds; the S-II stage provides powered flight for approximately 395 seconds. The S-IVB stage first burn of approximately 146 seconds inserts the S-IVB/IU/SLA/LM/ Command and Service Module (CSM) into a circular 90 n mi. altitude (referenced to the earth's equatorial radius) Earth Parking Orbit (EPO). Vehicle mass at orbit insertion is 306,791 lbm.

At approximately 10 seconds after EPO insertion, the vehicle is aligned with the local horizontal. Continuous hydrogen venting is initiated shortly after EPO insertion and the LV and Spacecraft (SC) systems are checked in preparation for the Translunar Injection (TLI) burn. Shortly after beginning the third revolution in EPO, the S-IVB stage is restarted and burns for approximately 345 seconds. This burn inserts the S-IVB/IU/SLA/LM/CSM into an earth-return translunar trajectory.

At 15 minutes after TLI, the vehicle initiates a maneuver to and holds inertial attitude for CSM separation and docking, and CSM/LM ejection. Following attitude acquisition the SLA panels are jettisoned and the CSM separates from the LV. The CSM then transposes and docks with the LM. After docking and latching, the CSM/LM is sprung ejected from the S-IVB/IU. Following separation of the combined CSM/LM from the S-IVB/IU, the S-IVB/IU performs a yaw maneuver and then an 80-second burn of the S-IVB Auxiliary Propulsion System (APS) ullage engines as an evasive maneuver to decrease the probability of S-IVB/IU recontact with the spacecraft. Subsequent to the completion of the S-IVB/IU evasive maneuver, the S-IVB/IU is placed on a trajectory such that it will impact the lunar surface in a target area located between the Apollo 14 and 16 landing sites. The lunar impact target is 7.0°S latitude and 8.0°W longitude. The impact trajectory is achieved by propulsive venting of hydrogen (H_2), dumping of residual liquid oxygen (LOX), and by ground-commanded firing of the APS ullage engines. The S-IVB/IU impact will be recorded by the seismographs deployed during the Apollo 12, 14, 15 and 16 missions. S-IVB/IU lunar impact is predicted to occur at 89 hours 16 minutes 08 seconds after launch for nominal flight.

Several inflight experiments will be flown on Apollo 17 including experiments conducted by use of the Scientific Instrument Module (SIM) located in Section I of the SM, and flight experiments during earth orbit, translunar coast, lunar orbit, and transearth coast mission phases.

During the 85-hour translunar coast, the astronauts will perform star-earth landmark sightings, Inertial Measurement Unit (IMU) alignments, general lunar navigation procedures, and midcourse corrections. At approximately 88 hours and 50 minutes, a Service Propulsion System (SPS), Lunar Orbit Insertion (LOI) burn of approximately 395 seconds is initiated to insert the CSM/LM into a 51 by 171 n mi. altitude parking orbit. Approximately two revolutions after LOI, a 22.9 second burn will adjust the orbit to 15 by 59 n mi. altitude. The LM is entered by astronauts Cernan and Scimmi, and checkout is accomplished. During the twelfth revolution in orbit, at 110 hours 28 minutes, the LM separates from the CSM and prepares for the lunar descent. The CSM is then inserted into an approximately 62 n mi. altitude circular orbit using a 4.0 second SPS burn. The LM Descent Propulsion System is used to brake the LM into the proper landing trajectory and to maneuver the LM during descent to the lunar surface. Landing at Taurus-Littrow is scheduled to occur at 113 hours 2 minutes. The landing site is

situated at 20°10' North latitude and 30°45' East longitude.

Following lunar landing, three EVA time periods of 7 hours each are scheduled during which the astronauts will explore the lunar surface in the LRV, collect surface samples, photograph the lunar surface, and deploy scientific instruments. Sorties in the LRV will be limited in radius such that the life support system capability will not be exceeded if LRV failure necessitates the astronauts walking back to the LM. Total stay time on the lunar surface is open-ended, with a planned maximum of 75.0 hours depending upon the outcome of current lunar surface operations planning and of real-time operational decisions.

The CSM performs an orbital plane change approximately 8 hours before rendezvous. LM liftoff nominally occurs at 189 hours 3 minutes into the mission. The ascent stage insertion into a 9 by 48 n mi. altitude lunar orbit occurs approximately 7 minutes later. At approximately 190.0 hours the rendezvous and docking with the CSM is accomplished.

Following docking, equipment transfer, and decontamination procedures, the LM ascent stage is jettisoned and targeted to impact the lunar surface at a point approximately 9 km from the Apollo 17 landing site. Transearth Injection (TEI) is accomplished at the end of revolution 75 at approximately 236 hours and 40 minutes with a 142.2 second SPS burn.

During the 68-hour transearth coast, the astronauts will perform navigation procedures, star-earth-moon sightings, the electro-phoretic separation demonstration, and as many as three midcourse corrections. The Command Module Pilot will also perform an EVA to retrieve film cassettes from the SIM bays. The SM separates from the CM before re-entry. Splashdown occurs in the Pacific Ocean 304 hours 31 minutes after liftoff.

After the recovery operations, a biological quarantine is not imposed on the crew and CM. However, biological isolation garments will be available for use in the event of unexplained crew illness.

FLIGHT SUMMARY

The tenth manned Saturn Apollo space vehicle, AS-512 (Apollo 17 Mission) was launched at 00:33:00 Eastern Standard Time on December 7, 1972, from Kennedy Space Center, Complex 39, Pad A. The performance of the launch vehicle and Lunar Roving Vehicle was satisfactory and all MSFC Mandatory and Desirable Objectives were accomplished except the precise determination of the S-IVB/IU lunar impact point. Preliminary assessments indicate that the final impact solution will satisfy the mission objective.

The ground systems supporting the countdown and launch performed satisfactorily with the exception of the Terminal Countdown Sequencer (TCS). The TCS malfunction resulted in a 2 hour 40 minute unscheduled hold. Damage to the pad, Launch Umbilical Tower and support equipment was considered minimal.

The vehicle was launched on an azimuth 90 degrees east of north. A roll maneuver was initiated at 13 seconds that placed the vehicle on a flight azimuth of 91.504 degrees east of north. In accordance with preflight targeting objectives, the translunar injection maneuver shortened the translunar coast period by 2 hours and 40 minutes to compensate for the launch delay so that the lunar landing could be made with the same lighting conditions as originally planned. Available C-Band radar and Unified S-Band tracking data plus telemetered guidance velocity data were used in the trajectory reconstruction. Because the velocity at S-II Outboard Engine Cutoff was higher than nominal, earth parking orbit insertion conditions were achieved 4.08 seconds earlier than nominal. Translunar Injection conditions were achieved 2.11 seconds later than nominal with altitude 5.8 kilometers greater than nominal and velocity 5.1 meters per second less than nominal. CSM separation was Commander initiated 57.9 seconds earlier than nominal resulting in an altitude 306.1 kilometers less than nominal and velocity 91.7 meters per second greater than nominal.

All S-IC propulsion systems performed satisfactorily. In all cases, the propulsion performance was very close to the predicted nominal. Overall stage site thrust was 0.30 percent higher than predicted. Total propellant consumption rate was 0.16 percent higher than predicted and the total consumed mixture ratio was 0.002 percent higher than predicted. Specific impulse was 0.14 percent higher than predicted. Total propellant consumption from Holdown Arm release to Outboard Engines Cutoff (OECO) was low by 0.14 percent. Center Engine Cutoff (CECO) was initiated by the Instrument Unit at 139.30 seconds, 0.02 seconds earlier than planned.

OECO was initiated by the fuel depletion sensors at 161.20 seconds, 0.47 seconds earlier than predicted. This is well within the +5.99, -4.22 second 3-sigma limits. At OECO, the LOX residual was 36,479 lbm compared to the predicted 37,235 lbm and the fuel residual was 26,305 lbm compared to the predicted 29,956 lbm.

The S-II propulsion systems performed satisfactorily throughout the flight. The S-II Engine Start Command (ESC), as sensed at the engines, occurred at 163.6 seconds. Center Engine Cutoff (CECO) was initiated by the Instrument Unit (IU) at 461.21 seconds, 0.47 seconds earlier than planned. Outboard Engine Cutoff (OECO), initiated by LOX depletion sensors, occurred at 559.66 seconds giving an outboard engine operating time of 396.1 seconds. Engine mainstage performance was satisfactory throughout flight. The total stage thrust at the standard time slice (61 seconds after S-II ESC) was 0.14 percent below predicted. Total propellant flowrate, including pressurization flow, was 0.19 percent below predicted, and the stage specific impulse was 0.05 percent above predicted at the standard time slice. Stage propellant mixture ratio was 0.36 percent below predicted. Engine thrust buildup and cutoff transients were within the predicted envelopes. The propellant management system performance was satisfactory throughout loading and flight, and all parameters were within expected limits except the LOX fine mass indication. Propellant residuals at OECO were 1401 lbm LOX, as predicted and 2752 lbm LH₂, 107 lbm less than predicted. Control of engine mixture ratio was accomplished with the two-position pneumatically operated Mixture Ratio Control Valves. Relative to ESC, the lower Engine Mixture Ratio step occurred 1.6 seconds earlier than predicted. The performance of the LOX and LH₂ tank pressurization system was satisfactory. Ullage pressure in both tanks was adequate to meet or exceed engine inlet Net Positive Suction Pressure minimum requirements throughout mainstage.

The S-IVB propulsion system performed satisfactorily throughout the operational phase of first and second burns and had normal start and cutoff transients. S-IVB first burn time was 138.8 seconds, 3.7 seconds shorter than predicted for the actual flight azimuth of 91.5 degrees. This difference is composed of -4.1 seconds due to the higher than expected S-II/S-IVB separation velocity and +0.4 second due to lower than predicted S-IVB performance. The engine performance during first burn, as determined from standard altitude reconstruction analysis, deviated from the predicted Start Tank Discharge Valve (STDV) open +135-second time slice by -0.68 percent for thrust and -0.14 percent for specific impulse. The S-IVB stage first burn Engine Cutoff (ECO) was initiated by the Launch Vehicle Digital Computer (LVDC) at 702.65 seconds. The Continuous Vent System adequately regulated LH₂ tank ullage pressure at an average level of 19.1 psia during orbit and the Oxygen/Hydrogen burner satisfactorily achieved LH₂ and LOX tank repressurization for restart. Engine restart conditions were within specified limits. S-IVB second burn time was 351.0 seconds, 4.0 seconds longer than predicted for the 91.5 degree flight azimuth. This difference is primarily due to the lower S-IVB performance and heavier vehicle mass during second burn. The engine

performance during second burn, as determined from the standard altitude reconstruction analysis, deviated from the STDV open +172-second time slice by -0.77 percent for thrust and -0.16 percent for specific impulse. Second burn ECO was initiated by the LVDC at 11,907.64 seconds, (08:51:27.64). Subsequent to second burn, the stage propellant tanks and helium spheres were safed satisfactorily. Sufficient impulse was derived from LOX dump, LH₂ CVS operation and auxiliary propulsion system (APS) ullage burn to achieve a successful lunar impact. Two subsequent planned APS burns were used to improve lunar impact targeting. The APS operation was nominal throughout the flight. No helium or propellant leaks were observed and the regulators functioned nominally.

The structural loads experienced during the S-IC boost phase were well below design values. The maximum bending moment was 96×10^6 lbf-in at the S-IC LOX tank (less than 36 percent of the design value). Thrust cutoff transients experienced by AS-512 were similar to those of previous flights. The maximum longitudinal dynamic responses at the Instrument Unit (IU) were ± 0.20 g and ± 0.27 g at S-IC Center Engine Cutoff and Outboard Engine Cutoff (OECO), respectively. The magnitudes of the thrust cutoff responses are considered normal. During S-IC stage boost, four to five hertz oscillations were detected beginning at approximately 100 seconds. The maximum amplitude measured at the IU was ± 0.06 g. Oscillations in the four to five hertz range have been observed on previous flights and are considered to be normal vehicle response to flight environment. POGO did not occur during S-IC boost. The S-II stage center engine LOX feedline accumulator successfully inhibited the 16 hertz POGO oscillations. A peak response of ± 0.4 g in the 14 to 20 hertz frequency range was measured on engine No. 5 gimbal pad during steady-state engine operation. As on previous flights, low amplitude 11 hertz oscillations were experienced near the end of S-II burn. Peak engine No. 1 gimbal pad response was ± 0.06 g. POGO did not occur during S-II boost. The POGO limiting backup cutoff system performed satisfactorily during the prelaunch and flight operations. The system did not produce any discrete outputs and should not have since there was no POGO. The structural loads experienced during the S-IVB stage burns were well below design values. During first burn the S-IVB experienced low amplitude, ± 0.14 g, 16 to 20 hertz oscillations. The amplitudes measured on the gimbal block were comparable to previous flights and within the expected range of values. Similarly, S-IVB second burn produced intermittent low amplitude oscillations of ± 0.10 g in the 11 to 16 hertz frequency range which peaked near second burn cutoff.

The Stabilized Platform and the Guidance Computer successfully supported the accomplishment of all guidance and navigation mission objectives with no discrepancies in performance of the hardware. The end conditions at Parking Orbit Insertion and Translunar Injection were attained with insignificant navigation error. Two anomalies related to the flight program did occur. At approximately 5421 seconds range time ($T_5 + 4718.8$) minor loop error telemetry indicated an unreasonable change in the yaw gimbal angle during one minor loop. At the re-initialization of boost navigation for

S-IVB second burn the extra accelerometer readings normally telemetered from GRR to liftoff plus 10 seconds were restarted and continued throughout second burn boost navigation. Neither of these anomalies significantly impacted navigation, guidance and control. A minor discrepancy occurred during S-II burn, when the yaw gimbal angle failed the zero reasonableness test twice, resulting in minor loop error telemetry at 478.3 seconds ($T_3 +317.2$) and 559.4 seconds ($T_3 +398.2$).

All control functions and separation events occurred as planned. Engine gimbal deflections were nominal and APS firings predictable throughout powered flight. All dynamics were within vehicle capability, and bending and slosh modes were adequately stabilized. The APS provided satisfactory orientation and stabilization during parking orbit and from translunar injection through the S-IVB/IU passive thermal control maneuver. APS propellant consumption for attitude control and propellant settling prior to the APS burn for lunar target impact was lower than the mean predicted requirements. All separation sequences were performed as planned. Transients due to spacecraft separation, docking, and Lunar Module ejection were nominal.

The launch vehicle electrical systems and Emergency Detection System performed satisfactorily throughout the required period of flight. However, the temperature of the S-IVB Aft Battery No. 1 Unit No. 1, increased significantly above the nominal control limit (90°F) at approximately 9 hours due to malfunction of the primary heater control system. Operation of the Aft Battery No. 1 remained nominal as did operation of all other batteries, power supplies, inverters, Exploding Bridge Wire firing units, and switch selectors.

The S-IC and S-II base pressure environments were consistent with trends and magnitudes observed on previous flights. The S-II base pressure environments were consistent with trends seen on previous flights, although the magnitudes were higher than seen on previous flights. The pressure environment during S-IC/S-II separation was well below maximum values.

The S-IC base region thermal environments exhibited trends and magnitudes similar to those seen on previous flights except that the ambient temperature under Engine No. 4 cocoon rose unexpectedly and at about 50 seconds and was approximately 13°C above the level experienced during previous flights. During the later portion of the S-IC boost, the temperature returned to normal. The maximum cocoon temperature reached was well below the upper limit of the components under the cocoon. The base thermal environments on the S-II stage were consistent with the trends and magnitudes seen on previous flights and were well below design limits. Aerodynamic heating environments and S-IVB base thermal environments were not measured.

The S-IC stage forward compartment thermal environment was adequately maintained although the temperature was lower than experienced during previous flights. The S-IC stage aft compartment environmental conditioning system performed satisfactorily. The S-II stage engine compartment conditioning system maintained the ambient temperature and thrust

cone surface temperatures within design ranges throughout the launch countdown. No equipment container temperature measurements were taken; however, since the external temperature were satisfactory and there were no problems with the equipment in the containers, the thermal control system apparently performed adequately. The IU stage Environmental Control System exhibited satisfactory performance for the duration of the IU mission. Coolant temperatures, pressures, and flowrates were continuously maintained within the required ranges and design limits. At 20,998 seconds the water valve logic was purposely inhibited (with the valve closed). Subsequent temperature increases were as predicted for this condition.

All data systems performed satisfactorily throughout the flight. Flight measurements from onboard telemetry were 99.8 percent reliable. Telemetry performance was normal except for noted problems. Radio Frequency propagation was satisfactory, though the usual interference due to flame effects and staging were experienced. Usable VHF data were received until 36,555 seconds (10:09:15). The Secure Range Safety Command Systems on the S-IC, S-II, and S-IVB stages were ready to perform their functions properly, on command, if flight conditions during launch phase had required destruct. The system properly safed the S-IVB destruct system on a command transmitted from Bermuda (BDA) at 723.1 seconds. The performance of the Command and Communications System (CCS) was satisfactory from liftoff through lunar impact at 313,181 seconds (86:59:41). Madrid, Goldstone were receiving CCS signal carrier at lunar impact. Good tracking data were received from the C-Band radar, with BDA indicating final Loss of Signal at 48,420 seconds (13:27:00).

Total vehicle mass, determined from postflight analysis, was within 0.68 percent of predicted from ground ignition through S-IVB stage final shutdown. This small variation indicates that hardware weights, propellant loads, and propellant utilization were close to predicted values during flight.

The S-IVB/IU Lunar Impact Mission objectives were to impact the stage within 350 km of the target, determine the impact time within 1 second, and determine the impact point within 5 km. The first two objectives have been met. Further analysis is required to satisfy the third objective. Based on analysis to date, the S-IVB/IU impacted the moon December 10, 1972, 20:32:40.99 GMT (313,180.99 seconds after range zero) at 4.33 degrees south latitude and 12.37 degrees west longitude. This location is 155 km (84 n mi) from the target of 7 degrees south latitude and 8 degrees west longitude. The velocity of the S-IVB/IU at impact relative to the lunar surface was 2,544 m/s (8,346 ft/s). The incoming heading angle was 83.0 degrees west of north and the angle relative to the local vertical was 35.0 degrees. The total mass impacting the moon was approximately 13,931 kg (approximately 30,712 lbm). Real-time targeting

activities modified the planned first APS lunar impact burn to reduce the APS ullage burn duration. A second APS burn was performed to minimize the trajectory dispersion from the targeted impact point.

Three MSFC Inflight Demonstrations were conducted during translunar coast. The purpose of the Demonstrations were to obtain data in a low g environment on:

- a. Convection in a Liquid Caused by Surface Tension Gradients.
- b. Heat Flow and Convection in a Confined Gas.
- c. Heat Flow and Convection in a Liquid.

The Demonstrations were conducted as planned. The data were collected by movie camera and crew observation, was of good quality, and is presently being analyzed.

The Lunar Roving Vehicle (LRV) satisfactorily supported the Apollo 17 Taurus-Littrow lunar surface exploration objectives. The total odometer distance traveled during the three EVA's was 35.7 kilometers at an average velocity of 7.75 km/hr on traverses. The maximum velocity attained was 18.0 km/hr and the maximum slopes negotiated were 18 degrees up and 20 degrees down. The average LRV energy consumption rate was 1.64 amp-hours/km with a total consumed energy of 73.4 amp-hours (including 14.8 amp-hours used by Lunar Communication Relay Unit) out of an approximate total available energy of 242 amp-hours. The navigation system gyro drift and closure error were negligible.

Controllability was good. There were no problems with steering, braking, or obstacle negotiation. Brakes were used at least partially on all downslopes. Driving down sun was difficult because the concealed shadows caused poor obstacle visibility.

While the LRV had no problems with the dust, stowed payload mechanical parts attached to the LRV tended to bind up. The crew described dust as being an anti-lubricant and reported that there was no EVA-4 capability in many of the stowed payload items because of dust intrusion. Large tolerance mechanical items such as locking bags on the gate and the pallet lock had problems toward the end of EVA-3. Only those items which had been protected from the dust performed without degradation.

All interfaces between crew, LRV and stowed payload were satisfactory.

The following LRV system anomalies were noted:

- a. At initial power-up, the LRV battery temperatures were higher than predicted.
- b. Battery No. 2 temperature indication was off scale low at start of EVA-3.

- c. The right rear fender extension was broken off at the Lunar Module site on EVA-1 prior to driving to the Apollo Lunar Surface Experiments Package site.

MISSION OBJECTIVES ACCOMPLISHMENT

Table 1 presents the MSFC Mandatory Objectives and Desirable Objectives as defined in the "Saturn V Apollo 17/AS-512 Mission Implementation Plan," MSFC Document PM-SAT-8010.10A, dated September 29, 1972. An assessment of the degree of accomplishment of each objective is shown. Discussion supporting the assessment can be found in other sections of this report as shown in Table 1.

Table 1. Mission Objectives Accomplishment

NO.	MSFC MANDATORY OBJECTIVES (MO) AND DESIRABLE OBJECTIVES (DO)	DEGREE OF ACCOMPLISHMENT	DISCREPANCIES	SECTION IN WHICH DISCUSSED
1	Launch on a flight azimuth between 72 and 100 degrees and insert the S-IVB/IU/SC into the planned circular earth parking orbit. (MO)	Complete	None	4.1
2	Restart the S-IVB on the first or second opportunity over the Atlantic and inject the S-IVB/IU/SC onto the planned translunar trajectory. (MO)	Complete	None	4.2.3, 7.6
3	Provide the required attitude control during TODE. (MO)	Complete	None	10.4.4
4	Perform an evasive maneuver after ejection of the CSM/LM from the S-IVB/IU (DO).	Complete	None	10.4.4
5	Target the S-IVB/IU stage for impact on the lunar surface at 7.0°S, 8.0°W. (DO)	Complete	None	17.4
6	Determine actual impact point within 5 kilometers, and time of impact within 1 second. (DO)	Analysis not complete, although the time of impact was determined within 1 sec.	None anticipated.	17.4
7	After final LV/SC separation, vent and dump the remaining gases and propellants to safe the S-IVB/IU. (DO)	Complete	None	7.4

FAILURES AND ANOMALIES

Evaluation of the Launch Vehicle and Lunar Roving Vehicle data revealed nine anomalies, one of which is considered significant. The significant anomaly is summarized in Table 2, and the other anomalies are summarized in Table 3.

Table 2. Summary of Significant Anomalies

ITEM	VEHICLE SYSTEM	ANOMALY IDENTIFICATION			RECOMMENDED CORRECTIVE ACTION	ACTION STATUS	VEHICLE EFFECTIVITY	PARA-REF.
		DESCRIPTION (CAUSE)	EFFECT ON MISSION	OCCURRENCE RANGE TIME (SEC)				
1	LVSSE/ESE	Toroidal Countdown Sequence (TCS) failed to provide S-100 LRE Task Preseparation command at T-167 seconds resulting in an automatic cutoff of the countdown at T-29 seconds. (Excessive reverse current leakage through diodes caused intericticant operation of certain TCS outputs.)	Launch delay of 2 hours and 60 minutes.	T-30 sec.	Replace all defective TCS diodes. Recomfigure LVSSE to provide 3 TCS's with 2 out of 3 voting logic at each Mobile Launcher, and ground unused outputs from each TCS.	EDP (EE 10-32746) Approved. Assembly cleaned.	SA-513 SA-206 Shr SA-208	3.3

Table 3. Summary of Anomalies

ITEM	VEHICLE SYSTEM	ANOMALY	PROBABLE CAUSE	SIGNIFICANCE	PAGE REF.
1	S-IC/Propulsion	S-IC engine start sequence was 2-1-1-1 instead of the planned 1-2-2.	By definition, two engines are considered to start together if their thrust chamber pressures reach 90% of a 100-millisecond time period. There is an apparent inability to consistently predict individual engine start times, within the 100 ms band, in the S-IC environment.	None on this mission or on the AS-513 mission since analysts using significantly larger start sequence dispersions than experienced on AS-512 have shown no problem. This anomaly is considered closed.	5.2 6.2.1
2	S-IC/Propulsion	The ambient temperature under Engine No. 1 caused a sudden rise early in the boost, peaking 13°C above the maximum previously experienced flight data at 50 seconds, then returned to the normal operation level for the remainder of S-IC boost.	1. Small leak (less than 0.003 lb/sec) in Gas Generator (GG) combustion body drives part plug the "popped itself" due to the deposition of hydrocarbons on the fuel-rich GG combustion gases. 2. Temporary loss of carbon insulation integrity, such as loose GG combustion drove access cover, which later corrected itself.	Apparently none on this mission since the problem was self-correcting and the maximum temperature reached was well below component design limits. Special attention will be given during prelaunch operations to inspection of the GG plug and access access covers.	5.3 13.2
3	S-IIW/Electrical	Aft Battery No. 1, Unit No. 1 temperature increased approximately 30 degrees above the nominal 50°F cutoff limit of the primary Master Control System during transverse coast.	Failure of Unit No. 1 heater power transistor.	None. Battery voltage and current remained normal. The battery temperature was kept below the upper limit by the high temperature thermostat (high temperature backup control). This anomaly is closed.	11.4.2
4	Postflight Program	Failure of the Two-Gyro Angle Reconciliation Test at 5421 seconds.	Progressing error, causing the reconciliation test to be performed improperly following a period of data compensation for telemetry of the backup gyros' angles.	None, since only one test failure was observed and 3 failures are required before champion to the backup system. The flight program for subsequent missions will be modified to preclude improper reconciliation test.	9.3.3
5	Postflight Program	Scheduled telemetry of certain 10 accelerometer readings during S-190 second burn.	A change to the Flight Program of AS-512 to lower the priority of certain accelerometer telemetry was accomplished by placing all related instructions in the Periodic Processor instead of in the Three-Hundred Second Unit (THSU) on AS-512 and AS-513. Because all instructions to the Periodic Processor are repeated for each guidance restart in preparation for TLI burn, the accelerometer readings were repositioned at T _g -7.2 seconds and continued through second burn.	None on this mission. Programming will not be changed because future flights do not call for a restart of heat-up navigation. This anomaly is closed.	9.3.4
6	LW Radar Subsystem	LW right rear radar antenna mounted off at LH site by Commandor.	Antenna carried in the right leg pocket of Commandor's Extravehicular Mobility Unit (EMU), caught the antenna and pulled it off.	Approximately 20 minutes of laser surface time was expended to implementing a fix. No further action is contemplated since this was the last planned United States laser surface exploration.	20.11
7	LW Batteries	High battery temperatures at initial LW power-up.	Hot holes (correlation of LW toward the sun) turned on massive thermal control during transverse coast.	No performance degradation. For alternate procedures, the batteries were cycled on 100% site during EVA-1 and on Station 6 during EVA-3 as alternate batteries while thermal limits. No further action is contemplated since this was the last planned United States laser surface exploration.	20.12
8	LW Batteries	Battery No. 2 temperature indication off scale for at start of EVA-1.	Shorted connector to the battery.	None. Battery No. 1 was used as an indicator and temperature trends had been established from initial data on EVA's 1 and 2. No further action is contemplated since this was the last planned United States laser surface exploration.	20.12

xxx111

SECTION 1

INTRODUCTION

1.1 PURPOSE

This report provides the National Aeronautics and Space Administration (NASA) Headquarters, and other interested agencies, with the launch vehicle and Lunar Roving Vehicle (LRV) evaluation results of the AS-512 flight (Apollo 17 Mission). The basic objective of flight evaluation is to acquire, reduce, analyze, evaluate and report on flight data to the extent required to assure future mission success and vehicle reliability. To accomplish this objective, actual flight problems are identified, their causes determined, and recommendations made for appropriate corrective action.

1.2 SCOPE

This report contains the performance evaluation of the major launch vehicle systems and LRV, with special emphasis on problems. Summaries of launch operations and spacecraft performance are included.

The official George C. Marshall Space Flight Center (MSFC) position at this time is represented by this report. It will not be followed by a similar report unless continued analysis or new information should prove the conclusions presented herein to be significantly incorrect.

SECTION 2
EVENT TIMES

2.1 SUMMARY OF EVENTS

Range zero occurred at 00:33:00 Eastern Standard Time (EST) (05:33:00 Universal Time [UT]) December 7, 1972. Range time is the elapsed time from range zero, and is the time used throughout this report unless otherwise noted. Time from base time is the elapsed time from the start of the indicated time base. Table 2-1 presents the time bases used in the flight sequence program.

Table 2-1. Time Base Summary

TIME BASE	VEHICLE TIME* SECONDS (HR:MIN:SEC)	GROUND TIME** SECONDS (HR:MIN:SEC)	SIGNAL START
T ₀	-16.96	-16.96	Guidance Reference Release
T ₁	0.63	0.63	IU Umbilical Disconnect Sensed by LVDC
T ₂	139.44	139.44	Initiated by LVDC 0.013 Seconds after T ₁ +138.8 Seconds
T ₃	161.22	161.22	S-IC OECO Sensed by LVDC
T ₄	559.65	559.65	S-II OECO Sensed by LVDC
T ₅	702.87	702.87	S-IVB ECO (Velocity) Sensed by LVDC
T ₆	10,978.65 (03:02:58.65)	10,978.65 (03:02:58.65)	Restart Equation Solution
T ₇	11,907.87 (03:18:27.87)	11,907.87 (03:18:27.87)	S-IVB ECO (Velocity) Sensed by LVDC
T ₈	18,179.88 (05:02:59.88)	18,180.00 (05:03:00.00)	Initiated by Ground Command

*Range Time of occurrence as indicated by uncorrected LVDC clock,
i.e., the time of event as tagged onboard, converted to range time.

**Range Time of Ground receipt of telemetered signal from vehicle.
Includes telemetry transmission time and LVDC clock correction.
Figure 2-1.

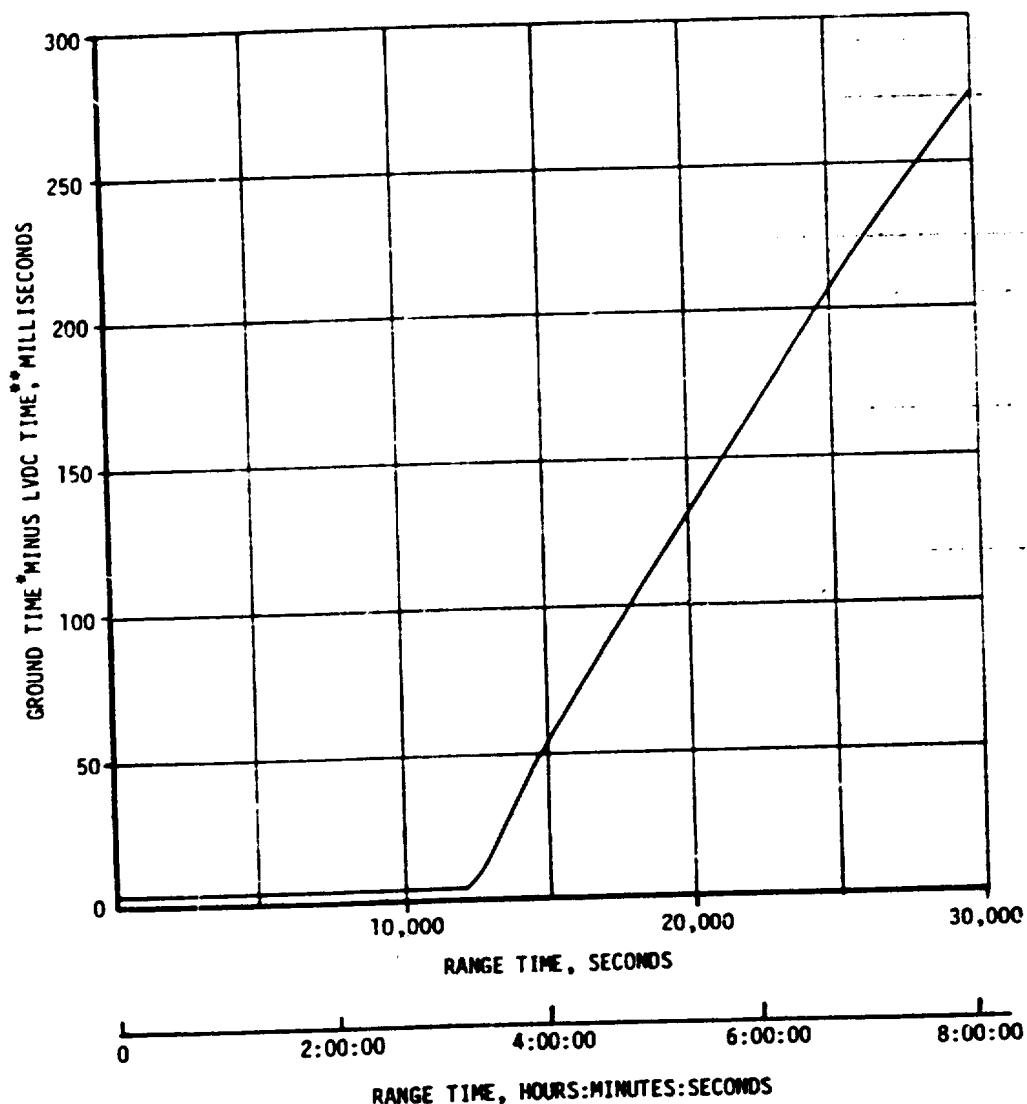
The start of Time Bases T₀, T₁, and T₂ were nominal. T₃, T₄ and T₅ were initiated approximately 0.5 seconds early, 0.4 seconds early, and 4.1 seconds early, respectively, due to variations in the stage burn times. These variations are discussed in Sections 5, 6 and 7 of this document. Start times of T₆ and T₇ were 1.9 seconds early and 2.1 seconds late, respectively. T₈ was initiated by the receipt of a ground command.

Figure 2-1 shows the mean difference between ground station receipt time and vehicle tagged time which may be used for precise comparisons between onboard guidance and navigation data that is time-tagged onboard and other data that is time-tagged by time of telemetry signal receipt at a ground station.

A summary of significant event times for AS-512 is given in Table 2-2. The preflight predicted times were adjusted to match the actual first motion time. The predicted times for establishing actual minus predicted times in Table 2-2 were taken from 40M33627D, "Interface Control Document Definition of Saturn SA-511, 512 and 514 Flight Sequence Program" and from the AS-512 Postlaunch Operational Trajectory (OT). The postlaunch operational trajectory, MSFC Memorandum S&E-AERO-MFT-200-72, correcting the earlier OT for the adjusted flight azimuth, was used because of the launch delay.

2.2 VARIABLE TIME AND COMMANDED SWITCH SELECTOR EVENTS

Table 2-3 lists the switch selector events which were issued during the flight, but were not programmed for specific times.



* RANGE TIME OF GROUND RECEIPT OF TELEMETRED SIGNAL FROM VEHICLE.
** RANGE TIME OF OCCURRENCE AS INDICATED BY UNCORRECTED LVDC CLOCK.

Figure 2-1. AS-512 Telemetry Time Difference

Table 2-2. Significant Event Times Summary

ITEM	EVENT DESCRIPTION	RANGE TIME		TIME FROM BASE	
		ACTUAL SEC	ACT-PREF SEC	ACTUAL SEC	ACT-PREF SEC
1	GUIDANCE REFERENCE RELEASE (GRR)	-17.0	0.0	-17.6	-0.4
2	S-IC ENGINE START SEQUENCE COMMAND (CROWNS)	-9.9	0.0	-9.5	0.0
3	S-IC ENGINE NO.5 START	-6.9	0.0	-7.5	0.0
4	S-IC ENGINE NO.1 START	-6.7	0.0	-7.3	0.1
5	S-IC ENGINE NO.3 START	-6.6	0.0	-7.2	0.0
6	S-IC ENGINE NO.2 START	-6.3	0.0	-6.9	0.1
7	S-IC ENGINE NO.4 START	-6.3	0.1	-7.0	0.0
8	ALL S-IC ENGINES THRUST OK	-1.6	-0.1	-2.3	-0.1
9	RANGE ZERO	0.0		-0.6	
10	ALL HOLDDOWN ARMS RELEASED (FIRST PULL)	0.2	0.0	-0.4	0.0
11	DU UNBILICAL DISCONNECT, START OF TIME BASE 1 (T1)	0.6	0.0	0.0	0.0
12	BEGIN TOWER CLEARANCE YAW MANEUVER	0.7	0.1	1.0	0.0
13	END YAW MANEUVER	9.7	0.1	9.1	0.1
14	BEGIN PITCH AND ROLL MANEUVER	12.9	0.4	12.3	0.5
15	S-IC OUTBOARD ENGINE CANT	20.6	0.0	20.0	0.0
16	END ROLL MANEUVER	14.3	-0.4	13.7	-0.4
17	MACH 1	67.5	0.0	66.9	0.1
18	MAXIMUM DYNAMIC PRESSURE (MAX C)	82.5	-1.1	81.9	-1.1
19	S-IC CENTER ENGINE CUTOFF (CECC)	139.30	-0.02	138.67	-0.01
20	START OF TIME BASE 2 (T2)	139.4	0.0	0.0	0.0
21	END PITCH MANEUVER (TILT ARREST)	160.1	0.2	20.6	0.1
22	S-IC OUTBOARD ENGINE CUTOFF (CECC)	161.20	-0.47	21.75	-0.47
23	START OF TIME BASE 3 (T3)	161.2	-0.5	0.0	0.0

Table 2-2. Significant Event Times Summary (Cont'd)

ITEM	EVENT DESCRIPTION	RANGE TIME		TIME FROM BASE	
		ACTUAL SEC	ACT-PRED SEC	ACTUAL SEC	ACT-PRED SEC
24	START S-II LH2 TANK HIGH PRESSURE VENT MODE	161.3	-0.5	0.1	-0.0
25	S-II LH2 RECIRCULATION PUMPS CFF	161.4	-0.5	0.2	0.0
26	S-IC/S-II SEPARATION COMMAND TO FIRE SEPARATION DEVICES AND RETRO MOTORS	162.9	-0.5	1.6	-0.1
27	S-II ENGINE SLEWING ACTIVATION (AVERAGE OF FIVE)	163.6	-0.5	2.4	0.0
28	S-II ENGINE START SEQUENCE COMMAND (ESCI)	163.6	-0.5	2.4	0.0
29	S-II IGNITION-STOVR OPEN	164.6	-0.5	3.4	0.0
30	S-II MAINSTAGE	166.4	-0.5	5.2	0.0
31	S-II CHILLODOWN VALVES CLOSE	166.5	-0.5	5.3	0.0
32	S-II HIGH (5.5) EPR NO. 1 ON	169.1	-0.5	7.9	0.0
33	S-II HIGH (5.5) EPR NO. 2 ON	169.3	-0.5	8.1	0.0
34	S-II SECOND PLANE SEPARATION COMMAND (JETTISON S-II AFT INTERSTAGE)	192.9	-0.5	31.7	0.0
35	LAUNCH ESCAPE TOWER (LET) JETTISON	*			
36	ITERATIVE GUIDANCE MODE (IGM) PHASE 1 INITIATED	204.1	0.0	42.9	0.5
37	S-II CENTER ENGINE CUTOFF (CECC)	461.21	-0.47	299.98	-0.02
38	START OF ARTIFICIAL TAU MODE	489.0	-1.9	327.8	-1.5
39	S-II LOW ENGINE MIXTURE RATIO (EMR) SHIFT (FACTUAL)	489.2	-2.1	328.0	-1.6
40	END OF ARTIFICIAL TAU MODE	499.0	-3.2	337.8	-2.8
41	S-II CUTBACK ENGINE CUTOFF (CECC)	559.66	-0.47	398.43	-0.02
42	S-II ENGINE CUTOFF INTERRUPT. START OF TIME BASE 4 (T4)	559.7	-0.4	0.0	0.0
43	S-IVB ULLAGE MOTOR IGNITION	560.5	-0.5	0.9	0.0
44	S-II/S-IVB SEPARATION COMMAND TO FIRE SEPARATION DEVICES AND RETRO MOTORS	560.6	-0.5	1.0	0.0

*Data not available.

Table 2-2. Significant Event Times Summary (Cont'd)

ITEM	EVENT DESCRIPTION	TIME		TIME FROM BASE	
		ACTUAL SEC	ACT-PART SEC	ACTUAL SEC	ACT-PART SEC
45	S-IVB ENGINE START COMMAND (FIRST FST)	560.7	-0.5	1.1	3.0
46	FUEL CHILLER TANK PUMP OFF	561.8	-0.5	2.2	3.0
47	S-IVB IGNITION (STEV OPEN)	563.8	-0.4	4.2	0.1
48	S-IVB MAIN STAGE	566.2	-0.5	6.6	0.0
49	START OF ARTIFICIAL TAU MDT	568.9	0.4	9.2	3.8
50	S-IVB ULLAGE CASE JETTISON	572.4	-0.5	12.8	0.0
51	END OF ARTIFICIAL TAU MDC	582.7	4.4	27.6	4.9
52	BEGIN TERMINAL GUIDANCE	669.7	-6.2	110.1	-5.7
53	FNO IGN PHASE 3	696.3	-3.7	136.7	-3.2
54	BEGIN CMI FREEZE	696.3	-3.7	136.7	-3.2
55	S-IVB VELOCITY CUTOFF COMMAND NO. 1 (FIRST ECO1)	702.65	-4.09	-0.23	-0.02
56	S-IVB VELOCITY CUTOFF COMMAND NO. 2	702.75	-4.10	-0.12	-0.02
57	S-IVB ENGINE CUTOFF INTERRUPT, START OF TIME BASE 5 (T5)	702.9	-4.1	0.0	0.0
58	S-IVB APS ULLAGE ENGINE NO. 1 IGNITION COMMAND	703.1	-4.1	0.3	0.0
59	S-IVB APS ULLAGE ENGINE NO. 2 IGNITION COMMAND	703.2	-4.1	0.4	0.0
60	LCX TANK PRESSURIZATION OFF	704.0	-4.2	1.2	0.0
61	PARKING CRIT INSERTION	712.6	-4.1	9.8	0.0
62	BEGIN MANEUVER TO LOCAL HORIZONTAL ATTITUDE	724.4	-2.7	21.5	1.3
63	S-IVB CONTINUOUS VENT SYSTEM (CVS) ON	761.8	-4.1	59.0	3.0
64	S-IVB APS ULLAGE ENGINE NO. 1 CUTOFF COMMAND	785.8	-4.1	87.0	3.0
65	S-IVB APS ULLAGE ENGINE NO. 2 CUTOFF COMMAND	785.9	-4.1	87.1	3.0
66	BEGIN ORBITAL NAVIGATION	*			
67	BEGIN S-IVB RESTART PREPARATIONS, START OF TIME BASE 6 (T6)	80578.6	-1.5	0.0	0.0

*Data not available.

Table 2-2. Significant Event Times Summary (Cont'd)

ITEM	EVENT DESCRIPTION	RANGE TIME		TIME FROM PASE	
		ACTUAL SEC	ACT-PREF SEC	ACTUAL SEC	ACT-PREF SEC
68	S-IVB C2/H2 BURNER LH2 ON	11019.9	-1.9	41.3	0.0
69	S-IVB C2/H2 BURNER EXITERS ON	11020.2	-1.9	41.6	0.0
70	S-IVB C2/H2 BURNER LOX ON (HELIUM HEATER ON)	11020.6	-1.9	42.0	0.0
71	S-IVB CVS OFF	11020.8	-1.9	42.2	0.0
72	S-IVB LH2 REPRESSURIZATION CONTROL VALVE ON	11026.7	-1.9	48.1	0.0
73	S-IVB LOX REPRESSURIZATION CONTROL VALVE ON	11026.9	-1.9	48.3	0.0
74	S-IVB ALX HYDRAULIC PUMP FLIGHT MUTE ON	11197.6	-1.9	219.0	0.0
75	S-IVB LOX CHILLEDFA PUMP ON	11227.6	-1.9	249.0	0.0
76	S-IVB LH2 CHILLEDFA PUMP ON	11232.6	-1.9	254.0	0.0
77	S-IVB PREVALVES CLOSED	11237.6	-1.9	259.0	0.0
78	S-IVB MIXTURE RATIO CONTROL VALVE OPEN	11428.7	-1.9	450.1	0.0
79	S-IVB APS ULLAGE ENGINE NO. 1 IGNITION COMMAND	11474.9	-1.9	496.3	0.0
80	S-IVB APS ULLAGE ENGINE NO. 2 IGNITION COMMAND	11475.0	-1.9	496.4	0.0
81	S-IVB C2/H2 BURNER LH2 OFF (HELIUM HEATER OFF)	11475.4	-1.9	496.8	0.0
82	S-IVB C2/H2 BURNER LOX OFF	11479.9	-1.9	501.3	0.0
83	S-IVB LH2 CHILLEDFA PUMP OFF	11548.0	-1.9	565.4	0.0
84	S-IVB LOX CHILLEDFA PUMP OFF	11548.2	-1.9	565.6	0.0
85	S-IVB ENGINE RESTART COMMAND (FUEL LEAD INITIATION) (SECNG ESC)	11548.6	-1.9	570.0	0.0
86	S-IVB APS ULLAGE ENGINE NO. 1 CUTOFF COMMAND	11551.6	-1.9	573.0	0.0
87	S-IVB APS ULLAGE ENGINE NO. 2 CUTOFF COMMAND	11551.7	-1.9	573.1	0.0
88	S-IVB SECOND IGNITION (STOV OPEN)	11556.6	-1.9	578.0	0.0
89	S-IVB MAINSTAGE	11559.2	-1.9	580.4	-0.1

Table 2-2. Significant Event Times Summary (Cont'd)

ITEM	EVENT DESCRIPTION	WANCS TIME		TIME FROM BASE	
		ACTUAL SEC	PREDICTED SEC	ACTUAL SEC	PREDICTED SEC
90	ENGINE MIXTURE RATIO (ENR) CONTROL VALVE SHIFT (PREGIN VALVE MOVEMENT)	11649.8	-0.7	671.7	1.7
91	S-IVB LH2 STEP PRESSURIZATION (SECOND BURN RELAY OFF)	11728.6	-1.9	850.0	0.0
92	BEGIN TERMINAL GUIDANCE	11879.1	-2.3	900.5	4.2
93	BEGIN CMI FREEZE	11905.7	0.7	976.6	2.6
94	S-IVB SECTION GUIDANCE CUTOFF COMMAND NO. 1 (SECOND EOD)	11907.64	2.10	-0.24	-0.04
95	S-IVB SECOND GUIDANCE CUTOFF COMMAND NO. 2	11907.76	2.12	-0.12	-0.02
96	S-IVB ENGINE CUTOFF INTERRUPT, START OF TIME BASE 7 (T7)	11907.9	2.1	0.0	0.0
97	S-IVB CVS ON	11908.3	2.1	0.5	0.0
98	TRANSLUNAR INJECTION (TLI)	11917.6	2.1	9.0	0.0
99	S-IVB CVS OFF	12058.7	2.1	150.9	0.3
100	BEGIN CRITICAL NAVIGATION	12059.6	3.0	151.7	0.8
101	BEGIN MANEUVER TO LOCAL HORIZONTAL ATTITUDE	12059.6	3.0	151.7	0.8
102	BEGIN MANEUVER TO TRANSPONDER AND DOCKING ATTITUDE (TCGE)	12808.9	**	901.0	
103	CSM SEPARATION	13347.6	**	1435.7	
104	CSM CCCX	14230.7	**	2322.8	
105	SC/LV FINAL SEPARATION	17102.3	**	5194.3	
106	START OF TIME BASE E (T8)	18179.9	**	0.0	0.0
107	S-IVB APS ULLAGE ENGINE NO. 1 IGNITION COMMAND	18181.1	**	1.2	0.0
108	S-IVB APS ULLAGE ENGINE NO. 2 IGNITION COMMAND	18181.2	**	1.4	0.0
109	S-IVB APS ULLAGE ENGINE NO. 1 CUTOFF COMMAND	18261.0	**	81.2	0.0
110	S-IVB APS ULLAGE ENGINE NO. 2 CUTOFF COMMAND	*			

*Data not available.

**Prediction not available.

Table 2-2. Significant Event Times Summary (Cont'd)

ITEM	EVENT DESCRIPTION	RANGE TIME		TIME FOR BASE	
		ACTUAL SEC	ACT-PRED SEC	ACTUAL SEC	ACT-PRED SEC
111	Initiate Maneuver to LOX Dump Attitude	18,760.0	**	40.1	0.0
112	S-IVB CVS ON	19,179.8	**	1000.0	0.0
113	S-IVB CVS OFF	19,480.0	**	1300.0	0.0
114	End LOX Dump Required for S-IVB APS Burn	19,507.9	**	1328.0	0.0
115	S-IVB APS Ullage Engine No. 1 Ignition Command	22,199.8	**	4020.0	
116	S-IVB APS Ullage Engine No. 2 Ignition	22,200.0	**	4020.2	
117	S-IVB APS Ullage Engine No. 1 Cutoff Command	22,297.8	**	4118.0	
118	S-IVB APS Ullage Engine No. 2 Cutoff Command	22,298.0	**	4118.2	
119	2nd Lunar Impact Maneuver Command	39,760.0	**		
120	S-IVB APS Ullage Engine No. 1 Ignition Command	40,499.8	**		
121	S-IVB APS Ullage Engine No. 2 Ignition Command	40,500.0	**		
122	S-IVB APS Ullage Engine No. 1 Cutoff Command	40,601.8	**		
123	S-IVB APS Ullage Engine No. 2 Cutoff Command	40,602.0	**		
124	Passive Thermal Control Maneuver	41,510	**		
125	Flight Control Computer Power Off	41,532	**		
126	CCS Subcarrier Off	49,260	**		
127	S-IVB/IU Lunar Impact (Hours) (HR:MIN:SEC)	86.995 86:59:41		103.951	

**Predictions not available.

Table 2-3. Variable Time and Commanded Switch Selector Events

FUNCTION	STAGE	RANGE TIME (SEC)	TIME FROM BASE (SEC)	REMARKS
Low (4.8) EMR No. 1 ON	S-II	489.0	$T_3 + 327.8$	LVDC Function
Low (4.8) EMR No. 2 ON	S-II	489.2	$T_3 + 328.0$	LVDC Function
Water Coolant Valve Closed	IU	780.5	$T_5 + 77.6$	LVDC Function
Telemetry Calibrator Inflight Calibrate ON	IU	3216.1	$T_5 + 2513.2$	Acquisition by Carnarvon Revolution 1
TM Calibrate ON	S-IVB	3216.5	$T_5 + 2513.6$	Acquisition by Carnarvon Revolution 1
TM Calibrate OFF	S-IVB	3217.5	$T_5 + 2514.6$	Acquisition by Carnarvon Revolution 1
Telemetry Calibrator Inflight Calibrate OFF	IU	3221.1	$T_5 + 2518.2$	Acquisition by Carnarvon Revolution 1
Water Coolant Valve Open	IU	3480.5	$T_5 + 2777.6$	LVDC Function
Telemetry Calibrator Inflight Calibrate ON	IU	4712.1	$T_5 + 4009.2$	Acquisition by Hawaii Rev. 1
TM Calibrate ON	S-IVB	4712.5	$T_5 + 4009.6$	Acquisition by Hawaii Rev. 1
TM Calibrate OFF	S-IVB	4713.5	$T_5 + 4010.6$	Acquisition by Hawaii Rev. 1
Telemetry Calibrator Inflight Calibrate OFF	IU	4717.1	$T_5 + 4014.2$	Acquisition by Goldstone Rev. 1
Telemetry Calibrator Inflight Calibrate ON	IU	5344.1	$T_5 + 4641.2$	Acquisition by Goldstone Rev. 1
TM Calibrate ON	S-IVB	5344.5	$T_5 + 4641.6$	Acquisition by Goldstone Rev. 1
TM Calibrate OFF	S-IVB	5345.5	$T_5 + 4642.6$	Acquisition by Goldstone Rev. 1
Telemetry Calibrator Inflight Calibrate OFF	IU	5349.1	$T_5 + 4646.2$	Acquisition by Goldstone Rev. 1

Table 2-3. Variable Time and Commanded Switch Selector Events (Contd)

FUNCTION	STAGE	RANGE TIME (SEC)	TIME FROM BASE (SEC)	REMARKS
Telemetry Calibrator Inflight Calibrate ON	IU	6928.1	$T_5 + 6225.2$	Acquisition by Ascension Rev. 2
TM Calibrate ON	S-IVB	6928.5	$T_5 + 6225.6$	Acquisition by Ascension Rev. 2
TM Calibrate OFF	S-IVB	6929.5	$T_5 + 6226.6$	Acquisition by Ascension Rev. 2
Telemetry Calibrator Inflight Calibrate OFF	IU	6935.1	$T_5 + 6232.2$	Acquisition by Ascension Rev. 2
Telemetry Calibrator Inflight ON	IU	8808.1	$T_5 + 8105.2$	Acquisition by Carnarvon Rev. 2
TM Calibrate ON	S-IVB	8808.5	$T_5 + 8105.6$	Acquisition by Carnarvon Rev. 2
TM Calibrate OFF	S-IVB	8809.5	$T_5 + 8106.6$	Acquisition by Carnarvon Rev. 2
Telemetry Calibrator Inflight OFF	IU	8813.1	$T_5 + 8110.2$	Acquisition by Carnarvon Rev. 2
Telemetry Calibrator Inflight Calibrate ON	IU	10264.1	$T_5 + 9561.2$	Acquisition by Hawaii Rev. 2
TM Calibrate ON	S-IVB	10264.5	$T_5 + 9561.6$	Acquisition by Hawaii Rev. 2
TM Calibrate OFF	S-IVB	10265.5	$T_5 + 9562.6$	Acquisition by Hawaii Rev. 2
Telemetry Calibrator Inflight Calibrate OFF	IU	10269.1	$T_5 + 9566.2$	Acquisition by Hawaii Rev. 2
Telemetry Calibrator Inflight Calibrate ON	IU	10888.1	$T_5 + 10185.2$	Acquisition by Goldstone Rev. 2
TM Calibrate ON	S-IVB	10888.5	$T_5 + 10185.6$	Acquisition by Goldstone Rev. 2
TM Calibrate OFF	S-IVB	10889.5	$T_5 + 10186.6$	Acquisition by Goldstone Rev. 2
Telemetry Calibrator Inflight Calibrate OFF	IU	10893.1	$T_5 + 10190.2$	Acquisition by Goldstone Rev. 2

Table 2-3. Variable Time and Commanded Switch Selector Events (Cont'd)

FUNCTION	STAGE	RANGE TIME (SEC)	TIME FROM BASE (SEC)	REMARKS
Telemetry Calibrator Inflight Calibrate ON	IU	12175.2	$T_7 + 267.3$	Acquisition by Ascension TLC
TM Calibrate ON	S-IVB	12175.6	$T_7 + 267.7$	Acquisition by Ascension TLC
TM Calibrate OFF	S-IVB	12176.6	$T_7 + 268.7$	Acquisition by Ascension TLC
Telemetry Calibrator Inflight Calibrate OFF	IU	12180.2	$T_7 + 272.3$	Acquisition by Ascension TLC
Water Coolant Valve Closed	IU	19079.8	$T_8 + 899.9$	LVDC Function
S-IVB Ullage Engine No. 1 ON	S-IVB	22199.8	$T_8 + 4020.0$	Lunar Impact Burn No. 1
S-IVB Ullage Engine No. 2 ON	S-IVB	22200.0	$T_8 + 4020.2$	Lunar Impact Burn No. 1
S-IVB Ullage Engine No. 1 OFF	S-IVB	22297.8	$T_8 + 4118.0$	Lunar Impact Burn No. 1
S-IVB Ullage Engine No. 2 OFF	S-IVB	22298.0	$T_8 + 4118.2$	Lunar Impact Burn No. 1
S-IVB Ullage Engine No. 1 ON	S-IVB	40499.8	$T_8 + 22320.0$	Lunar Impact Burn No. 2
S-IVB Ullage Engine No. 2 ON	S-IVB	40500.0	$T_8 + 22320.1$	Lunar Impact Burn No. 2
S-IVB Ullage Engine No. 1 OFF	S-IVB	40601.0	$T_8 + 22421.9$	Lunar Impact Burn No. 2
S-IVB Ullage Engine No. 2 OFF	S-IVB	40602.0	$T_8 + 22422.1$	Lunar Impact Burn No. 2
Flight Control Computer Power OFF A	IU	41521.0	$T_8 + 23341.1$	CCS Command
Flight Control Computer Power OFF B	IU	41532.1	$T_8 + 23352.2$	CCS Command
Water Coolant Valve Open	IU	41554.3	$T_8 + 23374.4$	LVDC Function

SECTION 3

LAUNCH OPERATIONS

3.1 SUMMARY

The ground systems supporting the AS-512/Apollo 17 countdown and launch performed satisfactorily with the exception of the Terminal Countdown Sequencer (TCS). The TCS malfunction, which is discussed in paragraph 3.3, resulted in a 2 hour and 40 minute launch delay. The space vehicle was launched at 00:33:00 Eastern Standard Time (EST) (05:33:00 UT) on December 7, 1972, from Pad 39A of the Kennedy Space Center, Saturn Complex. Damage to the pad, Launch Umbilical Tower (LUT) and support equipment was considered minimal.

3.2 PRELAUNCH MILESTONES

A chronological summary of prelaunch milestones for the AS-512 launch is contained in Table 3-1.

3.2.1 S-IC Stage

S-IC stage and GSE systems performed satisfactorily during countdown with the exception of three failures which were subsequently corrected. The failures were in the (1) Safe and Arm Devices (S&A), (2) Remote Digital Sub-Multiplexer, and (3) F-1 Engine No. 2 Gas Generator Igniter. The Safe and Arm Device failed to respond to a safe command. Possible causes for the failure were determined to be low voltage, improper installation, or a defective unit. The Safe and Arm Device and its mounting block were replaced and the replacement unit performed satisfactorily. Bench tests of the suspect unit failed to duplicate the problem and dimensional analysis of the unit and mounting block was satisfactory. Analysis did reveal, however, that output torque of the solenoid at the lower end of the voltage curve was marginal with respect to the torque requirements of the mechanical linkage of the S&A device. As a precautionary measure, the countdown procedure was changed to arm the device at T-33 minutes instead of T-5 minutes to eliminate the need for recycling to T-22 minutes in the event of a hold. In addition, the provision was made to increase the stage bus voltage to 30 V if the unit should fail to arm during the count.

At the T-9 hour scheduled hold the Remote Digital Sub-Multiplexer (RDSM) failed and an 8 ampere current surge of one minute duration was recorded. The RDSM was replaced and satisfactorily retested. The cause was isolated to shorted ceramic capacitor (C7) in the power supply card. As a result of failure analysis it was concluded that the failure was random and no corrective action is anticipated.

Table 3-1. AS-512/Apollo 17 Prelaunch Milestones

DATE	ACTIVITY OR EVENT
October 27, 1970	S-II-12 Stage Arrival
December 21, 1970	S-IVB-512 Stage Arrival
June 16, 1971	Lunar Module (LM)-12 Ascent Stage Arrival
June 17, 1971	Lunar Module (LM)-12 Descent Stage Arrival
March 24, 1972	Spacecraft/Lunar Module Adapter (SLA)-21 Arrival
March 24, 1972	Command and Service Moduie (CSM)-114 Arrival
May 11, 1972	S-IC-12 Stage Arrival
May 15, 1972	S-IC Erection on Mobile Launcher (ML)-3
May 19, 1972	S-II Erection
June 2, 1972	Lunar Roving Vehicle (LRV)-3 Arrival
June 7, 1972	Instrument Unit (IU)-512 Arrival
June 20, 1972	III Erection
June 23, 1972	S-IVB Erection
July 12, 1972	Launch Vehicle (LV) Electrical Systems Test Completed
August 1, 1972	LV Propellant Dispersion/Malfunction Overall Test (OAT) Complete
August 11, 1972	LV Service Arm OAT Complete
August 13, 1972	LRV Installation
August 23, 1972	Spacecraft (SC) Erection
August 28, 1972	Space Vehicle (SV)/ML Transfer to Pad 39A
October 11, 1972	SV Electrical Mate
October 12, 1972	SV OAT No. 1 (Plugs In) Complete
October 20, 1972	SV Flight Readiness Test (FRT) Completed
November 10, 1972	RP-1 Loading
November 20, 1972	Countdown Demonstration Test (CDOT) Completed (Wet)
November 21, 1972	CDOT Completed (Dry)
December 5, 1972	SV Terminal Countdown Started (T-28 Hours)
December 7, 1972 (EST)	SV Launch

The F-1 Engine No. 2 Gas Generator (GG) igniter installed indication was lost at T-23 hours. Both GG igniters on Engine No. 2 were replaced and the problem was determined to be due to igniter failure. Failure analysis revealed an error in manufacture in that solder had been omitted from an electrical pin in the igniter, allowing intermittent contact. The lack of solder was seen in the X-ray picture which is made during receiving inspection. Corrective action taken was to review all remaining igniter X-ray pictures to assure no more omissions exist.

3.2.2 S-II Stage

The S-II stage and GSE performed satisfactorily during the countdown. As a result of the unscheduled hold caused by the Terminal Countdown Sequencer (TCS) malfunction, some systems such as the J-2 engine start tank system were required to remain active.

During the first unscheduled hold at 02:52:30 UT (T-30 seconds), S-II stage systems were safed and recycled successfully during this 65.2 minute hold duration. At 03:57:41 UT (T-22 minutes), the countdown was resumed and continued to T-8 minutes when another hold occurred to resolve the TCS corrective action. This hold lasted 73.3 minutes and contingency hold Option 2 was utilized. S-II systems remaining active through this hold were LOX system helium injection, engine actuation hydraulic system temperature control, and engine helium and hydrogen tanks pressurized. It was necessary to manually control engine start tanks pressurized. The engine start tanks were chilled, pressurized, and then required one rechill cycle at 05:12:00 UT for proper temperature conditions. At 05:25:00 UT, the countdown resumed at T-8 minutes and proceeded without further problems to liftoff. Electrical batteries on the S-II stage were on internal power about 20 seconds longer than previous vehicles and were slightly more discharged at liftoff as a result of the repeated countdown.

3.2.3 S-IVB Stage

Overall performance of the S-IVB stage and GSE was satisfactory during the countdown operations.

A hazardous gas detection sensor located at the LH₂ tank vent disconnect on Swing Arm No. 7, showed an intermittent indication of GH₂ for approximately 1-1/2 hours from T-3 hours 30 minutes. The leak was not large enough to cause a problem and was dispositioned acceptable for launch.

To keep the engine control helium sphere pressure below the redline limit of 3400 psia, the sphere was vented six times using the emergency vent during the hold period.

Prior to resuming the countdown at T-8 minutes, the start tank was rechilled to bring the temperature below the maximum limit acceptable for launch. After rechilling, the start tank emergency vent valve was cycled three times to keep the start tank pressure below the maximum limit.

A long term decay was noted on Forward Battery No. 2, open circuit voltage. The open circuit voltage at the time of installation was 34.74 V. The voltage decayed 1.50 V over a 24-hour period. During the hold at T-9 hours, a power transfer test was performed to verify battery performance under loaded conditions. Battery performance was normal. At T-8 hours 53 minutes, Battery Monitor Enable was turned on to provide a small load in order to stabilize the battery. The battery voltage stabilized at T-4 hours. The voltage decay was attributed to a greater than nominal silver-peroxide level in the battery cells. The battery met all specifications and criteria.

3.2.4 IU Stage

The IU stage performed satisfactorily during the countdown.

3.3 TERMINAL COUNTDOWN

The AS-512/Apollo 17 Terminal Countdown was picked up at T-38 hours on December 5, 1972. Scheduled holds were initiated at T-9 hours for a duration of 9 hours, and at T-3 hours 30 minutes for a duration of one hour.

At T-167 seconds the Terminal Countdown Sequencer (TCS) failed to issue the "S-IVB LOX Tank Pressurization" command. When it was visually observed that the S-IVB LOX Tank was not being pressurized, the console operator initiated action to manually control S-IVB LOX Tank Pressurization. The tank was pressurized, but because an interlock relay was not energized when the TCS failed to issue the T-167 second command, a countdown hold was experienced at T-30 seconds. This hold lasted for 2 hours and 40 minutes during which time the TCS failure was confirmed, a "Work-Around" was investigated, and the "Work-Around" was verified at the MSFC Saturn V System Development Facility (SDF). Also during this hold the countdown was recycled to T-22 minutes. After investigation of the failure and verification of the "Work-Around" it was concluded that the countdown could be successfully and safely accomplished by using a jumper to bypass the "S-IVB LOX Tank Pressurized" interlock relay and manually pressurizing the LOX tank from the LCC. The countdown sequence was restarted at T-22 minutes and completed successfully.

Figure 3-1 shows the electrical circuits associated with this anomaly and the following is a description of the functional operation of the circuits.

The T-167 second command from the TCS (Channel 3) is supplied to the Mobile Launcher (ML) Integration Patch Distributor to energize relay K3 which supplies a 28V signal to the ML S-IVB Patch distributor. This signal is used to initiate 1) S-IVB LOX tank vent closed, 2) S-IVB LOX tank pressurization valve open, and 3) energize relay K577 "Time for LOX Tank Pressurization." Without relay K577 energized the "S-IVB LOX Tank Pressurized" interlock relay K536 cannot be energized even if

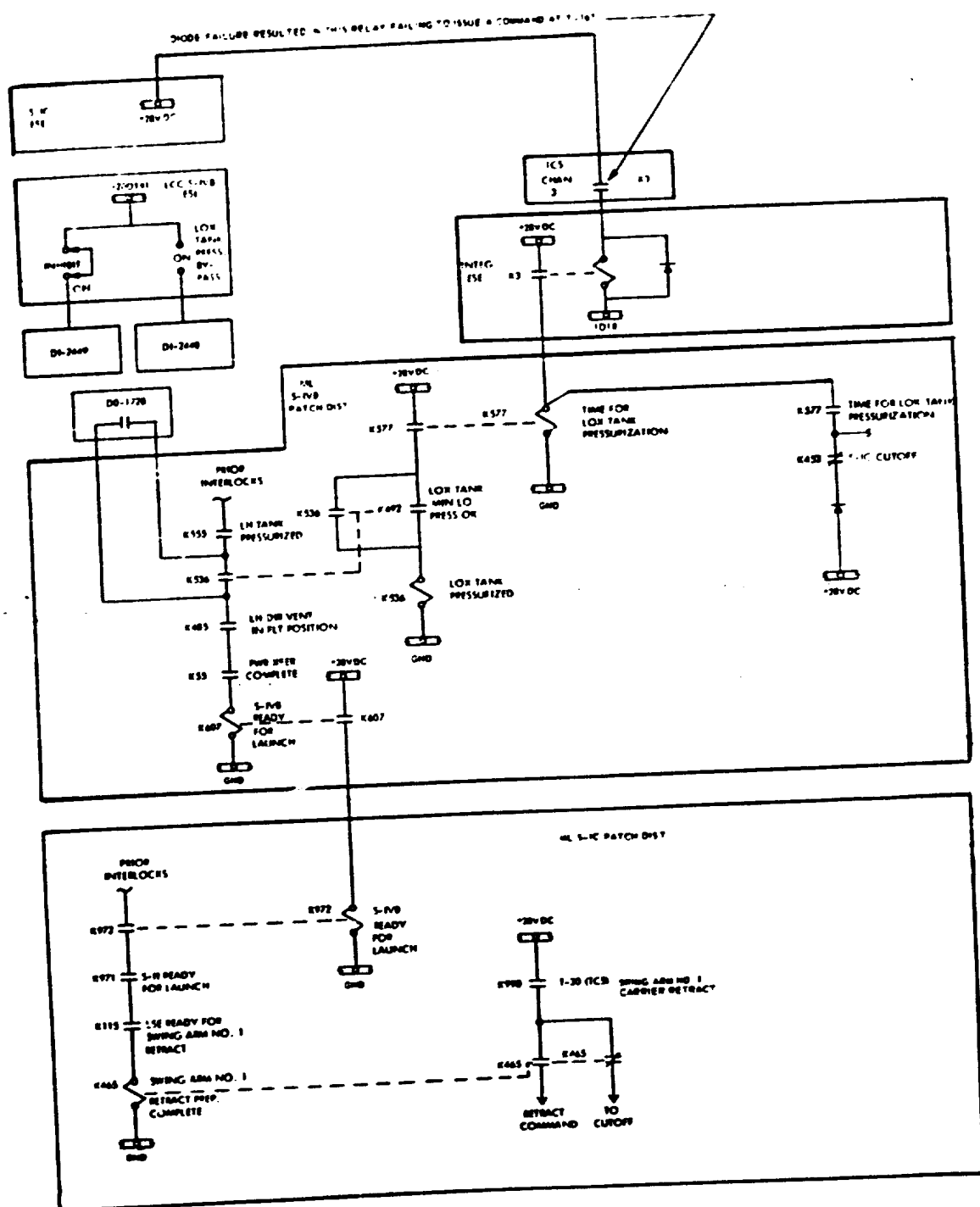


Figure 3-1. Electrical Support Equipment Partial Schematic

relay K492 "LOX Tank Minimum Low Pressure OK" is energized by manually pressurizing the LOX tank. When K536 is not energized the "S-IVB Ready for Launch" relay K607 will not provide a signal to the ML S-IC Patch Distributor "S-IVB Ready for Launch" relay K972 to complete the interlock chain to allow relay K465 "Swing Arm No. 1 Retract Preparation Complete" to be energized. If K465 is not energized when the T-30 second TCS command (Swing Arm No. 1 Carrier Retract) is received, a cutoff command will be initiated and a countdown hold will occur.

When the above condition occurred, the absence of the TCS T-167 second command was confirmed on the Digital Events Evaluator-6 (DEE-6) printout. Investigation of the DEE-6 printout disclosed that the T-176 second spare output from the TCS also did not occur. After investigation of various combinations of lost outputs and associated fixes, it was determined that the "LOX Tank Pressurized" relay K536 could be bypassed by moving the "LOX Tank Pressurized Bypass" jumper from "INHIBIT" to "ON" position. This jumper is located on S-IVB Patch Distributor in the LCC. The failure was simulated and the "Work-Around" was verified at the MSFC Saturn V SDF and a decision was made to proceed with the launch using the interlock bypass and manual pressurization. During the successful launch all TCS outputs were obtained except the T-176 second spare output. Therefore, the bypass and manual pressurization procedures were actually redundant to the normal circuitry.

Investigation of this failure at KSC subsequently centered on two diodes located in the logic circuitry of the TCS. One of these diodes inhibited the T-167 second S-IVB LOX Tank Pressurization command and the other inhibited the spare output. The two failures are functionally unrelated in the TCS circuitry. Excessive reverse current leakage through the partially shorted diodes caused intermittent operation of TCS outputs. The two failed diodes had been in service six years. Each TCS contains 1,827 of these diodes with approximately 1500 of these capable of causing a launch hold or scrub if they failed between CDDT and launch.

Testing of all similar diodes is being conducted where feasible. Of 2196 diodes tested, 7 additional diodes exhibited reverse current leakage in excess of the specification. The diodes that failed along with a number of non-failed diodes from the same printed circuit boards were subjected to extensive analysis. The following four causes of failure have been postulated: 1) inversion layer formation, 2) accumulation layer formation, 3) metallic precipitates in the depletion layer or 4) contamination in cracks partially or completely across the depletion layer.

Since deposition of contamination in microscopic cracks (Figure 3-2) was consistently observed in the failed diodes, this is considered to be the most probable failure mode. However, the investigation as to the cause of the cracks and subsequent contamination deposition is still underway and cannot be considered conclusive at this time.

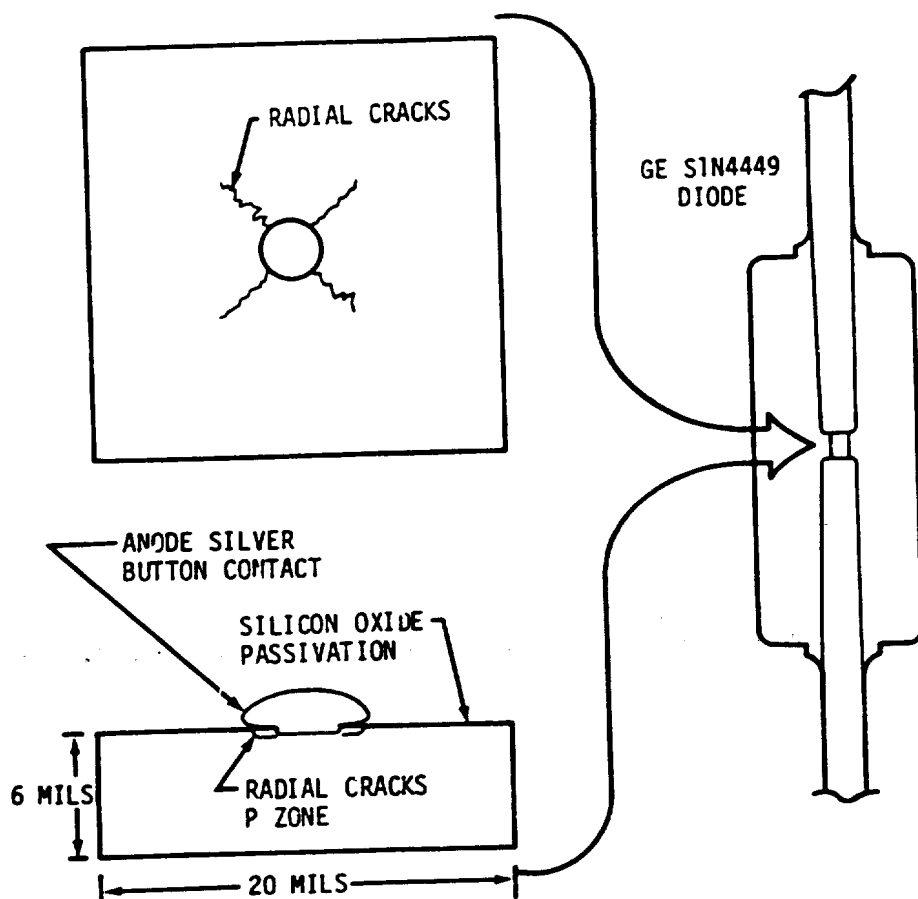


Figure 3-2. Diode Chip Detail

The "Work-Around" with the TCS at KSC that resulted in a satisfactory terminal countdown would not be acceptable if a problem occurred with the TCS during the Skylab-2, -3, and -4 countdowns due to the short launch windows.

The following activities will be accomplished prior to the Skylab launches in order to eliminate the possibility of another failure.

- a. The diodes will be tested and replaced as required in each of the existing TCS's to assure reliable performance.
- b. Pad 39A and Pad 39B will be modified to provide three TCS's in each launch vehicle ESE rather than the present one.
- c. Incorporate voting logic so that any two of the three TCS's will assure that the proper signals are provided.
- d. All unused signals from each TCS will be unpatched and grounded so there will be no possibility of them causing problems.

The above activities will reduce the probability of a false command being initiated and also assure that no single electrical failure will result in loss of the proper terminal countdown command.

3.4 PROPELLANT LOADING

3.4.1 RP-1 Loading

The RP-1 system successfully supported countdown and launch without incident. Tail Service Mast (TSM) 1-2 fill and replenish was accomplished at T-13 hours and S-IC level adjust and fill line inert occurred at about T-60 minutes. Both operations were satisfactory, there were no failures or anomalies. Launch countdown support consumed 213,304 gallons of RP-1.

3.4.2 LOX Loading

The LOX system supported countdown and launch satisfactorily. The fill sequence began with S-IVB fill command at 12:34 EST, December 6, 1972, and was completed 2 hours 40 minutes later with all stage replenish normal at 15:15 EST. Replenishment was automatic through the first Terminal Countdown Sequence but was switched to manual when S-IVB flight mass began cycling shortly before final countdown. This condition has been experienced during some previous loading operations and is a result of trapped LOX warming in the S-IVB inlet line. The LH₂/LOX Auto Load allows for manual replenishment when such cycling occurs.

When LOX loading was reinitiated shortly before recycling to T-22 minutes, LOX system logic did not reestablish replenish operations as

expected. Instead, it sequenced into a dual mode configuring simultaneously for both "vehicle replenishment" and "S-IC chilldown." In this posture, the S-IC slow fill valve was opened allowing LOX to be pumped directly into the stage resulting in a slight overfill. The system was manually reverted to prevent further overfill. Subsequent investigation revealed that an S-IC discrete necessary for normal replenishment was missing when loading operations were resumed.

A real time procedure change to LOX/LH₂ auto load, was prepared to initiate the discrete manually. Replenishment operations were reinitiated and continued normally through launch. This procedure change, which requires manual issue of Propellant Tanking Computer System (PTCS) discretes if tank level is at or above 98%, will prevent problem recurrence.

LOX consumption during launch countdown was 618,000 gallons.

3.4.3 LH₂ Loading

The LH₂ system successfully supported countdown and launch. The fill sequence began with start of S-II loading at 15:27 EST, December 6, 1972, and was completed 25 minutes later when all stage replenish was established at 16:52 EST. S-II replenish was automatic until terminated at initiation of the Terminal Countdown Sequencer. Intermittent overfill indications were experienced after S-IVB auto replenish was achieved and had to be inhibited to avoid unnecessarily cycling the replenish valve. S-IVB replenish was switched to manual at T-1 hour and left in that mode through start of Terminal Countdown Sequencer at T-187 seconds.

During recycle operations at T-30 seconds the LH₂ system was reverted normally. Fill operations were reestablished when count was resumed and both stages replenished normally to flight mass.

Launch countdown support consumed about 520,000 gallons of LH₂.

3.5 GROUND SUPPORT EQUIPMENT

3.5.1 Ground/Vehicle Interface

In general, performance of the ground service systems supporting all stages of the launch vehicle was satisfactory. Overall damage to the pad, LUT, and support equipment from blast and flame impingement was considered minimal.

The PTCS adequately supported all countdown operations and there was no damage or system failures.

The Environmental Control System (ECS) successfully supported the AS-512 countdown. All specifications for ECS flow rates, temperatures, and pressures were met and flow/pressure criteria were satisfactory during

the air to GN_2 changeover.

At T-48 hours, ECS chiller No. 1 shut down due to a low refrigerant charge. The redundant chillers were placed in operation and Freon added to chiller No. 1. No impact resulted.

At T-2 minutes the S-IC forward lower compartment temperature indication became inoperative. Redundant measurement systems were utilized and no impact resulted.

The Holddown Arms and Service Arm Control Switches (SACS) satisfactorily supported countdown and launch. All Holddown Arms released pneumatically within a six (6) millisecond period. The retraction and explosive release lanyard pull was accomplished in advance of ordnance actuation with a 42 millisecond margin. Pneumatic release valves 1 and 2 opened within 21 milliseconds after SACS armed signal. The SACS primary switches closed simultaneously at 449 milliseconds after commit. SACS secondary switches closed 1.154 and 1.163 seconds after commit.

Overall performance of the Tail Service Masts was satisfactory. Mast retraction times were nominal; 2.760 seconds for TSM 1-2, 1.980 seconds for TSM 3-2 and 2.685 seconds for TSM 3-4, measured from umbilical plate separation to mast retracted.

The preflight and inflight Service Arms (S/A's 1 through 8) supported the countdown in a satisfactory manner. Performance was nominal during terminal count and liftoff.

The DEE-3 system adequately supported all countdown operations. A discrepant printed circuit board was replaced in the FR 1 subsystem and a failed vacuum motor was replaced in the Pad A DEE-3D magnetic tape station. The Pad A DEE-3F magnetic tape station became inoperative subsequent to the propellant loading operations. The remainder of the countdown was supported by backup tape and line printer recordings. There was no launch damage.

3.5.2 MSFC Furnished Ground Support Equipment

Other than the TCS anomaly discussed in Section 3.3, the MSFC furnished electrical and mechanical ground support equipment successfully supported the Apollo 17 launch.

SECTION 4

TRAJECTORY

4.1 SUMMARY

The vehicle was launched on an azimuth 90 degrees east of north. A roll maneuver was initiated at 13.0 seconds that placed the vehicle on a flight azimuth of 91.504 degrees east of north. In accordance with preflight targeting objectives, the translunar injection maneuver shortened the translunar coast period by 2 hours and 40 minutes to compensate for the launch delay so that the lunar landing could be made with the same lighting conditions as originally planned. The reconstructed trajectory was generated by merging the following four trajectory segments: the ascent phase, the parking orbit phase, the injection phase, and the early translunar orbit phase. The analysis for each phase was conducted separately with appropriate end point constraints to provide trajectory continuity. Available C-Band radar and Unified S-Band (USB) tracking data plus telemetered guidance velocity data were used in the trajectory reconstruction.

The trajectory variables from launch to Command and Service Module (CSM) separation are discussed below and, in general, were close to nominal. Because the S-II Outboard Engine Cutoff velocity was higher than nominal, earth parking orbit insertion conditions were achieved 4.08 seconds earlier than nominal. Translunar Injection (TLI) conditions were achieved 2.11 seconds later than nominal with altitude 5.8 kilometers greater than nominal and velocity 5.1 meters per second less than nominal. CSM separation was Commander initiated 57.9 seconds earlier than nominal resulting in an altitude 306.1 kilometers less than nominal and velocity 91.7 meters per second greater than nominal.

4.2 TRAJECTORY EVALUATION

4.2.1 Ascent Phase

The ascent phase spans the interval from guidance reference release through parking orbit insertion. The ascent trajectory was established by using telemetered guidance velocity data as generating parameters to fit tracking data from six C-Band stations (Mer. itt Island, Patrick Air Force Base, Grand Turk, Bermuda FPQ-6, Bermuda FPS-16M and Antigua) and two S-Band stations (Merritt Island and Bermuda). Approximately 13 percent of the C-Band tracking data and 42 percent of the S-Band tracking data were not used because of inconsistencies. These values are consistent with past experience. The launch portion of the ascent phase (lift-off to approximately 20 seconds) was established by constraining integrated telemetered guidance accelerometer data to the best estimate trajectory.

Actual and nominal altitude, surface range, and crossrange for the ascent phase are presented in Figure 4-1. Actual and nominal space-fixed velocity and flight path angle during ascent are shown in Figure 4-2. Actual and nominal comparisons of total non-gravitational accelerations are shown in Figure 4-3. The maximum acceleration during S-IC burn was 3.87 g.

Mach number and dynamic pressure are shown in Figure 4-4. These parameters were calculated using meteorological data measured to an altitude of 58.3 kilometers (31.5 n mi). Above this altitude, the measured data were merged into the U.S. Standard Reference Atmosphere.

Actual and nominal values of parameters at significant trajectory event times, cutoff events, and separation events are shown in Tables 4-1, 4-2, and 4-3, respectively. All trajectory parameters were close to nominal throughout ascent. The space-fixed velocity was 25.6 m/s (84.0 ft/s) higher than predicted at the end of S-II powered flight. This difference is somewhat greater than usual and is discussed in Section 6.3.

4.2.2 Parking Orbit Phase

Orbital tracking was accomplished by the NASA Manned Space Flight Network. Three C-Band stations (Merritt Island, Antigua and Carnarvon) provided four data passes. Six S-Band stations (Goldstone, Bermuda, Texas, Merritt Island, Hawaii and Ascension) furnished eight additional tracking passes.

Velocity data generated by the ST-124M guidance platform were used to derive the orbital non-gravitational acceleration (venting) model. The parking orbit trajectory was obtained by integrating a comprehensive force model (gravity plus venting) with corrected insertion conditions forward to T6 at 10,978.65 seconds (03:02:58.65). The insertion conditions were obtained by using the force model and a differential correction procedure to fit the available tracking data.

A comparison of actual and nominal parking orbit insertion parameters is presented in Table 4-4. The groundtrack from insertion to S-IVB/CSM separation is given in Figure 4-5. All orbital trajectory variables were close to nominal.

4.2.3 Injection Phase

The injection phase spans the interval from T6 to TLI and was established in two parts (T6 to 11,500 seconds and 11,500 seconds to TLI). The first part was obtained by fitting data available from one C-Band station (Carnarvon) and three S-Band stations (Texas, Goldstone, and Merritt Island). The second part was obtained by integrating a state vector taken from the first part at 11,500 seconds (03:11:40) through second burn and constraining the integration to a final TLI state vector taken from the early translunar orbit trajectory. Telemetered guidance velocity data were used as generating parameters for both parts.

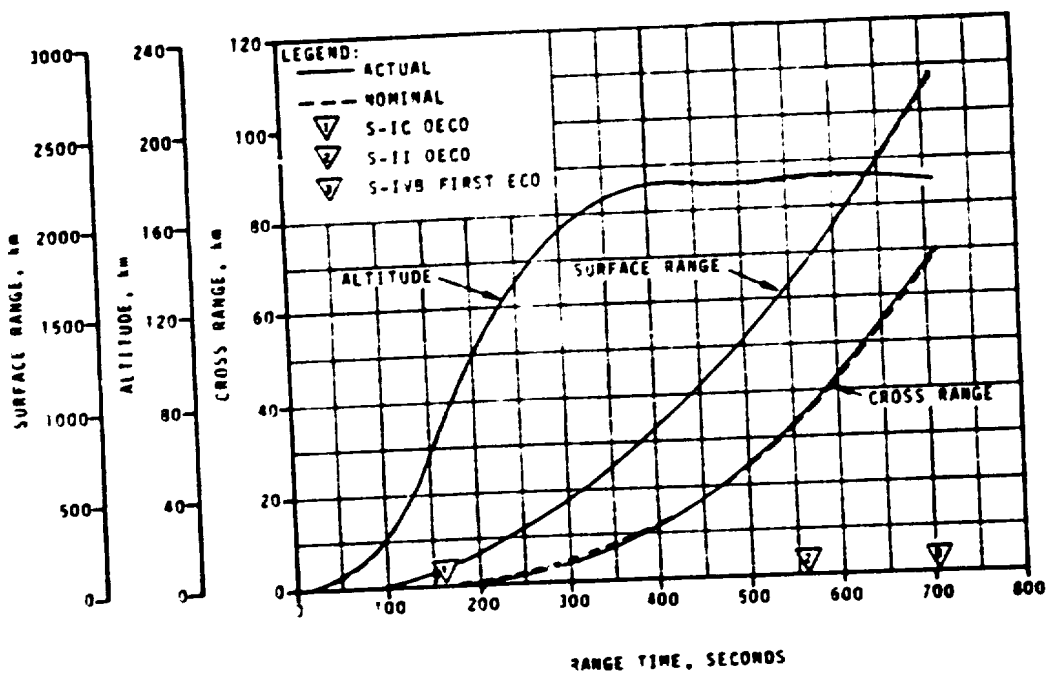


Figure 4-1. Ascent Trajectory Position Comparison

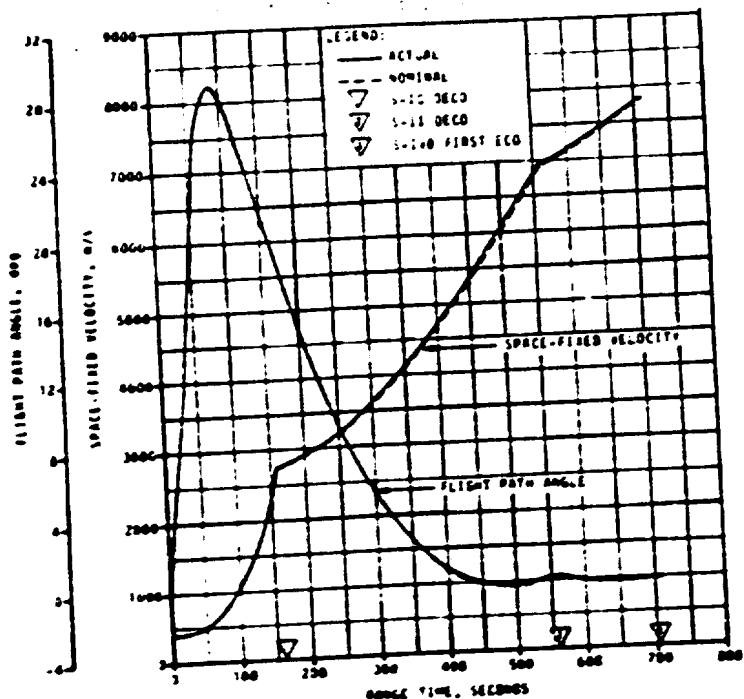


Figure 4-2. Ascent Trajectory Space-Fixed Velocity and Flight Path Angle Comparisons

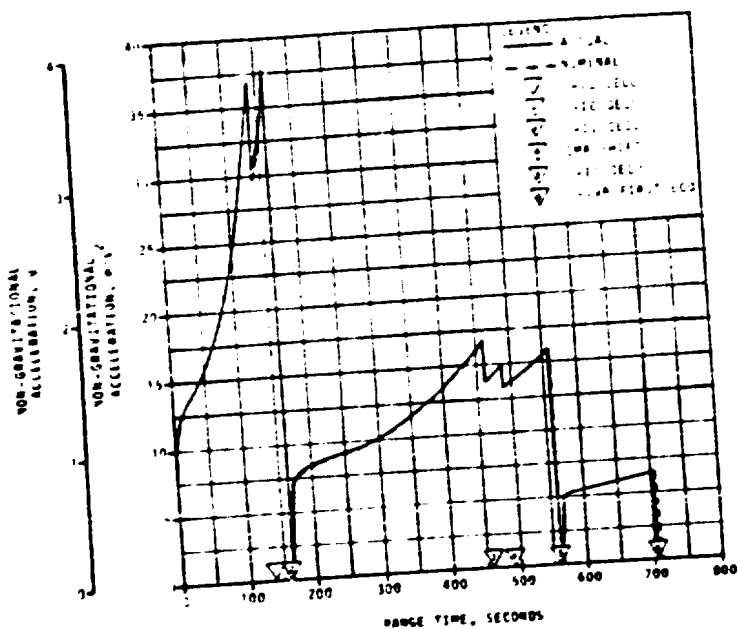


Figure 4-3. Ascent Trajectory Acceleration Comparison

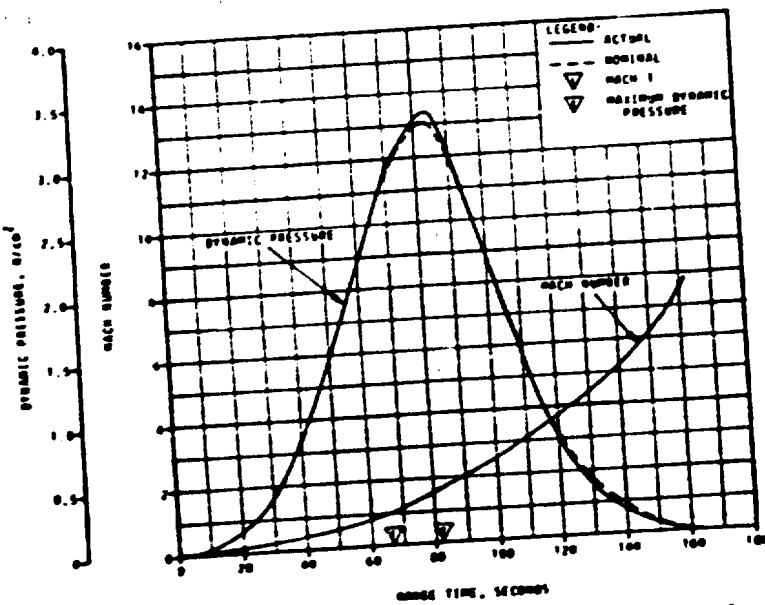


Figure 4-4. Dynamic Pressure and Mach Number Comparisons

Table 4-1. Comparison of Significant Trajectory Events

EVENT	PARAMETER	ACTUAL	NOMINAL	ACT-NOM
First Motion	Range Time, sec	0.24	0.24	0.00
	Total Non-Gravitational Acceleration, m/s^2 (ft/s 2) (g)	10.60 (34.70) (1.08)	10.55 (34.61) (1.08)	0.05 (0.17) (0.00)
Mach 1	Range Time, sec	67.5	67.4	0.1
	Altitude, km (nm)	8.0 (4.3)	7.9 (4.3)	0.1 (0.0)
Maxima Dynamic Pressure	Range Time, sec	82.5	83.5	-1.0
	Dynamic Pressure, n/cg^2 (lbf/ft 2)	3.36 (701.75)	3.27 (682.95)	0.09 (18.00)
	Altitude, km (nm)	13.1 (7.1)	13.3 (7.21)	-0.2 (-0.1)
Maxima Total Non-Gravitational Acceleration: S-1F	Range Time, sec	161.20	139.34	21.86
	Acceleration, m/s^2 (ft/s 2) (g)	37.95 (124.51) (3.82)	37.19 (122.01) (3.79)	0.76 (2.50) (0.00)
S-1I	Range Time, sec	461.21	461.60	-0.37
	Acceleration, m/s^2 (ft/s 2) (g)	17.07 (56.00) (1.74)	16.97 (55.68) (1.73)	0.10 (0.32) (0.91)
S-IVB First Burn	Range Time, sec	702.66	706.74	-4.08
	Acceleration, m/s^2 (ft/s 2) (g)	6.54 (21.86) (0.67)	6.62 (21.72) (0.68)	-0.08 (-0.26) (-0.01)
S-IVB Second Burn	Range Time, sec	11,907.65	11,905.54	2.11
	Acceleration, m/s^2 (ft/s 2) (g)	13.86 (45.47) (1.41)	14.10 (46.26) (1.44)	-0.24 (-0.79) (-0.03)
Maxima Earth-Fixed Velocity: S-IC	Range Time, sec	162.00	163.38	-1.38
	Velocity, m/s (ft/s)	2,376.4 (7,790.0)	2,362.0 (7,752.0)	11.6 (38.0)
S-II	Range Time, sec	560.60	561.14	-0.54
	Velocity, m/s (ft/s)	6,573.8 (21,567.6)	6,548.2 (21,483.6)	25.6 (84.0)
S-IVB First Burn	Range Time, sec	712.66	716.74	-4.08
	Velocity, m/s (ft/s)	7,385.6 (24,231.0)	7,385.9 (24,232.0)	-0.3 (-1.0)
S-IVB Second Burn	Range Time, sec	11,908.50	11,905.79	2.71
	Velocity, m/s (ft/s)	10,425.2 (34,203.6)	10,429.5 (34,217.5)	-4.3 (-14.1)

a Shortest Time Points Available

Table 4-2. Comparison of Cutoff Events

PARAMETER	ACTUAL	NOMINAL	ACT-NOM	ACTUAL	NOMINAL	ACT-NOM
	S-IC CECD (ENGINE SOLENOID)			S-IC DECO (ENGINE SOLENOID)		
S-IC CECD (ENGINE SOLENOID)						
Range Time, sec	139.30	139.34	-0.04	161.20	161.67	-0.47
Altitude, km (nm)	67.0 (24.6)	66.8 (25.3)	-0.2 (-0.1)	66.5 (35.9)	66.7 (36.0)	-0.2 (-0.1)
Space-Fixed Velocity, m/s (ft/s)	2,001.0 (62.9)	2,005.3 (63.5)	-0.3 (-0.1)	2,766.9 (9,912.1)	2,764.9 (9,005.6)	2.0 (-6.5)
Flight Path Angle, deg	23.199	23.296	-0.097	-0.829	20.473	-0.044
Heading Angle, deg	91.355	91.553	-0.198	-21.7	91.6 (89.5)	-0.6 (-0.4)
Surface Range, km (nm)	51.5 (27.8)	51.5 (27.8)	0.0 (0.0)	31.7 (49.1)	31.6 (49.5)	-0.1 (-0.4)
Cross Range, km (nm)	0.2 (0.1)	0.3 (0.2)	-0.1 (-0.1)	0.3 (0.2)	0.6 (0.3)	-0.3 (-0.1)
Cross Range Velocity, m/s (ft/s)	1.5 (4.9)	8.2 (26.9)	-6.7 (-22.0)	6.4 (21.0)	10.1 (46.3)	-7.7 (-25.3)
S-II DECO (ENGINE SOLENOID)						
Range Time, sec	461.21	461.68	-0.47	559.66	560.13	-0.47
Altitude, km (nm)	173.0 (93.4)	172.7 (93.3)	0.3 (-0.1)	172.6 (93.2)	172.1 (92.9)	0.5 (0.3)
Space-Fixed Velocity, m/s (ft/s)	5,620.4 (18,439.6)	5,601.4 (18,377.3)	19.0 (-62.3)	6,990.1 (22,933.4)	6,964.5 (22,849.4)	25.6 (-84.0)
Flight Path Angle, deg	-0.058	-0.005	0.027	0.254	0.247	0.007
Heading Angle, deg	97.647	97.571	0.076	100.395	100.333	0.062
Surface Range, km (nm)	1,095.0 (591.3)	1,093.0 (590.2)	2.0 (-1.1)	1,657.6 (895.0)	1,653.6 (892.9)	4.0 (2.1)
Cross Range, km (nm)	18.6 (10.0)	18.9 (10.2)	-0.3 (-0.2)	34.8 (18.0)	34.4 (18.6)	0.4 (0.2)
Cross Range Velocity, m/s (ft/s)	135.8 (444.2)	128.5 (421.6)	6.9 (22.6)	194.9 (639.4)	188.9 (619.0)	6.0 (19.6)
S-IIB 1ST GUIDANCE CUTOFF SIGNAL						
Range Time, sec	702.69	706.74	-4.05	11,907.64	11,905.54	2.10
Altitude, km (nm)	170.5 (92.1)	170.4 (92.0)	0.1 (-0.1)	300.9 (162.0)	294.5 (159.0)	5.5 (3.0)
Space-Fixed Velocity, m/s (ft/s)	7,002.3 (25,598.1)	7,002.6 (25,599.1)	-0.3 (-1.0)	10,644.6 (35,579.4)	10,849.3 (35,594.0)	-4.7 (-15.4)
Flight Path Angle, deg	0.001	-0.002	0.003	6.930	6.706	0.144
Heading Angle, deg	104.718	104.700	-0.062	118.046	117.967	0.079
Surface Range, km (nm)	2,625.2 (1,417.9)	2,643.7 (1,427.5)	-18.5 (-10.0)			
Cross Range, km (nm)	67.4 (36.4)	67.2 (36.3)	0.2 (-0.1)			
Cross Range Velocity, m/s (ft/s)	263.1 (856.6)	259.7 (852.0)	1.4 (-0.6)	28.673	28.423	0.050
Inclination, deg				86.061	86.149	-0.088
Descending Slope, deg				0.9707	0.9700	-0.0001
Eccentricity $e_3 \frac{m^2/s^2}{ft^2/s^2}$				-1,773.210 (-19,896.760)	-1,769.210 (-19,844.694)	-3.908 (-42.066)

Table 4-3. Comparison of Separation Events

PARAMETER	ACTUAL	NOMINAL	ACT-NOM
S-IC/S-II SEPARATION			
Range Time, sec	162.9	163.4	-0.5
Altitude, km (nmi)	68.1 (36.6)	68.4 (36.7)	-0.3 (-0.1)
Space-Fixed Velocity, m/s (ft/s)	2,754.2 (9,036.1)	2,751.7 (9,027.9)	2.5 (0.2)
Flight Path Angle, deg	20.151	20.208	-0.057
Heading Angle, deg	91.741	91.915	-0.174
Surface Range, km (nmi)	94.7 (51.1)	95.3 (51.5)	-0.6 (-0.4)
Cross Range, km (nmi)	0.3 (0.2)	0.6 (0.3)	-0.3 (-0.1)
Cross Range Velocity, m/s (ft/s)	6.7 (22.0)	14.5 (47.6)	-7.8 (-25.6)
Geodetic Latitude, deg N	28.580	28.577	0.003
Longitude, deg E	-79.637	-79.630	-0.007
S-II/S-IVB SEPARATION			
Range Time, sec	560.6	561.1	-0.5
Altitude, km (nmi)	172.6 (93.2)	172.1 (92.9)	0.5 (0.3)
Space-Fixed Velocity, m/s (ft/s)	6,992.8 (22,942.3)	6,967.2 (22,858.3)	(25.6) (84.0)
Flight Path Angle, deg	0.244	0.236	0.008
Heading Angle, deg	100.424	100.365	0.060
Surface Range, km (nmi)	1,663.6 (898.3)	1,660.1 (896.4)	3.5 (1.9)
Cross Range, km (nmi)	35.0 (18.9)	34.6 (18.7)	0.4 (0.2)
Cross Range Velocity, m/s (ft/s)	195.3 (640.7)	189.3 (621.1)	6.0 (19.6)
Geodetic Latitude, deg N	26.865	26.874	-0.009
Longitude, deg E	-63.831	-63.866	0.035
S-IVB/CSM SEPARATION			
Range Time, sec	13,347.6	13,405.5	-57.9
Altitude, km (nmi)	6,606.4 (3,567.2)	6,912.5 (3,732.5)	-306.1 (-165.3)
Space-Fixed Velocity, m/s (ft/s)	7,724.7 (25,343.5)	7,633.0 (25,042.7)	91.7 (300.8)
Flight Path Angle, deg	44.180	44.847	-0.667
Heading Angle, deg	102.797	102.166	0.631
Geodetic Latitude, deg N	-25.716	-25.944	0.228
Longitude, deg E	11.300	13.161	-1.261

Table 4-4. Parking Orbit Insertion Conditions

PARAMETER	ACTUAL	NOMINAL	ACT-NOM
Range Time, sec	712.66	716.74	-4.08
Altitude, km (nmi)	170.5 (92.1)	170.3 (92.0)	0.2 (0.1)
Space-Fixed Velocity, m/s (ft/s)	7,804.1 (25,604.0)	7,804.3 (25,604.7)	-0.2 (-0.7)
Flight Path Angle, deg	0.003	-0.001	0.004
Heading Angle, deg	105.021	105.082	-0.061
Inclination, deg	28.526	28.524	0.002
Descending Node, deg	86.978	87.024	-0.046
Eccentricity	0.0000	0.0001	-0.0001
Apogee, km (nmi)	167.2 (90.3)	167.4 (90.4)	-0.2 (-0.1)
Perigee, km (nmi)	166.6 (90.0)	166.6 (90.0)	0.0 (0.0)
Period, min	87.83	87.83	0.00
Geodetic Latitude, deg N	24.680	24.642	0.038
Longitude, deg E	-53.810	-53.633	0.177

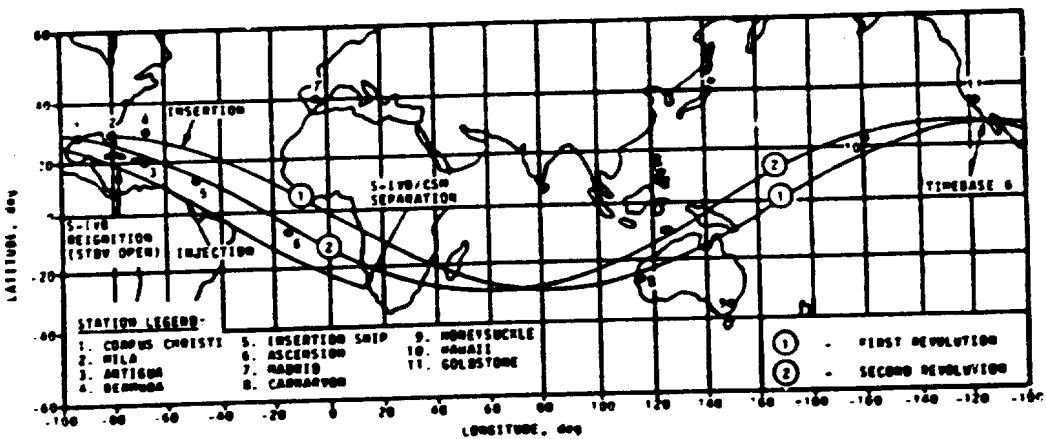


Figure 4-5. Launch Vehicle Groundtrack

Comparisons between the actual and nominal space-fixed velocity and flight path angle are shown in Figure 4-6. The actual and nominal total non-gravitational acceleration comparisons are presented in Figure 4-7. The lower than nominal velocity and acceleration shown in Figures 4-6 and 4-7, respectively, are due to the heavier S-IVB stage resulting from the 4.08 seconds early first S-IVB cutoff. The actual and nominal S-IVB second guidance cutoff conditions are presented in Table 4-2. The slightly longer than nominal burn compensated for the heavier S-IVB stage and resulted in near nominal conditions at cutoff.

4.2.4 Early Translunar Orbit Phase

The early translunar orbit trajectory spans the interval from translunar injection to S-IVB/CSM separation. Tracking data from one C-Band station (Carnarvon) and one S-Band station (Ascension) were fitted using the procedure outlined in 4.2.2. The actual and nominal translunar injection conditions are compared in Table 4-5. The S-IVB/CSM separation conditions are presented in Table 4-3. The large differences at CSM separation were due to the earlier than nominal separation time which was Commander initiated.

Table 4-5. Translunar Injection Conditions

PARAMETER	ACTUAL	NOMINAL	ACT-NOM
Range Time, sec	11,917.65	11,915.54	2.11
Altitude, km (nm)	313.5 (169.3)	307.7 (166.1)	5.8 (3.2)
Space-Fixed Velocity, m/s (ft/s)	10,837.0 (35,554.5)	10,842.1 (35,571.2)	-5.1 (-16.7)
Flight Path Angle, deg	7.384	7.240	0.144
Heading Angle, deg	118.116	118.039	0.077
Inclination, deg	28.474	28.423	0.051
Descending Node, deg	86.061	86.149	-0.088
Eccentricity	0.9720	0.9721	-0.0001
$C_3, \frac{m^2}{s^2}$ ($\frac{ft^2}{s^2}$)	-1,695.985 (-18,255,431)	-1,689.026 (-18,180,525)	-6,959 (-74,906)

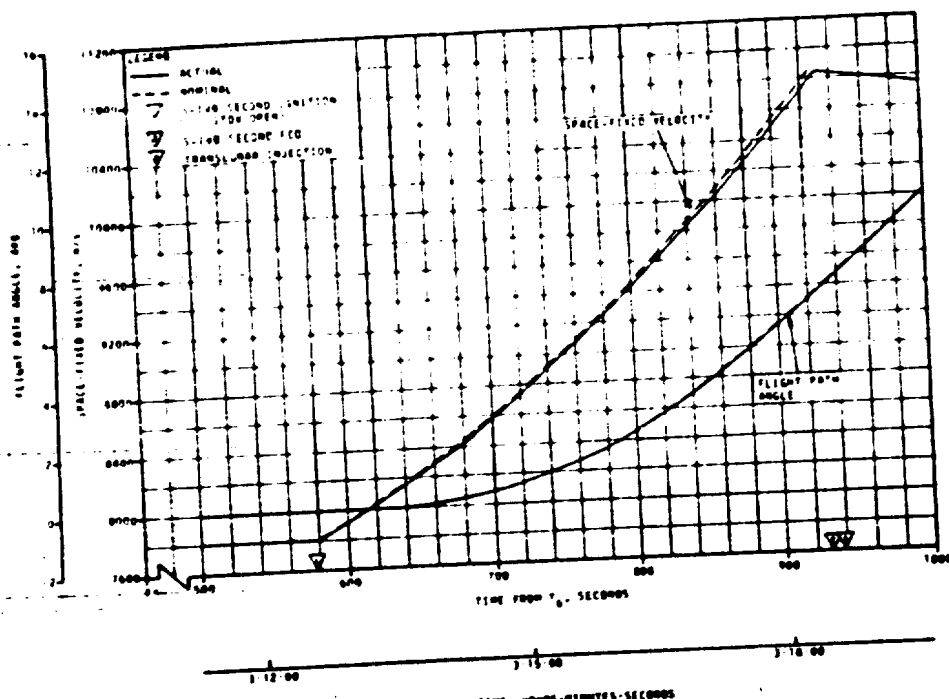


Figure 4-5. Injection Phase Space-Fixed Velocity and Flight Path Angle Comparisons

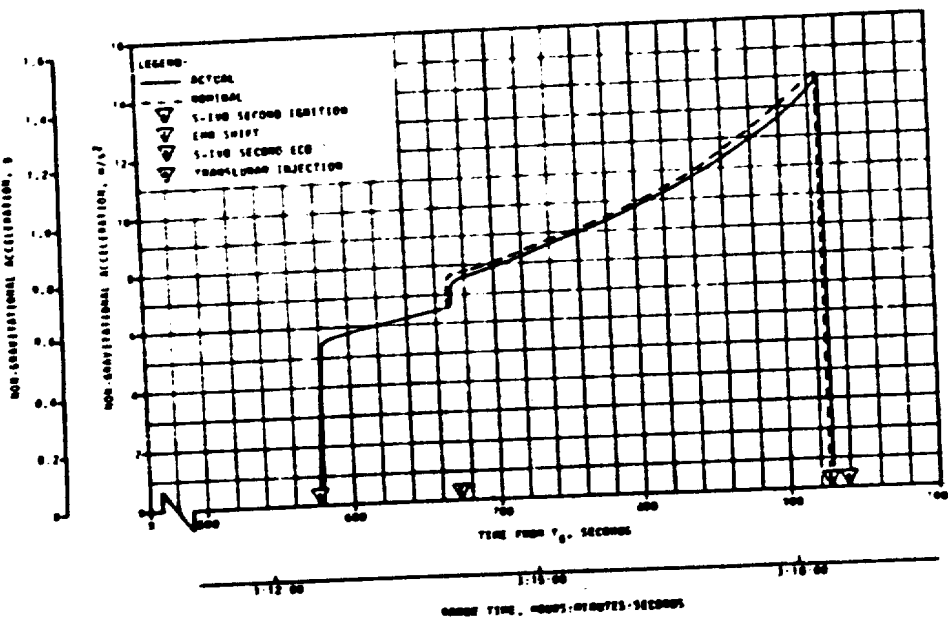


Figure 4-7. Injection Phase Acceleration Comparison

SECTION 5

S-IC PROPULSION

5.1 SUMMARY

All S-IC propulsion systems performed satisfactorily. In all cases, the propulsion performance was very close to the predicted nominal. Overall stage site thrust was 0.30 percent higher than predicted. Total propellant consumption rate was 0.16 percent higher than predicted and the total consumed mixture ratio was 0.002 percent higher than predicted. Specific impulse was 0.14 percent higher than predicted. Total propellant consumption from Holdown Arm (HDA) release to Outboard Engines Cutoff (OECO) was low by 0.14 percent.

Center Engine Cutoff (CECO) was initiated by the Instrument Unit (IU) at 139.30 seconds, 0.02 seconds earlier than planned. OECO was initiated by the fuel depletion sensors at 161.20 seconds, 0.47 seconds earlier than predicted. This is well within the +5.99, -4.22 second 3-sigma limits. At OECO, the LOX residual was 36,479 lbm compared to the predicted 37,235 lbm and the fuel residual was 26,305 lbm compared to the predicted 29,956 lbm.

The S-IC hydraulic system performed satisfactorily.

5.2 S-IC IGNITION TRANSIENT PERFORMANCE

The fuel pump inlet prestart pressure of 45.3 psia was within the F-1 engine acceptable starting region of 43.3 to 110 psia.

The LOX pump inlet prestart pressure and temperature were 81.3 psia and -287.3°F and were within F-1 engine acceptable starting region, as shown by Figure 5-1.

The planned 1-2-2 F-1 Engine start sequence (Engines 5, 3-1, 4-2) was not achieved. Two engines are considered to start together if both thrust chamber pressures reach 100 psig within 100 milliseconds. By this definition, the starting order was 2-1-1-1 (Engines 5-3, 1, 4, 2). The buildup times of all five engines as measured from engine control valve open signal to 100 psig chamber pressure, Table 5-1, were faster than predicted, although within specifications. The 2-1-1-1 start sequence had no adverse affect on either propulsion system performance or on the structure.

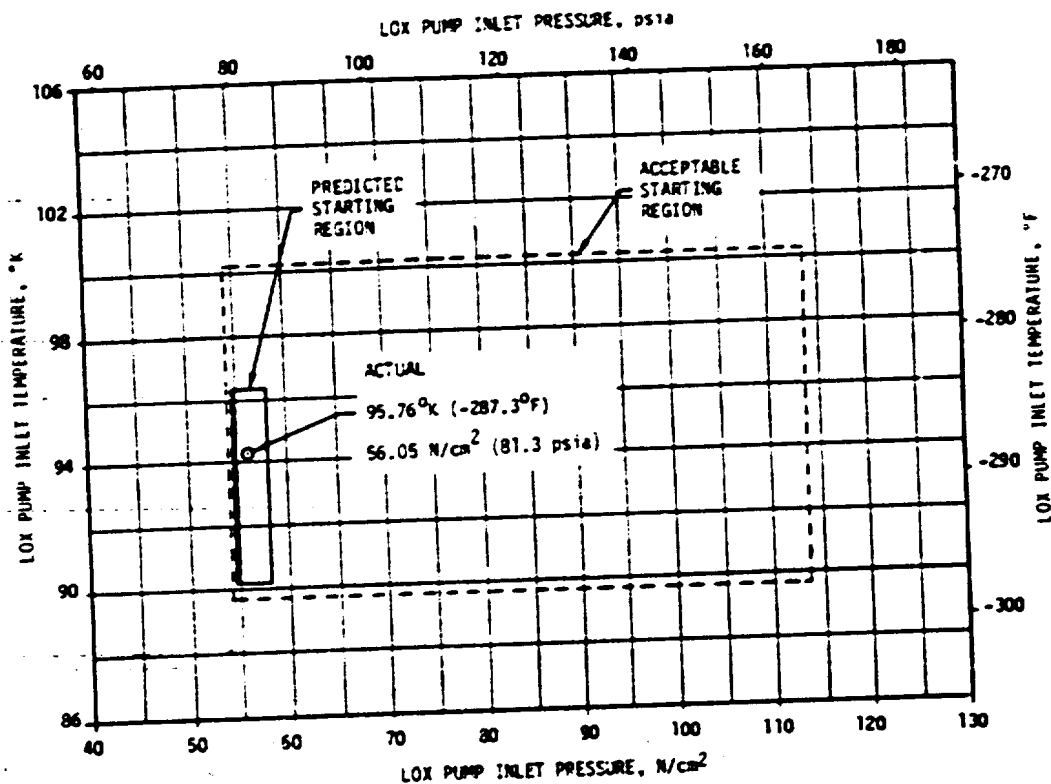


Figure 5-1. S-IC LOX Start Box Requirements

Table 5-1. F-1 Engine Systems Buildup Times

	BUILDUP TIME, SECONDS				
	ENGINE 1	ENGINE 2	ENGINE 3	ENGINE 4	ENGINE 5
Predicted*	4.057	3.365	3.925	3.990	3.933
Actual*	3.862	2.861	3.605	3.669	3.819
Difference	0.155	0.104	0.320	0.321	0.114
Direction	Fast	Fast	Fast	Fast	Fast

*Time from 4-way control valve open signal to 100 psig combustion chamber pressure
All times corrected to nominal prestart conditions

The desired 1-2-2 start sequence was also not achieved on flights AS-507, AS-508, and AS-510. The timing of the start signals to each engine is adjusted to achieve the desired start sequence and is based on data from individual engine firings and the single data sample in the stage environment obtained from static firing. Typically, a wide dispersion of start

times is observed at the stage static firing. This dispersion is attributed primarily to the differences between the stage conditions and single engine test stand conditions. Adjustments made between stage static firing and launch have been effective in reducing the dispersions substantially. However, it is apparent from review of data from all the Saturn V launches, that the system cannot be fine tuned accurately enough to consistently assure the desired start sequence within the 100 ms criterion. This fact is probably attributable to a combination of the limited data sample in the stage environment and typical engine start time dispersions even under controlled conditions.

The structural implications of a non-standard engine start sequence for the Skylab mission have been examined considering significantly larger dispersions than experienced on AS-512 and other Saturn V flights, and there is no concern. Accordingly, no modification of the present engine start sequence implementation is planned.

The reconstructed propellant consumption during holdown (from ignition command to holdown arm release) was 75,090 lbm LOX (67,031 lbm predicted) and 22,075 lbm fuel (18,764 lbm predicted). The greater than predicted propellant consumption during holdown was due to the faster engine start and longer burn before holdown release. The reconstructed propellant load at holdown arm release was 3,239,298 lbm LOX (3,243,932 lbm predicted) and 1,409,906 lbm fuel (1,415,766 lbm predicted).

Thrust buildup rates were as expected, as shown in Figure 5-2.

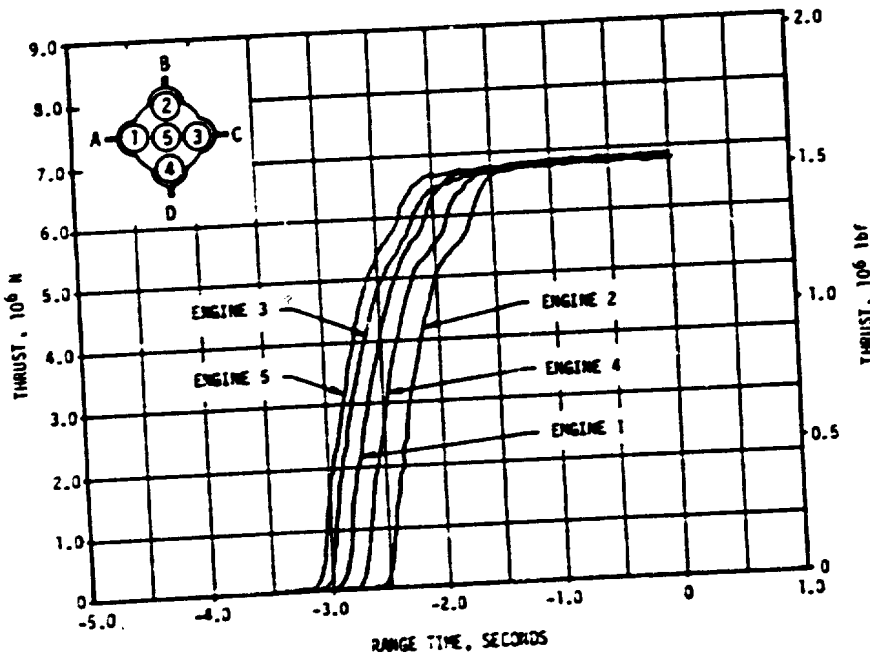


Figure 5-2. S-IC Engines Thrust Buildup

The engine Main Oxidizer Valve (MOV), Main Fuel Valve (MFV), and Gas Generator (GG) ball valve opening times were nominal.

5.3 S-IC MAINSTAGE PERFORMANCE

S-IC stage propulsion performance was satisfactory. Stage thrust, specific impulse, mixture ratio, and propellant flowrate were near nominal predictions as shown in Figure 5-3. The stage site thrust (averaged from time zero to OECO) was 0.30 percent higher than predicted. Total propellant consumption rate was 0.16 percent higher than predicted and the total consumed mixture ratio was 0.002 percent higher than predicted. The specific impulse was 0.14 percent higher than predicted. Total propellant consumption from HDA release to OECO was low by 0.14 percent.

For comparison of F-1 engine flight performance with predicted performance the flight performance has been analytically reduced to standard conditions and compared to the predicted performance which is based on ground firings and also reduced to standard conditions. These comparisons are shown in Table 5-2 for the 35 to 38-second time slice. The largest thrust deviation from the predicted value was -7 klbf for engine 2. Engines 1 and 5 had lower thrusts than predicted by 6 and 1 klbf, respectively. Engines 3 and 4 had higher thrust than predicted by 1 and 2 klbf, respectively. Total stage thrust was 11 Klbf lower than predicted for an average of -2.2 klbf/engine. These performance values are derived from a reconstruction math model that uses a chamber pressure and pump speed match.

An 11 Hz, 8 psi peak amplitude, oscillation was observed in the S-IC Engine No. 2 fuel suction line inlet pressure. This oscillation was also observed during S-IC-12 static test and disposed of at that time as no problem. This phenomenon is a self-induced oscillation characteristic of the F-1 fuel pump and has been observed on previous flights. The oscillation is Net Positive Suction Pressure (NPSP) dependent and its sensitivity varies from engine to engine. The stage accelerometer data are nominal at 11 Hz and comparable to that of previous flights, indicating the vehicle structural gain at this frequency is small.

The ambient gas temperature under Engine No. 1 cocoon increased shortly after liftoff and exceeded previous flight data from approximately 30 to 65 seconds by a maximum of about 13°C. After 100 seconds the temperature returned to a normal level and remained similar to the cocoon ambient temperature level for the other engines. The increase in the ambient gas temperature did not affect engine performance during flight. The two most probable causes of the temperature increase are: 1) a minor hot gas leakage from the Gas Generator drain port plug which subsequently sealed, 2) a temporary loss of cocoon insulation integrity (possible loose combustion drain access cover) which later corrected itself. Both of these possible causes for the cocoon ambient temperature rise are discussed in detail in Section 13.2 Vehicle Thermal Environment.

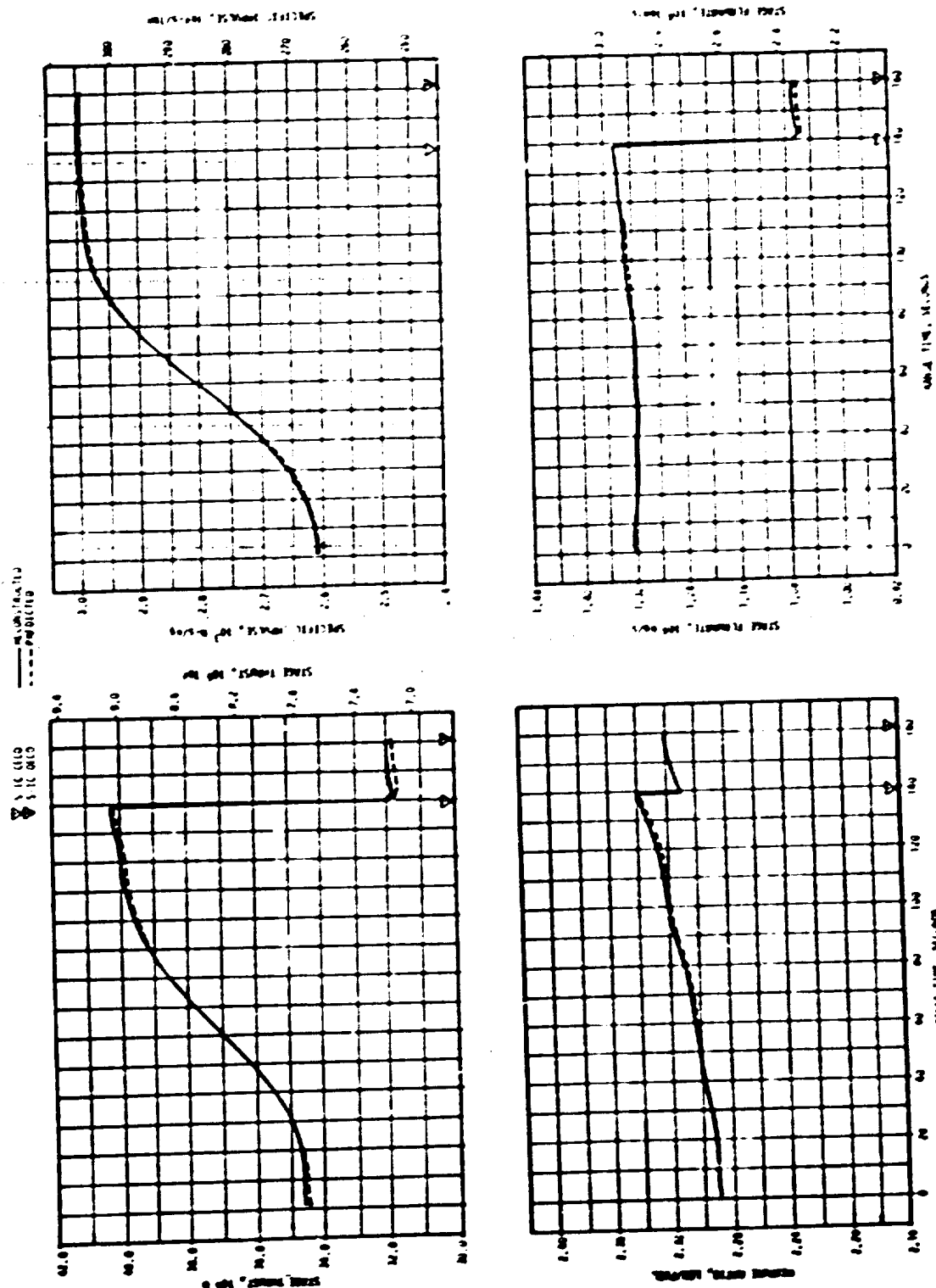


Figure 6-3. S-IC Stage Propulsion Performance

Table 5-2. S-IC Individual Standard Sea Level Engine Performance

PARAMETER	ENGINE	PREDICTED	RECONSTRUCTION ANALYSIS	DEVIATION PERCENT	STAGE DEVIATION PERCENT
T ₀₃ /T ₀₁	1522	1522	1516	-0.394	-0.145
	1522	1522	1515	-0.460	
	1522	1522	1523	0.066	
	1522	1522	1524	0.131	
	1522	1522	1521	-0.066	
	1522	1522	1522	0.023	
SPECIFIC IMPULSE 10 ³ ft/lbm	265.2	265.2	265.0	-0.075	
	265.9	265.9	265.7	-0.038	
	265.2	265.2	265.2	0	
	265.4	265.4	265.4	0	
	264.9	264.9	264.9	0	
TOTAL FLOWRATE lb/s	5741	5741	5722	-0.311	
	5745	5745	5702	-0.402	
	5739	5739	5742	0.052	
	5737	5737	5742	0.087	
	5746	5746	5741	0.087	
MIXTURE RATIO LOX/fuel	2.261	2.261	2.249	-0.131	
	2.287	2.287	2.284	-0.044	
	2.258	2.258	2.257	-0.132	
	2.266	2.266	2.263	-0.088	
	2.282	2.282	2.280	-0.107	

NOTE: Performance levels were reduced to standard sea level and pump inlet conditions.
Data were taken from the 35 to 36-second time slice.

5.4 S-IC ENGINE SHUTDOWNS: TRANSIENT PERFORMANCE

The F-1 engine thrust decay transient was nominal. The cutoff impulse, measured from cutoff signal to zero thrust, was 669,632 lbf-s for the center engine (0.1 percent less than predicted) and 2,593,423 lbf-s for all outboard engines (3.0 percent greater than predicted). The total stage cutoff impulse of 3,263,055 lbf-s was 2.3 percent greater than predicted.

Center engine cutoff was initiated by the IU at 139.30 seconds, 0.02 second earlier than planned. Cutoff signal to the outboard engines was initiated by fuel depletion and occurred 0.47 second earlier than the nominal predicted time of 161.67 seconds. The fuel depletion cutoff was caused by the higher than predicted fuel density due to chilldown of the fuel during the 2 hour 40 minute hold and the slightly higher than nominal batch fuel density for this flight. The early cutoff was due mainly to slightly higher than predicted stage site thrust (0.03 percent higher) and the accompanying higher propellant flowrates.

5.5 S-IC STAGE PROPELLANT MANAGEMENT

The S-IC stage does not have an active propellant utilization system. Minimum residuals are obtained by attempting to load the mixture ratio expected to be consumed by the engines plus the predicted unusable residuals. An analysis of the residuals experienced during a flight is a good measure of the performance of the passive propellant utilization system.

The residual LOX at OECN was 36,479 lbm compared to the predicted value of 37,235 lbm. The fuel residual at OECO was 26,305 lbm compared to the predicted value of 29,956 lbm. A summary of the propellants remaining at major event times is presented in Table 5-3.

5.6 S-IC PRESSURIZATION SYSTEMS

5.6.1 S-IC Fuel Pressurization System

The fuel tank pressurization system performed satisfactorily, keeping ullage pressure within acceptable limits during flight. Helium Flow Control Valves (HFCV) No. 1 through 4 opened as planned and HFCV No. 5 was not required.

The low flow prepressurization system was commanded on at -97.0 seconds. The low flow system was cycled on a second time at -3.1 seconds. High flow pressurization, accomplished by the onboard pressurization system, performed as expected. HFCV No. 1 was commanded on at -2.7 seconds and was supplemented by the ground high flow prepressurization system until umbilical disconnect.

Fuel tank ullage pressure was within the predicted limits throughout

Table 5-3. S-IC Propellant Mass History

EVENT	PREDICTED, LBM		LEVEL SENSOR DATA, LBM		RECONSTRUCTED, LBM (BEST ESTIMATE)	
	LOX	FUEL	LOX	FUEL	LOX	FUEL
Ignition Command	3,310,963	1,434,525	--	1,431,921	3,314,388	1,431,921
Holddown Arm Release	3,243,932	1,415,766	3,243,551	1,410,136	3,239,292	1,409,906
CECO	403,818	187,391	393,859	181,418	398,064	182,160
OECO	37,235	29,956	36,631	27,253	36,479	26,305
Separation	31,772	26,992	---	---	30,777	23,130
Zero Thrust	31,649	26,904	---	---	30,645	23,098

Predicted and reconstructed values do not include pressurization gas so they will compare with level sensor data.

flight as shown by Figure 5-4. HFCY No.'s 2, 3 and 4 were commanded open during flight by the switch selector within acceptable limits. Helium bottle pressure was 3000 psia at -2.8 seconds and decayed to 475 psia at OECO. Total helium flowrate was as expected.

Fuel pump inlet pressure was maintained above the required minimum Net Positive Suction Pressure (NPS) during flight.

5.6.2 S-IC LOX Pressurization System

The LOX pressurization system performed satisfactorily and all performance requirements were met. The ground prepressurization system maintained ullage pressure within acceptable limits until launch commit. The onboard pressurization system performed satisfactorily during flight.

The prepressurization system was initiated at -72.0 seconds. Ullage pressure increased to the prepressurization switch band and flow was terminated at -58.3 seconds. The low flow system was cycled on three additional times at -42.9, -26.8, and -5.4 seconds. At -4.7 seconds, the high flow system was commanded on and maintained ullage pressure within acceptable limits until launch commit.

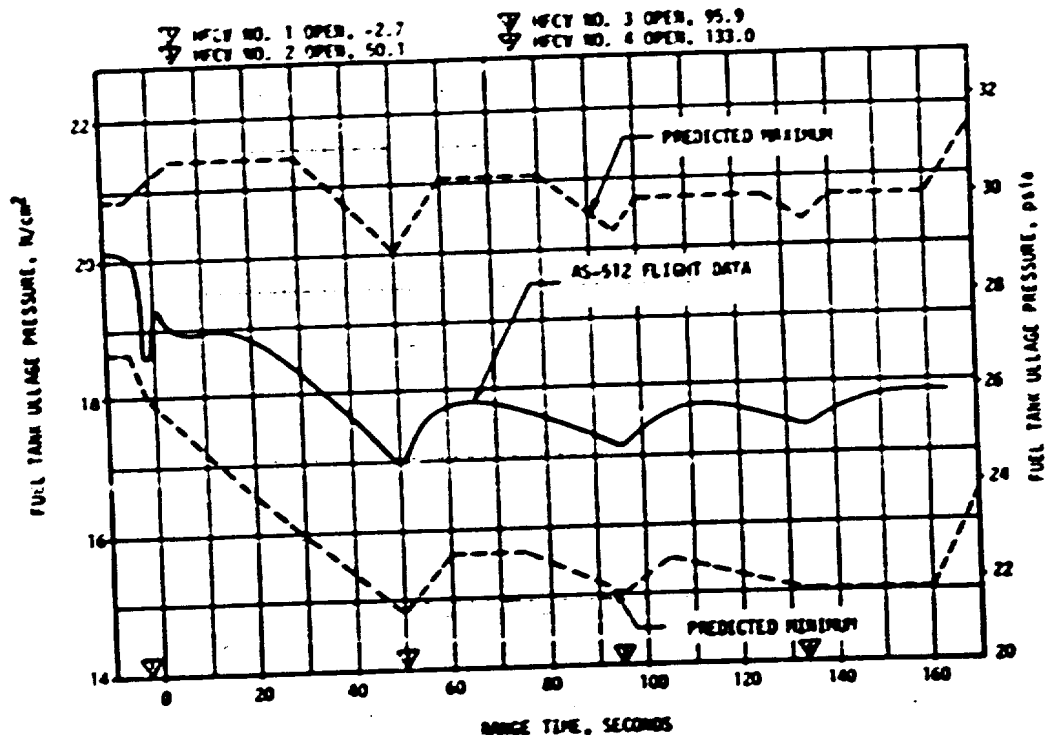


Figure 5-4. S-IC Fuel Tank Ullage Pressure

Ullage pressure was within the predicted limits throughout flight as shown in Figure 5-5. GOX flowrate to the tank was as expected. The maximum GOX flowrate after the initial transient was 48.3 lbm/s at CECO.

The LOX pump inlet pressure met the minimum RPSP requirement throughout flight.

5.7 S-IC PNEUMATIC CONTROL PRESSURE SYSTEM

The control pressure system functioned satisfactorily throughout the S-IC flight.

Sphere pressure was 2970 psia at liftoff and remained steady until CECO when it decreased to 2850 psia. The decrease was due to center engine prevalve actuation. There was a further decrease to 2475 psia after OECO. Pressure regulator performance was within limits.

The engine prevalves were closed after CECO and OECO as required.

5.8 S-IC PURGE SYSTEMS

Performance of the purge systems was satisfactory during flight.

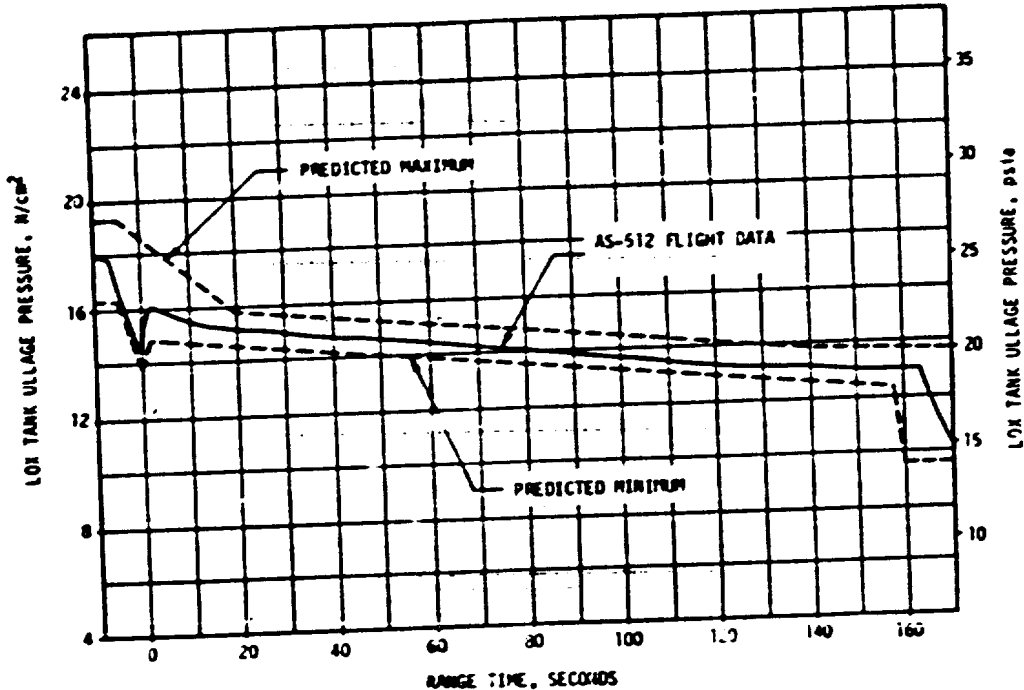


Figure 5-5. S-IC LOX Tank Ullage Pressure

The turbopump LOX seal storage sphere pressure of 2955 psia at liftoff was within the prestart limits of 2700 to 3300 psia. Pressure was within the predicted envelope throughout flight and was 2805 psia at OECO.

The pressure regulator performance throughout the flight was within the 85 ± 10 psig limits.

5.9 S-IC POGO SUPPRESSION SYSTEM

The POGO suppression system performed satisfactorily during S-IC flight.

Outboard LOX prevalve temperature measurements indicated that the prevalve cavities were filled with gas prior to liftoff as planned. The four resistance thermometers behaved during the AS-512 flight similarly to the flight of AS-511. The temperature measurements in the outboard LOX prevalve cavities remained warm (off scale high) throughout flight, indicating helium remained in the prevalves as planned. The two thermometers in the center engine prevalve were cold, indicating LOX in this valve as planned. The pressure and flowrate in the system were nominal.

5.10 S-IC HYDRAULIC SYSTEM

The performance of the S-IC hydraulic system was satisfactory. All servo-actuator supply pressures were within required limits.

Engine control system return pressures were within predicted limits and the engine hydraulic control system valves operated as planned.

SECTION 6

S-II PROPULSION

6.1 SUMMARY

The S-II propulsion systems performed satisfactorily throughout the flight. The S-II Engine Start Command (ESC), as sensed at the engines, occurred at 163.6 seconds. Center Engine Cutoff (CECO) was initiated by the Instrument Unit (IU) at 461.21 seconds, 0.47 seconds earlier than planned. Outboard Engine Cutoff (OECO), initiated by LOX depletion sensors, occurred at 559.66 seconds giving an outboard engine operating time of 396.1 seconds.

Engine mainstage performance was satisfactory throughout flight. The total stage thrust at the standard time slice (61 seconds after S-II ESC) was 0.14 percent below predicted. Total propellant flowrate, including pressurization flow, was 0.19 percent below predicted, and the stage specific impulse was 0.05 percent above predicted at the standard time slice. Stage propellant mixture ratio was 0.36 percent below predicted. Engine thrust buildup and cutoff transients were within the predicted envelopes.

The propellant management system performance was satisfactory throughout loading and flight, and all parameters were within expected limits except the LOX fine mass indication. Propellant residuals at OECO were 1401 lbm LOX, as predicted and 2752 lbm LH₂, 107 lbm less than predicted. Control of Engine Mixture Ratio (EMR) was accomplished with the two-position pneumatically operated Mixture Ratio Control Valves (MRCV). Relative to ESC, the low EMR step occurred 1.6 seconds earlier than predicted.

The performance of the LOX and LH₂ tank pressurization system was satisfactory. Ullage pressure in both tanks was adequate to meet or exceed engine inlet Net Positive Suction Pressure (NPSP) minimum requirements throughout mainstage.

Performance of the center engine LOX feedline accumulator system for POGO suppression was satisfactory. The accumulator bleed and fill subsystems operations were within predictions.

The engine servicing, recirculation, helium injection, and valve actuation systems performed satisfactorily.

S-II hydraulic system performance was normal throughout the flight.

6.2 S-II CHILDDOWN AND BUILDUP TRANSIENT PERFORMANCE

The engine servicing operations required to condition the engines prior to S-II engine start were satisfactorily accomplished. Thrust chamber

jacket temperatures were within predicted limits at both prelaunch and S-II ESC. Thrust chamber chilldown requirements are -200°F maximum at prelaunch commit and -150°F maximum at engine start. Thrust chamber temperatures ranged between -286 and -258°F at prelaunch commit and between -238 and -207°F at S-II ESC. Thrust chamber warmup rates during S-IC boost agreed closely with those experienced on previous flights.

Start tank system performance was satisfactory. Both temperature and pressure conditions of the engine start tanks were within the required prelaunch and engine start boxes as shown in Figure 6-1. Start tank temperature and pressure increase rates were normal during prelaunch and S-IC boost.

Start tank relief valve operation was noted on Engine No. 3. This characteristic had been predicted based upon results of the AS-512 Countdown Demonstration Test (CDDT) start tank relief valve setting test.

All engine helium tank pressures were within the prelaunch limits of 2800 to 3350 psia and engine start limits of 2800 to 3500 psia. Engine helium tank pressures ranged between 2940 and 3060 psia at prelaunch commit and between 3030 and 3160 psia at S-II ESC.

Engine helium tank pressures during start and initial mainstage operation were within the predicted limits as shown in Figure 6-2. The helium tank pressures decayed 350 to 370 psi during the engine start transient.

During the countdown hold initiated at -30 seconds, the hold options were exercised. The launch vehicle was maintained in the Hold Option 2 condition for approximately 73 minutes. This required control of the J-2 engine start tank and helium tank pressures to assure that they would remain within redline limits during the hold. Engine helium tank pressure was maintained by manual venting using the emergency vent solenoids. Start tank pressures were similarly controlled by use of the emergency vent solenoids until the start tank relief valves functioned to automatically maintain the tank pressures. A special test was run during the CDDT to determine the individual characteristic of each start tank relief valve and to show that it was comparable with existing stage redlines. Figure 6-3 shows the start tank pressures and temperatures during the option 2 hold. Figure 6-4 illustrates the repeatability of the start tank relief valves operation as evidenced during an Option 2 Hold.

During the hold period the prechilled start tanks warmed up at a rate of approximately 1.7°F/min. Fifty eight minutes after initiating the hold, engine 3 start tank had warmed up to the maximum temperature (-146°F) allowed by the redline requirements. At this point it was necessary to subject all five start tanks to a short rechill cycle in order to keep the respective temperatures within redline limits. Figure 6-5 shows the start tank and helium tank conditions during the rechill cycle. After the rechill and pressurizing, the start tank and helium tank pressures were controlled during the remainder of the hold and countdown using the emergency vent solenoids.

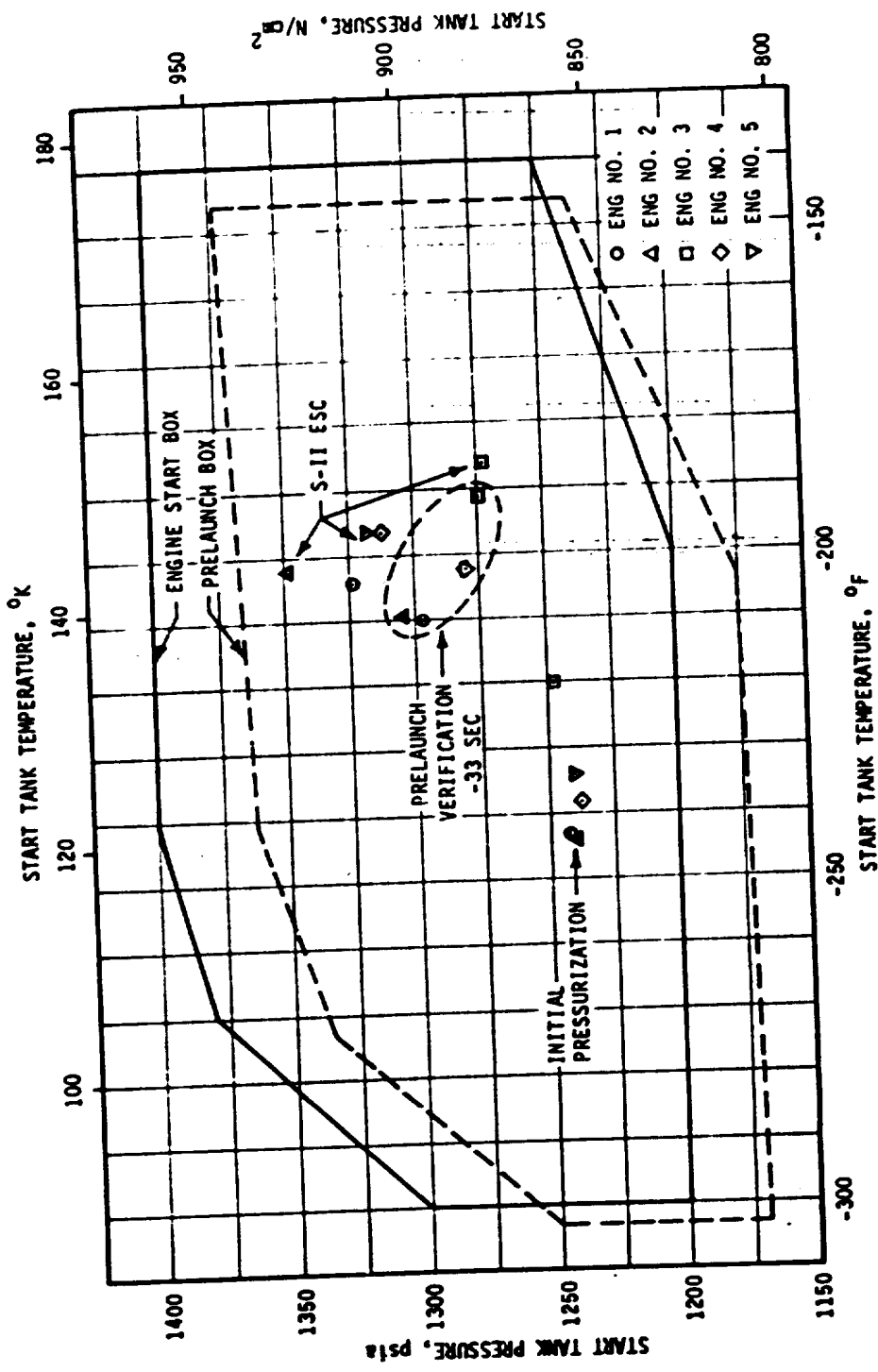


Figure 6-1. S-II Engine Start Tank Performance

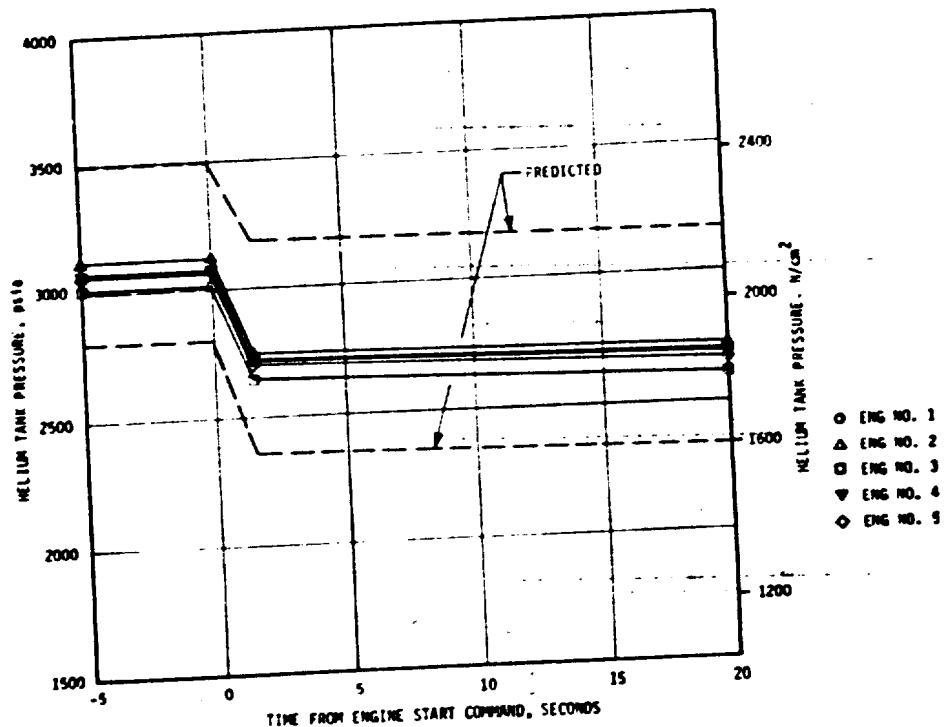


Figure 6-2. S-II Engine Helium Tank Pressures

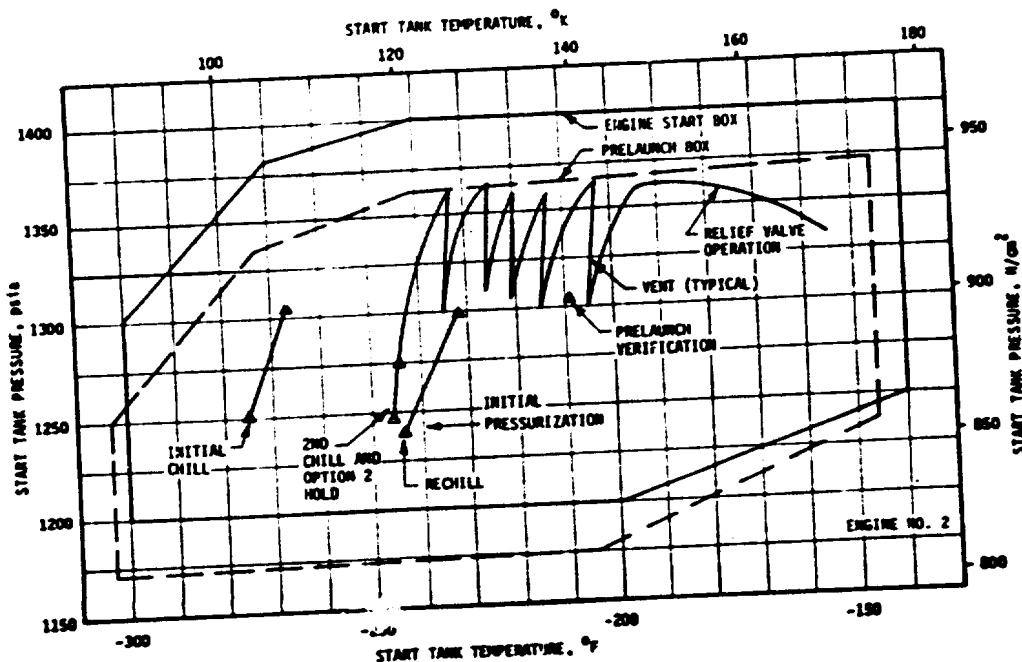


Figure 6-3. S-II Typical Start Tank Conditions During Hold Operations

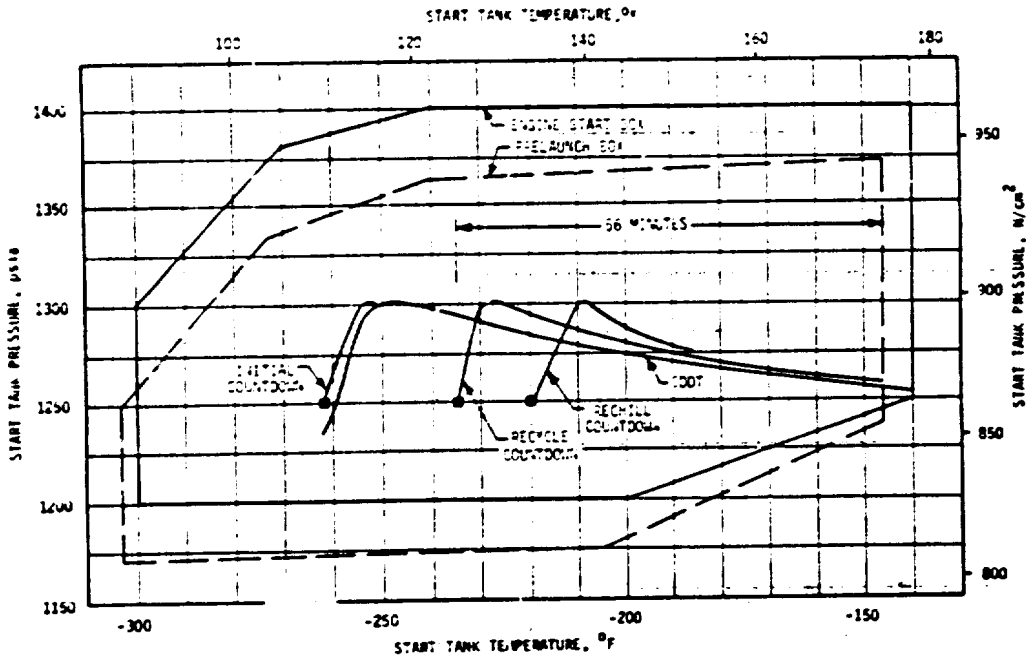


Figure 6-4. Comparison of S-II Start Tank Conditions During CDDT & Launch

This is the first time the S-II stage has been required to rechill its engine start tanks during an actual launch situation. Personnel, procedures, and hardware all performed as expected and all results were completely satisfactory.

The LOX and LH₂ recirculation systems, used to chill the feed ducts, turbo-pumps, and other engine components performed satisfactorily during prelaunch and S-IC boost. Engine pump inlet temperatures and pressures at S-II ESC were well within the requirements as shown in Figure 6-6. The LOX pump inlet pressure for all five engines was approximately 0.5 psi above the predicted envelope because the LOX tank experienced an approximate 1 psi increase in ullage pressure between S-IC OECO and S-II ESC. This pressure increase is attributed to the small ullage volume, coupled with the springback of the aft bulkhead at S-IC OECO, thus compressing the pressurant in the ullage. The LOX pump discharge temperatures at S-II ESC were approximately 14.0°F subcooled, well below the 3°F subcooling requirement.

Again, as --
not advr
perat"
and
--

S-511 the deletion of the S-II ullage motors did not affect the recirculation system. The characteristic temperature of the pump discharge temperature between S-IC OECO and S-II ESC was approximately 1.5°F, similar to that experienced on the ullage motors installed.

The pressurization of the propellant tanks was accomplished satisfactorily. The pressures at S-II ESC were 41.5 psia for LOX and 29.1 psia for LH₂, well above the minimum requirement of 33.0 and 27.0 psia, respectively.

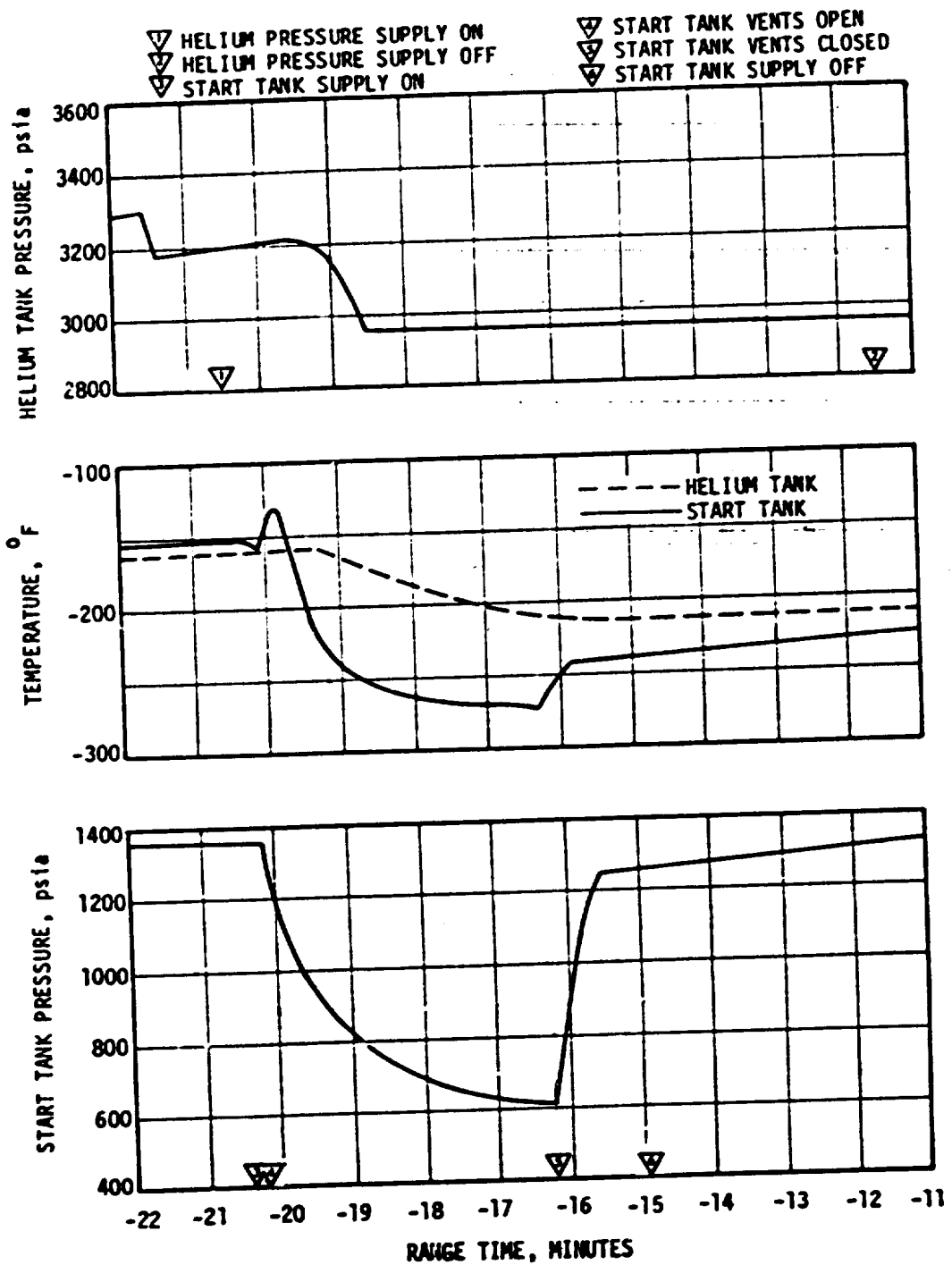


Figure 6-5. S-II Start Tank Rechill Sequence (Engine 1, Typical)

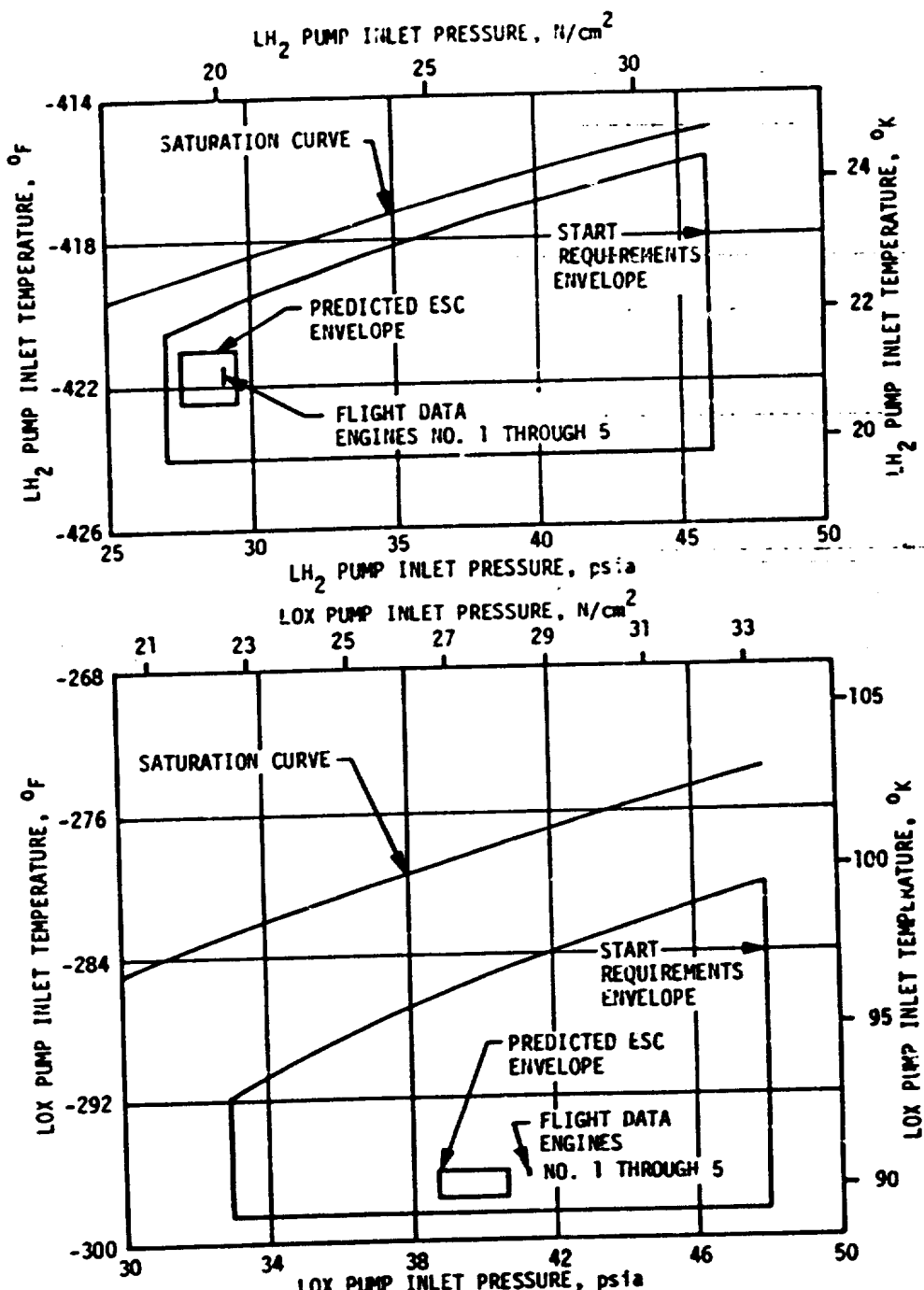


Figure 6-6. S-II Engine Pump Inlet Start Requirements

S-II ESC was received at 163.6 seconds and the Start Tank Discharge Valve (STDV) solenoid activation signal occurred 1.0 second later. The engine thrust buildup was satisfactory and well within the predicted thrust buildup envelope. All engines reached 90 percent thrust within 3.3 seconds after S-II ESC.

6.3 S-II MAINSTAGE PERFORMANCE

The propulsion reconstruction analysis showed that stage performance during mainstage operation was satisfactory. A comparison of predicted and reconstructed thrust, specific impulse, total flowrate, and mixture ratio versus time is shown in Figure 6-7. Stage performance was very close to predicted. At ESC +61 seconds, total stage thrust was 1,156.694 lbf which was 1585 lbf (0.14 percent) below the preflight prediction. Total propellant flowrate including pressurization flow, was 2743.4 ibm/s, 0.19 percent below predicted. Stage specific impulse, including the effect of pressurization gas flowrate, was 421.6 lbf-s/lbm, 0.05 percent above predicted. The stage propellant mixture ratio was 0.36 percent below predicted.

Center Engine Cutoff was initiated at ESC +297.62 seconds, 0.47 seconds earlier than planned. This action reduced total stage thrust by 234,131 lbf to a level of 920,746 lbf. The EMR shift from high to low occurred 325.6 seconds after ESC and the reduction in stage thrust occurred as expected. At ESC +351 seconds, the total stage thrust was 787,009 lbf; thus, a decrease in thrust of 133,737 lbf was indicated between high and low EMR operation. S-II burn duration was 396.1 seconds.

Individual J-2 engine data are presented in Table 6-1 for the ESC +61 second time slice. Good correlation exists between predicted and reconstructed flight performance. The performance levels shown in Table 6-1 have not been adjusted to standard J-2 altitude conditions and do not include the effects of pressurization flow.

Although the propulsion reconstruction was very close to the predicted, the trajectory reconstruction, Section 4.2.1, indicated that the S-II stage produced approximately 23 m/s more velocity than predicted. While this difference is within the normal range of trajectory dispersion, the unexpectedly poor correlation of the trajectory with the engine predicted and reconstructed performance is unique in the history of the S-II. From a review of the propulsion and trajectory as well as the history of stage and engine manufacturing and testing, it has been determined that the combined contribution of initial conditions, masses, base pressure, thrust, insulation erosion, propellant loading, propellant residuals, and reconstructed engine performance accounts for approximately 9 m/s of the additional velocity, leaving 14 m/s still to be explained.

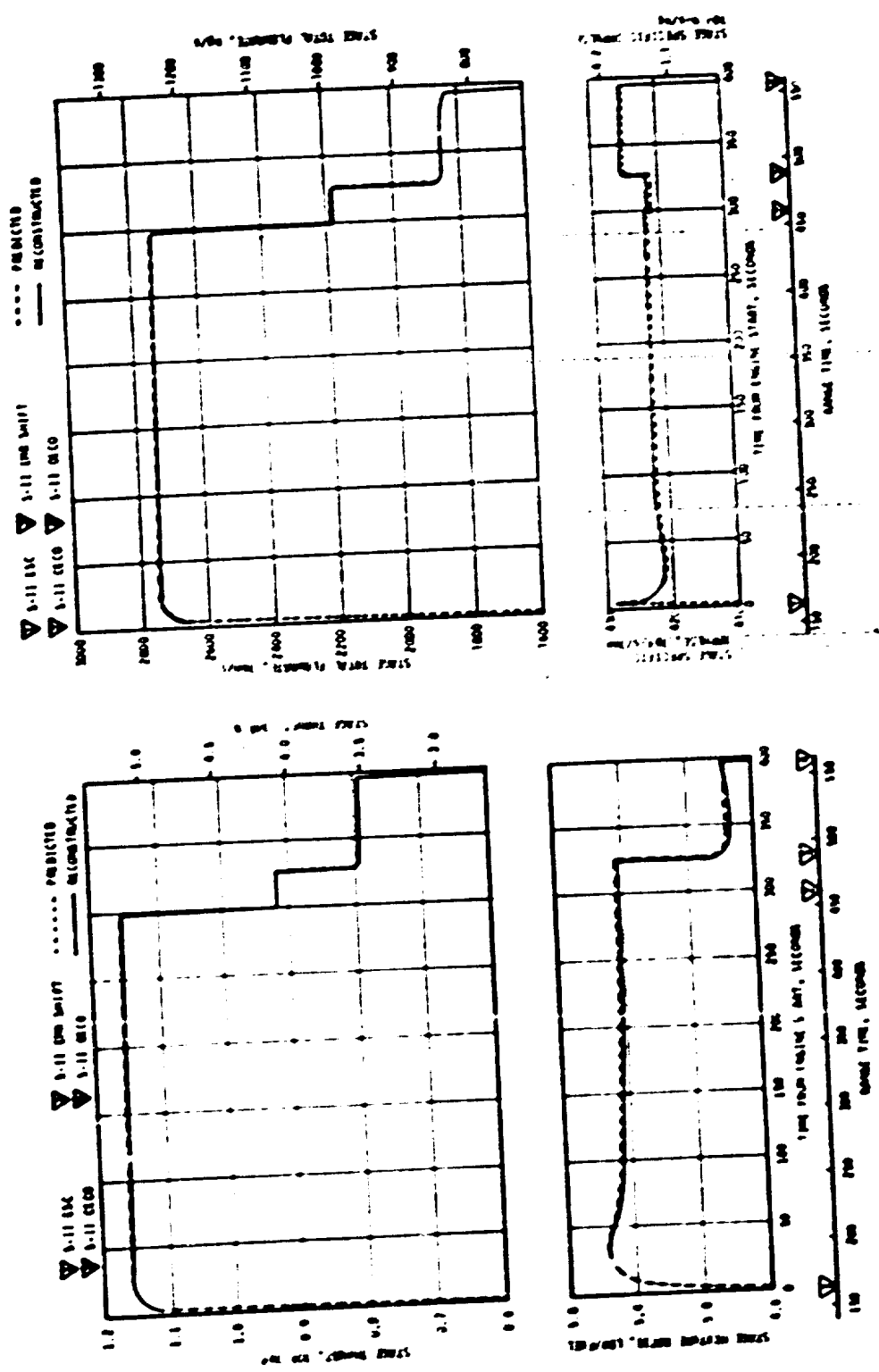


Figure 6-7. S-11 Steady State Operation

Most noteworthy is the fact that the S-engine average Specific Impulse (I_{sp}) on S-II-12 is the lowest of any S-II stage, and while there is no evidence that the engine log book I_{sp} values are improper, the predicted stage performance would have been very close to that indicated by the trajectory reconstruction if the average I_{sp} for the engines in this production block (Engines S/N 2060 through 2150) had been assumed. This would imply that the engine is approximately as repeatable as its associated instrumentation.

The differences involved are quite small. The difference between the block average I_{sp} and the S-II-12 average log book values (tags) is within the instrumentation noise level. The actual engine-to-engine repeatability is very similar to the instrumentation run-to-run repeatability. Therefore, it is reasonable to hypothesize that the lower than average engine performance indicated by the log book I_{sp} values may not have been real, and that actual engine performance may have been close to the block average. While the reconstruction would detect a flowrate contribution to an error in tag I_{sp} , it would not correct a thrust measurement error. If this latter situation were the case, a significant difference between predicted and reconstructed propulsion values would not be expected because the nozzle efficiency coefficient used in both the propulsion reconstruction and the prediction are derived from the same ground test data.

No change to the propulsion technique for SA-513 is required because the actual velocity increment from the S-II-13, which is programmed for an energy cutoff, is not affected and because the payload effect is minimal and the Skylab mission is not payload critical. Also the difference between S-II-13 tags and the block average is only about half as large as that for S-II-12.

Two LOX system measurements, engine No. 4 pump inlet temperature and engine No. 4 pump discharge pressure, exhibited unusual characteristics during the later part of high DMR operation. Since both measurements were within the same engine, a detailed examination was conducted to determine if this represented an engine performance change. The examination concluded that no engine performance change was indicated by the flight data. For further discussion of these measurements refer to Table 15-3.

6.4 S-II SHUTDOWN TRANSIENT PERFORMANCE

S-II DECO was initiated by the stage LOX depletion cutoff system as planned.

The LOX depletion cutoff system again included a 1.5 second delay timer. As in previous flights (AS-504 and subsequent), this resulted in engine

Table 6-1. S-II Engine Performance

PREDICTED	ENGINE	PREDICTED	RECONSTRUCTED OVERFLIGHT	PREDICTED DEVIATION IN FLIGHT	PREDICTED STAGE DEVIATION
Thrust, lbf	1	730,862	731,513	+0.31	
	2	732,265	732,752	+0.59	
	3	730,177	730,154	-0.21	
	4	731,526	731,670	+0.32	
	5	733,303	733,397	+0.36	
Specific Impulse, sec-lbf/lbm	1	424.1	424.1	0.00	
	2	423.8	424.1	+0.32	
	3	421.9	422.6	+0.16	
	4	423.3	423.7	+0.33	
	5	426.6	426.5	-0.02	
Engine Thrust, lbf	1	564.38	565.95	+0.32	
	2	560.91	562.22	+1.06	
	3	565.58	564.58	-0.10	
	4	567.44	566.76	-0.12	
	5	569.51	569.83	+0.32	
Engine Cut-off Ratio, LOX/LB	1	5.508	5.503	-0.25	
	2	5.515	5.509	-0.29	
	3	5.508	5.508	0.00	
	4	5.507	5.505	-0.21	
	5	5.522	5.523	+0.32	

Note: Performance values at TLE +61 seconds. Values are site conditions and do not include effect of pressurization flow.

thrust decay (observed as a drop in thrust chamber pressure) prior to receipt of the cutoff signal.

The outboard engine thrust decay performance was within the predicted band. First indications of thrust decay were noted 0.75 second prior to cutoff signal on engine 1. In order of engine position, thrust decay began at 0.75, 0.50, 0.55, and 0.30 seconds prior to cutoff signal and corresponding chamber pressure decays were 180, 180, 130 and 120 psi.

At S-II DECO total thrust was down to 612,126 lbf. Stage thrust dropped to five percent of this level within 0.4 second. The stage cutoff impulse through the five percent thrust level is estimated to be 121,100 lbf-s.

6.5 S-II STAGE PROPELLANT MANAGEMENT SYSTEM

Ground loading and flight performance of the S-II stage propellant management system were nominal and all parameters were within normal ranges. The only exception was the LOX fine mass measurement that exhibited a signal level reduction of one to two volts between -2.5 seconds and 15 seconds and then returned to normal for the remainder of the flight. This condition has not been observed during previous flights. A review of the LOX coarse mass and the Propellant Utilization (PU) error signal verifies that the PU computer LOX bridge servo did correspondingly move during this time period eliminating the possibility of a telemetry problem. After a thorough data review, this signal characteristic could not be explained by known tank conditions. Laboratory simulations with either series of parallel

resistance in the leadwire system between the capacitance probe and the PIV computer have duplicated this problem.

To preclude possible problems on future flights, an inspection of the leadwire system integrity will be conducted for S-II-13 and subsequent vehicles. This measurement is non-critical in flight and manual point sensor backup propellant loading could be used for ground loading should this problem recur.

The Propellant Tanking Computer System (PTCS) and the stage propellant management system properly controlled S-II loading and replenishment. All S-II stage LOX and LH₂ liquid level point sensors and capacitance probes operated without any problems during the propellant loading. Both LOX and LH₂ overfill point sensor percent wet indications were all within the loading redline at the -187 second commit point.

Open-loop control of EMR during flight was successfully accomplished through use of the engine two position pneumatically operated Mixture Ratio Control Valves (PMRV). At ESC, helium pressure drove the valves to the engine start position corresponding to the 4.8 EMR. The high EMR (5.5) command was received at ESC +5.5 seconds as expected, providing a nominal high EMR of 5.5 for the first phase of the Programmed Mixture Ratio (PMR).

The low EMR step occurred at ESC +325.6 seconds, which is 1.6 seconds earlier than predicted. This time difference is most likely caused by IU computational cycle errors or the Saturn vehicle reaching the preset step command velocity at an earlier time than planned. The average EMR at the low step was 4.78 as compared to a predicted 4.80. This lower than planned EMR is well within the two sigma ± 0.06 mixture ratio tolerance.

Outboard Engine Cutoff (OECO) was initiated by the LOX depletion ECO sensors at ESC +396.07 seconds which is 0.02 seconds later than planned. Liquid level point sensor data were not available to verify that LOX depletion occurred but engine parameters such as thrust chamber pressure, pump inlet temperatures, pump speeds and pump flows all exhibited characteristics similar to LOX depletion cutoff on previous flights.

Since liquid level data were not available, propellant residual mass in tanks determination was done by other means. Based on predicted LOX OECO mass, predicted LH₂ full load mass and flowmeter data, propellant residual mass in tanks at OECO were 1401 lbm LOX and 2752 lbm LH₂ versus 1401 lbm LOX and 2858 lbm LH₂ predicted. The open loop PU error at OECO was -107 lbm LH₂ which is well within the estimated three sigma dispersion of ± 2500 lbm LH₂.

Table 6-2 presents a comparison of propellant masses as measured by the PU probes and engine flowmeters. The full load mass could not be derived using point sensors (data not available) as a reference. The predicted value for LH₂ is used as the best estimate. The LOX full load mass was derived from the engine flowmeter integration and OECO residual values.

Table 6-2. AS-512 Flight S-II Propellant Mass History

EVENT	PREDICTED, LBM		PI SYSTEM ANALYSIS LBM		ENGINE FLOWMETER INTEGRATION, LBM (BEST ESTIMATE)	
	LOX	LH ₂	LOX	- ⁴²	LOX	LH ₂
Liftoff	844,150	160,220	844,059	160,220	842,469	160,220
S-II ESC	844,150	160,206	844,150	160,415	842,469	160,206
S-II PU Valve Step Command	107,586	25,061	111,129	24,367	109,354	25,467
2 Percent Point Sensor	112,263	4268	--	--	--	--
S-II DECO	1401	2858	2502	2859	1401	2752
S-II Residual After Thrust Decay	1179	2744	Data not useable	Data not useable	1222	2676

Note: Table is based on mass in tanks and sump only. Propellant trapped external to tanks and LOX sump is not included. PU data are not corrected for tank/probe mismatch.

--Point sensor discrete data not available due to Bermuda Ground Station problem.

6.6 S-II PRESSURIZATION SYSTEM

6.6.1 S-II Fuel Pressurization System

LH₂ tank ullage pressure, actual and predicted, is presented in Figure 6-8 for autosequence, S-IC boost, and S-II boost. The LH₂ vent valves were closed at -94.08 seconds and the ullage volume pressurized to 35.8 psia in 17.5 seconds. One make-up cycle was required at approximately -43 seconds and the ullage pressure was increased from 34.8 psia to 35.8 psia. Ullage pressure at -19 seconds (launch commit) was 35.4 psia which is within the redline limits of 33.0 to 38.0 psia. Ullage pressure decayed to 35.1 psia at S-IC ESC at which time the pressure decay rate increased for about 20 seconds. (The increased decay rate was attributed to an increase in cooling due to LH₂ surface agitation caused by S-IC engine firing.) This decay is normal and seen on previous launches.

During S-IC boost, the differential pressure across the vent valve, was

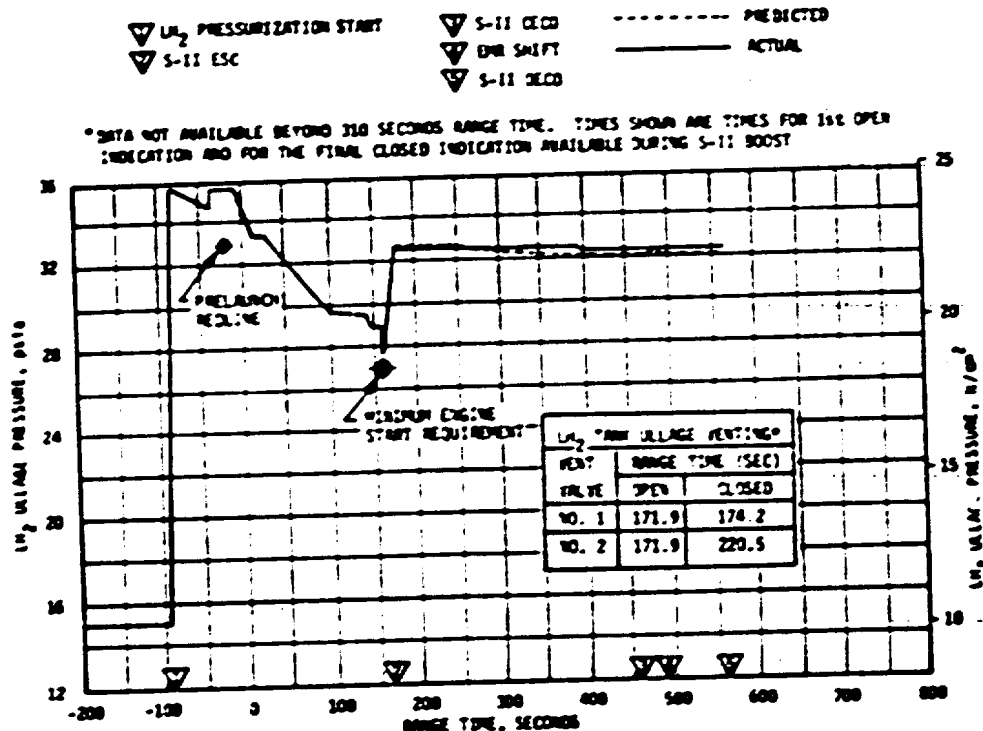


Figure 6-8. S-II Fuel Tank Ullage Pressure

within the allowable low-mode band of 27.5 to 29.5 psia. The LH₂ vent valve No. 2 cycled open at 140.3 seconds and closed at 141.1 seconds. Ullage pressure at S-II engine start was 29.1 psia exceeding the minimum engine start requirement of 27 psia. The LH₂ vent valves were switched to the high vent mode (30.5 to 33.0 psia) prior to S-II engine start.

During S-II boost, the GH₂ for pressurizing the LH₂ tank was controlled by a flow control orifice in the LH₂ tank pressurization line with maximum tank pressure controlled by the LH₂ vent valves. Except for the normal low pressure spike during start transient, the ullage pressure throughout the S-II boost period was controlled by the LH₂ vent valves within the 30.5 to 33 psia allowable band. LH₂ vent valve 1 opened at 171.9 seconds and remained open until 174.2 seconds. Vent Valve No. 2 cracked open five (5) times during the first 156 seconds of S-II boost. Vent valve discrete measurements are not available beyond 310.9 seconds due to data acquisition problems. The LH₂ ullage pressure was a maximum of 0.3 psi higher than the predicted pressure.

Figure 6-9 shows LH₂ pure total inlet pressure, temperature, and Net Positive Suction Pressure (NPSP) for the J-2 engines. The parameters were in close agreement with the predicted values throughout the S-II flight period. NPSP remained above the minimum requirement throughout the S-II burn phase.

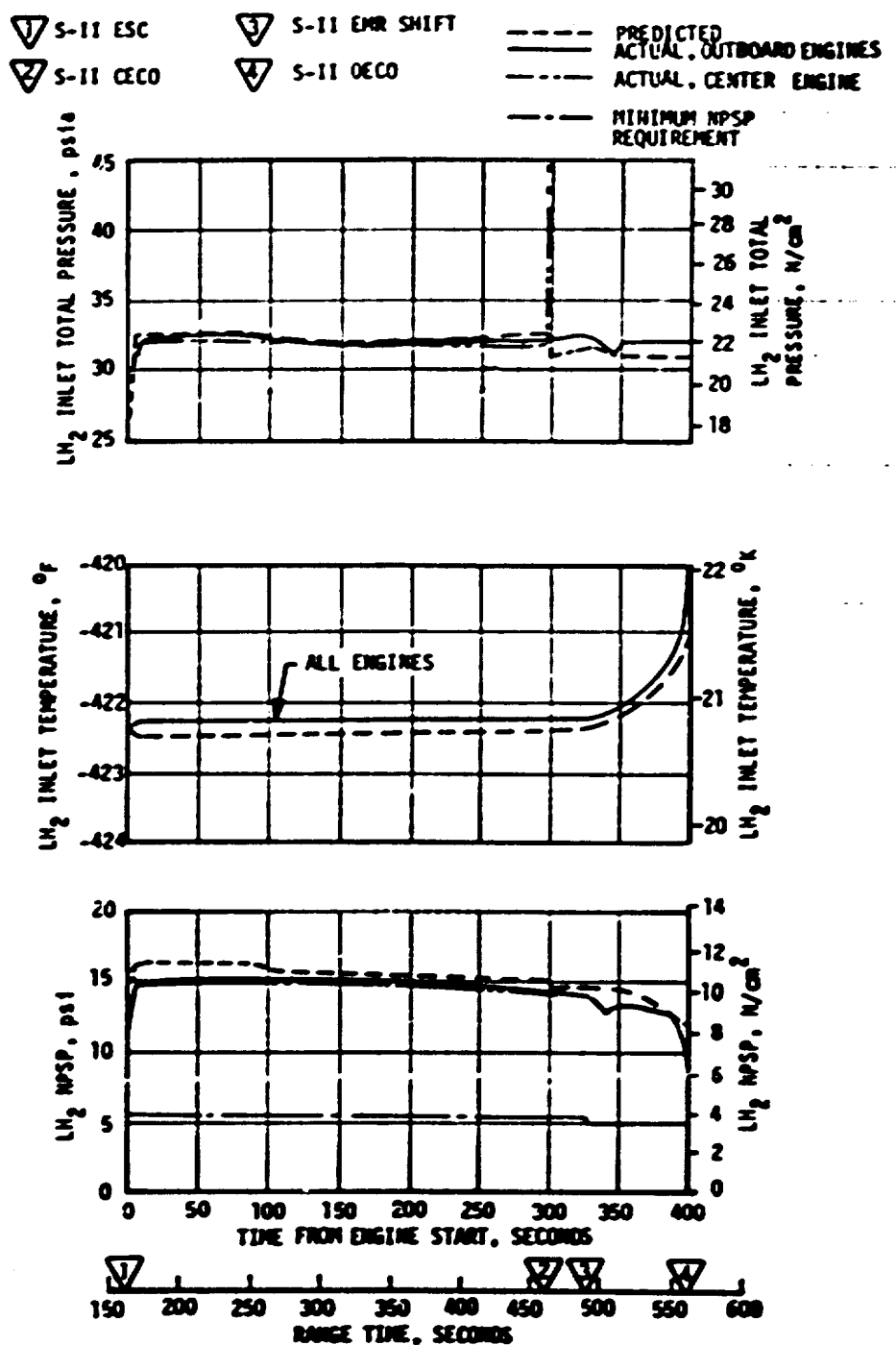


Figure 6-9. S-II Fuel Pump Inlet Conditions

6.6.2 S-II LOX Pressurization System

LOX tank ullage pressure, actual and predicted, is presented in Figure 6-10 for autosequence, S-IC boost, and S-II burn. After a 107 second cold helium chilldown flow through the LOX tank, the chilldown flow was terminated at -200 seconds. The vent valves were closed at -184 seconds and the LOX tank was pressurized to the pressure switch setting of 38.5 psia in 31.0 seconds. No pressure make-up cycles were required. The LOX tank ullage pressure increased to 40.0 psia because of common bulk-head flexure during LH₂ tank prepressurization. Ullage pressure at -19 seconds (launch commit) was 40.2 psia which is within the redline limits of 36 to 43 psia. The LOX vent valves performed satisfactorily during all prelaunch operations.

*DATA NOT AVAILABLE BEYOND 310 SECONDS RANGE TIME. TIMES SHOWN ARE TIMES FOR FIRST OPEN INDICATION AND FOR THE FINAL CLOSED INDICATION AVAILABLE

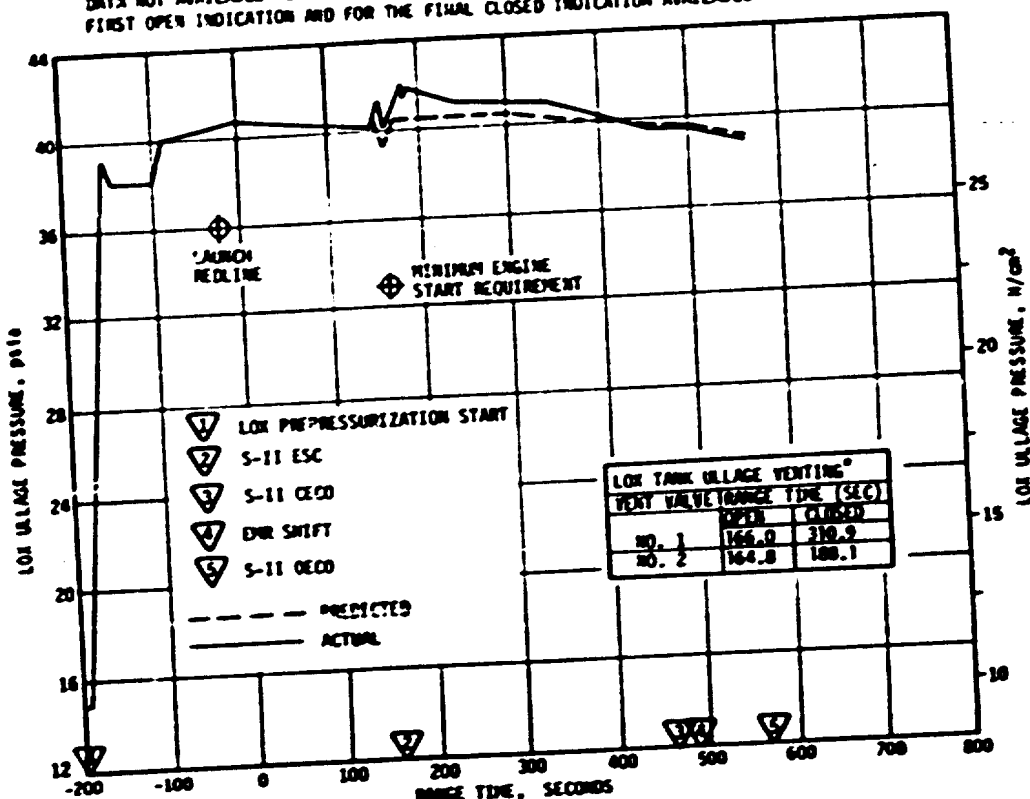


Figure 6-10. S-II LOX Tank Ullage Pressure

The LOX vent valves remained closed during the S-IC boost mode and the LOX tank ullage pressure prior to S-II engine start was 41.5 psia. During the S-II boost mode, the LOX tank pressure varied from a maximum of 42.0 psia at 182.0 seconds to a minimum of 39.0 psia at S-II OECO. Similarly to AS-510 and AS-511 the GOX for pressurizing the LOX tank was controlled by a flow control orifice in the LOX tank pressurization line with the LOX tank vent valves controlling excessive pressure buildup within a pressure range setting of 39.0 to 42.0 psia. The LOX vent valve No. 2 first opened at 164.8 seconds and reseated at 165.5 seconds. LOX vent valve No. 2 opened and reseated a total of five (5) times between 164.8 seconds and 188.1 seconds. The LOX vent valve No. 1 cracked open 18 times between 166.0 seconds and 310.9 seconds. Vent valve position discrete indications are not available beyond 310.9 seconds due to data acquisition problems.

The LOX tank ullage pressure was controlled within one psi of the pressure predicted for S-II boost as shown in Figure 6-10. Comparisons of the LOX pump total inlet pressure, temperature and NPSP are presented in Figure 6-11. Throughout S-II boost, the LOX pump NPSP was well above the minimum requirement.

This was the second flight using the LOX tank pressure switch purge. The purge system was incorporated to preclude a potential LOX/GOX incompatibility situation within the LOX pressure switch assembly. The purge is connected to the helium injection and accumulator fill helium supply system. No instrumentation is available to evaluate the purge system. However, since both the helium injection and accumulator fill systems operated successfully, it is concluded that the purge system also functioned properly.

6.7 S-II PNEUMATIC CONTROL PRESSURE SYSTEM

The pneumatic control system functioned satisfactorily throughout the S-IC and S-II boost periods. Bottle pressure was 2990 psia at -30 seconds and with normal valve activities during S-II burn, pressure decayed to approximately 2590 psia after S-II OECO.

Regulator outlet pressure during flight remained at a constant 715 psia, except for the expected momentary pressure drops when the recirculation or prevalves were actuated closed just after engine start, at CECO, and at OECO.

6.8 S-II HELIUM INJECTION SYSTEM

The performance of the helium injection system was satisfactory. The supply bottle was pressurized to 2976 psia prior to liftoff and by S-II ESC the pressure was 1663 psia. Helium injection average total flowrate during supply bottle blowdown (-30 to 161.4 seconds) was 74 SCFM. During the prelaunch countdown, the helium injection bottle decay test was repeated to assure no adverse trends existed. The initial and final decay tests were within predicted limits.

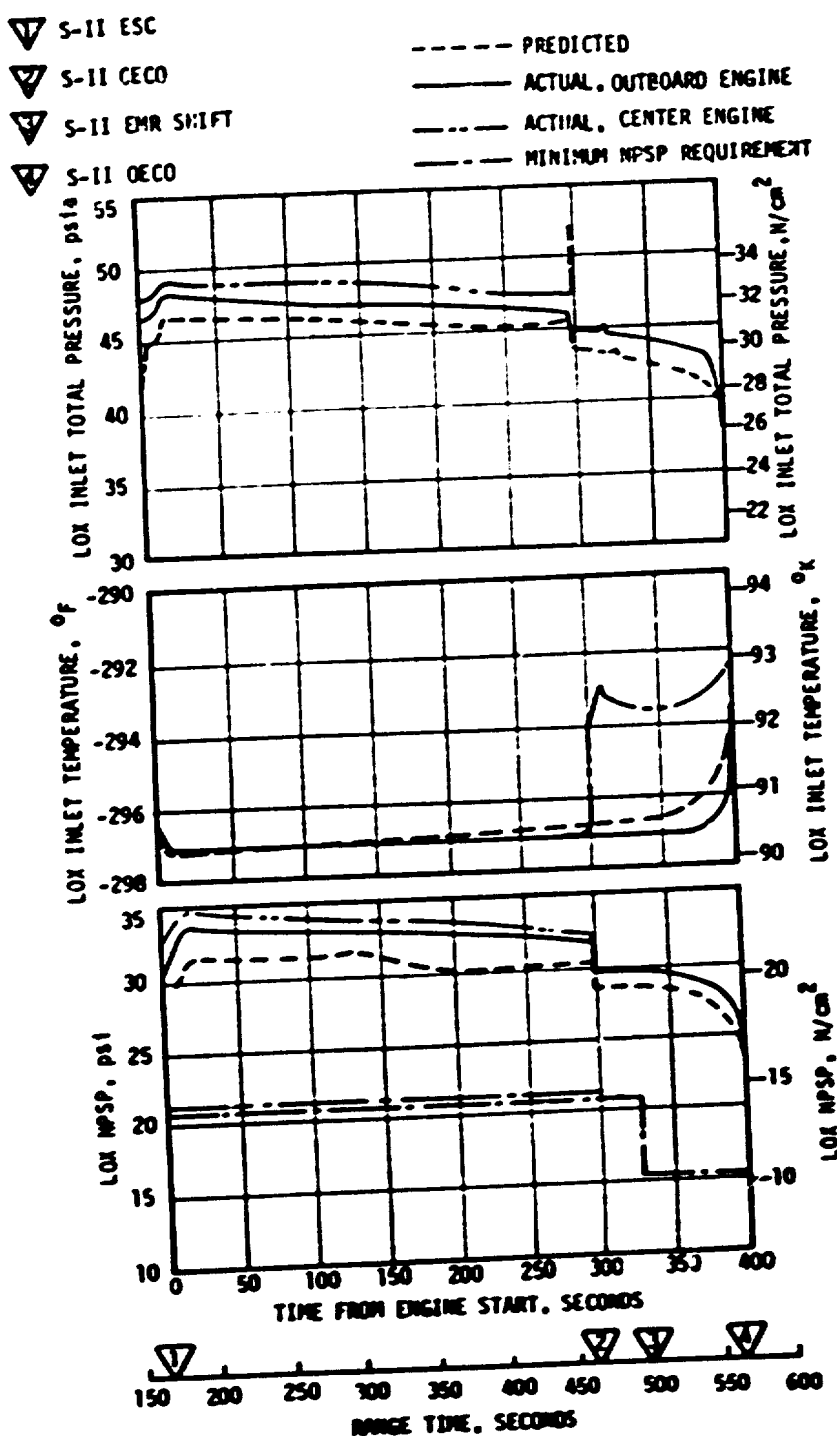


Figure 6-11. S-II LOX Pump Inlet Conditions

6.9 POGO SUPPRESSION SYSTEM

A center engine LOX feedline accumulator is installed on the S-II stage as a POGO suppression device. Analysis indicates that there was no S-II POGO.

The accumulator system consists of 1) a bleed system to maintain sub-cooled LOX in the accumulator during S-IC boost and S-II engine start, and 2) a fill system to fill the accumulator with helium subsequent to engine start and maintain a helium filled accumulator through S-II CECO.

The accumulator bleed subsystem performance was satisfactory. Figure 6-12 shows the required accumulator temperature at engine start, the predicted temperatures during prelaunch and S-IC boost, and the actual temperatures experienced during AS-512 flight. The maximum allowable temperature of -281.5°F at engine start was adequately met (-293.8°F actual).

Accumulator fill was initiated 4.1 seconds after engine start. Figure 6-13 shows the accumulator LOX level versus time during accumulator fill. The fill time was 6.6 seconds, within the required 5 to 7 seconds. The helium fill flow rate, during the fill transient, was 0.0055 lbm/s and the accumulator pressure was 45.72 psia.

After the accumulator was filled with helium, it remained in that state until S-II CECO when the helium flow was terminated by closing the two fill solenoid valves.

The accumulator bottom temperature measurement indicated there was liquid propellant splashing on the bottom temperature probe shortly after the accumulator was filled with helium gas. This type of phenomena was observed during the ground static firing test of the S-II-14 vehicle and to a lesser degree during the flights of S-II-9, -10, and -11. This splashing is not considered to be a problem. Figure 6-14 shows the helium injection and accumulator fill supply pressure during accumulator fill operation. As can be seen, the supply bottle pressure was within the predicted band, indicating that the helium usage rates were as predicted.

6.10 S-II HYDRAULIC SYSTEM

S-II hydraulic system performance was nominal with all pressures, temperatures, and volumes within nominal predicted limits throughout countdown and flight. Actuator positions followed actuator commands with good accuracy and showed normal transient responses. The maximum engine deflection was approximately 1.3 degrees in pitch on engines 3 and 4 in response to separation and engine start transients. Actuator loads were well within design limits. The maximum actuator load was approximately 6800 lbf for the pitch actuator of engine 1. This load also occurred shortly after engine start.

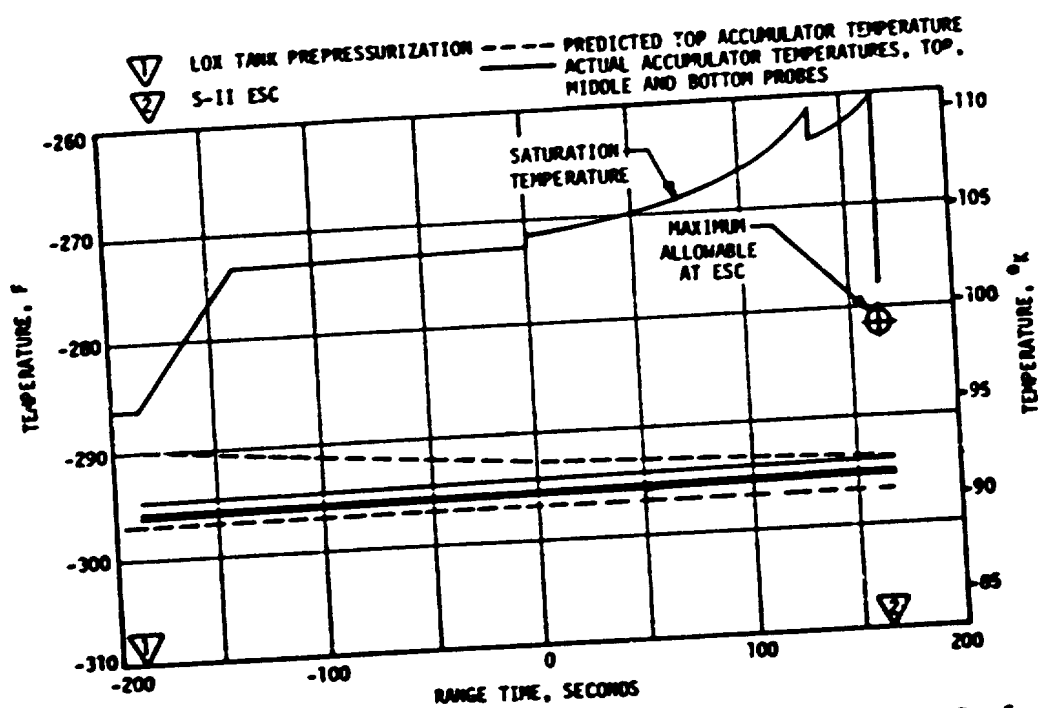


Figure 6-12. S-II Center Engine LOX Feedline Accumulator Bleed System Performance

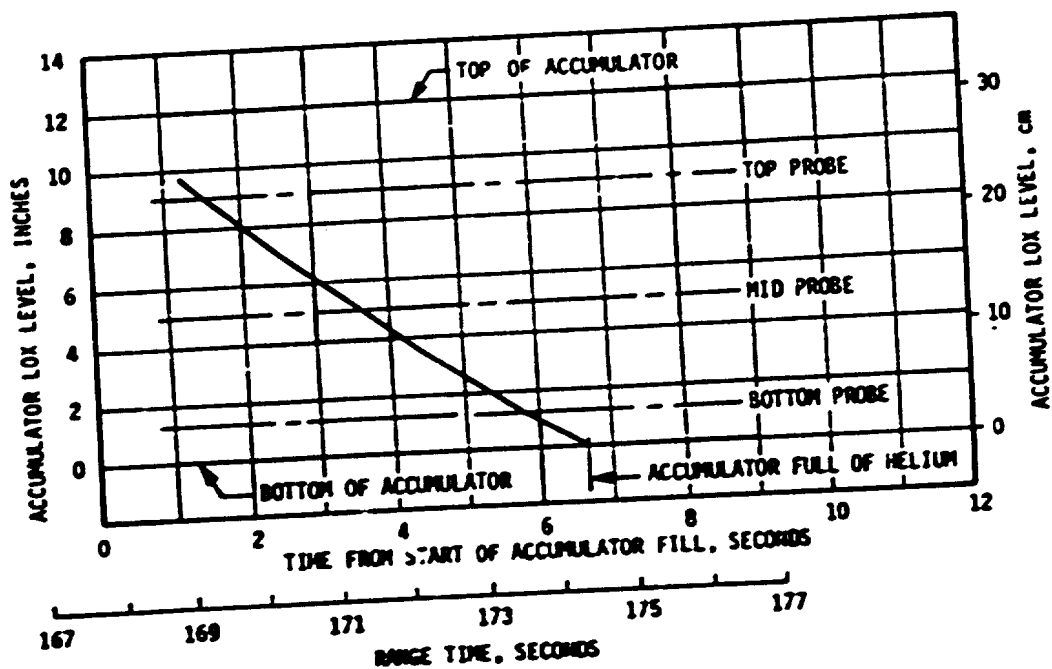


Figure 6-13. S-II Center Engine LOX Feedline Accumulator Fill Transient

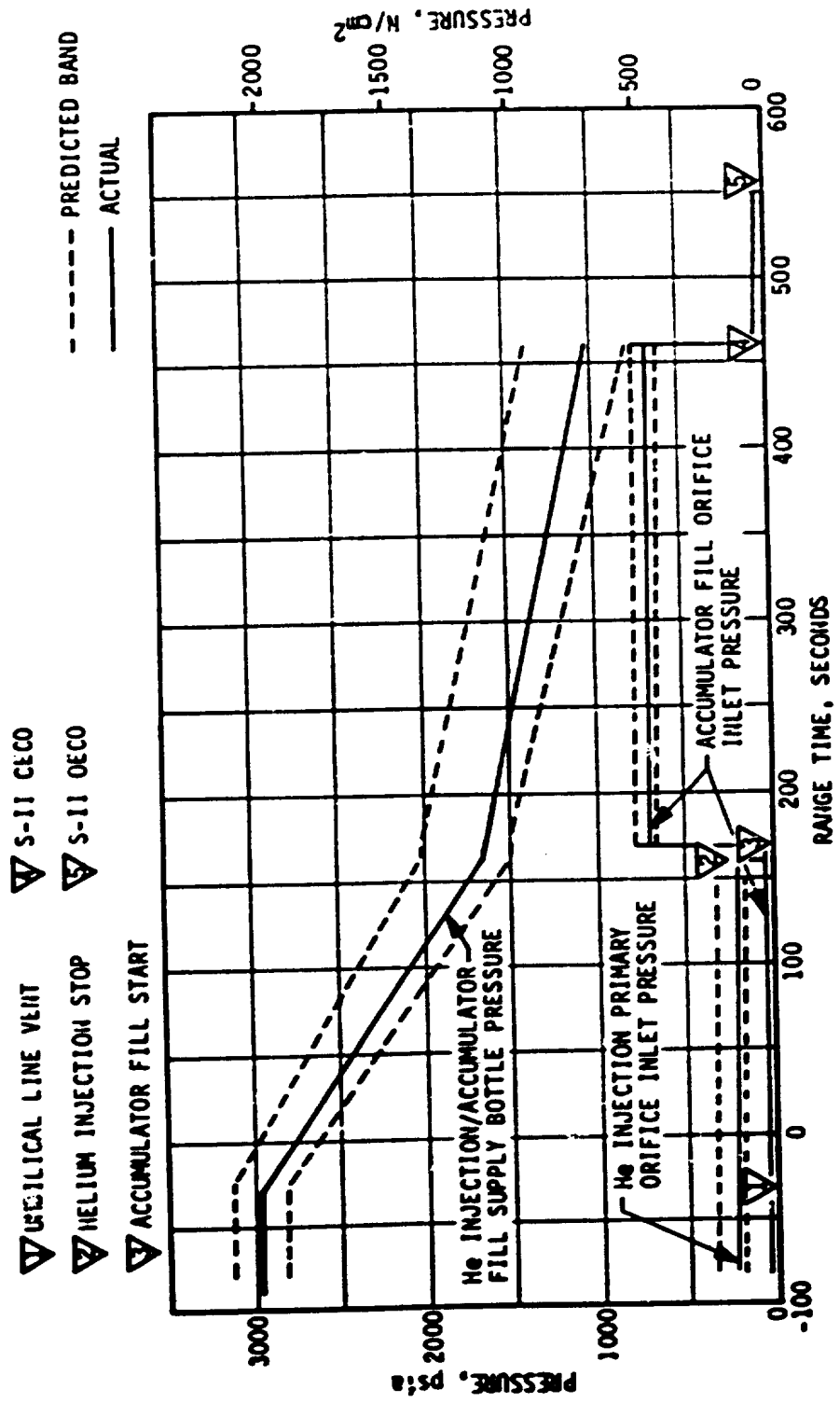


Figure 6-14. S-II Center Engine LOX Feedline Accumulator Helium Supply System Performance

SECTION 7

S-IVB PROPULSION

7.1 SUMMARY

The S-IVB propulsion system performed satisfactorily throughout the operational phase of first and second burns and had normal start and cutoff transients.

S-IVB first burn time was 138.8 seconds, 3.7 seconds shorter than predicted for the actual flight azimuth of 91.5 degrees. This difference is composed of -4.1 seconds due to the higher than expected S-II/S-IVB separation velocity and +0.4 second due to lower than predicted S-IVB performance. The engine performance during first burn, as determined from standard altitude reconstruction analysis, deviated from the predicted Start Tank Discharge Valve (STDV) open +135-second time slice by -0.68 percent for thrust and -0.14 percent for specific impulse. The S-IVB stage first burn Engine Cutoff (ECO) was initiated by the Launch Vehicle Digital Computer (LVDC) at 702.65 seconds.

The Continuous Vent System (CVS) adequately regulated LH₂ tank ullage pressure at an average level of 19.1 psia during orbit and the Oxygen/Hydrogen (O₂/H₂) burner satisfactorily achieved LH₂ and LOX tank resurization for restart. Engine restart conditions were within specified limits.

S-IVB second burn time was 351.0 seconds, 4.0 seconds longer than predicted for the 91.5 degree flight azimuth. This difference is primarily due to the lower S-IVB performance and heavier vehicle mass during second burn. The engine performance during second burn, as determined from the standard altitude reconstruction analysis, deviated from the STDV open +172-second time slice by -0.77 percent for thrust and -0.16 percent for specific impulse. Second burn ECO was initiated by the LVDC at 11,907.64 seconds, (08:51:27.64).

Subsequent to second burn, the stage propellant tanks and helium spheres were safed satisfactorily. Sufficient impulse was derived from LOX dump, LH₂ CVS operation and auxiliary propulsion system (APS) ullage burn to achieve a successful lunar impact. Two subsequent planned APS burns were used to improve lunar impact targeting.

The APS operation was nominal throughout the flight. No helium or propellant leaks were observed and the regulators functioned nominally.

The hydraulic system performance was nominal throughout flight.

7.2 S-IVB CHILDDOWN AND BUILDUP TRANSIENT PERFORMANCE FOR FIRST BURN

The thrust chamber temperature at launch was -177°F , which was below the maximum allowable redline limit of -130°F . At S-IVB first burn Engine Start Command (ESC), the temperature was -136°F , which was within the requirements of $-189.6 \pm 110^{\circ}\text{F}$.

The chilldown and loading of the engine GH₂ start tank and pneumatic control bottle prior to liftoff was satisfactory.

The engine control sphere pressure and temperature at liftoff were 3070 psia and -155.7°F . At first burn ESC the start tank conditions were 1310 psia and -157.7°F , within the required region of 1325 ± 75 psia and $-170 \pm 30^{\circ}\text{F}$ for start. The discharge was completed and the refill initiated at first burn ESC +3.8 seconds. The refill was satisfactory with 1173 psia and -223°F at cutoff.

The propellant recirculation systems operation, which was continuous from before liftoff until just prior to first ESC, was satisfactory. Start and run box requirements for both fuel and LOX were met, as shown in Figure 7-1. At first ESC the LOX pump inlet temperature was -295°F and the LH₂ pump inlet temperature was -421.5°F .

First burn fuel lead followed the expected pattern and resulted in satisfactory conditions as indicated by the fuel injector temperature.

The first burn start transient was satisfactory, and the thrust buildup was within the limits set by the engine manufacturer. Thrust data during the start transient is presented in Figure 7-2. This buildup was similar to the thrust buildups observed on previous flights. The Mixture Ratio Control Valve (MRCV) was in the closed position (5.0 EMR) prior to first start, and performance indicates it remained closed during the first burn. The total impulse from STDV open to STDV open +2.5 seconds was 187,271 lbf-s.

7.3 S-IVB MAINSTAGE PERFORMANCE FOR FIRST BURN

The propulsion reconstruction analysis showed that the stage performance during mainstage operation was satisfactory. A comparison of predicted and actual performance of thrust, specific impulse, total flowrate, and Engine Mixture Ratio (EMR) versus time is shown in Figure 7-3. Table 7-1 shows the thrust, specific impulse, flowrates, and EMR deviations from the predicted at the STDV open +135-second time slice at standard altitude conditions.

Thrust, specific impulse, and EMR were slightly less than the nominal prediction but well within the predicted bands. These deviations from predicted are very minor considering the S-IVB-512 stage was not static fired. Based on engine performance reconstruction the MRCV setting was within the requirement of 30.0 ± 1 degrees.

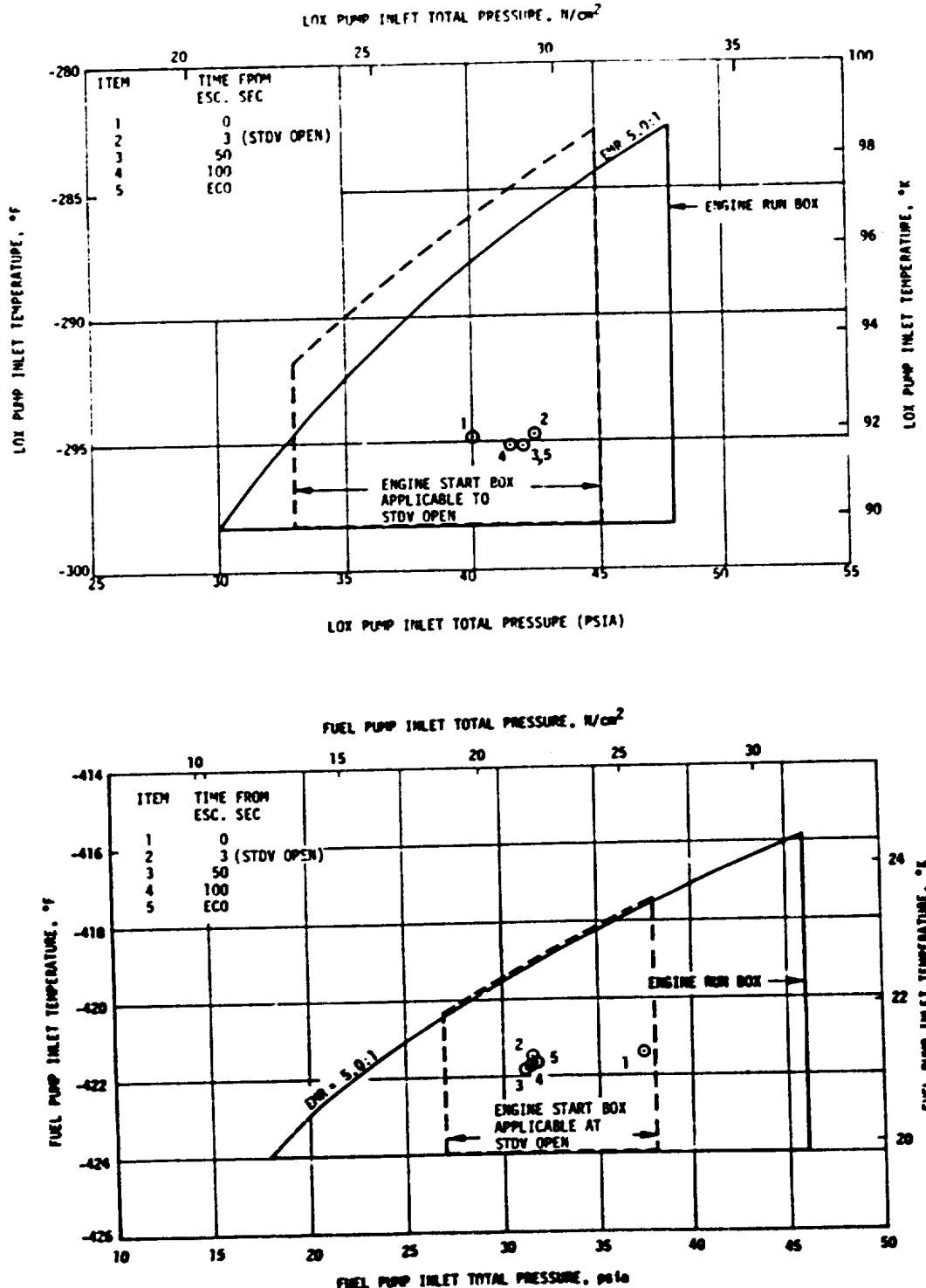


Figure 7-1. S-IVB Start Box and Run Requirements - First Burn

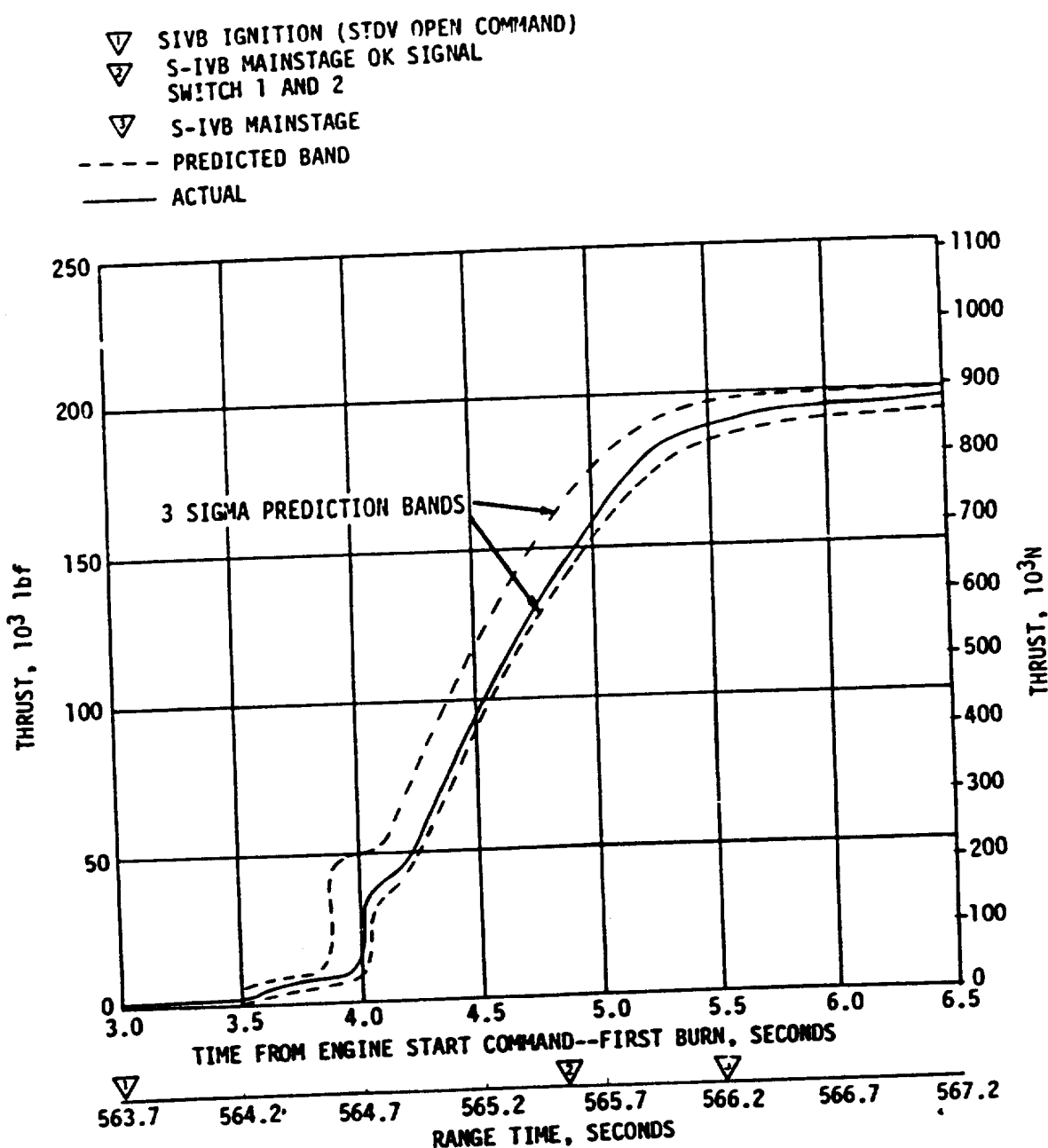


Figure 7-2. S-IVB Thrust Buildup Transient for First Burn

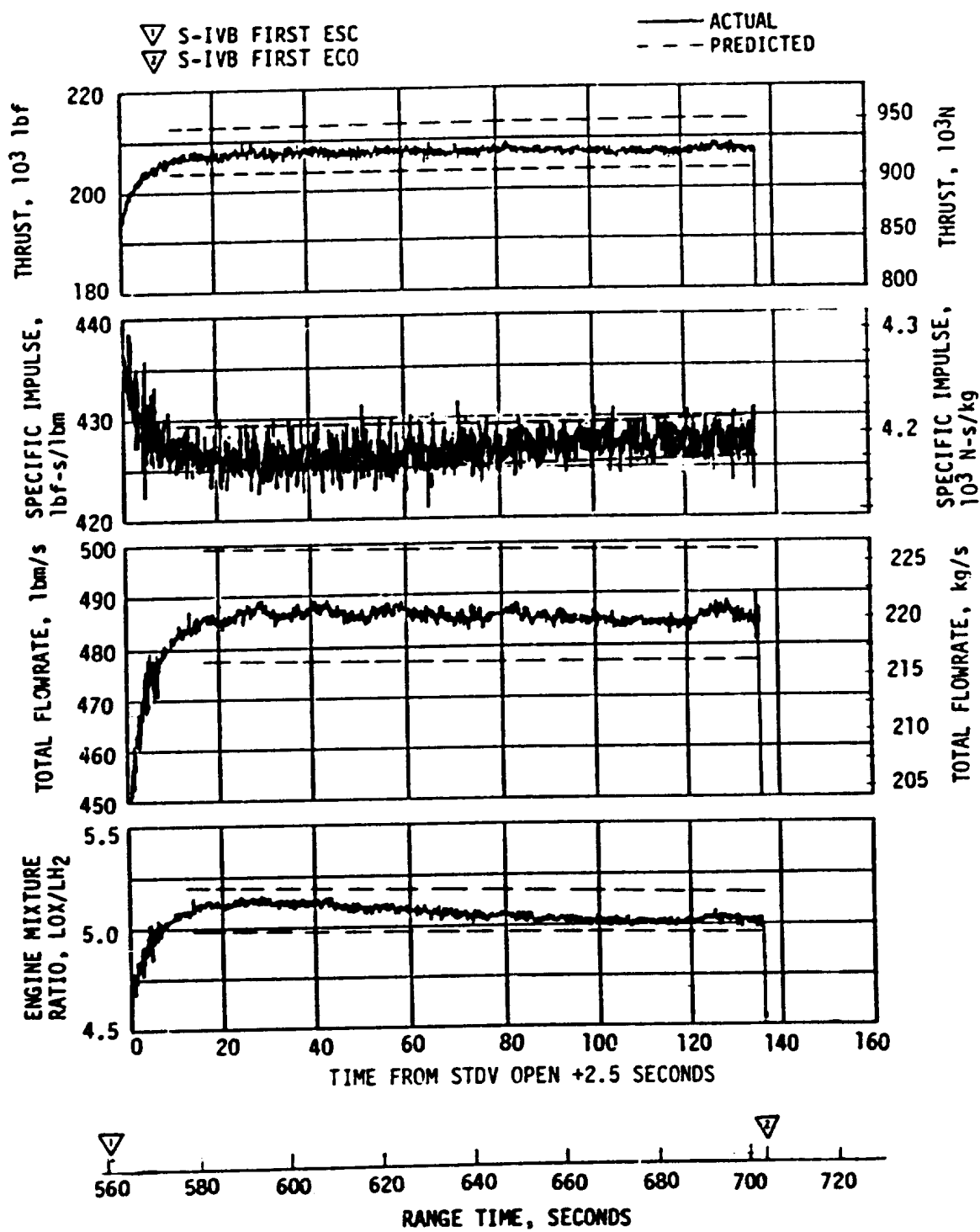


Figure 7-3. S-IVB Steady-State Performance

Table 7-1. S-IVB Steady State Performance - First Burn
(STDV Open +135-Second Time Slice at Standard Altitude Conditions)

PARAMETER	PREDICTED	RECONSTRUCTION	FLIGHT DEVIATION	PERCENT DEVIATION FROM PREDICTED
Thrust, lbf	207,197	205,797	-1,400	-0.68
Specific Impulse, lbf-s/lbm	428.3	427.7	-0.6	-0.14
LOX Flowrate, lbm/s	403.40	401.26	-2.14	-0.53
Fuel Flowrate, lbm/s	80.37	79.96	-0.41	-0.51
Engine Mixture Ratio, LOX/Fuel	5.019	5.018	-.001	-0.02

The first burn time was 138.8 seconds, terminated by a guidance velocity cutoff command, which was 3.7 seconds less than predicted for the actual flight azimuth of 91.5 degrees. This difference is composed of 4.1 seconds less due to the higher than expected S-II/S-IVB separation velocity and 0.4 second longer due to lower S-IVB performance. Total impulse from STDV open +2.5-seconds to ECO was 28.23×10^6 lbf-s which was 874,949 lbf-s less than predicted.

The engine helium control system performed satisfactorily during main-stage operation. An estimated 0.30 lbm of helium was consumed during first burn.

7.4 S-IVB SHUTDOWN TRANSIENT PERFORMANCE FOR FIRST BURN

S-IVB first ECO was initiated at 702.65 seconds and the ECO transient was satisfactory. The total cutoff impulse to zero thrust was 46,401 lbf-s which was 1237 lbf-s lower than the nominal predicted value of 47,638 lbf-s and within the ± 4100 lbf-s predicted band. Cutoff occurred with the MRCV in the 5.0 EMR position. Thrust data during the cutoff transient is presented in Figure 7-4.

The J-2 engine bleed valves normally open within seven seconds from Engine Cutoff Command (ECC) based on previous flight experience. However, the engine helium control package was modified for this flight to allow the purge valve to open and close at a higher pressure. This results in a longer time to adequately reduce the accumulator pressure to allow the bleed valves to open.

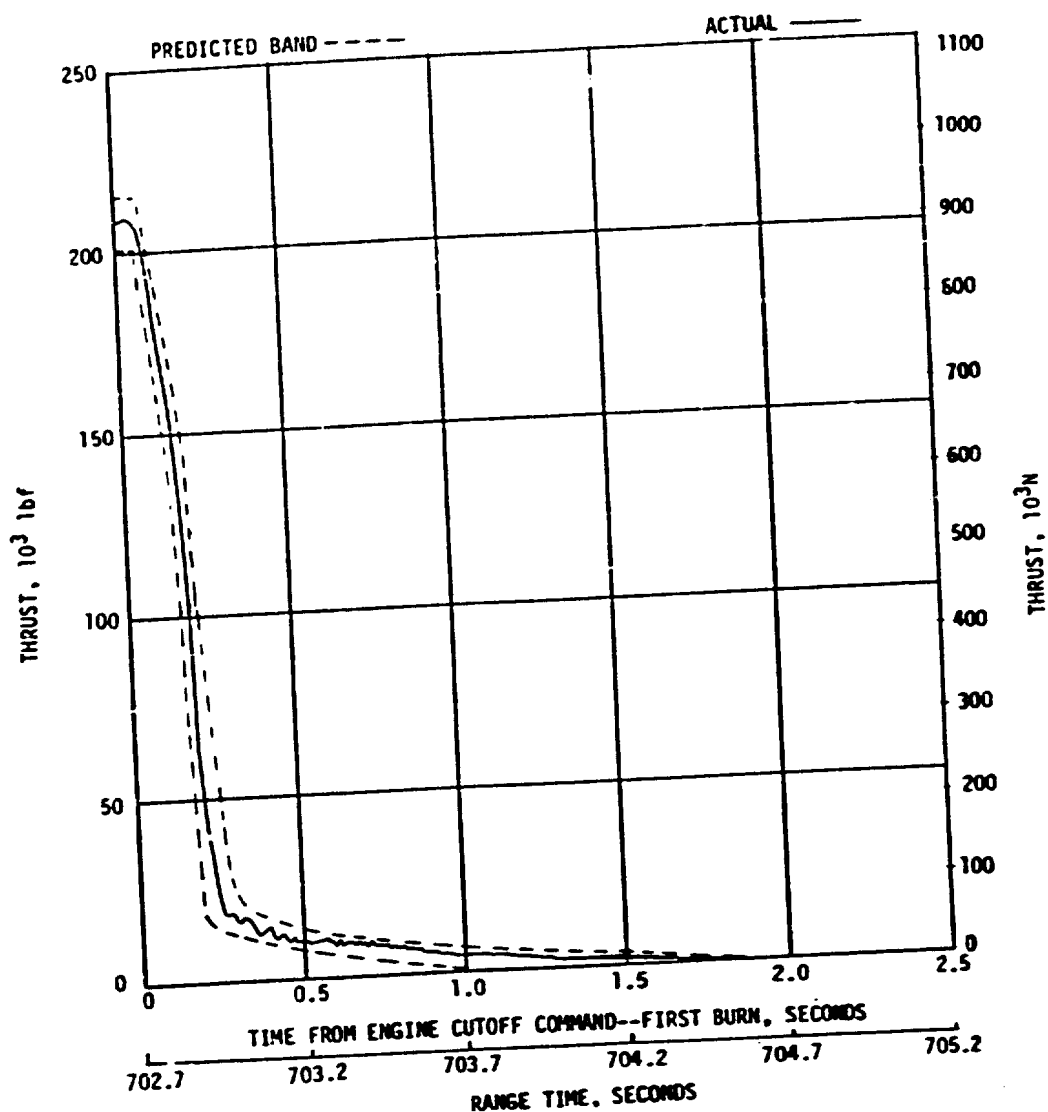


Figure 7-4. S-IVB Thrust Decay

Consequently, the bleed valves' opening time from ECC was increased from approximately 7 to 14 seconds.

7.5 S-IVB PARKING ORBIT COAST PHASE CONDITIONING

The LH₂ CVS performed satisfactorily, maintaining the fuel tank ullage pressure at an average level of 19.1 psia. This was well within the 18 to 21 psia band of the inflight specification.

The continuous vent regulator was activated at 761.8 seconds and was terminated at 11,020.8 seconds (03:03:40.8). The CVS performance is shown in Figure 7-5.

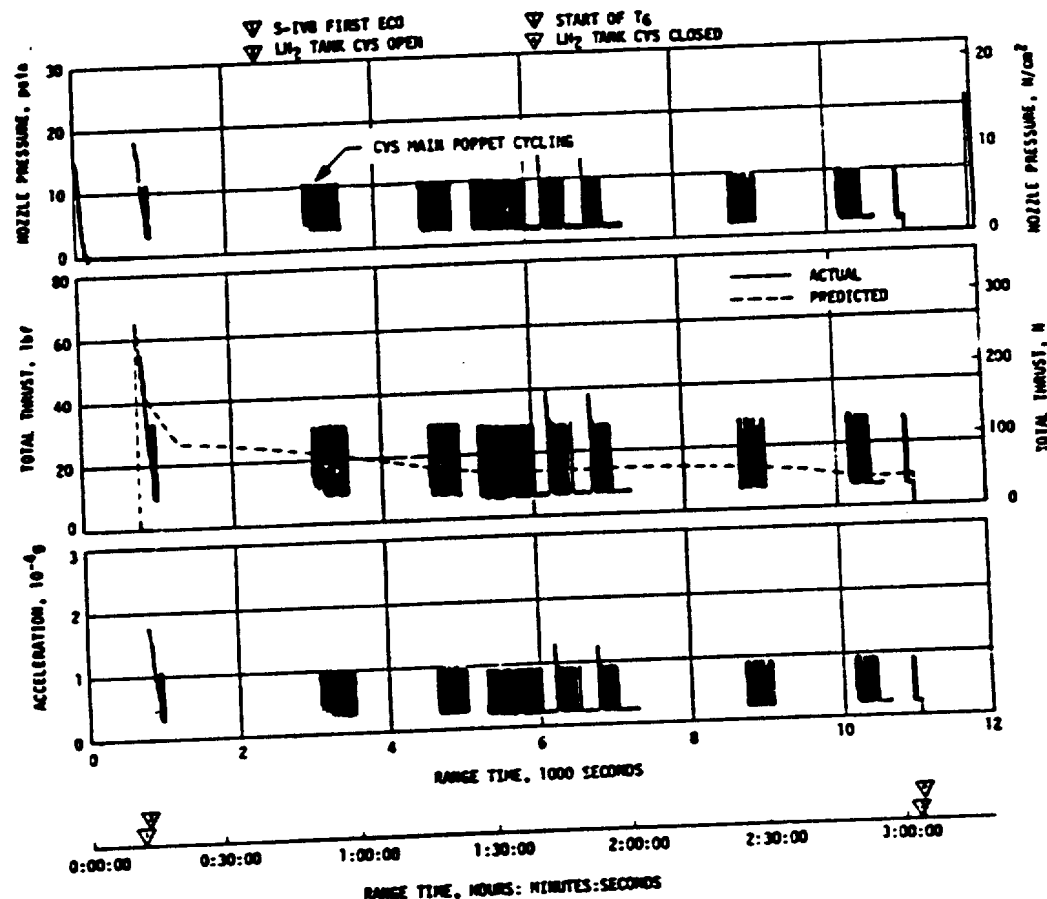


Figure 7-5. S-IVB CVS Performance - Coast Phase

The CVS regulator began cycling at 900 seconds, about 30 minutes earlier than on previous flights. The extended hold during launch countdown and the atmospheric conditions provided low initial LH₂ tank and propellant temperatures, which resulted in low boiloff and permitted regulator cycling early in the orbital coast period.

Calculations based on estimated temperatures indicate that the mass vented from the fuel tank during parking orbit was 2195 lbm and that the boiloff mass was 2405 lbm, compared to predicted values of 2330 lbm and 2540 lbm, respectively.

LOX boiloff during the parking orbit coast phase was approximately 10 lbm.

7.6 S-IVB CHILDDOWN AND BUILDUP TRANSIENT PERFORMANCE FOR SECOND BURN

Repressurization of the LOX and LH₂ tanks was satisfactorily accomplished by the O₂/H₂ burner. Burner "ON" command was initiated at 11,020.6 seconds (3:03:40.6). The LH₂ repressurization control valves were opened at burner "ON" +6.1 seconds, and the fuel tank was repressurized from 19.1 to 30.5 psia in 191 seconds. There were 26.2 lbm of cold helium used to repressurize the LH₂ tank. The LOX repressurization control valves were opened at burner "ON" +6.3 seconds, and the LOX tank was repressurized from 36.5 to 40.1 psia in 130 seconds. There were 3.7 lbm of cold helium used to repressurize the LOX tank. LH₂ and LOX ullage pressures are shown in Figure 7-6. The burner continued to operate for a total of 459 seconds providing nominal propellant settling forces. The performance of the AS-512 O₂/H₂ burner was satisfactory as shown in Figure 7-7.

The S-IVB LOX recirculation system satisfactorily provided conditioned oxidizer to the J-2 engine for restart. Fuel recirculation system performance was adequate and conditions at the pump inlet conditions were satisfactory at second STDV open. The LOX and fuel pump inlet conditions are plotted in the start and run boxes in Figure 7-8. At second ESC, the LOX and fuel pump inlet temperatures were -294.4 and -418.5°F, respectively.

Second burn fuel lead generally followed the predicted pattern and resulted in satisfactory conditions, as indicated by the fuel injector temperature. Since J-2 start system performance was nominal during coast and restart, no helium recharge was required from the LOX ambient repressurization system (bottle No. 2). The start tank performed satisfactorily during second burn blowdown and recharge sequence. The engine start tank was recharged properly and it maintained sufficient pressure during coast. The engine control sphere first burn gas usage was as predicted; the ambient helium spheres recharged the control sphere to a nominal level for restart.

The second burn start transient was satisfactory. The thrust buildup was

▽ BURNER START COMMAND
 ▽ LOX AND H₂ TANK REPRESSURIZATION VALVES OPEN
 ▽ IGNITION OF LOX TANK REPRESSURIZATION
 ▽ IGNITION OF H₂ TANK REPRESSURIZATION
 ▽ BURNER CUTOFF

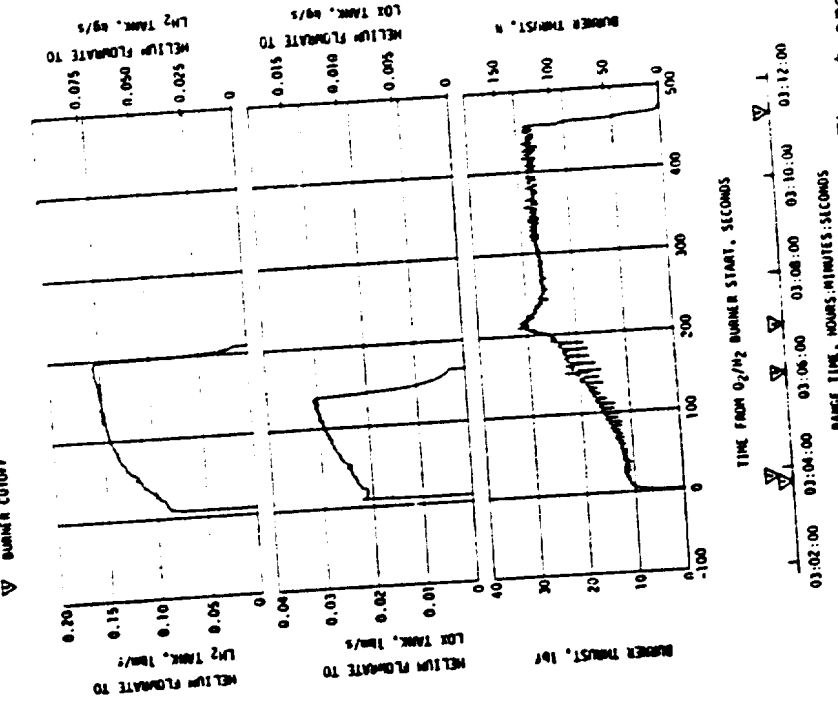


Figure 7-7. S-IVB 02/H₂ Burner Thrust and Pressurant Flowrate

▽ O₂/H₂ BURNER ON
 ▽ LOX AND LOX CRYOGENIC REPRESSURIZATION
 ▽ TERMINATION OF LOX TANK REPRESSURIZATION
 ▽ TERMINATION OF H₂ TANK REPRESSURIZATION
 ▽ O₂/H₂ BURNER OFF

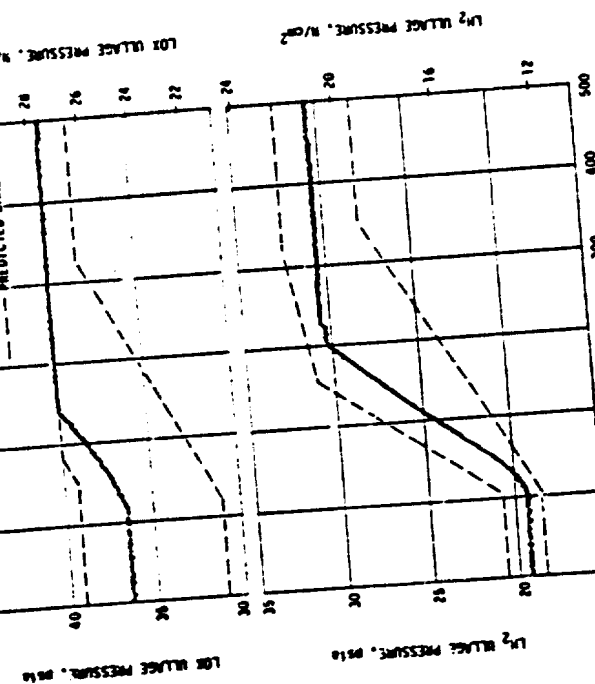


Figure 7-6. S-IVB Ullage Conditions During Repressurization Using 02/H₂ Burner

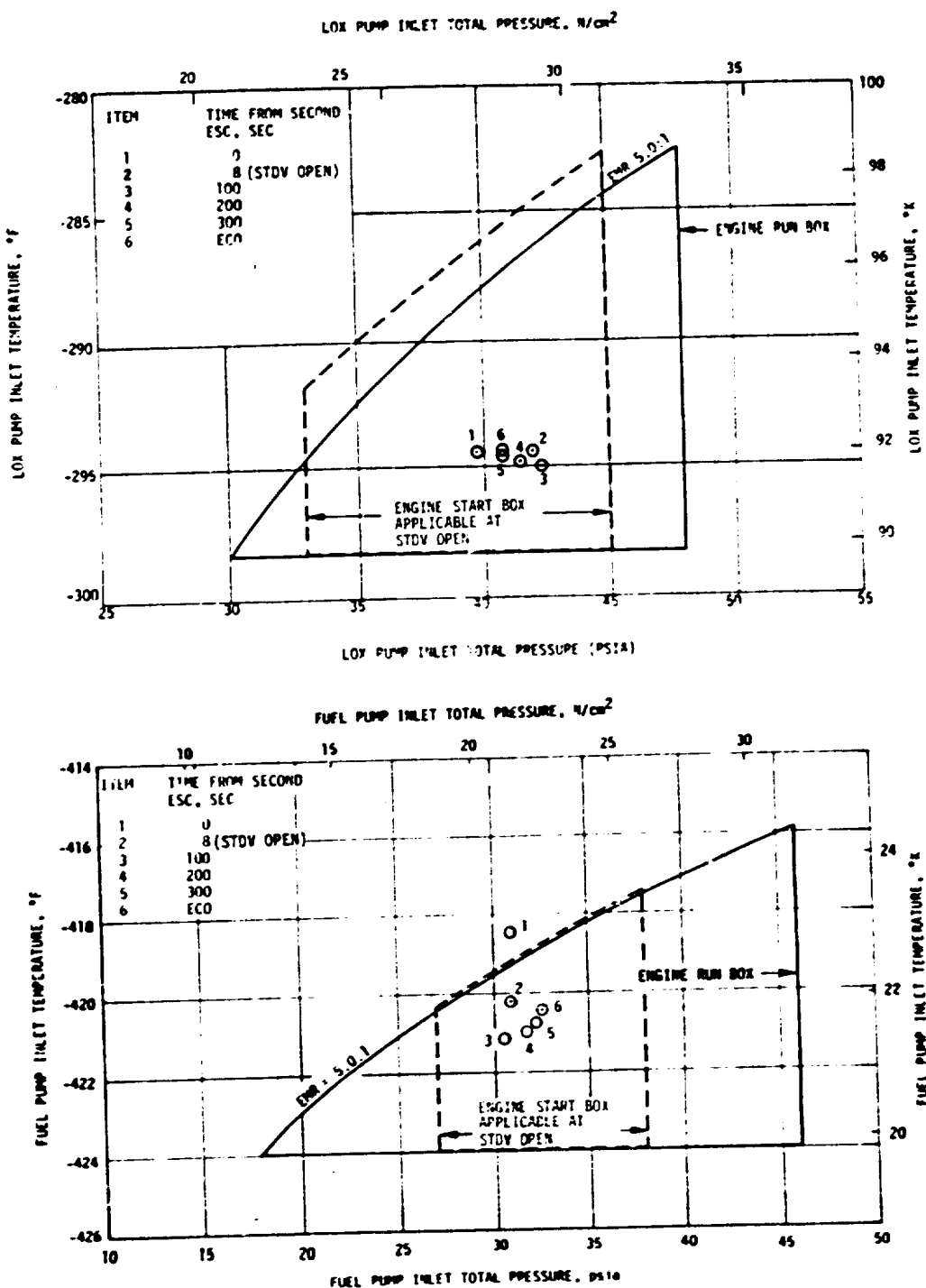


Figure 7-8. S-IVB Start Box and Run Requirements - Second Burn

within the limits set by the engine manufacturer and was similar to the thrust buildups observed on previous flights. The MRCV was in the proper full open (4.5 EMR) position prior to the second start. The total impulse from STDV open to STDV open +2.5 seconds was 182,502 lbf-s.

7.7 S-IVB MAINSTAGE PERFORMANCE FOR SECOND BURN

The propulsion reconstruction analysis showed that the stage performance during mainstage operation was satisfactory. A comparison of predicted and actual performance of thrust, specific impulse, total flowrate, and EMR versus time is shown in Figure 7-9. Table 7-2 shows the thrust, specific impulse, flowrates, and EMR deviations from the predicted at the STDV open +172-second time slice at standard altitude conditions. This time slice performance is the standard altitude performance which is comparable to the first burn slice at STDV open +135 seconds.

Thrust, specific impulse, and EMR were well within the predicted bands. The thrust and propellant flowrates were slightly lower than predicted.

The second burn time was 351.0 seconds which was 4.0 seconds longer than predicted. This difference is primarily due to the slightly lower S-IVB performance and heavier second burn vehicle mass. The total impulse from STDV open +2.5 seconds to ECO was 69.59×10^6 lbf-s which was 466,296 lbf-s more than predicted.

The engine helium control system performed satisfactorily during mainstage operation. An estimated 1.1 lbm of helium was consumed during second burn.

7.8 S-IVB SHUTDOWN TRANSIENT PERFORMANCE FOR SECOND BURN

S-IVB second ECO was initiated at 11,907.64 seconds. The ECO transient was satisfactory. The total cutoff impulse to zero thrust was 46,260 lbf-s which was 2123 lbf-s lower than the nominal predicted value of 48,383 lbf-s and within the +4100 lbf-s predicted band. Cutoff occurred with the MRCV in the 5.0 EMR position.

7.9 S-IVB STAGE PROPELLANT MANAGEMENT

A comparison of propellant masses at critical flight events, as determined by various analyses, is presented in Table 7-3. The best estimate full load propellant masses were 0.027 percent greater for LOX and 0.005 percent greater for LH₂ than predicted. This deviation was well within the required loading accuracy.

Extrapolation of best estimate residuals data to depletion, using the propellant flowrates, indicated that a LOX depletion would have occurred approximately 9.22 seconds after the second burn velocity cutoff.

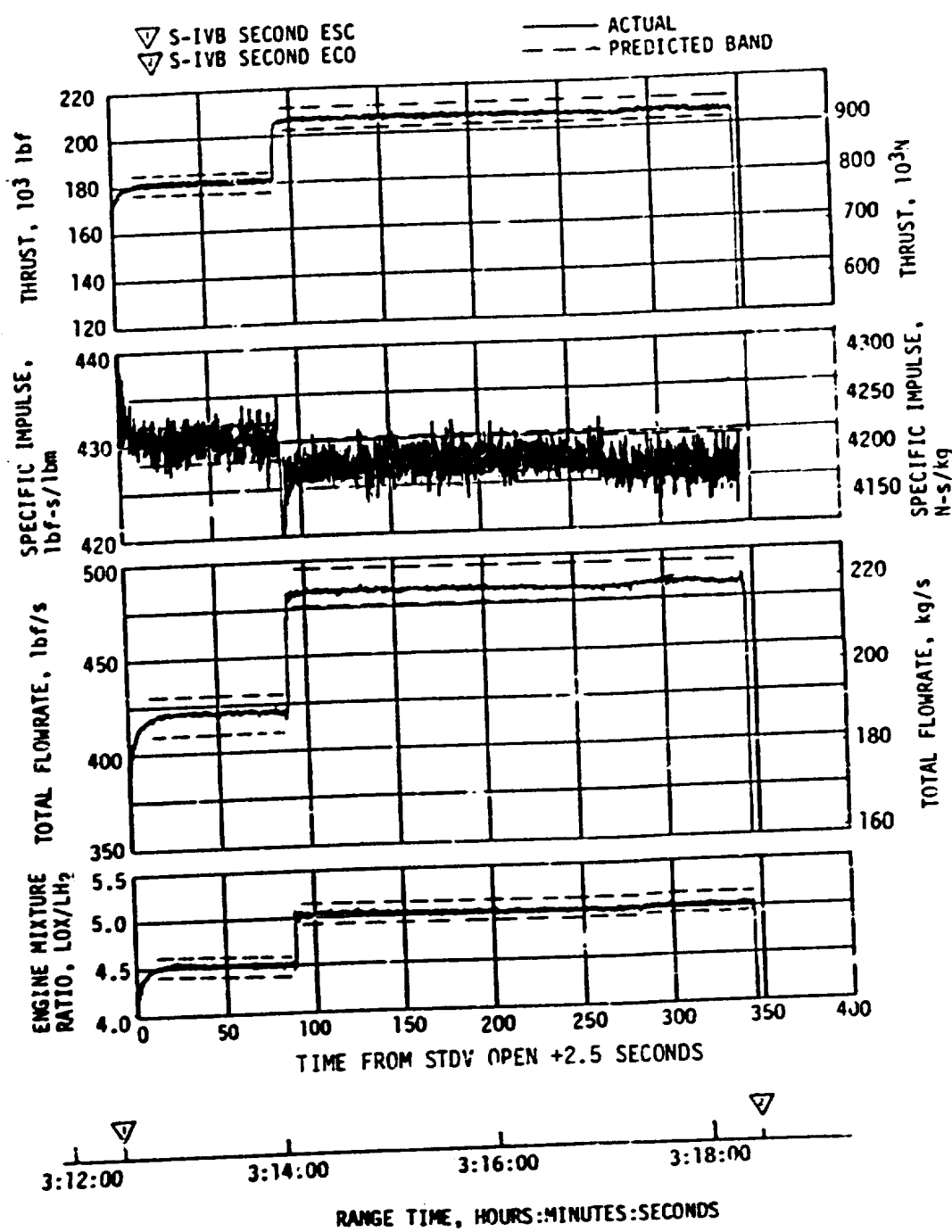


Figure 7-9. S-IVB Steady-State Performance - Second Burn

Table 7-2. S-IVB Steady State Performance - Second Burn
 (STDV Open +172-Second Time Slice at Standard Altitude Conditions)

PARAMETER	PREDICTED	RECONSTRUCTION	FLIGHT DEVIATION	PERCENT DEVIATION FROM PREDICTED
Thrust, lbf	207,197	205,608	-1,589	-0.77
Specific Impulse, lbf-s/lbm	428.3	427.6	-0.7	-0.16
LOX Flowrate, lbm/s	403.40	400.95	-2.45	-0.61
Fuel Flowrate, lbm/s	80.37	79.91	-.46	-0.57
Engine Mixture Ratio, LOX/Fuel	5.019	5.018	-.001	-0.02

Table 7-3. S-IVB Stage Propellant Mass History

EVENT	UNITS	PREDICTED		PU INDICATED (CORRECTED)		PU VOLUMETRIC		FLOW INTEGRAL		BEST ESTIMATE	
		LOX	LH ₂	LOX	LH ₂	LOX	LH ₂	LOX	LH ₂	LOX	LH ₂
S-IC Liftoff	lbm	195,584	43,750	195,421	43,724	195,421	43,944	195,495	43,600	195,636	43,752
First S-IVB ESC	lbm	195,574	43,749	195,421	43,724	195,421	43,944	195,495	43,600	195,636	43,750
First S-IVB Cutoff	lbm	138,265	32,297	140,141	32,536	140,141	32,700	139,840	32,536	140,017	32,675
Second S-IVB ESC	lbm	138,142	29,774	139,985	30,040	139,985	30,163	139,684	30,040	139,879	30,075
Second S-IVB Cutoff	lbm	3784	2097	4392	2240	4392	2251	4269	2224	4249	2224

The masses shown do not include mass below the main engine valves, as presented in Section 16.

During first burn, the pneumatically controlled two position Mixture Ratio Control Valve (MRCV) was positioned at the closed position for start and remained there, as programmed, for the duration of the burn.

The MRCV was commanded to the 4.5 EMR position 119.9 seconds prior to second ESC. The MRCV, however, did not actually move until it received engine pneumatic power.

At second ESC +100.0 seconds, the MRCV was commanded to the closed position (approximately 5.0 EMR) and remained there throughout the remainder of the flight.

7.10 S-IVB PRESSURIZATION SYSTEM

7.10.1 S-IVB Fuel Pressurization System

Performance of the LH₂ pressurization system was satisfactory during prepressurization, boost, first burn, coast phase, and second burn.

The LH₂ tank prepressurization command was received at -96.3 seconds and the tank pressurized signal was received 11.1 seconds later. Following the termination of prepressurization, the ullage pressure reached relief conditions (approximately 31.5 psia) and remained at that level until liftoff, as shown in Figure 7-10. A small ullage collapse occurred during the first 10 seconds of boost. The ullage pressure returned to the relief level by 130 seconds due to self pressurization. A similar ullage collapse occurred at S-IC/S-II separation. The ullage pressure returned to the relief level 35 seconds later. Ullage collapse during boost has been experienced on previous flights and is considered normal.

During first burn, the average pressurization flowrate was approximately 0.67 lbm/s, providing a total flow of 92.2 lbm. Throughout the burn, the ullage pressure was at the relief level, as predicted.

The LH₂ tank was satisfactorily repressurized for restart by the O₂/H₂ burner. The LH₂ ullage pressure was 30.6 psia at second burn ESC, as shown in Figure 7-10. The average second burn pressurization flowrate was 0.69 lbm/s until step pressurization, when it increased to 1.34 lbm/s. This provided a total flow of 288.2 lbm during second burn. Due to lower than expected ullage collapse, the ullage pressure was slightly above the predicted value, but well within acceptable limits, during the initial portion of second burn. The increase in pressurization flowrate resulting from the EMR change increased the ullage pressure to relief pressure (31.7 psia) at second ESC +195 seconds. The initiation of step pressurization at second ESC +280 seconds increased the relief level to 32.4 psia.

The LH₂ pump inlet Net Positive Suction Pressure (NPSP) was calculated from the pump interface temperature and total pressure. These values indicated that the NPSP at first burn ESC was 15.5 psi. At the minimum point, the

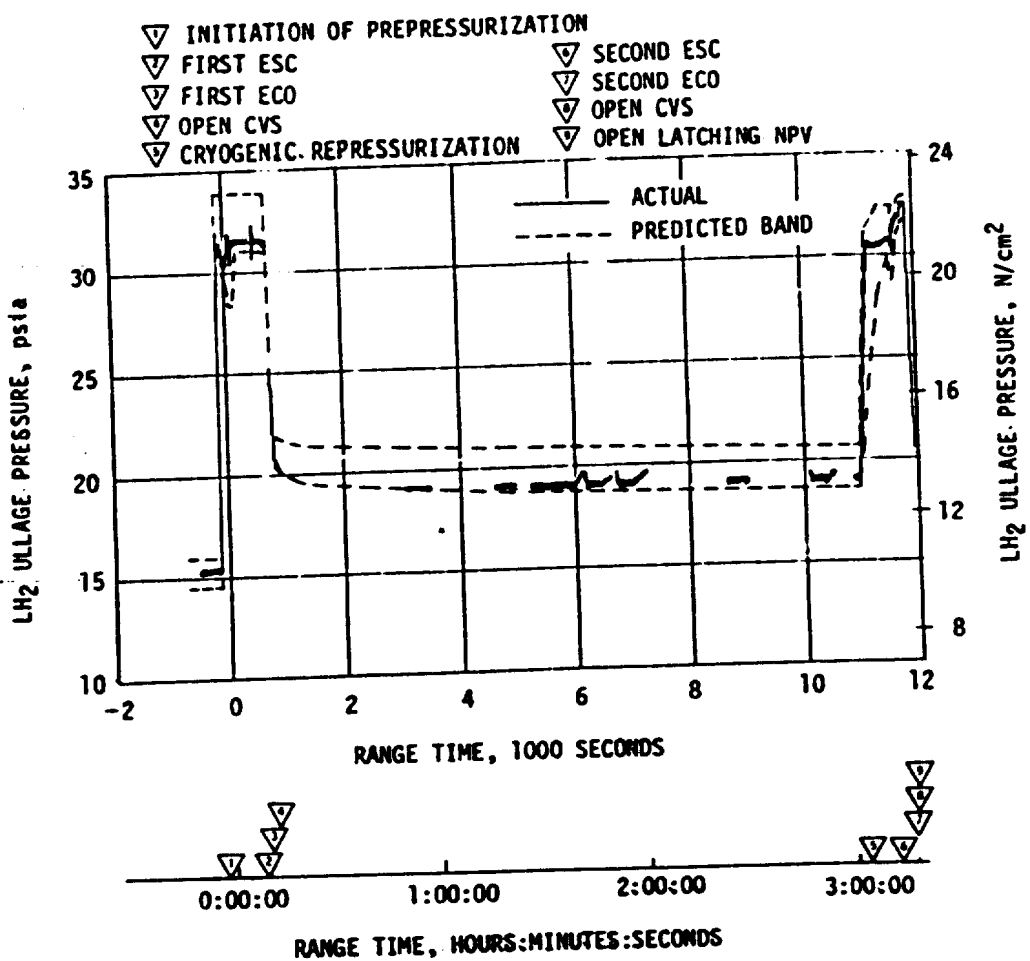


Figure 7-10. S-IVB LH₂ Ullage Pressure - First Burn, Parking Orbit and Second Burn

NPSP had satisfactory agreement with the predicted values. The NPSP at second burn STDV open was 7.0 psi, which was 2.5 psi above the minimum required value. Figures 7-11 and 7-12 summarize the fuel pump inlet conditions for first and second burns.

7.10.2 S-IVB LOX Pressurization System

LOX tank prepressurization was initiated at -167 seconds and increased the LOX tank ullage pressure from ambient to 40.1 psia in 14.9 seconds, as shown in Figure 7-13. Three makeup cycles were required to maintain the LOX tank ullage pressure before the ullage temperature stabilized.

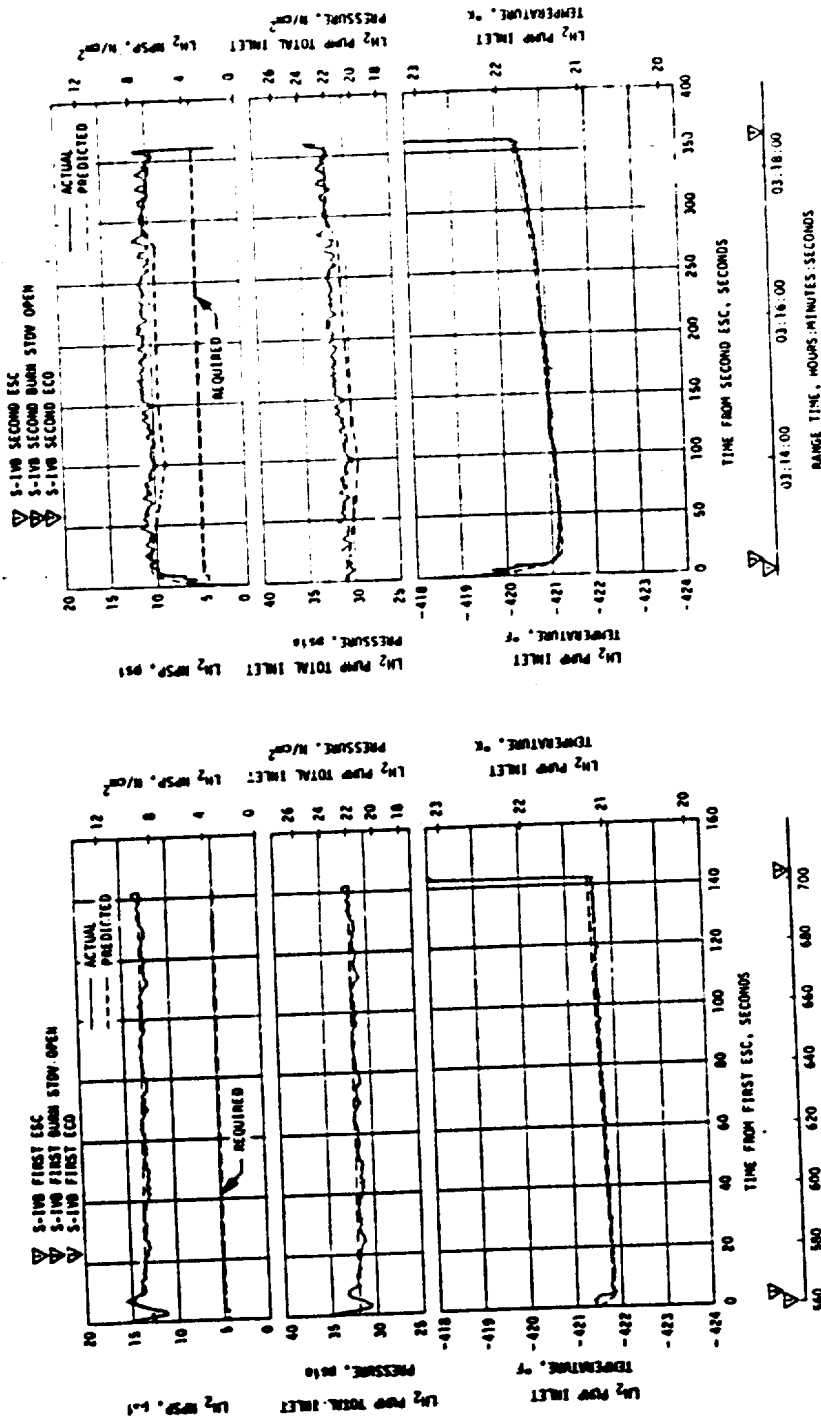


Figure 7-11. S-IVB Fuel Pump Inlet Conditions - First Burn

▼ 03:14:00
▼ 03:16:00
▼ 03:18:00

RANGE TIME, HOURS:MINUTES:SECONDS

▼ 03:14:00 03:16:00 03:18:00

RANGE TIME, HOURS:MINUTES:SECONDS

▼ 03:14:00 03:16:00 03:18:00

RANGE TIME, HOURS:MINUTES:SECONDS

Figure 7-12. S-IVB Fuel Pump Inlet Conditions - Second Burn

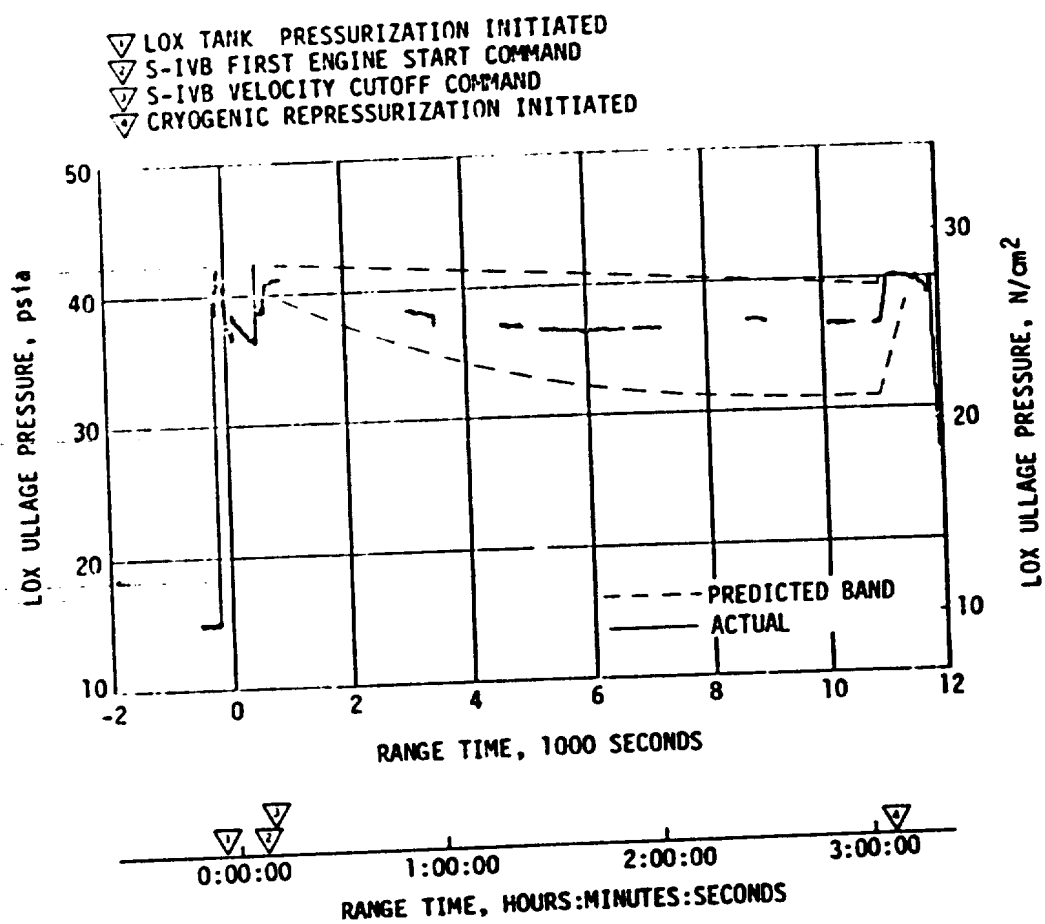


Figure 7-13. S-IVB LOX Tank Ullage Pressure - First Burn, Earth Parking Orbit, and Second Burn

At -96 seconds, fuel tank pressurization caused the LOX tank pressure to increase from 39.7 to 42.2 psia and unseat the tank pressure relief valve (NPV). The valve reseated at 40.6 psia and the ullage pressure then increased to 41.2 psia at liftoff.

During boost there was a nominal rate of ullage pressure decay caused by tank volume increase (acceleration effect) and ullage temperature decrease. No makeup cycles can occur because of an inhibit until after Timebase 4 (T4). LOX tank ullage pressure was 36.3 psia just prior to ESC and was increasing at ESC due to a makeup cycle.

During first burn, six over-control cycles were initiated, including the programmed over-control cycle initiated prior to ESC. The LOX tank pressurization flowrate variation was 0.24 to 0.29 lbm/s during under-control and 0.33 to 0.41 lbm/s during over-control system operation. This

variation is normal and is caused by temperature effects. Heat exchanger performance during first burn was satisfactory.

The LOX NPSP calculated at the interface was 21.7 psi at the first burn ESC. This was 8.9 psi above the NPSP minimum requirement for start. The LOX pump static interface pressure during first burn follows the cyclic trends of the LOX tank ullage pressure.

During orbital coast, the LOX tank ullage pressure experienced a decay similar to that experienced in the AS-511 flight. This decay was within the predicted band, and was not a problem.

The vehicle pitch maneuver at insertion resulted in minimal LOX sloshing and no tank venting. Mass addition to the ullage from LOX evaporation was minimal and the ullage pressure stayed below the relief range.

Repressurization of the LOX tank prior to second burn was required and was satisfactorily accomplished by the O₂/H₂ burner. The tank ullage pressure was 39.9 psia at second ESC and satisfied the engine start requirements.

Pressurization system performance during second burn was satisfactory. There was one over-control cycle, which was nominal. Helium flowrate varied between 0.33 and 0.41 lbm/s. Heat exchanger performance was satisfactory.

The LOX NPSP calculated at the engine interface was 22.5 psi at second burn ESC. This was 10.7 psi above the minimum required NPSP for second engine start. At all times during second burn, NPSP was above the required level. Figures 7-14 and 7-15 summarize the LOX pump conditions for first burn and second burn, respectively. The LOX pump run requirements for first and second burns were satisfactorily met.

The cold helium supply was adequate to meet all flight requirements. At first burn ESC, the cold helium spheres contained 382 lbm of helium. At the end of second burn, the helium mass had decreased to 165 lbm. Figure 7-16 shows helium supply pressure history.

7.11 S-IVB PNEUMATIC CONTROL PRESSURE SYSTEM

The stage pneumatic system performed satisfactorily during all phases of the mission. The pneumatic sphere pressure was 2390 psia at initiation of safing.

7.12 S-IVB AUXILIARY PROPULSION SYSTEM

The APS demonstrated close to nominal performance throughout flight and met control system demands as required out to the time of flight control computer shutoff at approximately 41,532 seconds (11:32:13).

The oxidizer and fuel supply systems performed as expected during the flight. The propellant temperatures measured in the propellant control

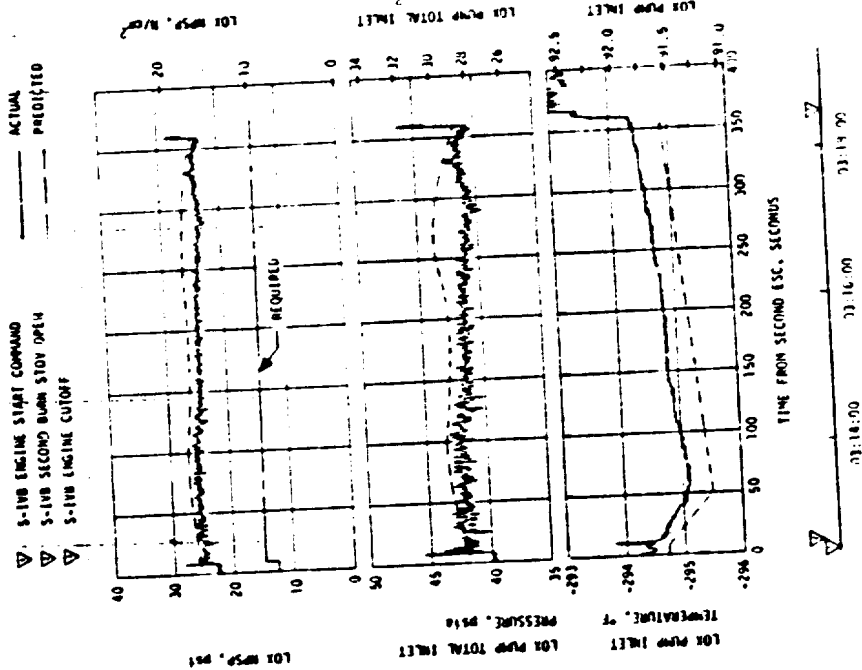


Figure 7-15. S-IVB LOX Pump Inlet Conditions -
Second Burn

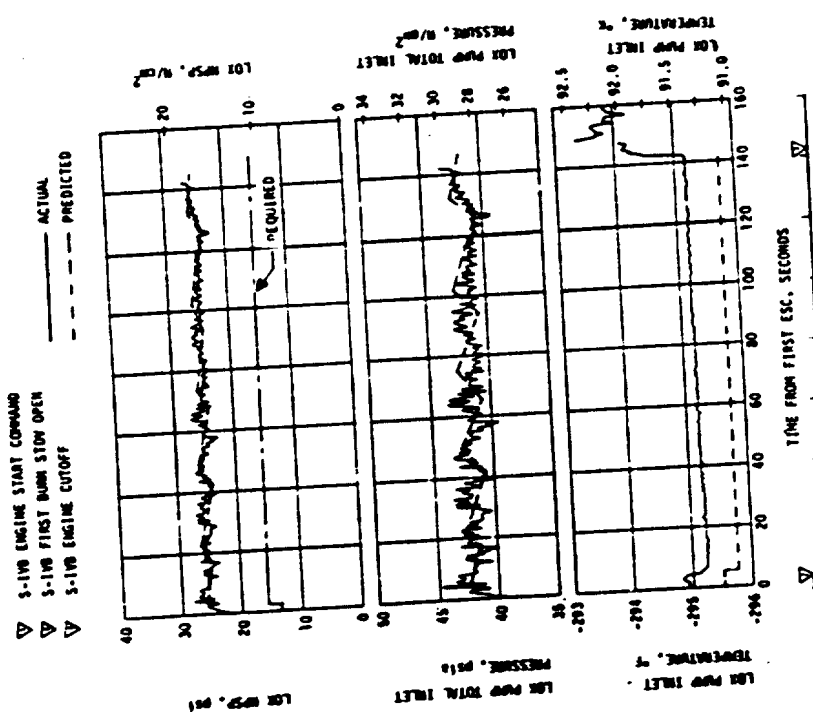


Figure 7-14. S-IVB LOX Pump Inlet Conditions -
First Burn

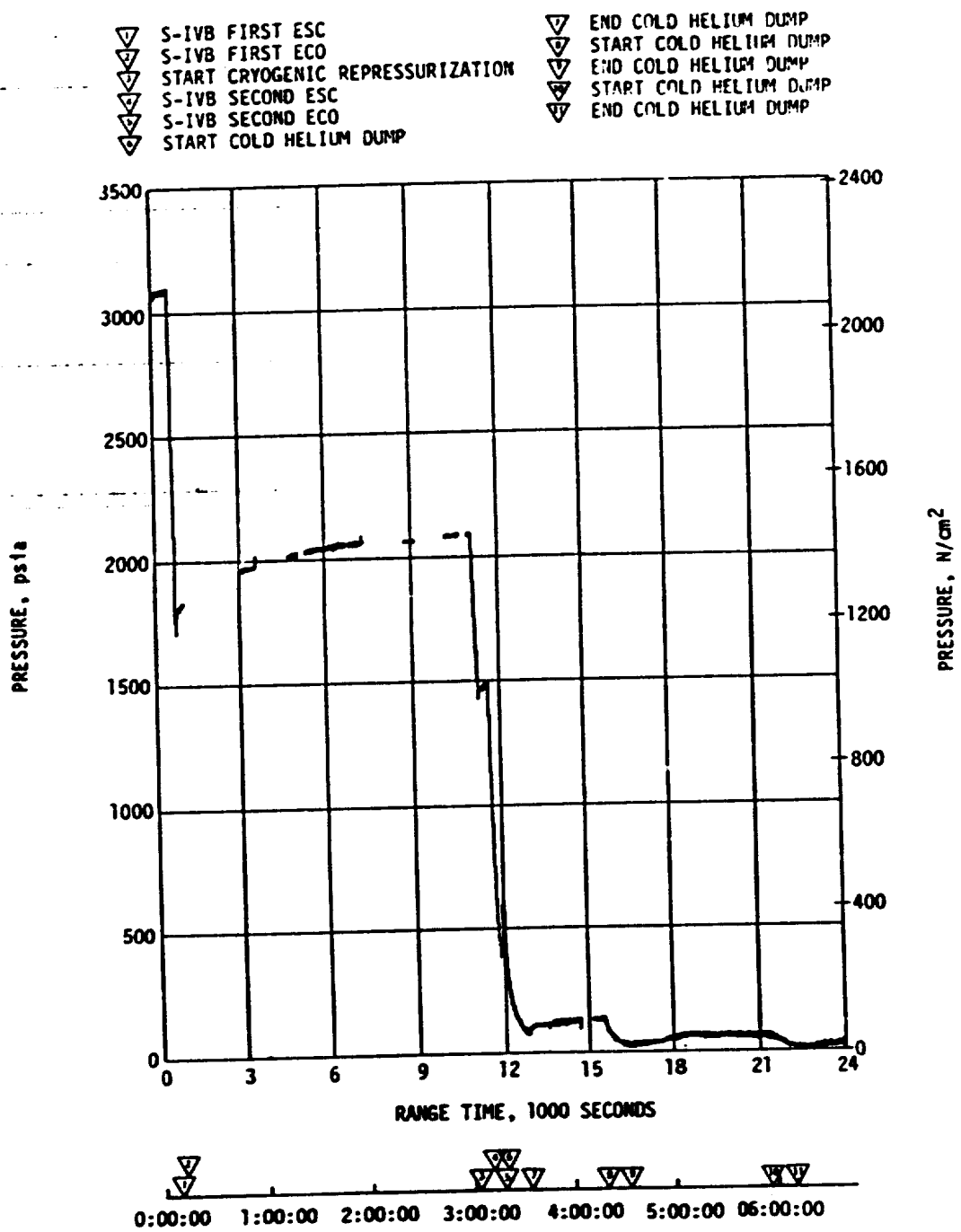


Figure 7-16. S-IVB Cold Helium Supply History

modules ranged from 60 to 107°F. The APS propellant usage was nominal. Table 7-4 presents the APS propellant usage during specific portions of the mission.

Table 7-4. S-IVB APS Propellant Consumption

	MODULE NO. 1				MODULE NO. 2			
	OXIDIZER		FUEL		OXIDIZER		FUEL	
	LBM	PERCENT	LBM	PERCENT	LBM	PERCENT	LBM	PERCENT
Initial Load	203.8		126.1		203.6		126.1	
First Burn (Roll Control)	0.5	0.2	0.3	.2	0.5	0.2	0.3	0.2
ECO to End of First APS Ullaging (86.7 sec time period)	14.6	7.2	11.3	9.0	12.5	6.1	10.0	7.9
End of First Ullage Burn to Start of Second Ullage Burn	11.2	5.5	7.0	5.6	5.8	2.9	3.6	2.9
Second Ullage Burn (76.7 sec Duration)	12.5	6.1	9.5	7.5	12.5	6.1	9.4	7.5
Second Burn (Roll Control)	0.3	0.1	0.2	.2	0.3	0.1	0.2	.2
ECO to Start of First Lunar Impact Burn at 22,200 sec.	28.0	13.7	18.8	14.9	36.5	17.9	25.1	19.9
First Lunar Impact Ullage (APS-1) Burn (98 sec Duration)	15.0	7.4	11.6	9.2	15.5	7.6	12.0	9.5
From End of First Lunar Impact Burn to Start of Second Lunar Impact Burn at 40,500 sec.	7.0	3.4	4.4	3.5	7.0	3.4	4.8	3.8
From Start of Second Lunar Impact (APS-2) Burn to FCC Cutoff (approximately 41,533 sec)	15.2	7.5	12.0	9.5	16.0	7.8	12.2	9.7
Total Propellant Usage	104.3	51.1	75.1	59.6	106.6	52.1	77.6	61.6

NOTE: The APS propellant consumption presented in this table calculated from helium bottle pressure and temperature measurements.

Both regulators functioned nominally during the mission. The module No. 1 regulator outlet pressure increased from 194 psia to 206 psia as the helium bottle temperature decreased from 80°F to -40°F. The module No. 2 regulator outlet pressure decreased from 194 psia to 186.5 psia as the helium bottle temperature increased from 85°F to 166°F. This thermal effect on the regulator outlet pressure is normal and has been observed on previous flights. The APS ullage pressures in the propellant tanks ranged from 182 psia to 200 psia.

The performance of the attitude control thrusters and the ullage thrusters was satisfactory throughout the mission. The thruster chamber pressures ranged from 95 to 101 psia. The ullage thrusters successfully completed the three sequenced burns of 86.7, 76.7, and 80.0 seconds; and the two ground commanded lunar impact burns of 98 seconds at 22,200 seconds (6:10:00) and 102 seconds at 40,500 seconds (11:15:00). The Passive Thermal Control (PTC) Maneuver was successfully completed prior to flight control computer shutdown.

The longest attitude control engine firing recorded during the mission was 0.890 seconds on the module No. 2 pitch engine at 12,810 seconds during the Transportation Docking and Ejection (TDE) maneuver.

The average specific impulse of the attitude control thrusters was approximately 220 lbf-s/lbm for both modules.

The sealing and transducer mounting block changes incorporated in the AS-512 APS modules to prevent helium leakage such as occurred during the AS-511 mission were apparently successful. No leakage occurred during the AS-512 mission.

7.13 S-IVB ORBITAL SAFING OPERATIONS

The S-IVB high pressure systems were safed following J-2 engine second ECO. The thrust developed during the LOX dump was utilized to provide a velocity change for S-IVB lunar impact. The manner and sequence in which the safing was performed is presented in Figure 7-17, and in the following paragraphs.

7.13.1 Fuel Tank Safing

The LH₂ tank was satisfactorily safed by utilizing both the Nonpropulsive Vent (NPV) and the CVS, as indicated in Figure 7-17. The LH₂ tank ullage pressure during safing is shown in Figure 7-18. At second ECO, the LH₂ tank ullage pressure was 32.4 psia; after three vent cycles, this decayed to zero at approximately 25,000 seconds (06:56:40). The mass of vented GH₂ agrees with the 2224 lbm of residual liquid and approximately 610 lbm of GH₂ in the tank at the end of powered flight.

7.13.2 LOX Tank Dumping and Safing

LOX dump performance in thrust, LOX flowrate, oxidizer mass, and LOX ullage pressure is shown in Figure 7-19.

At 22 seconds into the programmed LOX tank vent following second burn cutoff, vent system pressures and temperatures indicated momentary (less than 4 seconds) liquid venting. The amount of liquid vented is estimated at less than 20 pounds.

Probable cause was a combination of a later engine LOX bleed valve opening than on previous flights and a vehicle pitch rate correction at J-2 engine cutoff. The engine helium control package was modified, effective on AS-512, in response to a problem on the previous flight in which a S-II stage J-2 engine He purge valve failed to completely close for 10 seconds. This modification consisted of a change to the J-2 engine LOX Dome/Gas Generator Purge System to incorporate a Purge Control Valve with readjusted operating pressures, a redundant Purge Check Valve and Purge Control Valve Vent Line Orifice. These changes resulted in delaying the bleed valve opening from 7 to 14 seconds after engine cutoff command (reference paragraph 7.4). After second burn shutdown and prevalve/chilldown shutoff valve closure, the LOX pump inlet pressure increased to

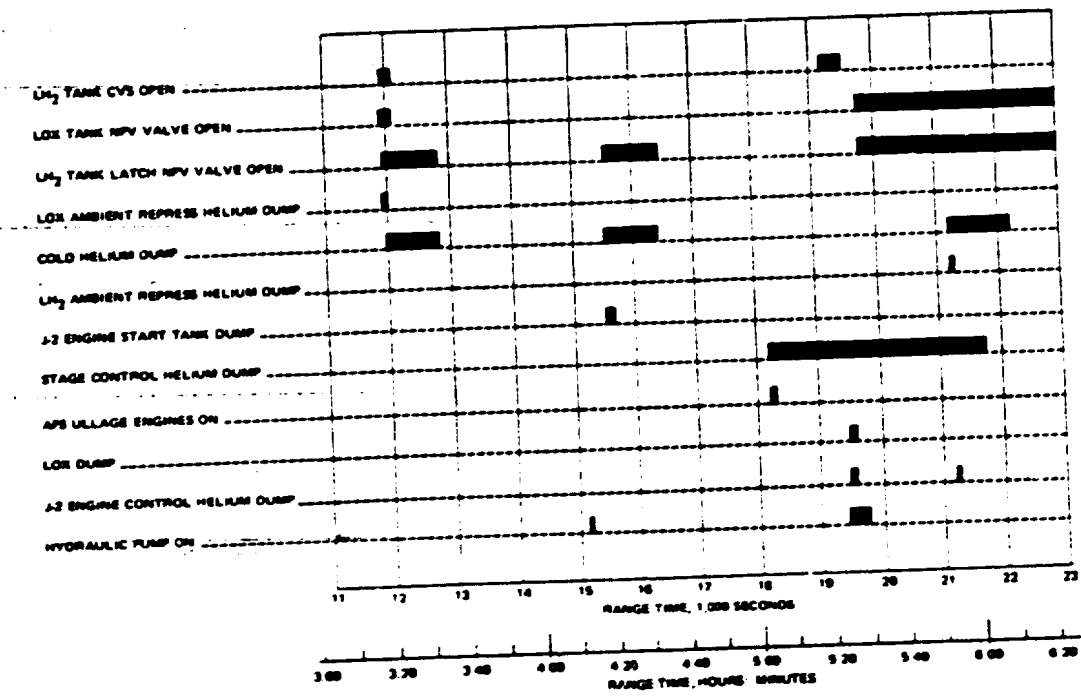


Figure 7-17. S-IVB LOX Dump and Orbital Safing Sequence

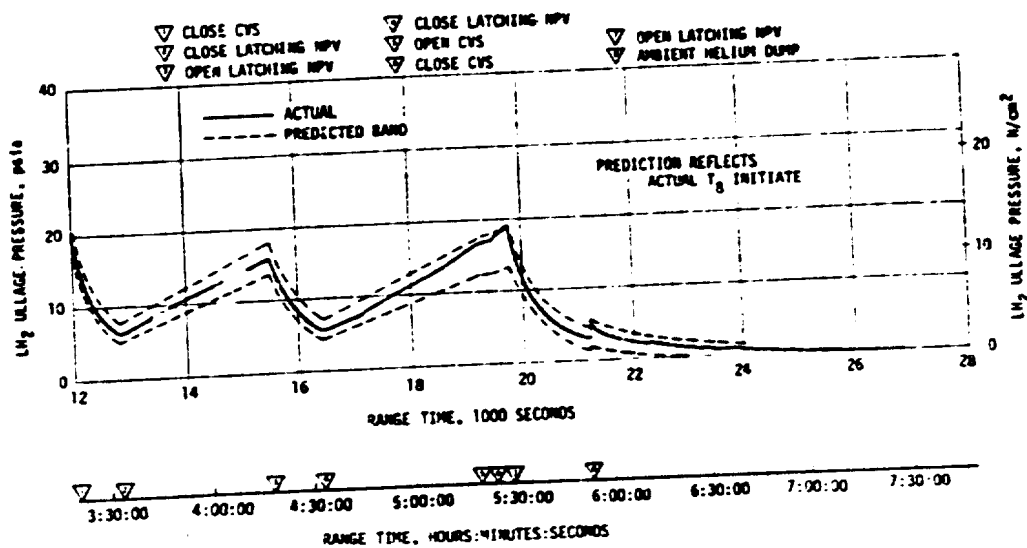


Figure 7-18. S-IVB LH₂ Ullage Pressure - Translunar Coast

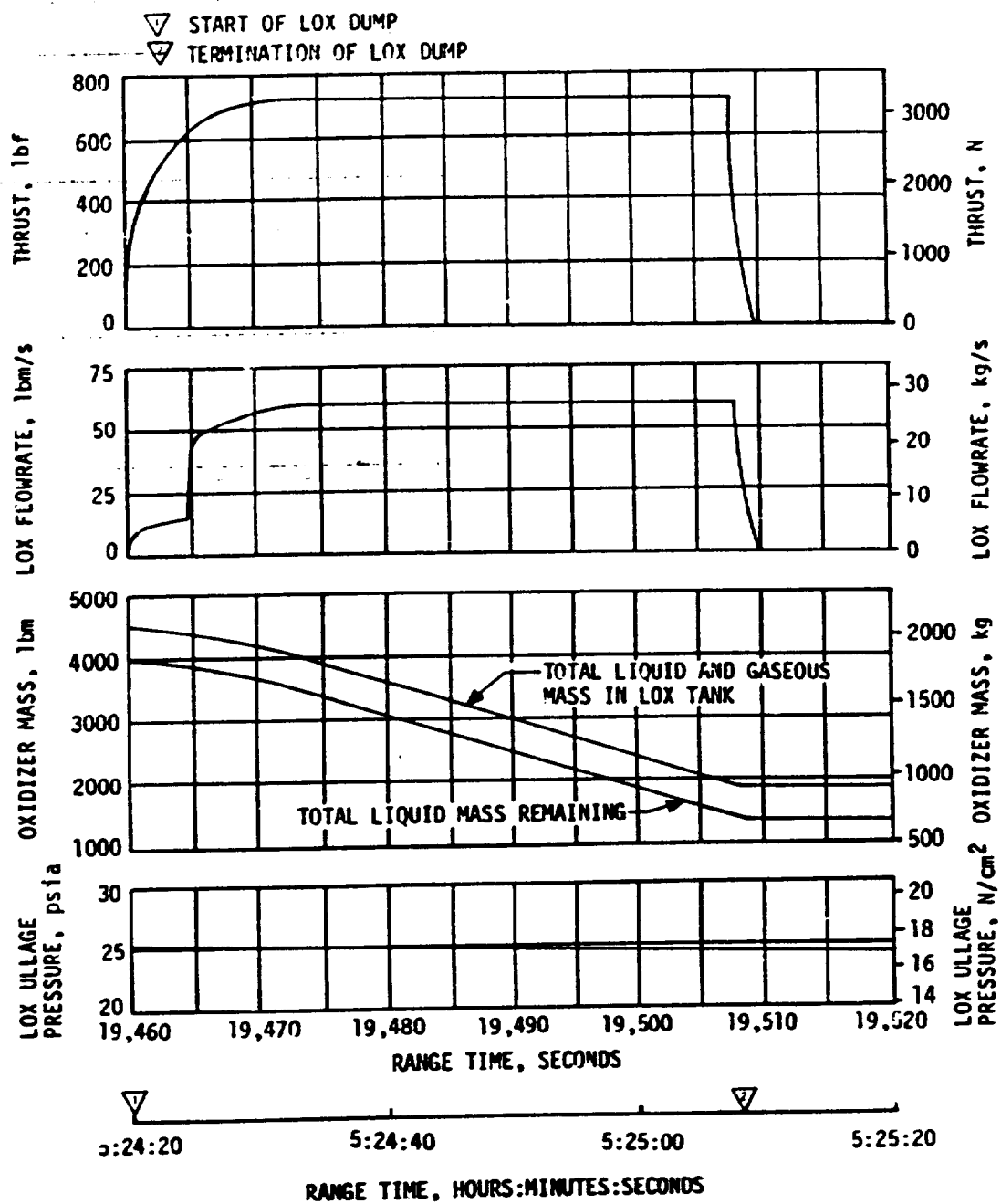


Figure 7-19. S-IVB LOX Dump Parameter Histories

a greater value than that seen on past flights due to the delayed bleed valve opening and consequent added heat transfer. At the same time LOX tank venting had reduced the LOX tank pressure. These two factors produce a greater pressure differential between the bleed valve inlet and the tank at the time of bleed valve opening than was seen on previous flights. This increased pressure differential would cause the bleed valve return flow velocity to be greater than normal. The probable sequence of events that led to liquid venting would be: slosh activity following cutoff and pitch attitude corrections momentarily submerged the LOX chilldown return line diffuser during the higher than normal return flow through this line from the bleed valve; the higher velocity flow into the small amount of remaining liquid dispersed LOX in the tank in such a manner that liquid was ingested into the non-propulsive vent system.

This LOX venting is not significant for an Apollo mission. However, it is of concern for a Skylab mission because of the need to conserve residuals for deorbiting the S-IVB/IU. In order to eliminate similar liquid venting on Skylab missions a procedural change to delay closing the chilldown valve has been incorporated.

Following vent completion, the ullage pressure rose gradually, due to self-pressurization, to 23.5 psia by the time of initiation of the transposition, docking, and ejection (TD&E) maneuver.

The LOX dump was initiated at 19,460.2 seconds (05:24:20.2) and was satisfactorily accomplished. A steady liquid flow of 368 gpm was reached in 13.3 seconds. The LOX residual at the start of dump was 3928 lbm. Calculations indicate that 2564 lbm was dumped. During dump, the ullage pressure decreased from 25.1 to 24.4 psia. A steady state LOX dump thrust of 720 lbf was attained. There was no ullage gas ingestion, and LOX dump ended at 19,507.9 seconds (05:25:01.9) as scheduled, by closing the Main Oxidizer Valve (MOV). The total impulse before MOV closure was 33,650 ibf-s, resulting in a calculated velocity change of 29.3 ft/sec.

At LOX dump termination +242 seconds, the LOX NPV valve was opened and latched. The LOX tank ullage pressure decayed from 24.4 psia at 19,750 seconds (05:29:10) to near zero pressure at approximately 24,000 seconds (06:40:00) as shown in Figure 7-20. Sufficient impulse was derived from the LOX dump, LH₂ CVS operation, and APS ullage burn to achieve lunar impact. For further discussion of the lunar impact, refer to Section 17.

7.13.3 Cold Helium Dump

A total of approximately 159 lbm of cold helium from the bottles submerged in the LH₂ tank was dumped through the cold He dump module during the three programmed dumps which occurred as shown in Figure 7-17.

7.13.4 Ambient Helium Dump

The two LOX ambient repressurization spheres were dumped through the LOX

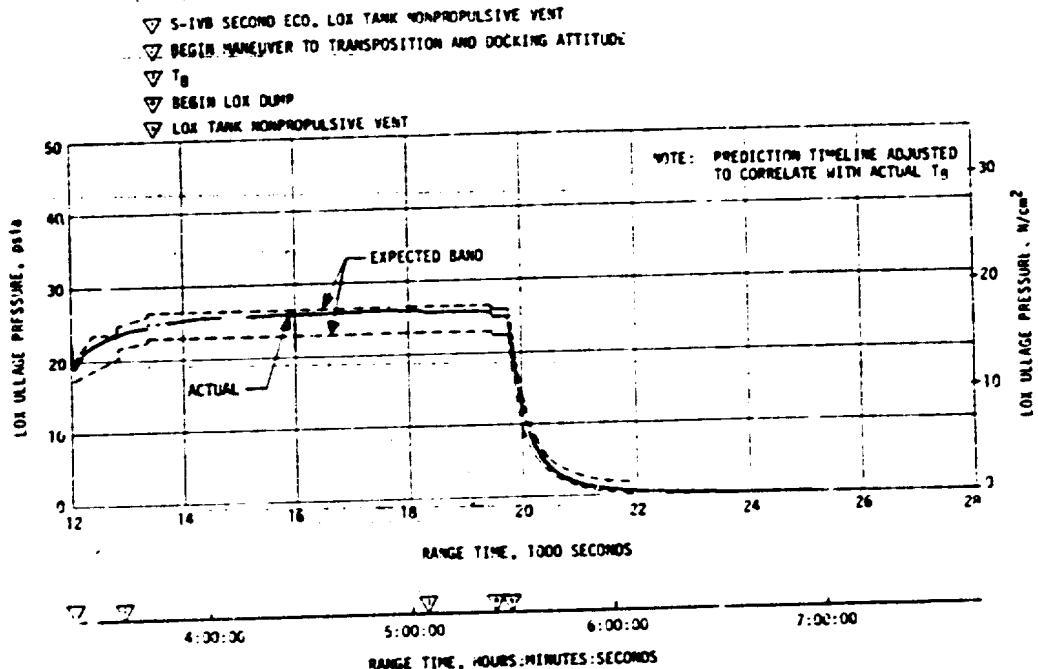


Figure 7-20. S-IVB LOX Tank Ullage Pressure - Translunar Coast

ambient repressurization control module into the LCX tank NPV system for 40 seconds beginning at 11,938 seconds (03:18:58). During this dump, the pressure decayed from 2900 psia to approximately 1200 psia.

A modification to the stage ambient He system, effective with AS-512, provided an interconnect through a normally closed valve to the APS He bottles. This interconnect provides an APS recharge capability in the event that He losses, similar to those seen on AS-511, occur. In order to retain the recharge capability through the initiation of the first APS lunar impact burn (APS-1), the AS-512 LH₂ ambient repressurization sphere dump time was reduced to 15 seconds as opposed to the AS-511 dump time of 1070 seconds. The 15-second dump began at 21,196 seconds (05:53:16) and approximately 16.3 lbm of He was dumped via the fuel tank and the non-propulsive vent.

7.13.5 Stage Pneumatic Control Sphere Safing

The stage pneumatic control sphere and the LOX repressurization spheres were safed by initiating the J-2 engine pump purge for a one-hour period. This activity began at 18,180 seconds (05:03:00) and satisfactorily reduced the pressure in the spheres from 2390 to 1300 psia.

7.13.6 Engine Start Tank Safing

The engine start tank was safed during a period of approximately 150 seconds beginning at 15,509 seconds (04:18:29). Safing was accomplished by opening the start tank vent valve. Pressure was decreased from 1300 to 20 psia with approximately 2.78 lbm of hydrogen being vented.

7.13.7 Engine Control Sphere Safing

The engine control sphere He dump was reduced to 16 sec on AS-512 as opposed to 1000 seconds on AS-511 to retain an APS He recharge capability as discussed in 7.13.4.

The safing of the engine control sphere began at 21,216.4 (05:53:36.4) by energizing the helium control solenoid to vent helium through the engine purge system. The helium control sphere vented until 21,232.4 seconds (05:53:52.4) with the initial pressure of 2970 psia reduced to 1340 psia at vent termination.

7.14 S-IVB HYDRAULIC SYSTEM

7.14.1 Boost and First Burn

The S-IVB Hydraulic System performed within the predicted limits after liftoff with no overboard venting of system fluid as a result of hydraulic fluid expansion. Prior to start of propellant loading, the accumulator was precharged to 2440 psia at 85°F. Reservoir oil level (auxiliary pump off) was 82 percent at 65°F at 20 minutes prior to launch.

During S-IC/S-II boost, all system fluid temperatures rose steadily when the auxiliary pump was operating and convection cooling was decreasing. The supply pressure during the S-IVB first burn was 3570 psia which was within the allowable limits of 3515 to 3665 psia.

The engine driven hydraulic pump operated properly as indicated by the current drop at engine start. Due to the close pressure settings of the pumps and the minimum demand by the system, the auxiliary pump provided the system internal fluid leakage rate of 0.63 gal/min (0.4 to 0.8 gpm allowable) for the burn. This is characterized by the pump motor current draw of 42 amperes.

7.14.2 Parking Orbit and Second Burn

The auxiliary hydraulic pump was programmed to flight mode "ON" at 11,198 seconds for engine restart preparations. System pressure stabilized at 3530 psia. At engine start, system pressure increased to 3580 psia and remained steady for approximately 140 seconds. The engine driven pump furnished most of the leakage flow during this period as evident by a current draw from Aft Battery No. 2 of 22 amperes. Following the first 140 seconds, the auxiliary hydraulic pump began sharing a portion of the leakage flow as indicated by an increase in current to

29 amps and a slight decrease in system pressure. Later, during the burn, the engine driven pump again furnished the leakage flow requirements for approximately 30 seconds followed by the auxiliary pump furnishing most of the leakage flow as evident by shifts in Aft Battery No. 2 current. System temperatures were normal during the burn. Pump inlet oil temperature responded to the changes in Aft Battery No. 2 current as the pressure and flow output varied between the two pumps.

The most probable cause for the interaction between the two pumps is the close pressure settings between the two pumps and frictional hysteresis in the engine drive pump flow-regulating mechanism. The operation of the hydraulic system during the first and second burns was nominal and the interaction between the two pumps is within the design specification of the system. It should be noted that this interaction between the two pumps does not indicate an impending malfunction and does not degrade the reliability of the engine driven pump or auxiliary hydraulic pump.

SECTION 8

STRUCTURES

8.1 SUMMARY

The structural loads experienced during the S-IC boost phase were well below design values. The maximum bending moment was 96×10^6 lbf-in at the S-IC LOX tank (less than 36 percent of the design value). Thrust cutoff transients experienced by AS-512 were similar to those of previous flights. The maximum longitudinal dynamic responses at the Instrument Unit (IU) were ± 0.20 g and ± 0.27 g at S-IC Center Engine Cutoff and Outboard Engine Cutoff (OECO), respectively. The magnitudes of the thrust cutoff responses are considered normal.

During S-IC stage boost, four to five hertz oscillations were detected beginning at approximately 100 seconds. The maximum amplitude measured at the IU was ± 0.06 g. Oscillations in the four to five hertz range have been observed on previous flights and are considered to be normal vehicle response to flight environment. POGO did not occur during S-IC boost.

The S-II stage center engine LOX feedline accumulator successfully inhibited the 16 hertz POGO oscillations. A peak response of ± 0.4 g in the 14 to 20 hertz frequency range was measured on engine No. 5 gimbal pad during steady-state engine operation. As on previous flights, low amplitude 11 hertz oscillations were experienced near the end of S-II burn. Peak engine No. 1 gimbal pad response was ± 0.06 g. POGO did not occur during S-II boost. The POGO limiting backup cutoff system performed satisfactorily during the prelaunch and flight operations. The system did not produce any discrete outputs and should not have since there was no POGO.

The structural loads experienced during the S-IVB stage burns were well below design values. During first burn the S-IVB experienced low amplitude, ± 0.14 g, 16 to 20 hertz oscillations. The amplitudes measured on the gimbal block were comparable to previous flights and within the expected range of values. Similarly, S-IVB second burn produced intermittent low amplitude oscillations of ± 0.10 g in the 11 to 16 hertz frequency range which peaked near second burn cutoff.

8.2 TOTAL VEHICLE STRUCTURES EVALUATION

8.2.1 Longitudinal Loads

The structural loads experienced during boost were well below design values. The AS-512 vehicle liftoff steady-state acceleration of 1.21 g was slightly higher than predicted (1.19 g), resulting in slightly higher

longitudinal loads but no associated problems. Maximum longitudinal dynamic response measured during thrust buildup and release was +0.21 g in the IU and +0.40 g at the Command Module (CM), Figure 8-1. Comparable values have been seen on previous flights.

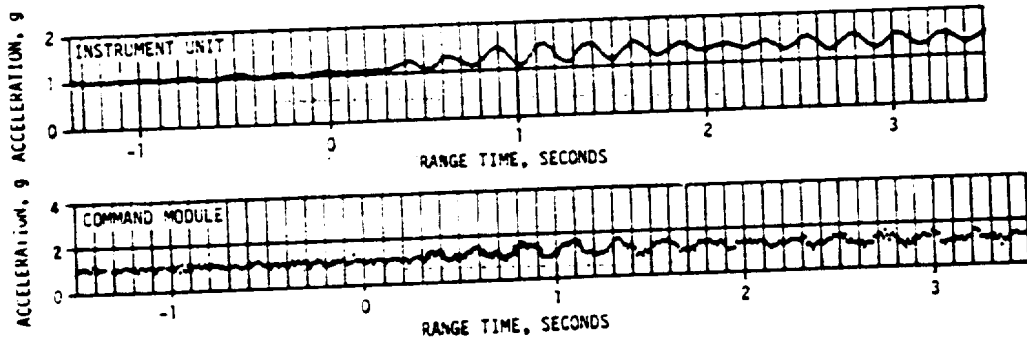


Figure 8-1. AS-512 Longitudinal Acceleration at IU and CM During Thrust Build-up and Launch

The F-1 engine thrust buildup rates were normal. The ignition sequence was 2-1-1-1 with engines 3 and 4 igniting early relative to the center engine. While the desired 1-2-2 start sequence was not achieved, the time deltas between pairs of diametrically opposed engines were within the 3σ dispersion used in preflight loads analyses (229 ms). The desired start sequence apparently cannot be expected with high confidence, but the structural loads on the SA-513 vehicle have been analyzed using start sequence stagger times both less and significantly larger than experienced on AS-512 with no problems arising. Thus the AS-512 ignition sequence has been established as not detrimental to SA-513.

The longitudinal loads experienced at the time of maximum bending moment (79 seconds) were as expected and are shown in Figure 8-2. The steady-state longitudinal acceleration was 2.02 g.

Figure 8-2 also shows that the maximum longitudinal loads imposed on the S-IC stage thrust structure, fuel tank, and intertank area occurred at S-IC CECO (139.3 seconds) at a longitudinal acceleration of 3.79 g. The maximum longitudinal loads imposed on all vehicle structure above the S-IC intertank area occurred at S-IC OECO (161.2 seconds) at an acceleration of 3.87 g.

Combined compression and tension loads were computed for the maximum bending moment, CECO and OECO conditions, using the loads shown in Figures 8-2 and 8-3 and measured ullage pressures. Those loads which produced minimum safety margins are plotted versus vehicle station along with the associated capabilities in Figure 8-4. The minimum ratio of capability to load is at Station 1541 for the OECO condition.

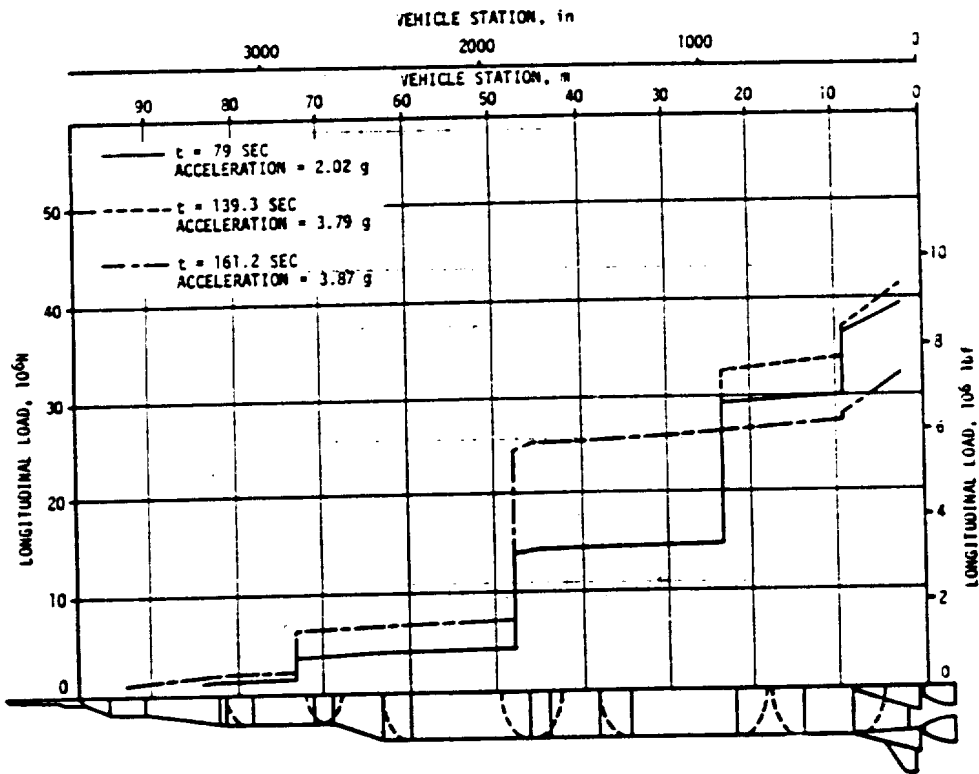


Figure 8-2. Longitudinal Load Distribution at Time of Maximum Bending Moment, CECO and OECO

8.2.2 Bending Moments

The peak vehicle bending moment occurred during the maximum dynamic pressure phase of boost at 79 seconds, Figure 8-3. The maximum bending moment of 96×10^6 lbf-in at vehicle station 1156 was less than 36 percent of design value.

8.2.3 Vehicle Dynamic Characteristics

8.2.3.1 Longitudinal Dynamic Characteristics

During S-IC stage boost, the significant vehicle response was the expected four to five hertz first longitudinal mode response. The low amplitude oscillations began at approximately 100 seconds and continued until S-IC CECO. The peak amplitude measured in the IU was ± 0.06 g, the same as seen on AS-510 and AS-511. The AS-512 IU response during the oscillatory period is compared with previous flight data in Figure 8-5. Spectral analysis of engine chamber pressure measurements shows no detectable buildup of structural/propulsion coupled oscillations. POGO did not occur during S-IC boost.

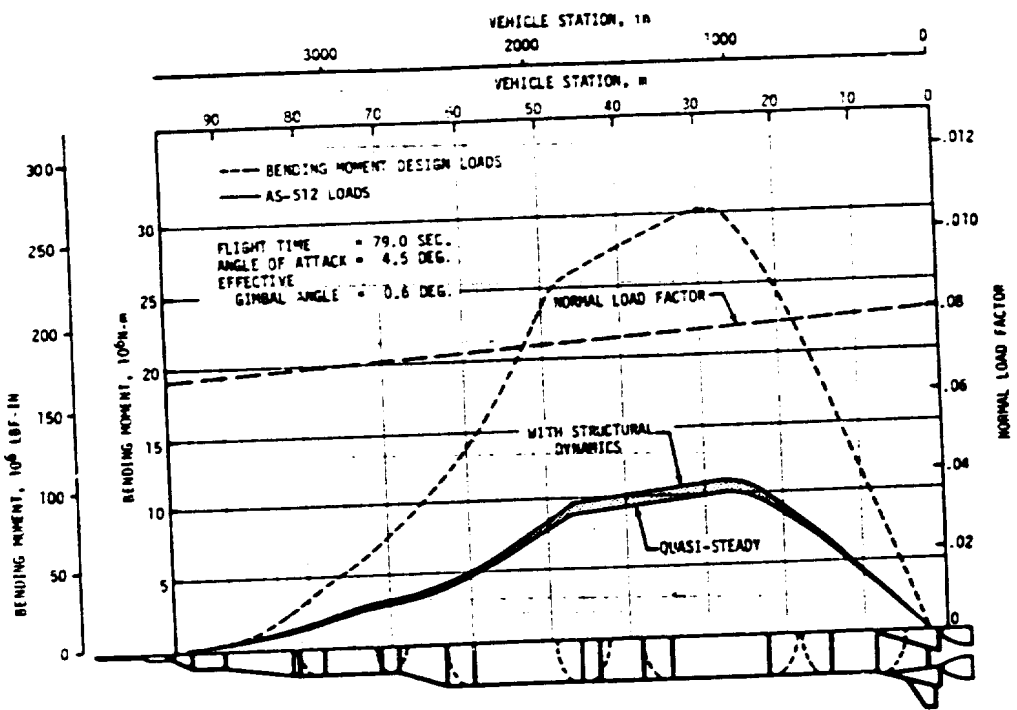


Figure 8-3. Bending Moment and Load Factor Distribution at Time of Maximum Bending Moment

Engine 2 outboard fuel suction duct 1 pressure data (D146-115) showed a high amplitude (8 psi peak) 11 Hz oscillation throughout most of the S-IC stage burn. The 11 Hz frequency content was also found in the related fuel suction inlet pressure measurement D4-102 where it appears as an aliased 1 Hz frequency of similar amplitude.

This 11 Hz oscillation has been observed on previous flights for various time periods and comparable amplitudes. In particular, the fuel inlets on Engine 5 on AS-501 (D146-115 and D149-115) exhibited a 12.5 Hz, 8 psi peak amplitude oscillation throughout flight.

This observed oscillation is a combined pump-propellant feed line pressure oscillation that occurs under certain Net Positive Suction Pressure (NPSP) conditions which were met for Engine 2 for most of the AS-512 S-IC burn time. This is not a POGO phenomenon. No significant vehicle response occurred at this frequency.

The AS-512 S-IC CECO and OECO transient responses were equal to or less than those of previous flights. The maximum longitudinal dynamics resulting from CECO were +0.20 g at the IU and +0.50 g at the CM, Figure 8-6. For OECO the maximum dynamics at the IU were +0.27 g and +0.80 g at the CM, Figure 8-7. The minimum CM acceleration level of -0.60 g occurred at approximately the same time and is somewhat lower

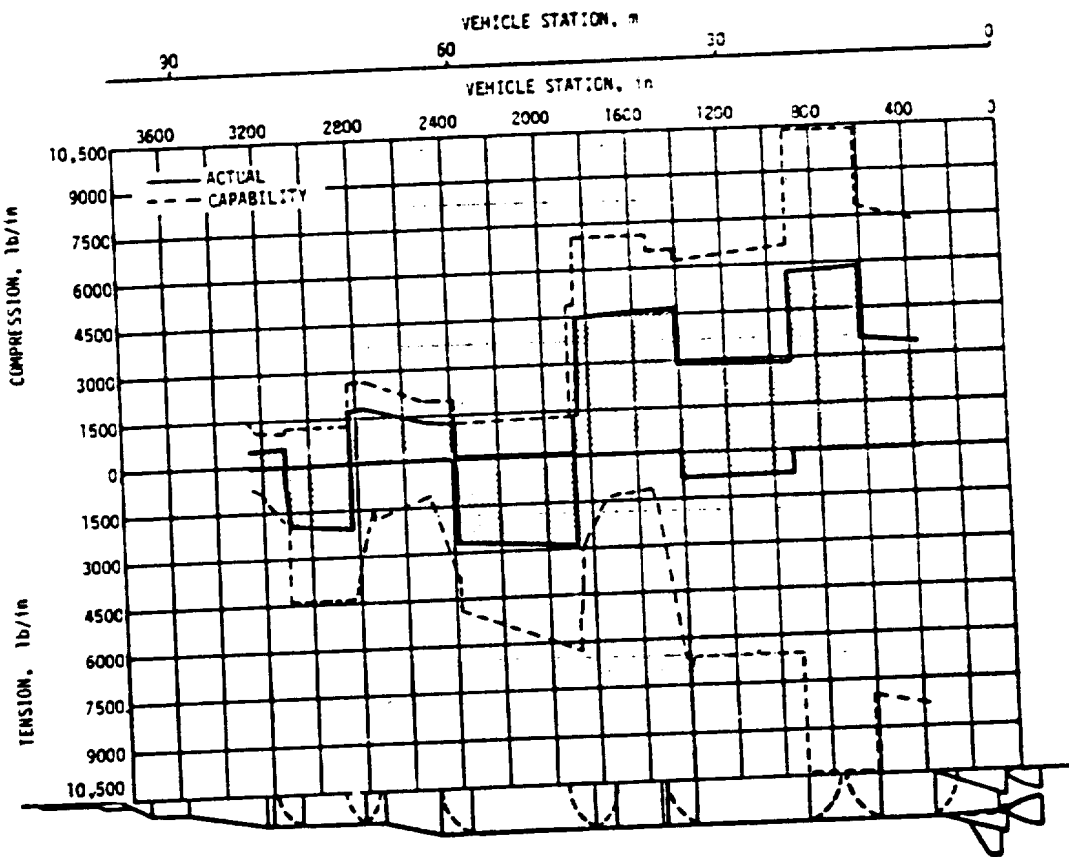


Figure 8-4. AS-512 Envelope of Combined Loads Producing Minimum Safety Margins for S-IC Flight

than on previous flights but considered normal.

The S-II stage center engine accumulator effectively suppressed the 16 hertz POGO phenomenon. The flight data show that the 16 hertz oscillations were inhibited with amplitudes comparable to those seen on AS-511, Figure 8-8. The peak 14 to 20 hertz center engine gimbal response was approximately ± 0.4 g, as compared to ± 0.5 g on AS-511. POGO did not occur.

The usual transient response in the center engine LOX pump inlet pressure was experienced shortly after accumulator fill was initiated. The peak response was approximately 34 psi peak-to-peak with a frequency of approximately 70 hertz, Figure 8-9. The LOX pump inlet pressure on AS-511 had a higher frequency content, a longer duration, and lower amplitude (13 psi peak-to-peak) but AS-512 is similar to AS-510 (45 psi peak-to-peak at 68 hertz). Such variations are not unique and the causes are attributed to the individual pump characteristics. There are no parallel increases in responses among the other engine pressures and the structural accelerations which again indicates the lack of strong coupling between the transient pressure response and the structural accelerations.

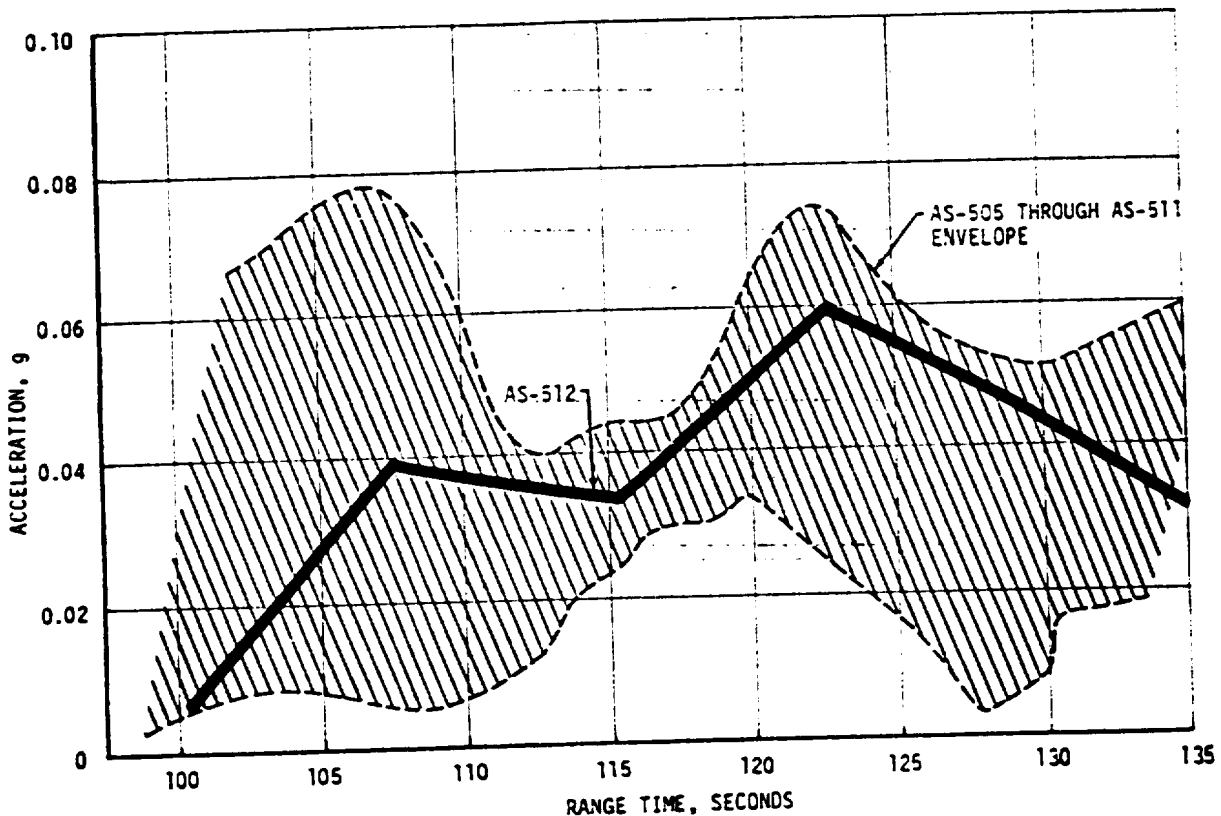


Figure 8-5. IU Vibration During S-IC Burn (Longitudinal)

As on prior flights, very low 11 hertz oscillations were noted near the end of S-II burn. The AS-512 peak engine No. 1 gimbal pad response was ± 0.06 g as compared to ± 0.07 g on AS-511.

During S-II burn, between 184 and 207 seconds range time, the vibration level on the S-IVB gimbal block was discernible above the noise floor, Figure 8-10. The maximum acceleration of the gimbal block in this interval was about ± 0.06 g. The signature of this signal appears to be wide band random. No signature similar to the S-IVB gimbal block oscillation was apparent on the various S-II dynamic parameters, i.e., the structural vibrations, the LOX pump inlet pressure fluctuations and the combustion chamber pressure fluctuation. Figure 8-11 compares the spectrum of the S-IVB gimbal block signal with the spectrum of the S-II center engine thrust pad. The spectrum associated with the center engine indicates a very low level response concentrated in the 20 hertz region. The S-IVB gimbal block has the character of a random response across the frequency spectrum. This demonstrates that the S-IVB phenomena is

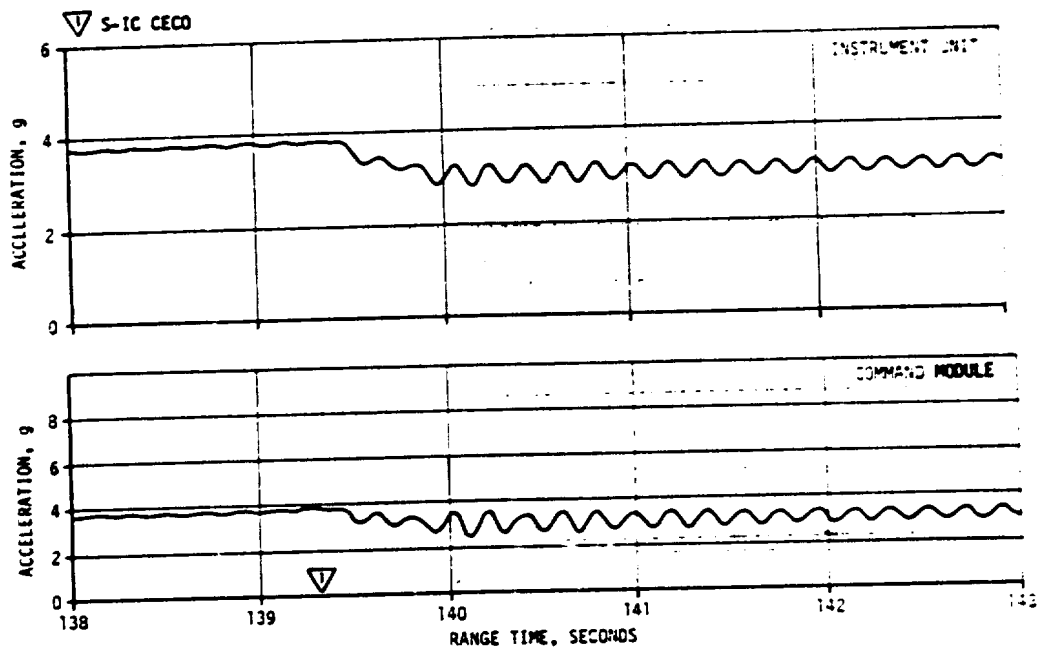


Figure 8-6. AS-512 Longitudinal Acceleration at IU and CM
During Center Engine Cutoff

not the result of a forced response due to an excitation emanating from the S-II. The S-IVB gimbal block vibration spectrum shows an order of magnitude increase when the noise occurs whereas the S-IVB LOX pump inlet pressure shows little change, Figure 8-12. The higher levels at frequencies from 5 to 20 hertz on the gimbal block do not occur in the LOX pump inlet pressure. Therefore it is concluded that the disturbance is not valid vibration data. Also, the amplitude during this disturbance, if valid, would produce insignificant dynamic loads on the stage.

During AS-512 S-IVB first burn, low frequency (16 to 20 hertz) longitudinal oscillations very similar to those observed on AS-511 were evident. The AS-512 amplitudes (± 0.14 g at gimbal block) were well below the maximum measured on AS-505 (± 0.30 g) and within the expected range of values.

AS-512 S-IVB second burn produced intermittent 11 to 16 hertz oscillations similar to those experienced on previous flights. The oscillations began approximately 135 seconds prior to cutoff and had a maximum value of ± 0.10 g measured on the gimbal block. This compared to ± 0.05 g on AS-510 and ± 0.08 g on AS-511.

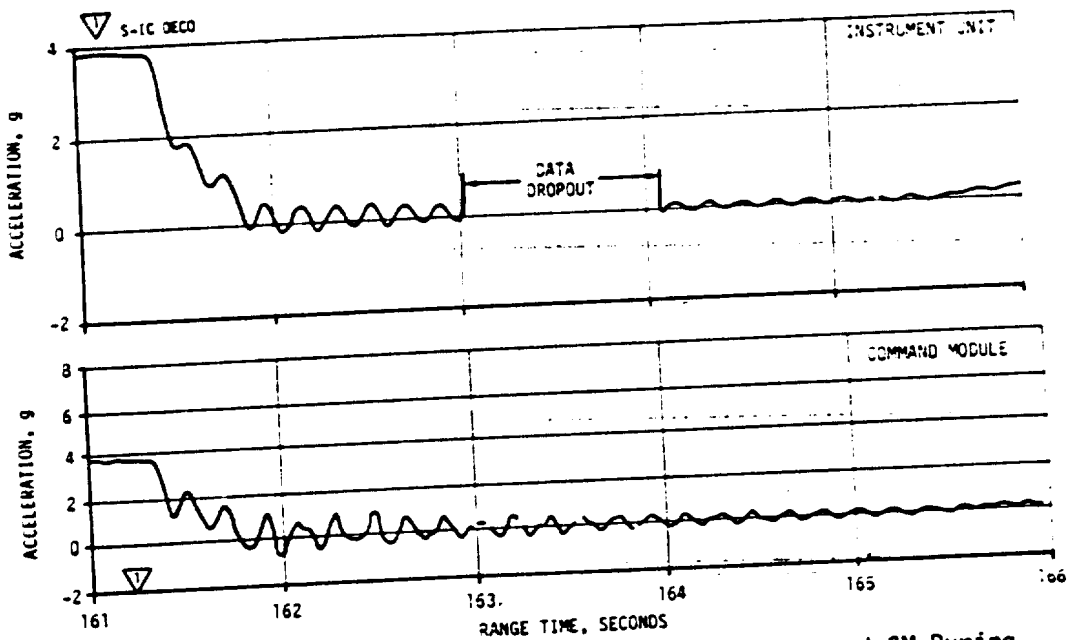


Figure 8-7. AS-512 Longitudinal Acceleration at IU and CM During Outboard Engine Cutoff

8.2.4 Vibration

There were no significant vibration environments identified on AS-512. A comparison of AS-512 data with data from previous flights show similar trends and magnitudes.

The "buzz" reported by the astronauts on AS-511 flight is again apparent on AS-512 at approximately 63 hertz in the pump inlet pressure measurement as it has been on previous flights. The vibrations can also be seen on selected propulsion pressure measurements (Figure 8-13). The AS-512 data show amplitudes similar to AS-511 (less than 1.0 psi rms). A review of AS-510 data showed similar vibration at approximately 72 hertz. The vibration is related to normal stage propulsion system operation and probably characteristic of the J-2 turbomachinery. These vibrations pose no POGO or any other structural concerns, and are of very low amplitude.

8.3 S-II POGO LIMITING BACKUP CUTOFF SYSTEM

The backup cutoff system provides for automatic S-II CECO if vibration response levels exceed predetermined levels within the preselected frequency band. The system consists of three sensors, a two-out-of-three voting logic, an engine cutoff arming function, and an automatic disable function which is effective until the arming operation has occurred.

The system did not produce discrete outputs at any time. The accelerometer analog outputs were well below the levels which would produce a

discrete output even during the engine start period when the system was not armed. After arming, the analog output did not exceed one g.

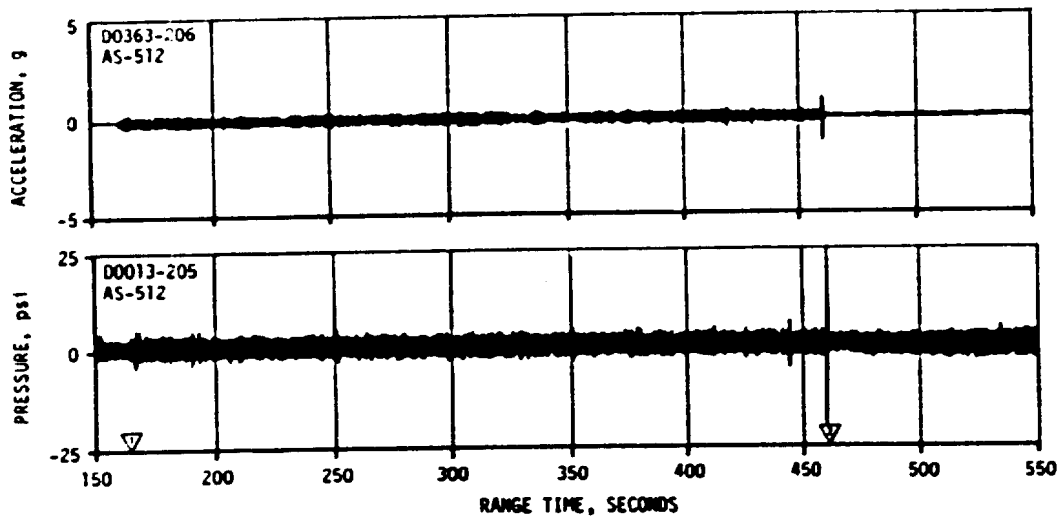
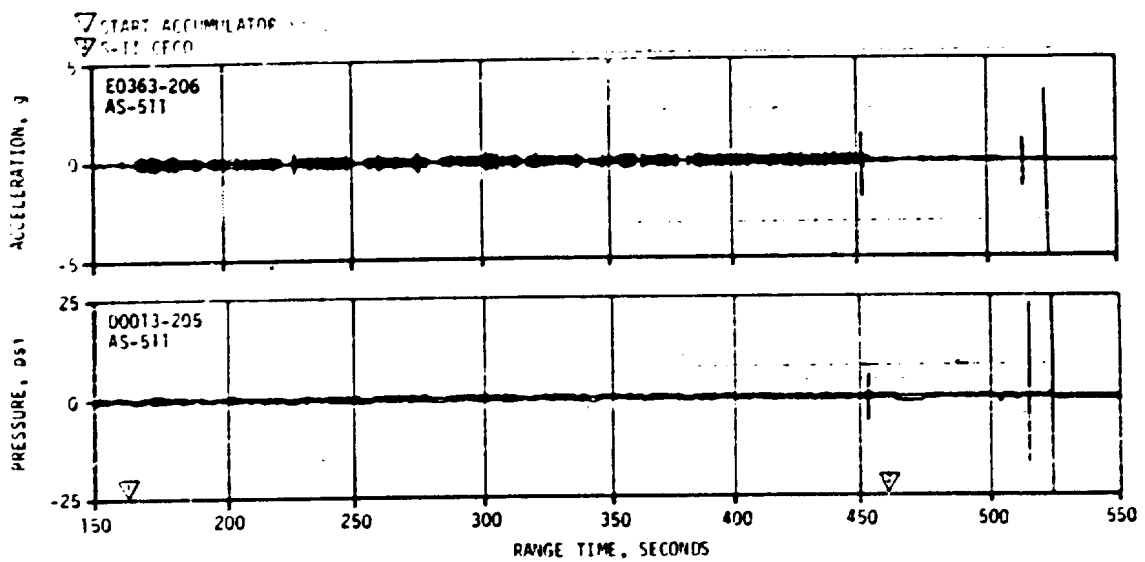


Figure 8-8. AS-512 Center Engine Chamber Pressure and Gimbal Pad Acceleration During S-II Burn (8 to 20 Hz Filter) Compared to AS-511

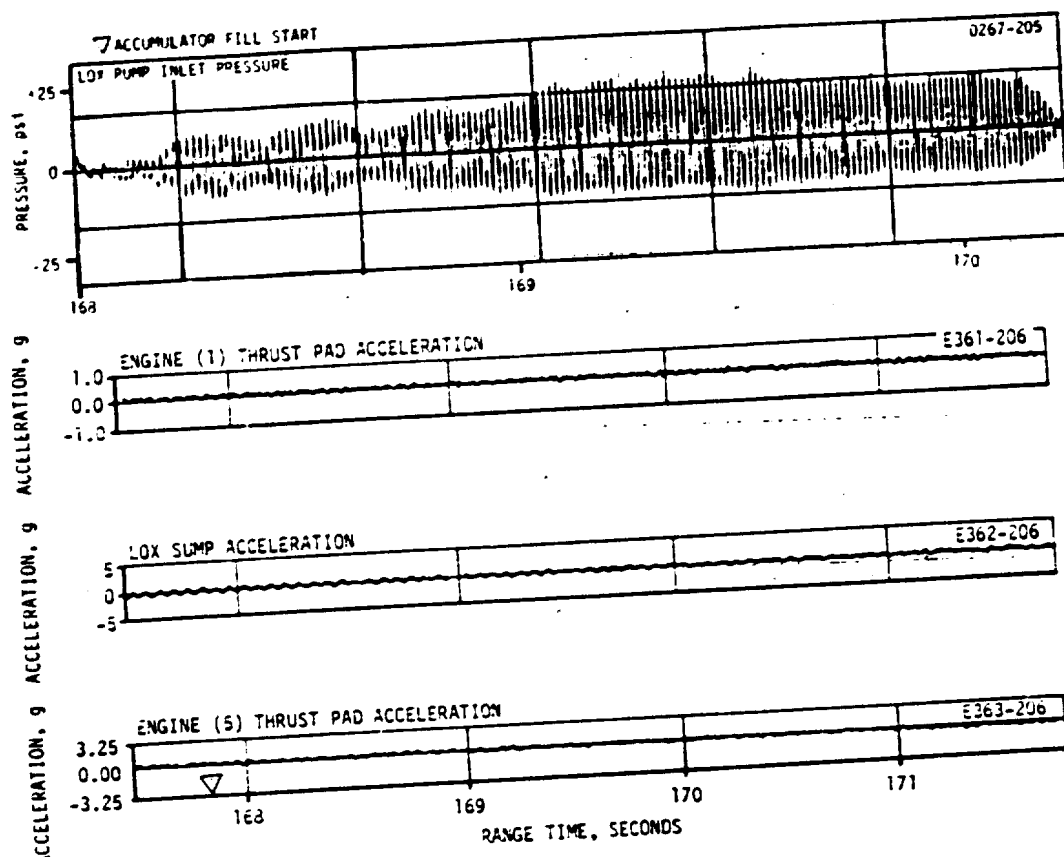


Figure 8-9. AS-512 Dynamic Responses During S-II Accumulator Fill
(1-110 Hz Filter)

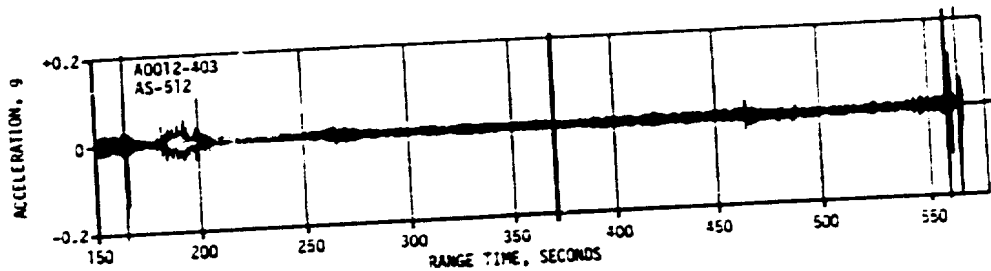


Figure 8-10. AS-512 S-IVB Gimbal Block Acceleration During S-II Burn -
Longitudinal (8 to 20 Hz Filter)

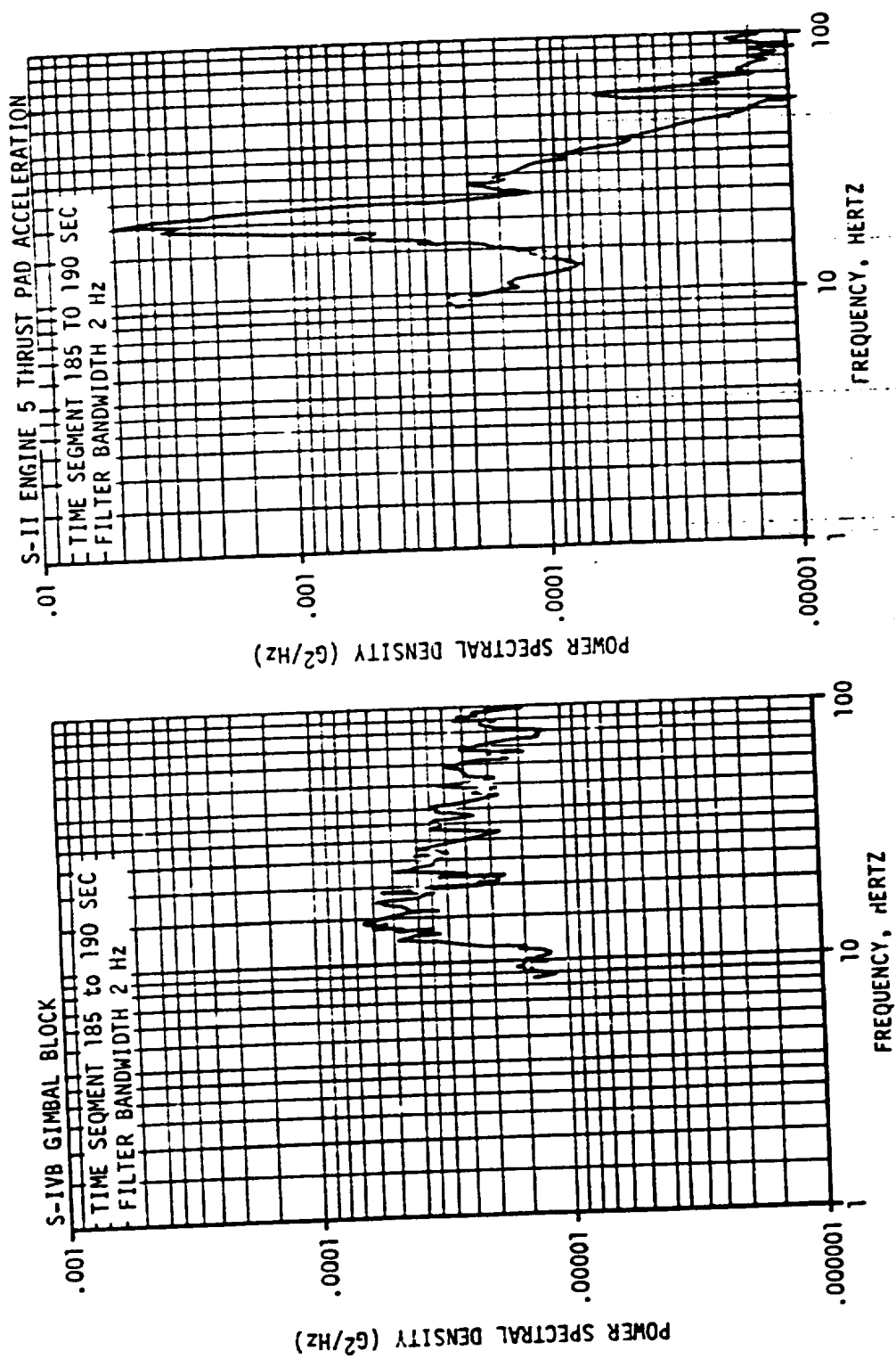


Figure 8-11. S-IVB Gimbal Block Acceleration and S-II Center Engine Thrust Pad Acceleration Spectra at $T + 185$ to 190 Seconds

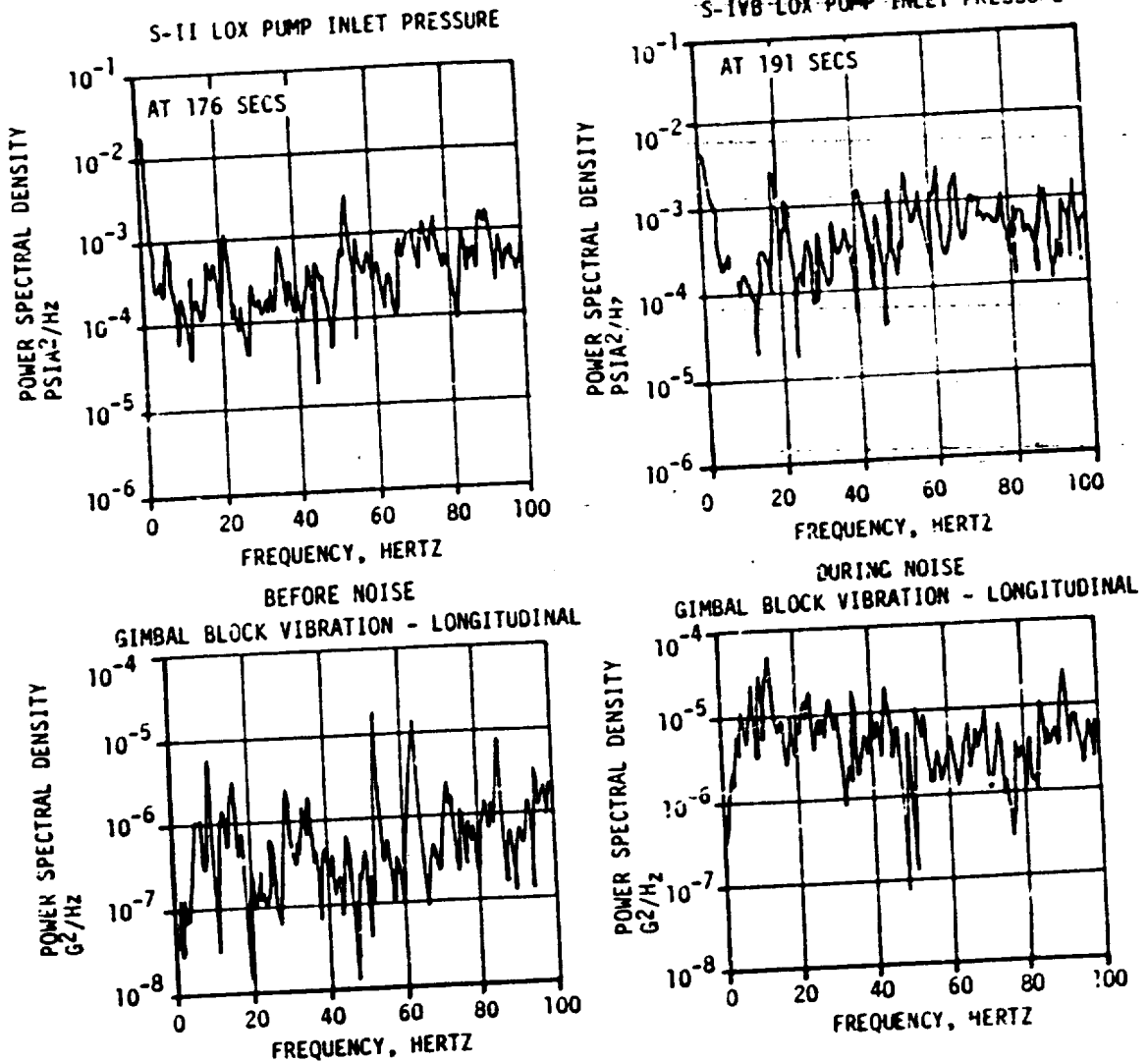


Figure 8-12. Noise on S-IVB Gimbal Block During S-II Burn

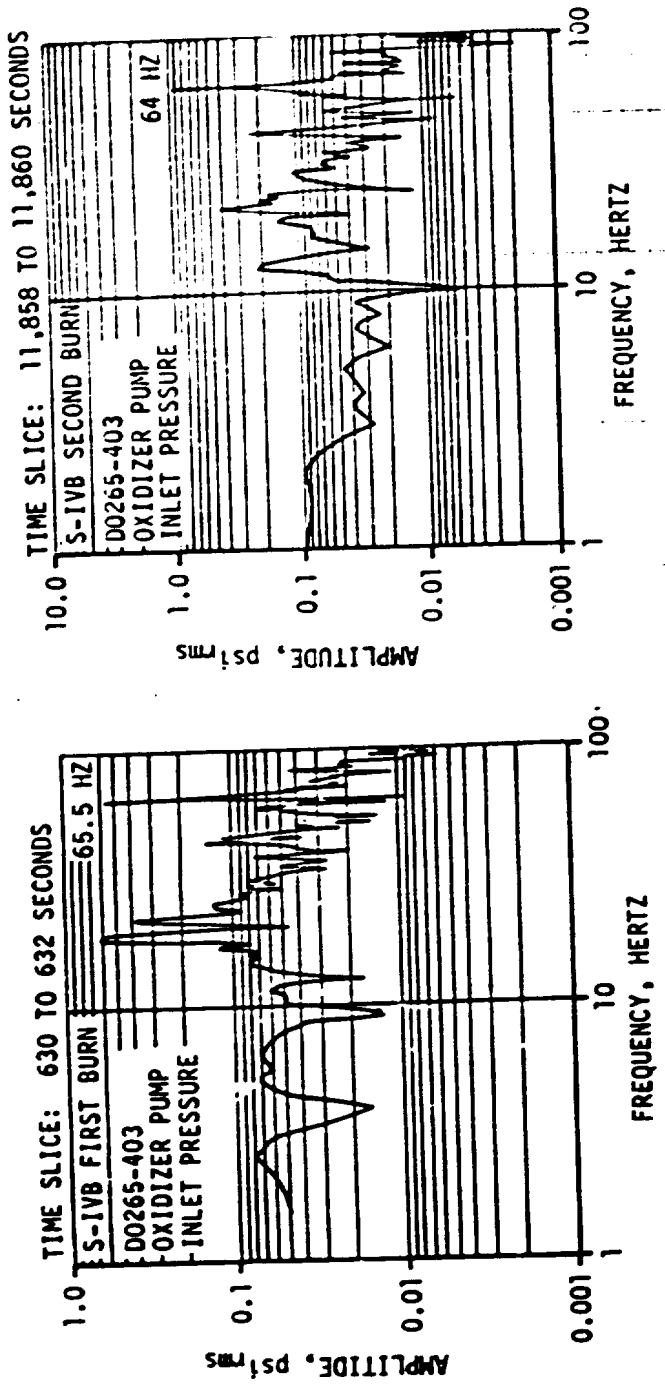


Figure 8-13. AS-512 S-IVB Pump Inlet Pressure Spectra

SECTION 9

GUIDANCE AND NAVIGATION

9.1 SUMMARY

The Stabilized Platform and the Guidance Computer successfully supported the accomplishment of all guidance and navigation mission objectives with no discrepancies in performance of the hardware. The end conditions at Parking Orbit Insertion and Translunar Injection were attained with insignificant navigation error.

Two anomalies related to the flight program did occur. At approximately 5421 seconds range time ($T_5 +4718.8$) minor loop error telemetry indicated an unreasonable change in the yaw gimbal angle during one minor loop. At the re-initialization of boost navigation for S-IVB second burn the extra accelerometer readings normally telemetered from Guidance Reference Release (GRR) to liftoff plus 10 seconds were restarted and continued throughout second burn boost navigation. Neither of these anomalies significantly impacted navigation, guidance and control. A detailed discussion is included in Section 9.3.3 and 9.3.4.

A minor discrepancy occurred during S-II burn, when the yaw gimbal angle failed the zero reasonableness test twice, resulting in minor loop error telemetry at 478.3 seconds ($T_3 +317.2$) and 559.4 seconds ($T_3 +398.2$). Detailed discussion of this occurrence is included in Section 9.3.2.

9.2 GUIDANCE COMPARISONS

The postflight guidance error analysis was based on comparisons of telemetered position and velocity data with corresponding values from the final postflight trajectory (21 day observed mass point trajectory) as established from telemetry and external tracking (see paragraph 4.2). Comparisons of the inertial platform measured velocities (PACSS 12) with corresponding postflight trajectory values from launch to earth parking orbit (EPO) are shown in Figure 9-1. At EPO insertion these differences were 0.47 m/s (1.54 ft/s), 3.07 m/s (10.07 ft/s), and 0.18 m/s (0.59 ft/s) for vertical, crossrange and downrange velocities, respectively. The inplane differences are very small. The crossrange velocity difference is somewhat larger than expected from laboratory measured hardware errors. However, this difference includes trajectory errors as well as platform measurement errors and is well within the combined accuracies. There was no indication of either inplane or crossrange velocity error caused by an accelerometer hitting its mechanical stop during thrust buildup on AS-512.

Platform velocity differences for the translunar injection burn are shown

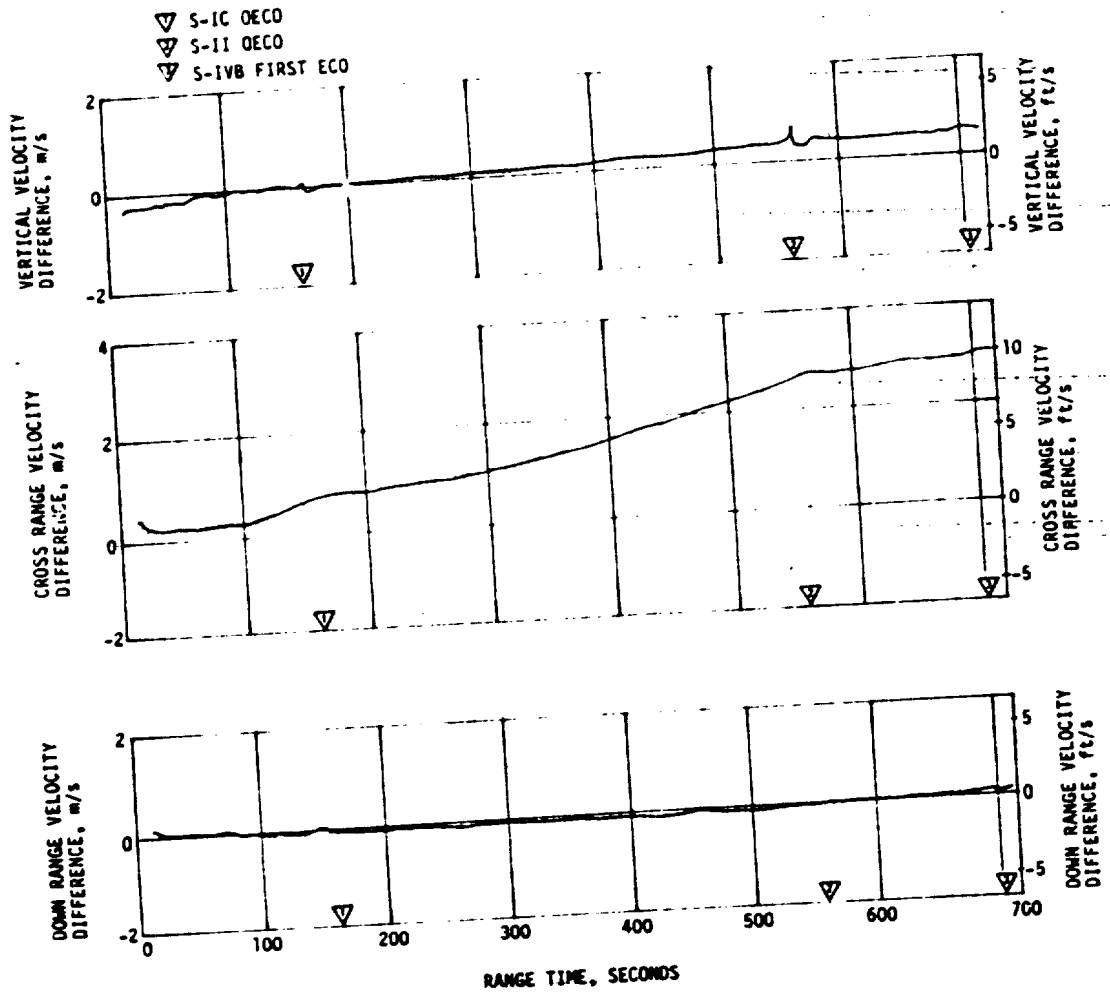


Figure 9-1. Trajectory and ST-124M Platform Velocity Comparisons, Boost-to-EPO (Trajectory Minus LVDC)

in Figure 9-2. At Time Base 6 (T6) minus 7.21 seconds, the platform velocity measurements were properly set to zero in the LVDC and the corresponding trajectory data were adjusted accordingly for comparison with the LVDC outputs. The differences shown in Figure 9-2 reflect adjustments made to the telemetered platform velocities during construction of the trajectory initialized to a parking orbit state vector and constrained to a state vector near TLI which was determined from post TLI tracking. The inplane (vertical and downrange) velocity difference profiles are not characteristic of hardware errors. However, the deviations are small and reflect an inconsistency between the initial and terminal trajectory state vectors. The crossrange velocity difference is greater than expected but well within the accuracy of the trajectory and 3 sigma hardware errors and the error profile is characteristic of platform misalignment due to drift over the long coast before second burn.

Telemetered platform system velocity measurements at significant event times are shown in Table 9-1 along with corresponding data from both the postflight and Operational (predicted) Trajectories (OT). The differences between the telemetered and postflight trajectory data reflect some combination of small guidance hardware errors and tracking errors. The differences between the LVDC and OT values reflect differences between actual and nominal performance and environmental conditions. The values shown for the second burn are velocity changes from T6. The characteristic velocity accumulated during second burn was 0.44 m/s (1.44 ft/s) greater than the OT which indicates slightly more stage performance was required to meet the targeted end conditions. The telemetered data indicated 0.32 m/s (1.05 ft/s) less than the postflight trajectory. The difference in indicated performance between the telemetered and postflight trajectory data reflects small errors in the state vectors to which the guidance velocities were constrained to generate the boost-to-TLI trajectory. The velocity increase due to thrust decay was 0.01 m/s (0.033 ft/s) less than the OT after first ECO and 0.05 m/s (0.16 ft/s) greater than the OT after second ECO, indicating very good prediction in both cases.

Comparisons of navigation (PACSS 13) positions, velocities and flight path angle at significant event times are presented in Table 9-2. Differences between the LVDC and OT values reflect off-nominal flight environment and vehicle performance. At first S-IVB ECO total velocity was 0.20 m/s (0.66 ft/s) less than the OT and the radius vector was 30.8 m (101.0 ft) greater than the OT. At S-IVB second ECO orbital energy (C_3) was $1849 \text{ m}^2/\text{s}^2$ greater than the OT value of $-1,769,443 \text{ m}^2/\text{s}^2$. The LVDC and postflight trajectory were in excellent agreement, except for crossrange, for the boost-to-EPO portion of flight. The crossrange component differences are within the accuracy of the data compared. The state vector differences during parking orbit were very small as compared to prior Saturn V flights. These small differences during parking orbit indicate that the vent thrust was effectively the same as programmed in the LVDC. The postflight trajectory and LVDC state vectors at TLI were in relatively good agreement. The difference in C_3

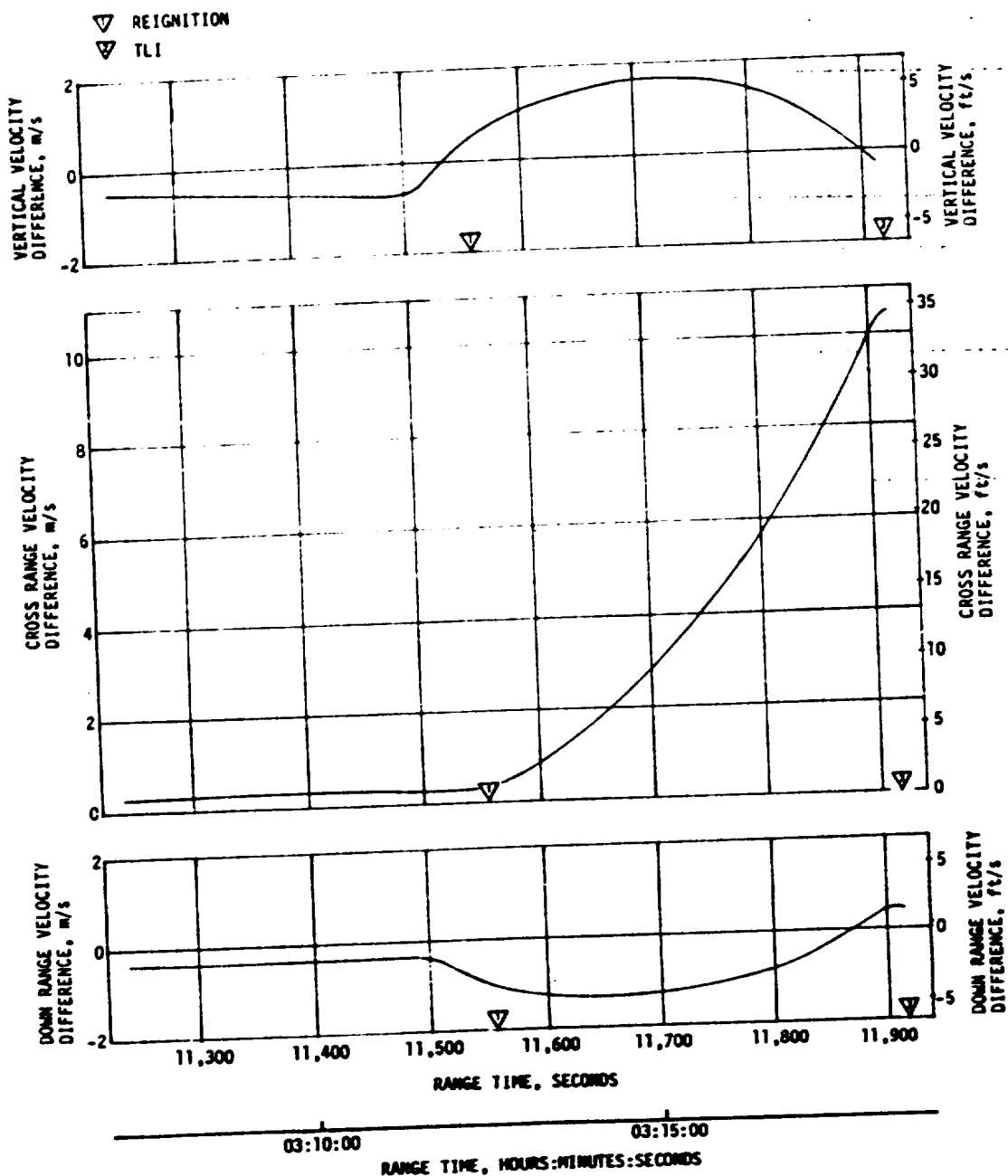


Figure 9-2. Trajectory and ST-124M Platform Velocity Comparisons,
Boost-to-TLI (Trajectory Minus LVDC)

Table 9-1. Inertial Platform Velocity Comparisons
(PACSS-12 Coordinate System)

EVENT	DATA SOURCE	VELOCITY - M/S (FT/S)		
		VERTICAL (X)	CROSS RANGE (Y)	DOWN RANGE (Z)
S-IC DECO	Guidance (LVDC)	2 631.75 (8 634.35)	-11.80 (-38.71)	2 204.15 (7 231.46)
	Postflight Trajectory	2 631.68 (8 634.12)	-11.07 (-36.32)	2 203.74 (7 230.12)
	Operational Trajectory	2 637.75 (8 654.03)	-3.37 (-11.05)	2 201.44 (7 222.56)
S-II DECO	Guidance (LVDC)	3 408.84 (11 183.86)	4.50 (14.76)	6 812.20 (22 349.74)
	Postflight Trajectory	3 409.52 (11 186.09)	7.07 (23.20)	6 810.92 (22 345.54)
	Operational Trajectory	3 425.35 (11 238.04)	1.87 (6.14)	6 787.06 (22 267.25)
S-IVB FIRST ECO	Guidance (LVDC)	3 212.45 (10 539.53)	-1.57 (-5.15)	7 603.88 (24 947.11)
	Postflight Trajectory	3 212.95 (10 541.18)	1.45 (4.76)	7 603.99 (24 947.49)
	Operational Trajectory	3 226.31 (10 584.99)	-1.18 (-3.88)	7 606.72 (24 956.44)
PARKING ORBIT INSERTION	Guidance (LVDC)	3 211.95 (10 537.89)	-1.65 (-5.41)	7 605.55 (24 952.59)
	Postflight Trajectory	3 212.42 (10 539.44)	1.42 (4.66)	7 605.73 (24 953.18)
	Operational Trajectory	3 225.76 (10 583.19)	-1.19 (-3.91)	7 608.39 (24 961.89)
S-IVB SECOND ECO*	Guidance (LVDC)	-2 766.68 (-9 077.03)	-22.40 (-73.49)	1 499.70 (4 920.28)
	Postflight Trajectory	-2 766.91 (-9 077.79)	-11.97 (-39.27)	1 500.07 (4 921.49)
	Operational Trajectory	-2 769.00 (-9 084.63)	-22.71 (-74.51)	1 494.47 (4 903.13)
TRANSLUNAR INJECTION*	Guidance (LVDC)	-2 770.20 (-9 088.58)	-22.40 (-73.49)	1 501.00 (4 924.54)
	Postflight Trajectory	-2 770.33 (-9 089.01)	-11.87 (-38.94)	1 501.47 (4 926.08)
	Operational Trajectory	-2 772.47 (-9 096.04)	-22.72 (-74.55)	1 495.75 (4 907.33)

*Values represent velocity change from Time Base 6.

Table 9-2. Navigation Comparisons (PACSS-13)

EVENT	DATA SOURCE	POSITIONS METERS (FT)				VELOCITIES M/S (FT/S)				FLIGHT PATH ANGLE (DEG)	
		x_1	y_1	z_1	\dot{x}_1	\dot{y}_1	\dot{z}_1	V_x	V_y	V_z	γ
S-1C DECO	Guidance (LVDC)	6,437,688.5 (21,120,894.0)	15,480,2 (50,820,9)	165,955.0 (544,411,8)	6,139,805.8 (21,127,971,8)	891,84 (2,926,0)	-24,78 (-81,30)	2,597,69 (8,522,61)	2,746,63 (9,011,25)	20,4234	
	Postflight Trajectory	6,437,631.7 (21,120,845,6)	15,515.2 (51,001,3)	165,952.9 (544,464,9)	6,139,791.1 (21,127,923,6)	892,18 (2,927,10)	-24,04 (-78,87)	2,597,84 (8,523,10)	2,746,98 (9,012,07)	20,4285	
	Operational Trajectory	6,437,851.0 (21,121,558,2)	15,798.4 (51,832,0)	166,811.6 (547,282,1)	6,140,031.1 (21,128,711,0)	893,18 (2,930,31)	-16,36 (-53,67)	2,595,42 (8,515,16)	2,744,86 (9,005,44)	20,47	
	Guidance (LVDC)	6,259,576.5 (20,336,668,3)	9,757.1 (12,011,5)	1,916,333.8 (6,287,184,4)	6,566,343.5 (21,477,504,9)	-2,017,25 (-6,618,21)	-30,54 (-34,59)	6,694,22 (21,962,66)	6,991,56 (22,938,19)	0,2518	
S-1I DECO	Postflight Trajectory	6,259,610.8 (20,336,700,0)	10,395.6 (34,106,3)	1,916,322.0 (6,287,309,7)	6,566,389.3 (21,477,681,4)	-2,016,60 (-6,616,14)	-8,15 (-26,74)	6,692,92 (21,958,40)	6,990,13 (22,933,50)	0,2541	
	Operational Trajectory	6,250,276.7 (20,336,912,0)	10,073.0 (33,047,6)	1,912,514.3 (6,274,850,0)	6,545,924.8 (21,476,131,0)	-2,006,09 (-5,581,67)	-13,65 (-44,76)	6,689,33 (21,881,00)	6,984,52 (22,889,48)	0,25	
	Guidance (LVDC)	5,810,178.5 (19,250,115,9)	7,882.0 (25,052,6)	2,894,103.6 (9,495,090,6)	6,544,837.2 (21,472,563,0)	-3,450,47 (-11,320,44)	-16,89 (-55,41)	6,997,92 (22,959,06)	7,002,36 (25,538,29)	-0,0056	
S-1V First ECO	Postflight Trajectory	5,810,255.5 (19,259,384,4)	8,897.3 (29,190,6)	2,894,196.6 (9,495,395,7)	6,544,948.6 (21,472,928,5)	-3,450,06 (-11,319,09)	-14,18 (-46,52)	6,998,10 (22,959,65)	7,002,34 (25,538,23)	-0,00118	
	Operational Trajectory	5,840,963.2 (19,228,882,0)	7,842.3 (25,729,4)	2,912,651.6 (9,555,943,5)	6,544,806.4 (21,472,461,8)	-3,472,64 (-11,393,18)	-16,93 (-55,67)	6,987,16 (22,923,75)	7,002,56 (25,538,95)	0,00	
	Guidance (LVDC)	5,835,269.7 (19,146,914,1)	7,712.7 (25,304,1)	2,963,891.8 (9,721,054,1)	6,544,833.6 (21,472,551,5)	-3,534,26 (-11,598,34)	-16,97 (-55,68)	6,957,97 (22,797,99)	7,004,14 (25,604,13)	0,00086	
	Postflight Trajectory	5,835,333.7 (19,144,795,6)	8,755.1 (28,724,1)	2,963,993.8 (9,724,366,3)	6,544,952.0 (21,472,939,6)	-3,533,85 (-11,599,00)	-16,93 (-46,69)	6,958,09 (22,888,38)	7,004,06 (25,603,87)	0,00264	
	Parking Orbit Insertion	5,825,815.4 (19,113,567,2)	7,672.5 (25,172,4)	2,982,330.4 (9,781,588,6)	6,544,805.4 (21,472,458,8)	-3,566,35 (-11,667,82)	-16,98 (-55,72)	6,946,91 (22,797,69)	7,004,32 (25,504,73)	0,00	
	Operational Trajectory	5,825,815.4 (19,113,567,2)	22,080.5 (75,067,3)	973,574.5 (3,194,142,1)	6,554,101.6 (21,502,958,0)	-1,158,39 (-3,800,49)	46,04 (151,05)	7,11,69 (25,300,82)	7,798,35 (25,585,14)	0,00002	
	Guidance (LVDC)	5,841,345.9 (21,264,550,2)	22,071.7 (75,038,4)	971,916.3 (3,188,701,8)	6,554,911.5 (21,505,818,6)	-1,152,23 (-3,290,12)	48,38 (160,04)	7,11,14 (25,299,02)	7,798,52 (25,585,70)	0,00078	
	Time Base	6,482,477.0 (21,267,911,8)	23,195.8 (76,101,7)	971,916.3 (3,188,701,8)	6,554,911.5 (21,505,818,6)	-1,156,78 (-3,295,21)	46,03 (151,01)	7,11,14 (25,299,02)	7,798,52 (25,585,70)	0,00	
	Postflight Trajectory	6,481,597.4 (21,265,063,2)	22,071.7 (75,038,4)	971,900.0 (3,188,648,2)	6,554,099.3 (21,502,950,3)	-1,156,78 (-3,295,21)	46,03 (151,01)	7,11,14 (25,299,02)	7,798,52 (25,585,70)	0,00	
	Operational Trajectory	1,610,938.6 (5,499,436,6)	44,193.3 (145,302,9)	6,472,355.5 (21,188,662,1)	6,677,276.2 (21,907,074,1)	-10,113,30 (-31,180,12)	-19,41 (-63,68)	12,850,03 (112,850,68)	10,845,26 (135,581,56)	6,94314	
	Guidance (LVDC)	1,539,656.6 (5,051,386,5)	43,991.1 (157,311,0)	6,471,985.6 (21,233,548,6)	6,677,983.5 (21,909,394,7)	-10,111,18 (-33,173,16)	-8,20 (-26,90)	3,920,35 (12,862,04)	3,844,59 (35,579,36)	6,929,63	
	Postflight Trajectory	1,545,164.6 (5,397,521,7)	47,865.5 (157,039,0)	6,510,767.9 (21,360,767,1)	6,691,492.5 (21,891,302,8)	-10,135,79 (-33,155,16)	-19,48 (-63,91)	3,947,43 (12,850,89)	10,849,31 (35,594,86)	6,79	
	Translunar Injection	1,575,027.2 (5,167,411,9)	44,090.5 (144,654,0)	6,497,391.8 (21,316,902,0)	6,685,712.7 (21,934,752,8)	-10,130,96 (-33,238,06)	-20,06 (-65,93)	3,861,93 (12,670,36)	10,842,70 (35,571,21)	7,24	

at TLI was $-1887 \text{ m}^2/\text{s}^2$ (trajectory minus LVDC). Figure 9-3 presents the state vector comparisons during EPO. The LVDC data not received because of non-continuous station coverage were simulated by initializing to a telemetered state vector and integrating a trajectory using flight program navigation equations and programmed vent accelerations. At T6, the differences in total position and velocity were 872 meters in radius and 1 m/s in velocity and are not significant.

The AS-512 vehicle was guided to the targeted end conditions with a high degree of accuracy. Vent thrust was effectively nominal during EPO. Figure 9-4 presents the continuous vent thrust reconstruction along with OT predictions and three-sigma envelope. The upper portion of Figure 9-4 shows the orbital acceleration derived from the platform measurements adjusted for accelerometer bias. The LVDC programmed acceleration is also shown. The oscillations in acceleration from orbital navigation (804.2 seconds) to about 2500 seconds may not be real. During this period only compressed data were available for a curve fit of the telemetered velocity outputs. However, the area under the curve which represents the accumulated velocity over this time span is essentially nominal.

The LVDC state vector at TLI was compared with the OT and postflight trajectories and the differences are presented in Table 9-3. The LVDC radius vector was 5093.1 meters (16,709.6 ft) higher than the OT and 686.7 meters (2253.0 ft) lower than the postflight trajectory value. Telemetered total velocity was 4.24 m/s (13.91 ft/s) less than the OT and 0.83 m/s (2.72 ft/s) higher than the postflight trajectory. The guidance system was highly successful in measuring the vehicle performance and generating proper commands to guide the vehicle to desired conditions as shown in Table 9-4.

9.3 NAVIGATION AND GUIDANCE SCHEME EVALUATION

The LVDC flight program performed all required functions properly. Two anomalies are reported in paragraphs 9.3.3 and 9.3.4. Neither significantly affected flight program performance.

9.3.1 Variable Launch Azimuth

Due to the unscheduled hold in the countdown at approximately T-30 seconds, the variable launch azimuth function of the flight program was required to perform over a time variation greater than for any previous Saturn V vehicle. The two hour 40 minute launch delay resulted in a change of the flight azimuth from 72.141 degrees to 91.504 degrees East of North. The performance of flight program in achieving the targeted parameters was satisfactory.

9.3.2 First Boost Period

All first stage maneuvers were performed within predicted tolerances and Iterative Guidance Mode (IGM) performance for first boost was nominal. The steering commands telemetered during first boost are illustrated in Figure 9-5. Table 9-4 shows the terminal end conditions for first

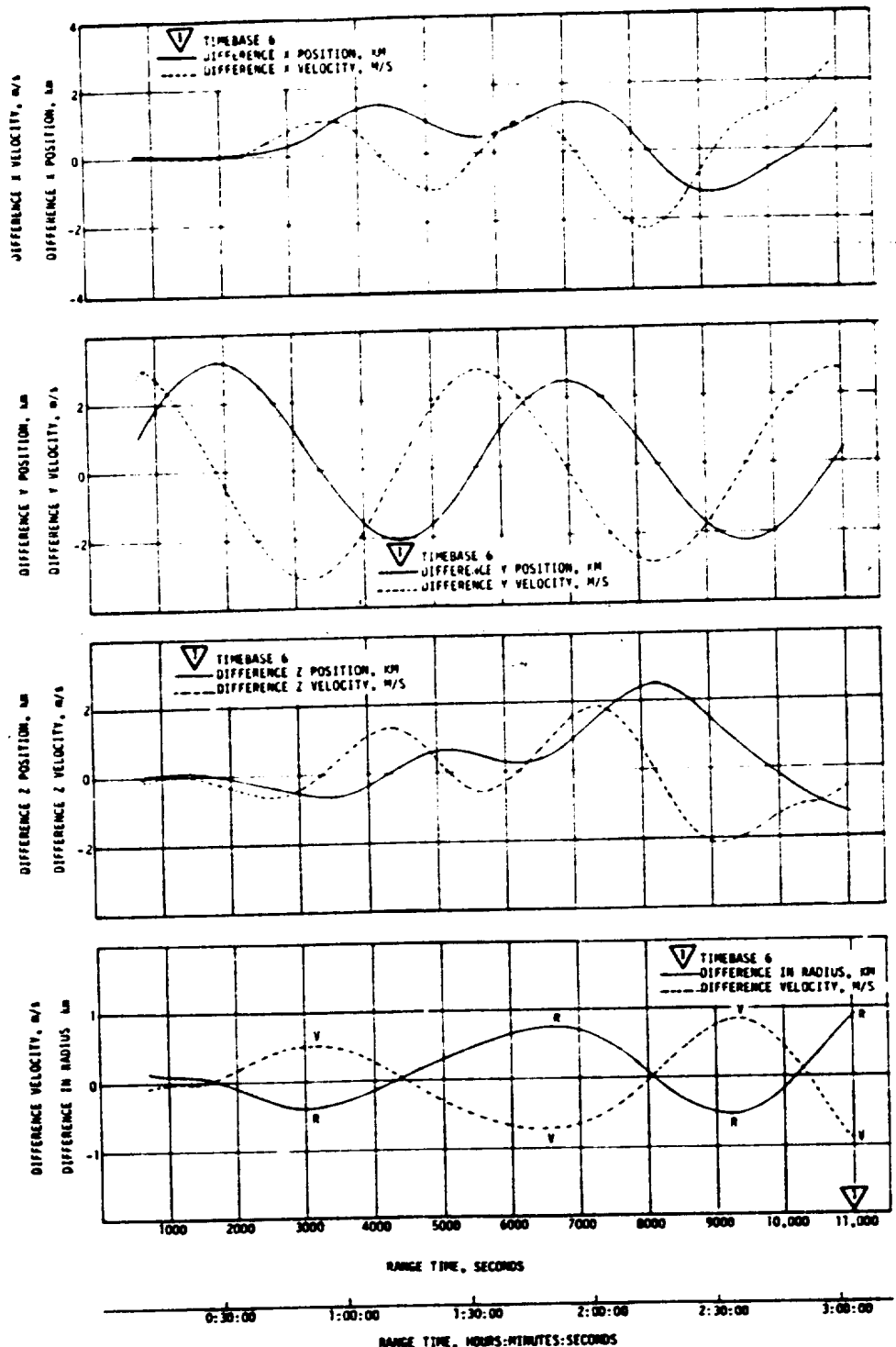


Figure 9-3. Comparison of LVDC and Postflight Trajectory During EPO

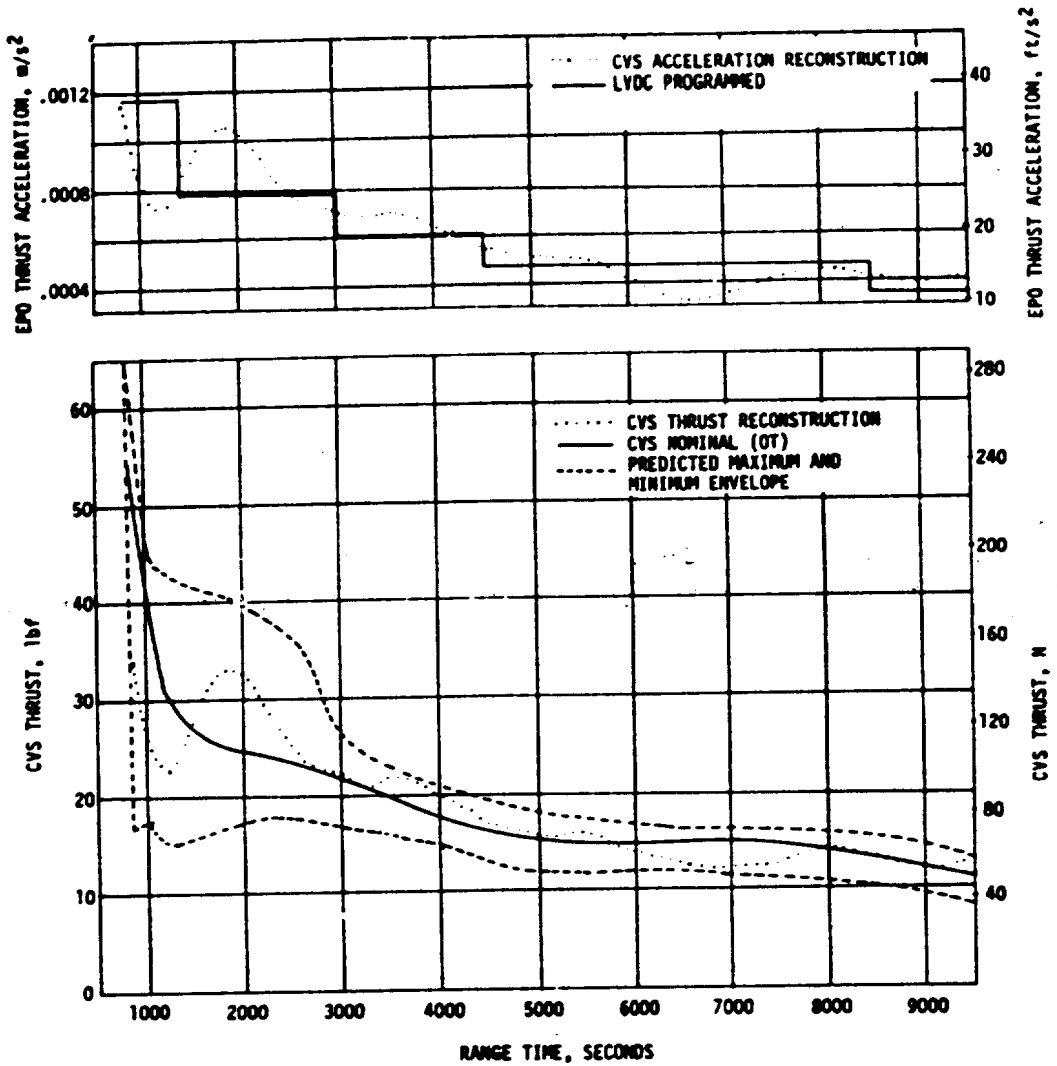


Figure 9-4. Continuous Vent System (CVS) Thrust and Acceleration During EPO

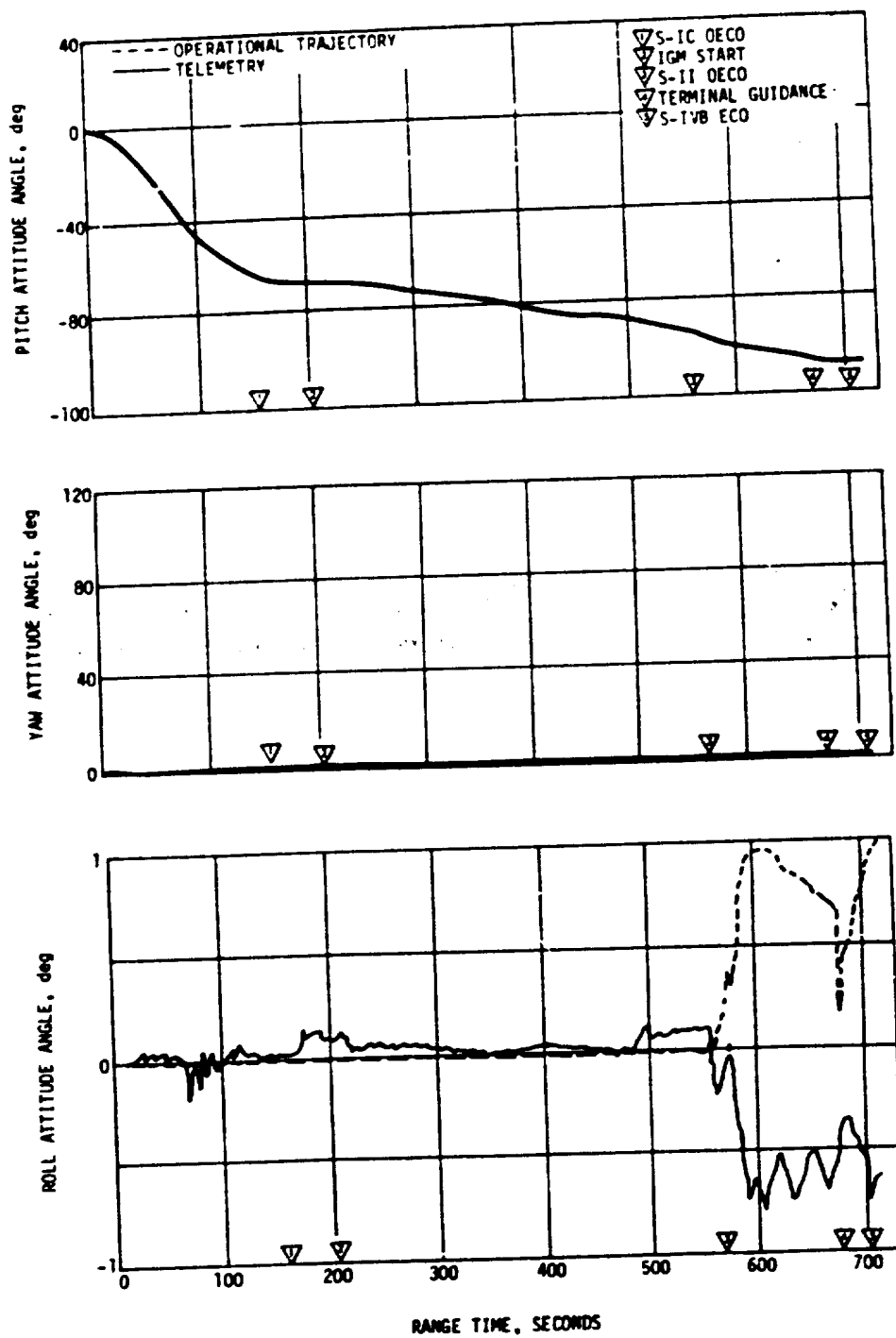


Figure 9-5. Steering Commands, First Boost

Table 9-3. State Vector Differences at Translunar Injection

PARAMETER	OPERATIONAL TRAJECTORY MINUS LVDC	POSTFLIGHT TRAJECTORY MINUS LVDC
ΔX_S , meters (feet)	35 370.6 (11° 045.3)	4 261.1 (13 980.0)
ΔY_S , meters (feet)	93.6 (307.1)	3 868.6 (12 692.3)
ΔZ_S , meters (feet)	-13 706.7 (-44 969.5)	-330.6 (-1 084.6)
ΔR , meters (feet)	-5 093.1 (-16 709.6)	687.7 (2 253.0)
$\Delta \dot{X}_S$, m/s (ft/s)	7.13 (23.39)	2.30 (7.55)
$\Delta \dot{Y}_S$, m/s (ft/s)	-0.15 (-0.49)	11.19 (36.71)
$\Delta \dot{Z}_S$, m/s (ft/s)	30.74 (100.85)	3.76 (12.34)
ΔV , m/s (ft/s)	4.24 (13.91)	-0.83 (-2.72)

burn. Terminal conditions were obtained by linear forward extrapolation using the velocity bias $\Delta V_b = 1.514$ meters/second to establish the extrapolation interval beyond velocity cutoff.

Minor loop error telemetry indicated an unreasonable zero reading of the yaw (Z) gimbal at 478.4 seconds ($T_3 +317.2$) and again at 559.4 seconds ($T_3 +398.2$). The test for an unreasonable zero reading was designed to detect a failure of the gimbal resolver power source. If two successive readings of the gimbal are found to be zero while the past attitude error magnitude exceeds the test constant (0.06 degrees) the zero reasonableness test is failed and minor loop error telemetry is generated. If the fine resolver fails the zero test three times in 0.8 seconds during boost, a failure of the fine resolver is assumed and the corresponding backup resolver is selected for attitude information for the remainder of the mission. Since gimbal and ladder data at the times of the error telemetry indicate zero yaw with yaw ladders (indicative of yaw attitude error) greater than the test constant, the flight

Table 9-4. AS-512 End Conditions

FIRST BURN

PARAMETER	DESIRED	ACHIEVED	ERROR (ACHIEVED-DESIRED)
Terminal Velocity, V_T (m/s)	7804.0613	7803.8796	-0.1817
Radius, R_T (meters)	6,544,846.0	6,544,838.51	-7.49
Path Angle, θ_T (degrees)	0.0	-0.000741	-0.000741
Inclination, I (degrees)	28.523855	28.524201	0.000346
Descending Node, λ (degrees)	87.019862	87.018449	-0.001413

SECOND BURN

PARAMETER	DESIRED	ACHIEVED	ERROR (ACHIEVED-DESIRED)
Eccentricity, E	0.97220895	0.97219893	-0.00001002
Inclination, I (degrees)	28.424498	28.424998	0.000500
Descending Node, λ (degrees)	86.143262	86.142845	-0.000417
Argument of Perigee, ω (degrees)	24.936942	24.925433	-0.011509
Energy, C_3 (m^2/sec^2)	-1,683,990.0	-1,684,562.323	-572.323

program apparently responded correctly. Only one unreasonable zero reading was found in each case and no change to backup readings was initiated. Although the improper selection of a backup resolver would not significantly degrade system accuracy, the current zero test is being studied for possible changes to either the test method or the magnitude of the test constant for future missions.

9.3.3 Earth Parking Orbit

Parking orbit guidance proceeded as expected. Table 9-5 presents the commanded steering angles for major events.

Orbital navigation was within the required tolerances for parking orbit. Termination of orbital navigation occurred at 10,971.4 seconds (T6 -7.2).

Table 9-5. Coast Phase Guidance Steering Commands at Major Events

FLIGHT PERIOD	EVENT	TIME, SECONDS	COMMANDED STEERING ANGLES, DEGREES		
			ROLL (X)	PITCH (Y)	YAW (Z)
Earth Parking Orbit	Initiate Orbital Guidance Chi Freeze	T5 +0.0	-0.7422	-106.8471	-0.5898
	Initiate Maneuver to Local Horizontal	T5 +21.538	0.0000	-117.6803	-0.1265
	Initiate Orbital Navigation	T5 +101.378	--	--	--
Post TLI	Initiate Orbital Guidance Chi Freeze	T7 +0.0	0.3404	-159.9386	0.0084
	Initiate Orbital Navigation	T7 +152.003	--	--	--
	Initiate Maneuver to Local Horizontal	T7 +152.033	0.0000	-179.2931	-0.2341
	Initiate TD&E Maneuver	T7 +401.032	180.0000	-105.1028	40.2581
	TD&E Maneuver Complete	T7 +5194.4	--	--	--
	Initiate Lunar Impact Local Reference Maneuver	T8 +581.014	180.0000	-94.3543	-18.6886

Minor loop error telemetry issued at approximately 5421 seconds (T5 +4718.8) indicated an unreasonable change in successive readings of the yaw gimbal angle. The test for a reasonable change is made by comparing the difference in past and current gimbal readings with a preset test constant. If the change between past and current gimbal readings exceeds the respective test constant for pitch, yaw, or roll the change is considered unreasonable. The magnitude of the yaw test constant at the time of the failure was 0.2 degree/minor loop. If a fine resolver fails the reasonableness test three times in one second during orbit the corresponding backup (coarse) resolver reading is selected for attitude information for the remainder of the mission. Since only one unreasonable change was found, the backup yaw gimbal was not selected.

Evaluation of the gimbal angle data from the time of the error telemetry indicated that the yaw (Z) backup gimbal reading was erroneously compared with a fine resolver reading instead of the proper comparison of two successive fine resolver readings. Further investigation revealed the initiation of the once per 100 second data compression module at the time of the minor loop interrupt. The occurrence of the minor loop interrupt during a particular six instruction interval at the start of

the data compression resulted in the replacement of the fine yaw gimbal reading by the backup yaw gimbal. Since the backup reading was rejected as unreasonable, the next fine gimbal reading was properly compared with the last reasonable fine gimbal reading and all subsequent reasonableness tests were passed. The possibility of a similar occurrence on subsequent missions has been eliminated by starting a read of the currently selected Z gimbal resolver (fine or backup) at the end of data compression.

9.3.4 Second Boost Period

The December 6 target objectives resulted in nearly constant-time-of-arrival trajectories across the launch window. Therefore the targeting parameters calculated in preparation for second burn defined a higher energy transfer orbit which compensated for the 2 hour 40 minute launch delay and enabled completion of the lunar landing and exploration on the originally planned timeline.

Sequencing of restart preparations occurred as scheduled. T6 was initiated at 10,978.6 seconds. Extra accelerometer telemetry was noted throughout the second boost navigation periods. This is discussed in the following paragraphs.

Upon reinitiation of boost navigation at 10,971.4 seconds the extra accelerometer readings, that should have been telemetered only from GRR to T +10, were reinitiated and continued throughout second boost navigation. This resulted from the extra accelerometer read module being queued in with the periodic processor at GRR and again at second boost initialize. The readings were not stopped as in first boost, because there was no counterpart to the T +10 second cue during second boost. In previous flight programs the extra accelerometer readings were queued in separately after GRR and were not queued in again at second boost. A class II change effective with AS-512 reduced the priority of these accelerometer readings and placed their start time at GRR. The only effect of this problem was a slight lengthening of the computation cycle during second boost but this was accounted for by the flight program without adverse results. Since no further missions with a S-IVB second burn are planned no program changes are recommended but documentation of the occurrence has been accomplished for future reference.

IGM for the S-IVB second burn was implemented at 11,562.7 seconds (T6 +584.1). Pitch, yaw and roll attitude angles for second burn are shown in Figure 9-6.

Table 9-4 shows the terminal end conditions for the S-IVB second burn. Desired values are the telemetered target values and actual terminal values were obtained by linear forward extrapolation using a velocity bias of $\Delta V_{\text{bias}} = 3.660 \text{ meters/second}$.

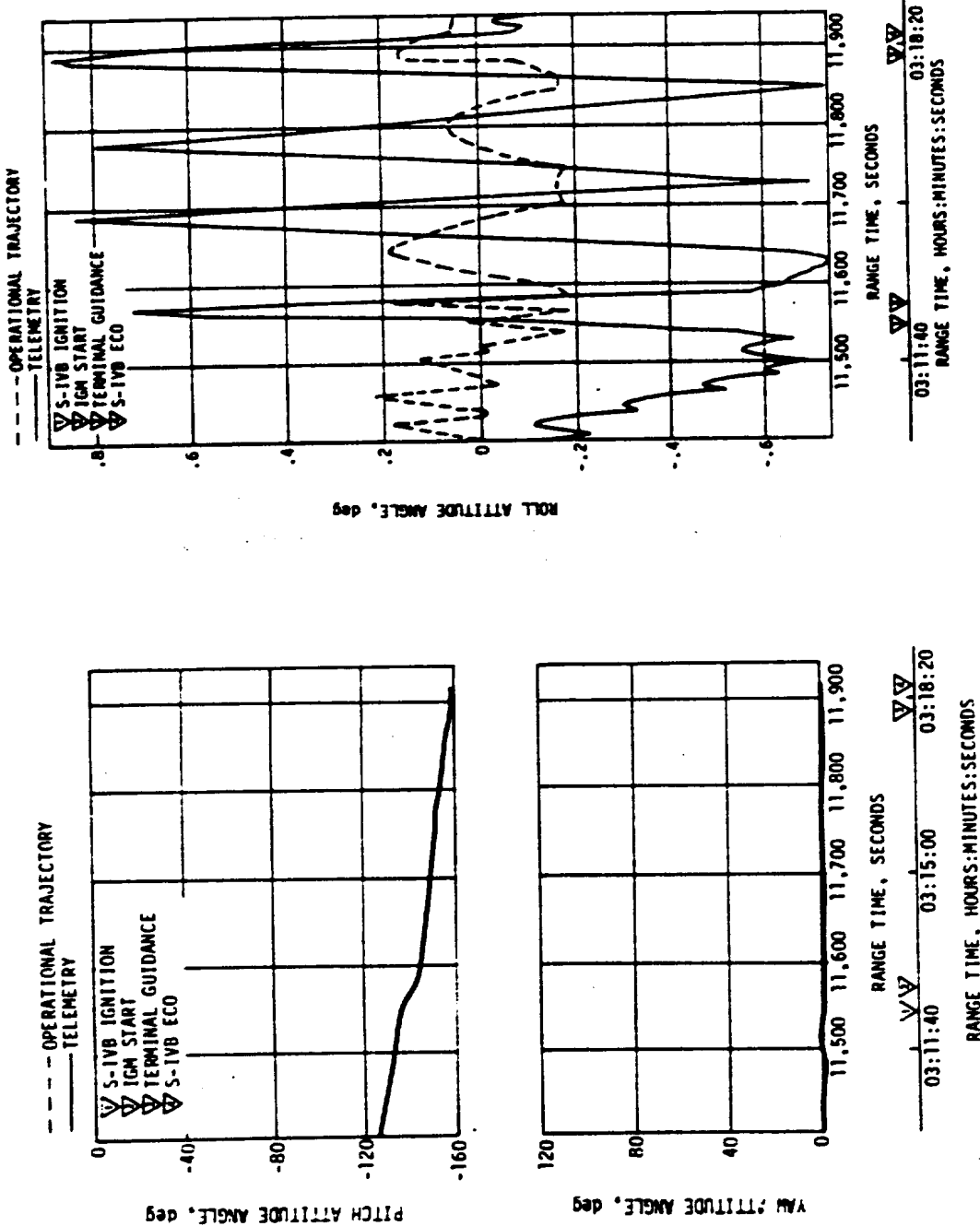


Figure 9-6. Steering Commands, Second Burn

9.3.5 Post-TLI Period

Post TLI guidance proceeded as expected. Table 9-5 presents the commanded steering angles for some major events.

Two lunar impact APS burns were commanded from Mission Control Center-Houston (MCC-H) at 21,735 seconds (6:02:15) and 39,754 (11:02:34), respectively. The first burn of 98 seconds duration was started at the commanded time of 22,200 seconds (6:10:00). The second burn was commanded to start at 40,500 seconds (1:15:00) with a duration of 102 seconds. Both burns were properly implemented by the flight program with the desired attitude changes occurring upon acceptance of the Digital Command System (DCS) commands, ignition times and burn durations occurring as commanded.

The three-axis tumble was started by a zero burn set of lunar impact commands beginning at 41,502 seconds. Changes of +31 degrees to pitch, yaw and roll were commanded establishing tumble rates, followed by Flight Control Computer power off "A" and "B" commands at 41,519 seconds and 41,530 seconds, respectively. (Power off "A" and "B" switch selectors were issued at 41,521 and 41,532 seconds, respectively.)

The telemetry subcarrier oscillator was commanded off by the flight program at 49,620 seconds after which no further telemetry data was available.

9.4 NAVIGATION AND GUIDANCE SYSTEM COMPONENTS

The navigation and guidance hardware satisfactorily supported the accomplishment of mission objectives. No anomalies were observed during the AS-512 flight.

9.4.1 ST-124M Stabilized Platform System

The three gyro servo loops responded properly to all vehicle perturbations. Maximum deflection during the liftoff period was 0.3 degree on the Z gyro pickoff. As on previous vehicles the 5 Hz oscillation (0.2° peak-to-peak) occurred from S-IC CECO to S-IC OECO.

The largest disturbance occurred at Spacecraft/IU separation when the X gyro pickoff deflected 0.8 degree, well within limits for proper control.

The three accelerometer servo loops operated within previously experienced limits. Peak deflections of the accelerometer gyro pickoffs occurred during the heavy vehicle vibration period at liftoff. Maximum excursions were as follows:

X	Y	Z
Positive 2.5 deg.	5.0 deg.	3.0 deg.
Negative 2.1 deg.	4.5 deg.	2.9 deg.

9.4.2 Guidance Computer

The LVDC and LVDA performed satisfactorily, and no hardware anomalies were observed during any phase of the AS-512 mission.

SECTION 10

CONTROL AND SEPARATION

10.1 SUMMARY

All control functions and separation events occurred as planned. Engine gimbal deflections were nominal and Auxiliary Propulsion System (APS) firings predictable throughout powered flight. All dynamics were within vehicle capability, and bending and slosh modes were adequately stabilized.

The APS provided satisfactory orientation and stabilization during parking orbit and from Translunar Injection (TLI) through the S-IVB/IU passive thermal control maneuver. APS propellant consumption for attitude control and propellant settling prior to the APS burn for lunar target impact was lower than the mean predicted requirements.

All AS-512 separation sequences were performed as planned with no anomalies. Transients due to spacecraft separation, docking, and Lunar Module ejection appeared to be nominal.

10.2 S-IC CONTROL SYSTEM EVALUATION

10.2.1 Liftoff

The liftoff tower clearance maneuver occurred as planned. Table 10-1 summarizes liftoff conditions and misalignments.

10.2.2 Inflight Dynamics

The AS-512 control system performed satisfactorily during S-IC boost. JimspHERE measurements indicate that the peak wind speed encountered was 45.1 meters/second at 12.2 kilometers altitude with an azimuth of 311 degrees. The peak wind speed calculated from the Q-ball data was 40.5 meters/second at 12.2 kilometers with an azimuth of 313.1 degrees. The yaw wind component in both cases was 28.6 meters/second, which is near the 99 Percentile yaw wind component for December (29.7 meters/second for a 90 degree launch azimuth). The pitch component was near 50 percentile. The control system adequately stabilized the vehicle in this wind. About 12% of the available yaw plane engine deflection was used in the region of the peak wind speed, and less than 10% was used in pitch (based on the average engine gimbal angles in pitch and yaw).

Table 10-1. AS-512 Misalignment and Liftoff Conditions Summary

PARAMETER	PREDICTED 3 σ RANGE			LAUNCH		
	PITCH	YAW	ROLL	PITCH	YAW	ROLL
Thrust Misalignment, deg	-0.31	-0.31	-0.37	-0.13	0.11	-0.04
Center Engine Cant, deg	-0.31	-0.31	-	0.02	0.30	-
Vehicle Stacking and Pad Misalignment, deg	-0.27	-0.27	0.00	0.00	0.00	0.00
Attitude Error at Holddown Arm Release, deg	-	-	-	-0.12	0.12	-0.06
Peak Soft Release Force Per Rod, N(lbf)	415,900 (93,500)			*		
Wind	19.55 M/S (38 Knots) at 161.5 Meters (530 Feet)			5.4 M/S (10.5 Knots) at 161.5 Meters (530 Feet) at 335°		
Thrust to Weight	1.189			*		

*Data not available.

Time histories of pitch and yaw control parameters are shown in Figures 10-1 through 10-3, with peaks summarized in Table 10-2. Dynamics in the region between 0 and 40 seconds resulted primarily from guidance commands. Between 40 and 110 seconds vehicle dynamics were caused by the pitch guidance program and the wind. Dynamics from 110 seconds to S-IC outboard engine cutoff were caused by separated airflow aero-dynamics, inboard engine shutdown, tilt arrest, and high altitude winds.

The attitude errors between liftoff and 20 seconds indicate that the equivalent thrust vector misalignments present before the outboard engines canted were -0.13, 0.11, and -0.04 degrees in pitch, yaw, and roll, respectively. After outboard engine cant the misalignments became 0.04, 0.06, and 0.01 degrees. The attitude error transients at center engine cutoff indicate that the center engine misalignments were 0.02 and 0.30 degrees in pitch and yaw.

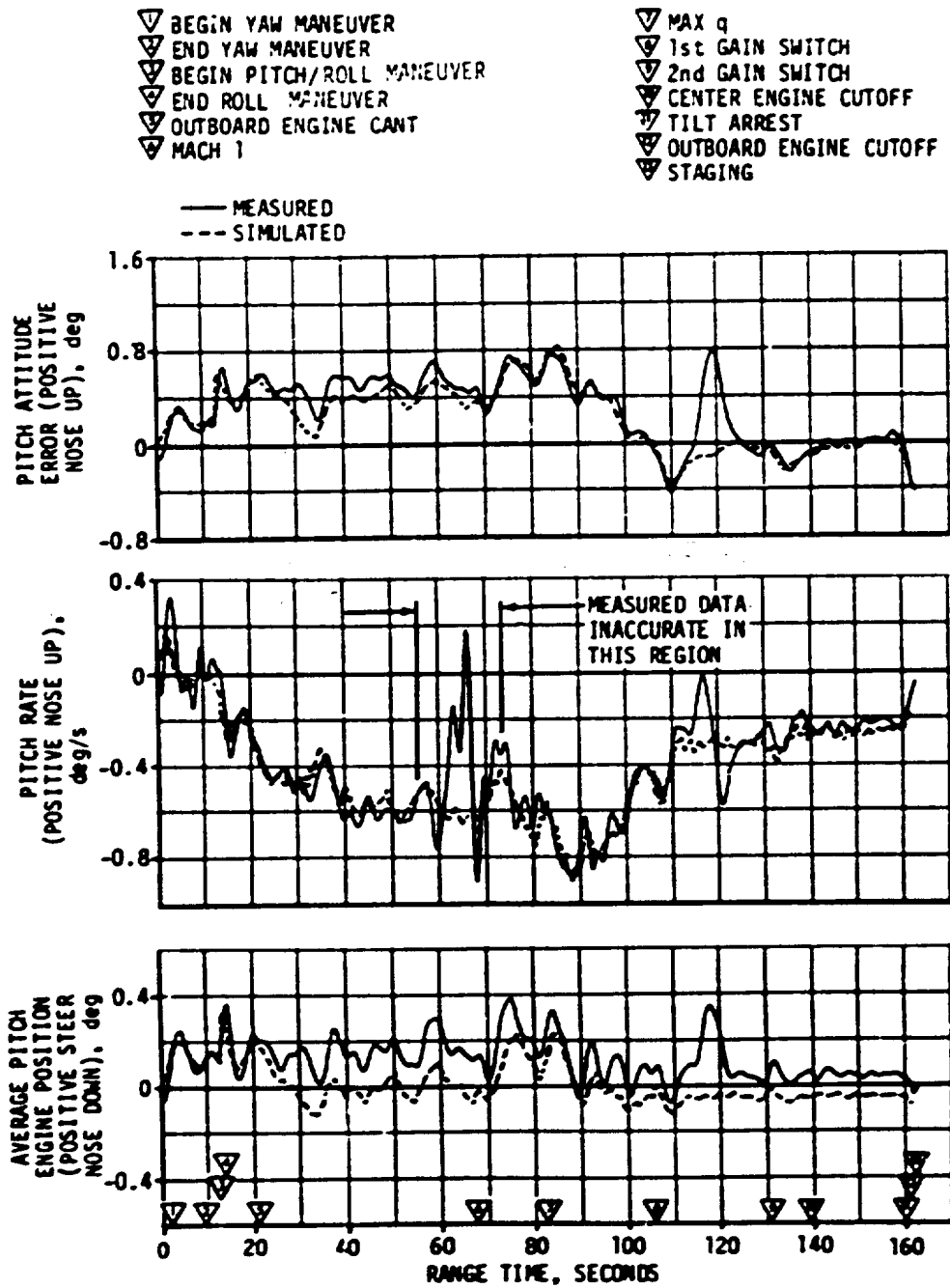


Figure 10-1. Pitch Plane Dynamics During S-IC Burn

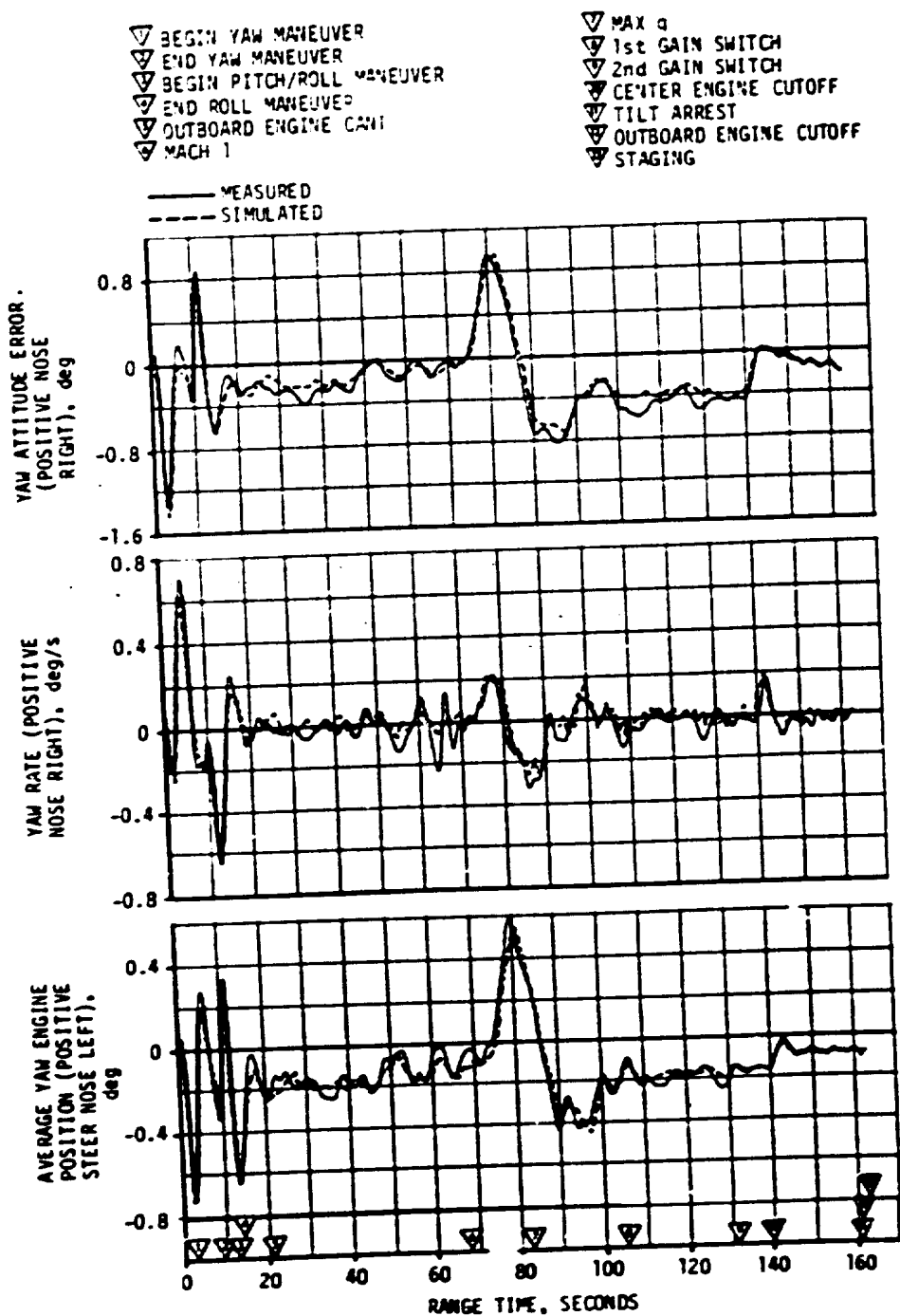


Figure 10-2. Yaw Plane Dynamics During S-IC Burn

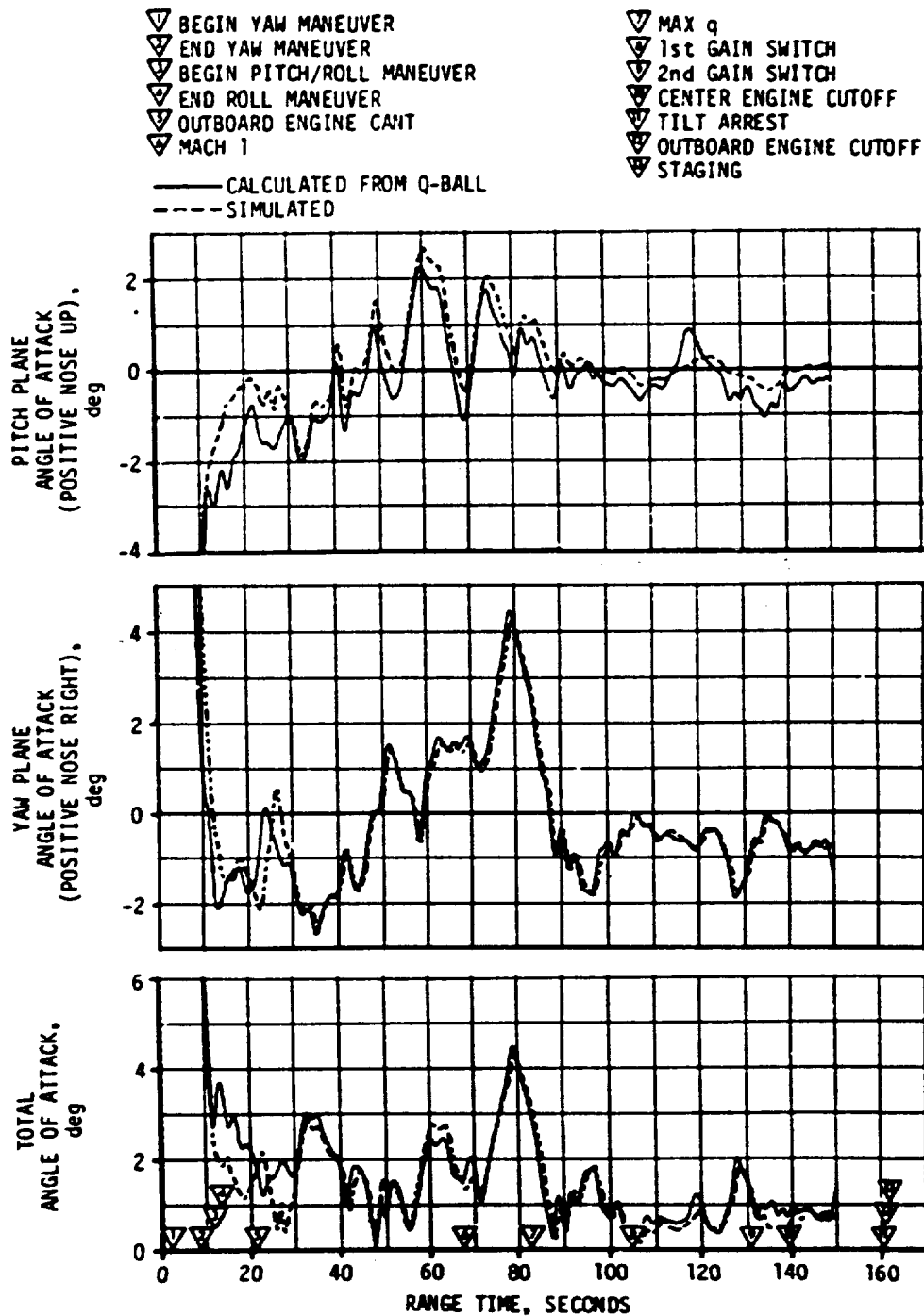


Figure 10-3. Pitch and Yaw Plane Free Stream Angle of Attack During S-IC Burn

Table 10-2. Maximum Control Parameters During S-IC Burn

PARAMETERS	PITCH PLANE		YAW PLANE		ROLL PLANE	
	AMPLITUDE	RANGE TIME (SEC)	AMPLITUDE	RANGE TIME (SEC)	AMPLITUDE	RANGE TIME (SEC)
Attitude Error*, deg	0.84	119.4	-1.26	3.3	1.02	14.0
Angular Rate, deg/s	-0.89	88.4	0.71	5.0	-1.18	14.7
Average Gimbal Angle, deg	0.38	75.0	-0.73	3.2		
Angle of Attack, deg	2.23	59.6	4.45	78.9		
Angle of Attack-Dynamic Pressure Product, deg-N/cm ² (deg-lbf/ft ²)	5.48 (1140)	74.4	14.45 (3018)	78.9		
Normal Acceleration, m/s ² (ft/s ²)	-0.45 (-1.5)	66	0.52 (1.7)	31		

* Biases removed

All dynamics were within vehicle capability. The attitude errors required to trim out the effects of thrust unbalance, offset center of gravity, thrust vector misalignment, and control system misalignments were within predicted envelopes. The peak angles of attack in the maximum dynamic pressure region were 2.23 degrees in pitch and 4.45 degrees in yaw. The peak average engine deflections required to trim out the aerodynamic moments in this region were 0.38 degree in pitch and 0.58 degree in yaw. No divergent bending or slosh dynamics were observed, indicating that both bending and slosh were adequately stabilized. Vehicle dynamics prior to S-IC/S-II first plane separation were within staging requirements.

10.3 S-II CONTROL SYSTEM EVALUATION

The S-II stage attitude control system performance was satisfactory. The vehicle dynamics were within expectations at all times. The maximum values of pitch parameters occurred in response to Iterative Guidance Mode (IGM) Phase I initiation. The maximum values of yaw and roll control parameters occurred in response to S-IC/S-II separation conditions. The maximum control parameter values for the period of S-II burn are shown in Table 10-3.

Between S-IC OECO and initiation of IGM Phase I, commands were held constant. Significant events occurring during this interval were S-IC/S-II separation, S-II stage J-2 engine start, second plane separation, and Launch Escape Tower (LET) jettison. Pitch and yaw dynamics during

Table 10-3. Maximum Control Parameters During S-II Burn

PARAMETER	PITCH PLANE		YAW PLANE		ROLL PLANE	
	AMPLITUDE	RANGE TIME (SEC)	AMPLITUDE	RANGE TIME (SEC)	AMPLITUDE	RANGE TIME (SEC)
Attitude Error*, deg	-1.5	471	-0.5	206	-2.7	166
Angular Rate, deg/sec	1.0	471	0.5	204	2.5	166
Average Gimbal Angle, deg	0.5	206	0.4	206	-	-

* Biases removed

this interval indicated adequate control stability as shown in Figures 10-4 and 10-5, respectively. Steady state attitudes were achieved within 10 seconds from S-IC/S-II separation.

Flight and simulated data comparison, Figures 10-4 and 10-5, show agreement at those events of greatest control system activity. Differences between the two can be accounted for largely by engine location misalignments, thrust vector misalignments, and uncertainties in engine thrust buildup characteristics.

10.4 S-IVB CONTROL SYSTEM EVALUATION

The S-IVB thrust vector control system provided satisfactory pitch and yaw control during powered flight. The APS provided satisfactory roll control during first and second burns.

During S-IVB first and second burns, control system transients were experienced at S-II/S-IVB separation, guidance initiation, Engine Mixture Ratio (MR) shift, terminal guidance mode, and S-IVB Engine Cut-off (ECO). These transients were expected and were well within the capabilities of the control system.

10.4.1 Control System Evaluation During First Burn

S-IVB first burn pitch attitude error, angular rate, and actuator position are presented in Figure 10-6. First burn yaw plane dynamics are presented in Figure 10-7. The maximum attitude errors and rates occurred at IGM initiation. A summary of the first burn maximum values of critical flight control parameters is presented in Table 10-4.

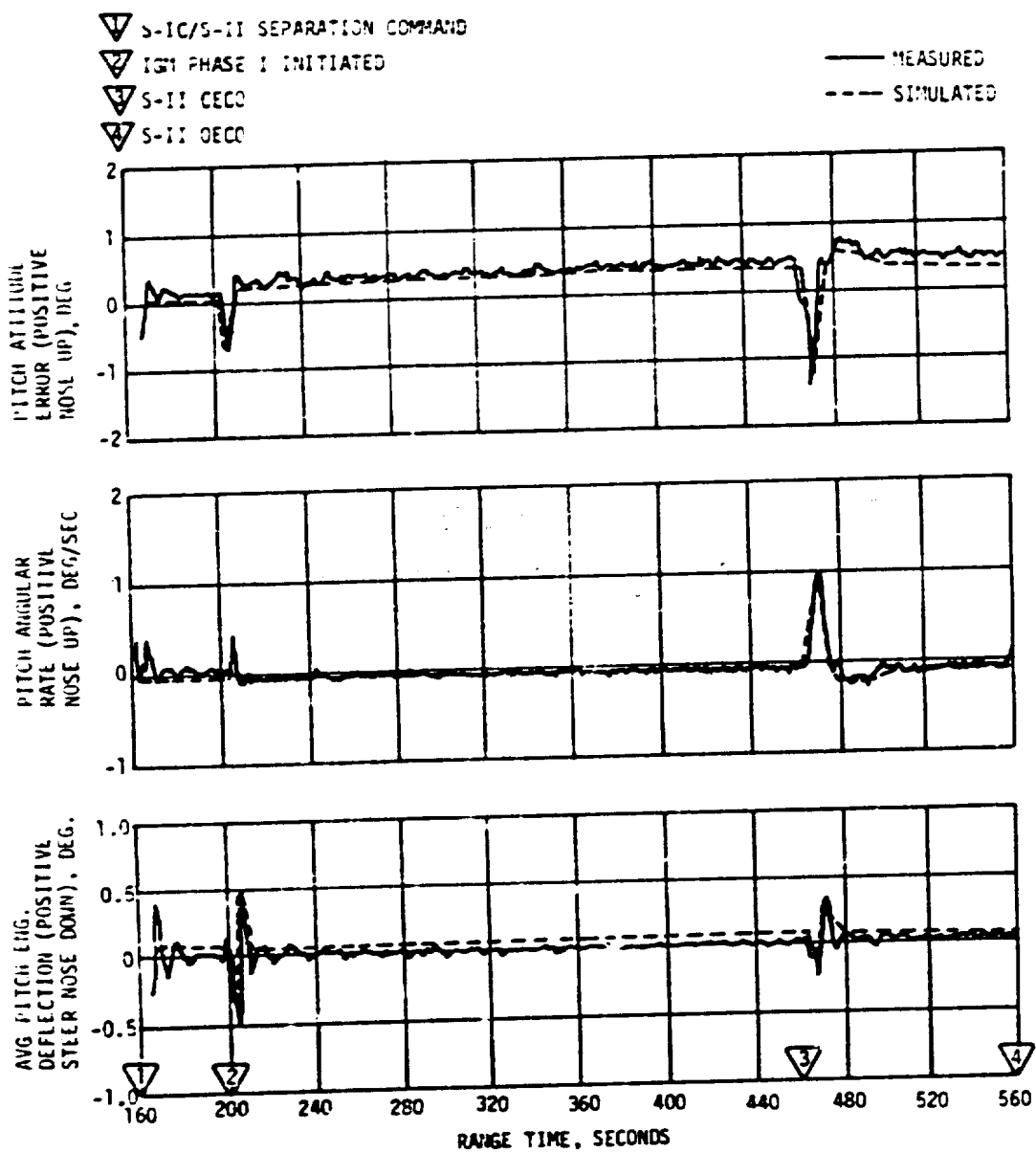


Figure 10-4. Pitch Plane Dynamics During S-II Burn

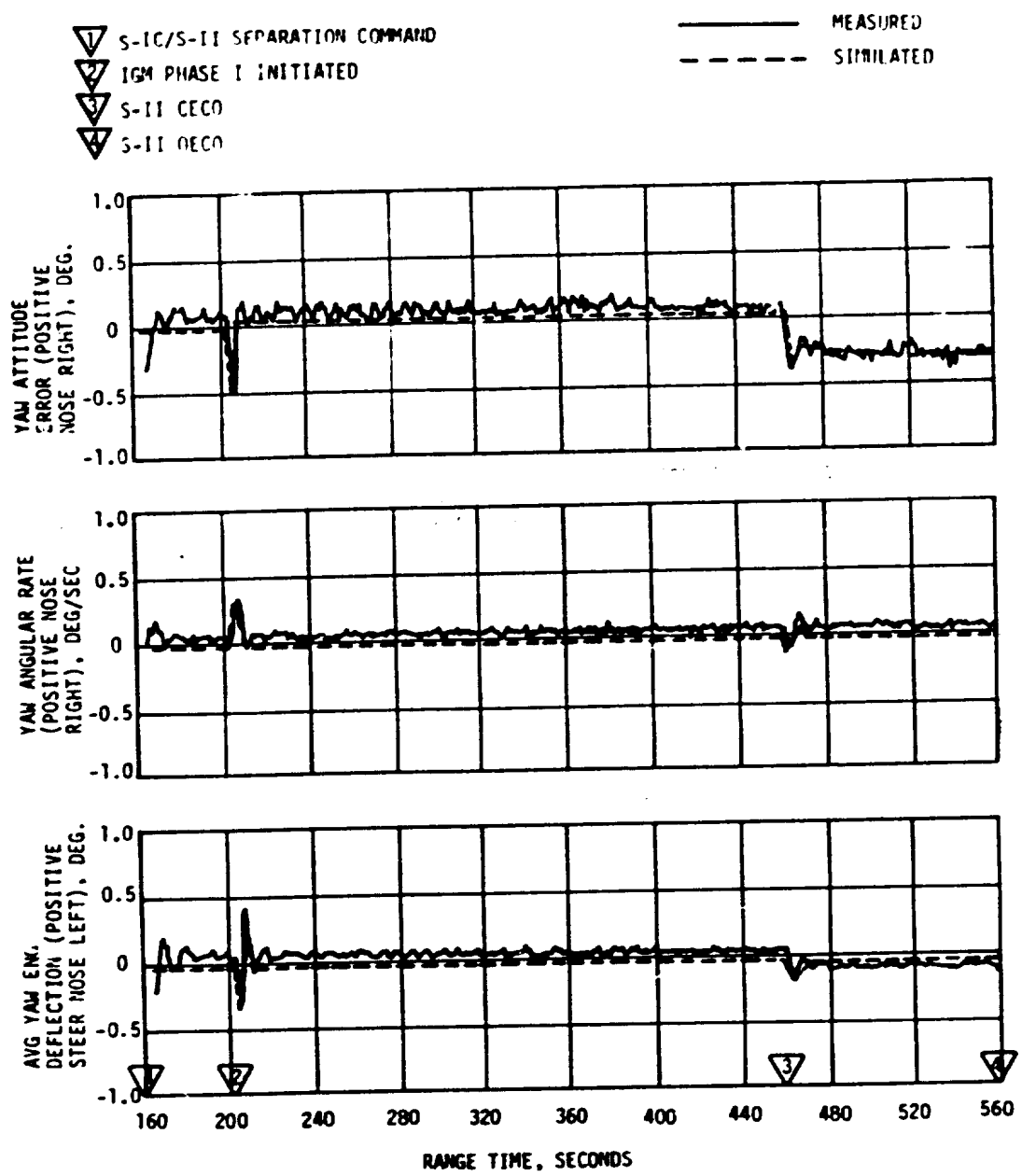


Figure 10-5. Yaw Plane Dynamics During S-II Burn

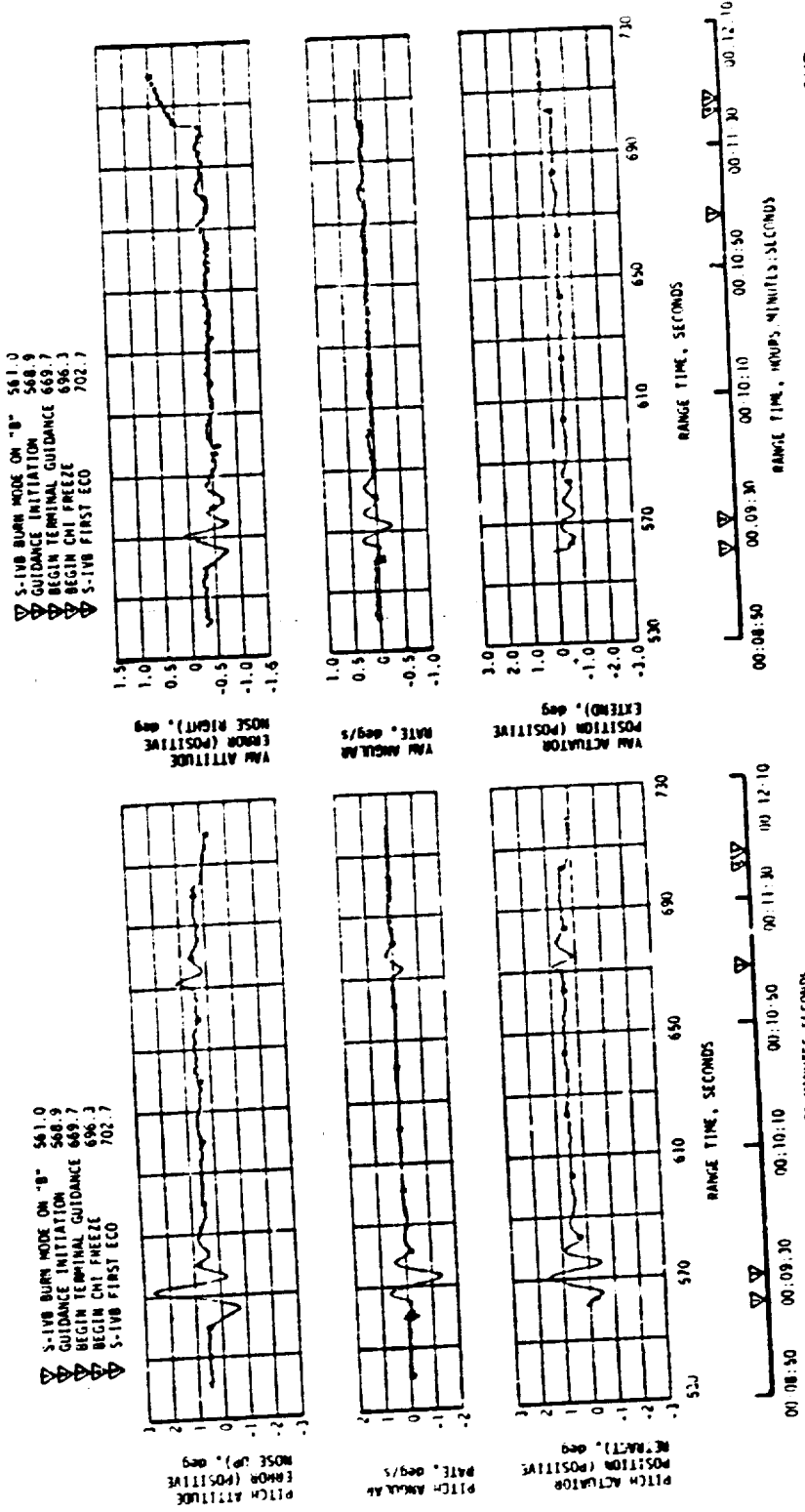


Figure 10-6. Pitch Plane Dynamics During S-IVB First Burn



Figure 10-7. Yaw Plane Dynamics During S-IVB First Burn

Table 10-4. Maximum Control Parameters During S-IVB First Burn

PARAMETER	PITCH PLANE		YAW PLANE		ROLL PLANE	
	AMPLITUDE	RANGE TIME (SEC)	AMPLITUDE	RANGE TIME (SEC)	AMPLITUDE	RANGE TIME (SEC)
Attitude Error*, deg	2.4	571.5	-0.7	574.0	-0.8	606.0
Angular Rate, deg/s	-1.4	573.0	-0.3	572.0	-0.5	561.4
Maximum Gimbol Angle, deg	1.5	570.5	-0.7	574.0	-	-

* Stages removed

The pitch and yaw effective thrust vector misalignments during first burn were 0.37 and -0.18 degrees, respectively. A steady state roll torque of 7.4 N-m (5.4 lbf-ft) counterclockwise looking forward required roll APS firings during first burn. The steady state roll torque experienced on previous flights has ranged between 61.4 N-m (45.3 lbf-ft) counterclockwise and 54.2 N-m (40.0 lbf-ft) clockwise.

Propellant sloshing during first burn was observed on data obtained from the Propellant Utilization (PU) mass sensors. The propellant slosh did not have any noticeable effect on the operation of the attitude control system.

10.4.2 Control System Evaluation During Parking Orbit

The APS provided satisfactory orientation and stabilization during parking orbit. Following S-IVB first ECO, the vehicle was maneuvered to the in-plane local horizontal, and the orbital pitch rate was established. The pitch attitude error and pitch angular rate for this maneuver are shown in Figure 10-8. Available data indicate that sloshing disturbances which caused venting of LOX on AS-510 were minimized on AS-512. The LOX ullage pressure remained below the relief setting throughout parking orbit.

10.4.3 Control System Evaluation During Second Burn

S-IVB second burn pitch attitude error, angular rate, and actuator position are presented in Figure 10-9. Second burn yaw plane dynamics are presented in Figure 10-10. The maximum attitude errors and rates occurred following guidance initiation. Transients were also observed as a result of the pitch and yaw attitude commands at the termination of the Artificial Tau guidance mode (27 seconds before ECO).

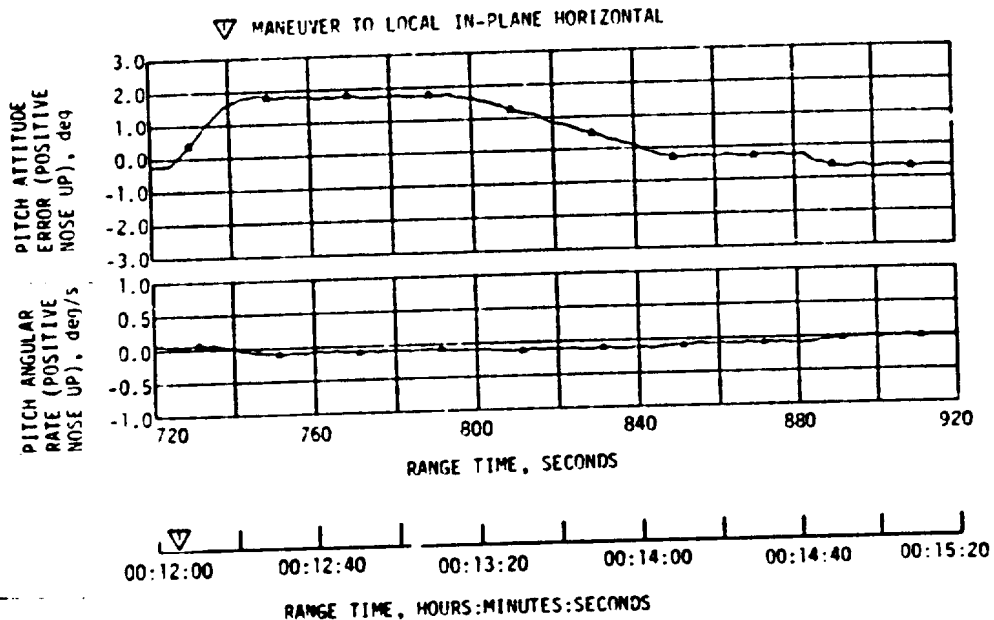


Figure 10-8. Pitch Plane Dynamics During Parking Orbit

A summary of the second burn maximum flight control parameter values is presented in Table 10-5.

Table 10-5. Maximum Control Parameters During S-IVB Second Burn

PARAMETER	PITCH PLANE		YAW PLANE		ROLL PLANE	
	AMPLITUDE	RANGE TIME (SEC)	AMPLITUDE	RANGE TIME (SEC)	AMPLITUDE	RANGE TIME (SEC)
Attitude Error*, deg	2.2	11567.5	-0.8	11579.0	+0.9	11885.0
Angular Rate, deg/s	-1.4	11569.0	0.3	11581.0	0.15	11560.0
Maximum Gimbal Angle, deg	1.3	11567.0	-0.7	11570.0	-	-

* Biases removed

The pitch and yaw effective thrust vector misalignments early in second burn (prior to MR shift) were 0.36 and -0.16 degrees, respectively. Following the MR shift the misalignments were 0.50 and -0.24 for pitch and yaw, respectively. The steady state roll torque during second burn was essentially zero as minimum impulse firings were observed at alternating sides of the roll deadband.

Normal propellant sloshing during second burn was observed on data obtained from the PU mass sensors. The slosh activity did not have any noticeable effect on the operation of the Attitude Control System.

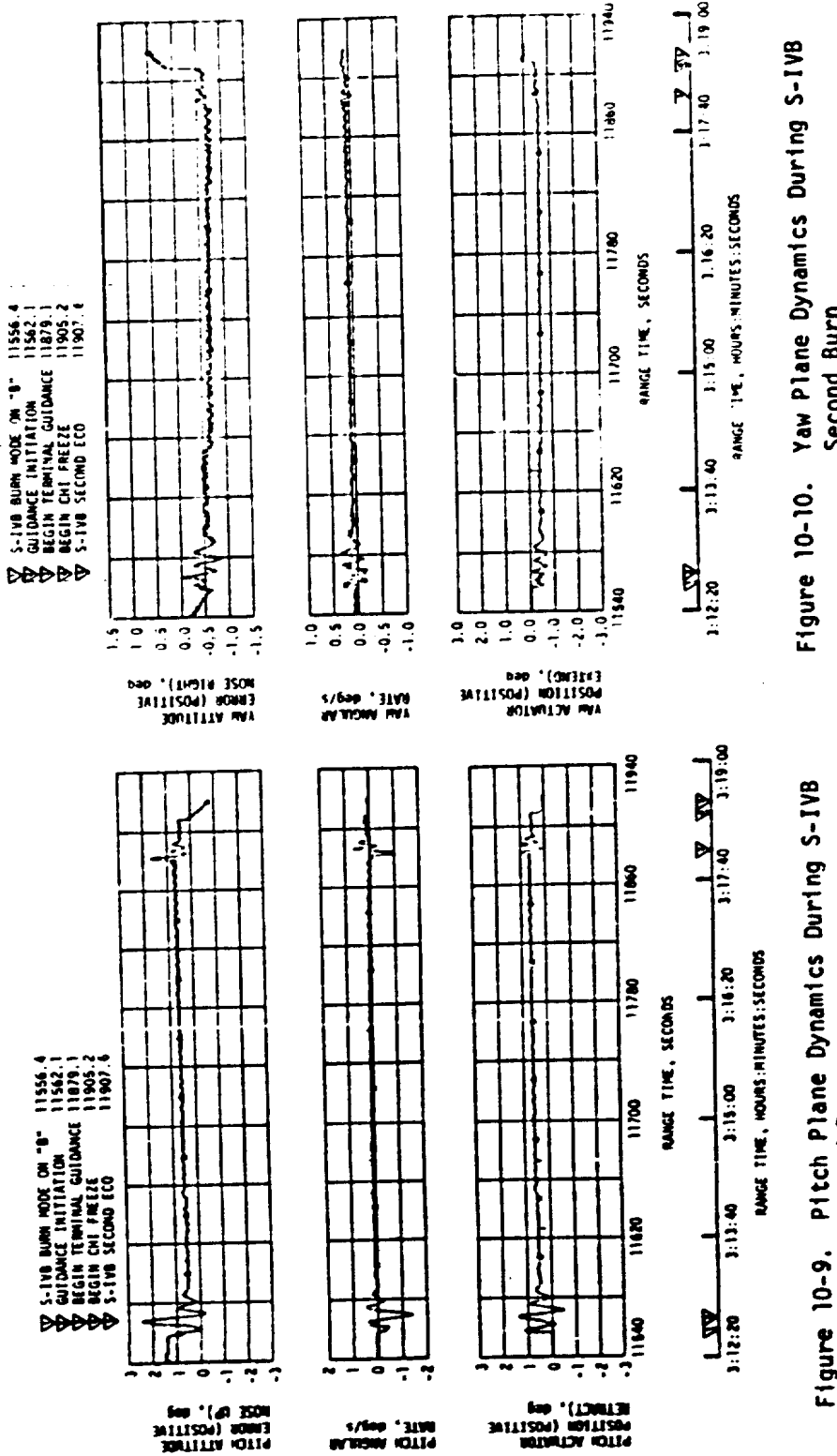


Figure 10-9. Pitch Plane Dynamics During S-IVB Second Burn

Figure 10-10. Yaw Plane Dynamics During S-IVB Second Burn

10.4.4 Control System Evaluation After S-IVB Second Burn

The APS provided satisfactory orientation and stabilization from Translunar Injection (TLI) through the S-IVB/IU Passive Thermal Control (PTC) maneuver [Three-Axis Tumble Maneuver]. Each of the planned maneuvers was performed satisfactorily.

Significant events related to translunar coast attitude control were the maneuver to the in-plane local horizontal following second burn cutoff, the maneuver to the Transportation Docking and Ejection (TD&E) attitude, spacecraft separation, spacecraft docking, lunar module extraction, the maneuver to the evasive ullage burn attitude, the maneuver to the LOX dump attitude, the maneuver to the optimum lunar impact ullage burn attitude, the maneuver to the solar heating control attitude, the maneuver to the vernier lunar impact ullage burn attitude, and the PTC maneuver.

The pitch attitude error and angular rate for events during which telemetry data were available are shown in Figure 10-11.

Following S-IVB second cutoff, the vehicle was maneuvered to the in-plane local horizontal at 12,059 seconds (03:20:59) (through approximately -19.4 degrees in pitch and -0.2 degree in yaw), and an orbital pitch rate was established. At 12,809 seconds (03:33:29), the vehicle was commanded to maneuver to the separation TD&E attitude (through approximately 120, 40 and -180 degrees in pitch, yaw and roll, respectively).

Spacecraft separation, which occurred at 13,347 seconds (03:42:27), appeared nominal, as indicated by the relatively small disturbances induced on the S-IVB.

Disturbances during spacecraft docking, which occurred at 14,231 seconds (03:57:11), were less than on previous flights. Docking disturbances required 2,160 N-sec (485 lbf-sec) of impulse from Module 1 and 1,160 N-sec (261 lbf-sec) of impulse from Module 2. The largest docking disturbances on previous flights occurred on AS-510 and required 3,480 N-sec (783 lbf-sec) of impulse from Module 1 and 3,040 N-sec (683 lbf-sec) of impulse from Module 2. Lunar module extraction occurred at 17,102 seconds (04:45:02) with nominal disturbances.

At 17,520 seconds (04:52:00) a yaw maneuver from 40.3 degrees (TD&E attitude) to -40.0 degrees was initiated to attain the desired attitude for the evasive ullage burn. At 18,181 seconds (05:03:01) the APS ullage engines were commanded on for 80 seconds to provide the necessary separation distance between the S-IVB and spacecraft.

The maneuver to the LOX dump attitude was performed at 18,760 seconds (05:12:40). This was a two-axis maneuver with pitch commanded from 179.5

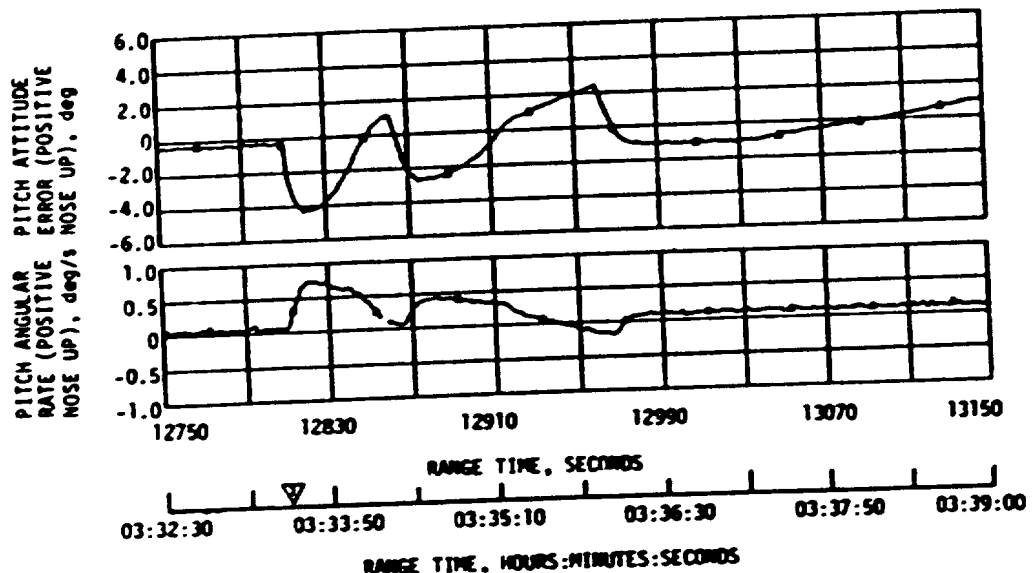
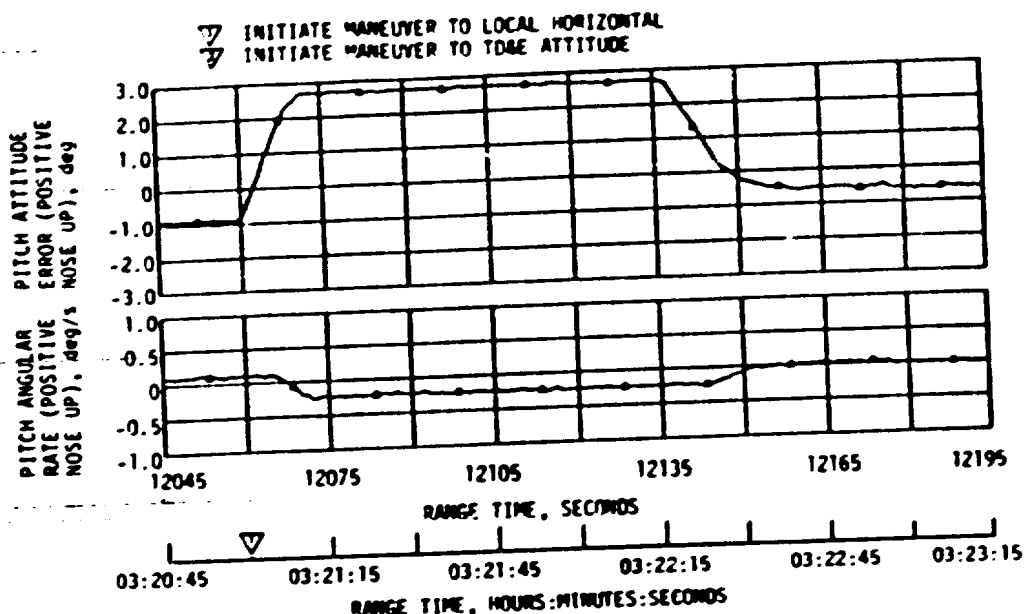


Figure 10-11. Pitch Plane Dynamics During Translunar Coast (Sheet 1 of 6)

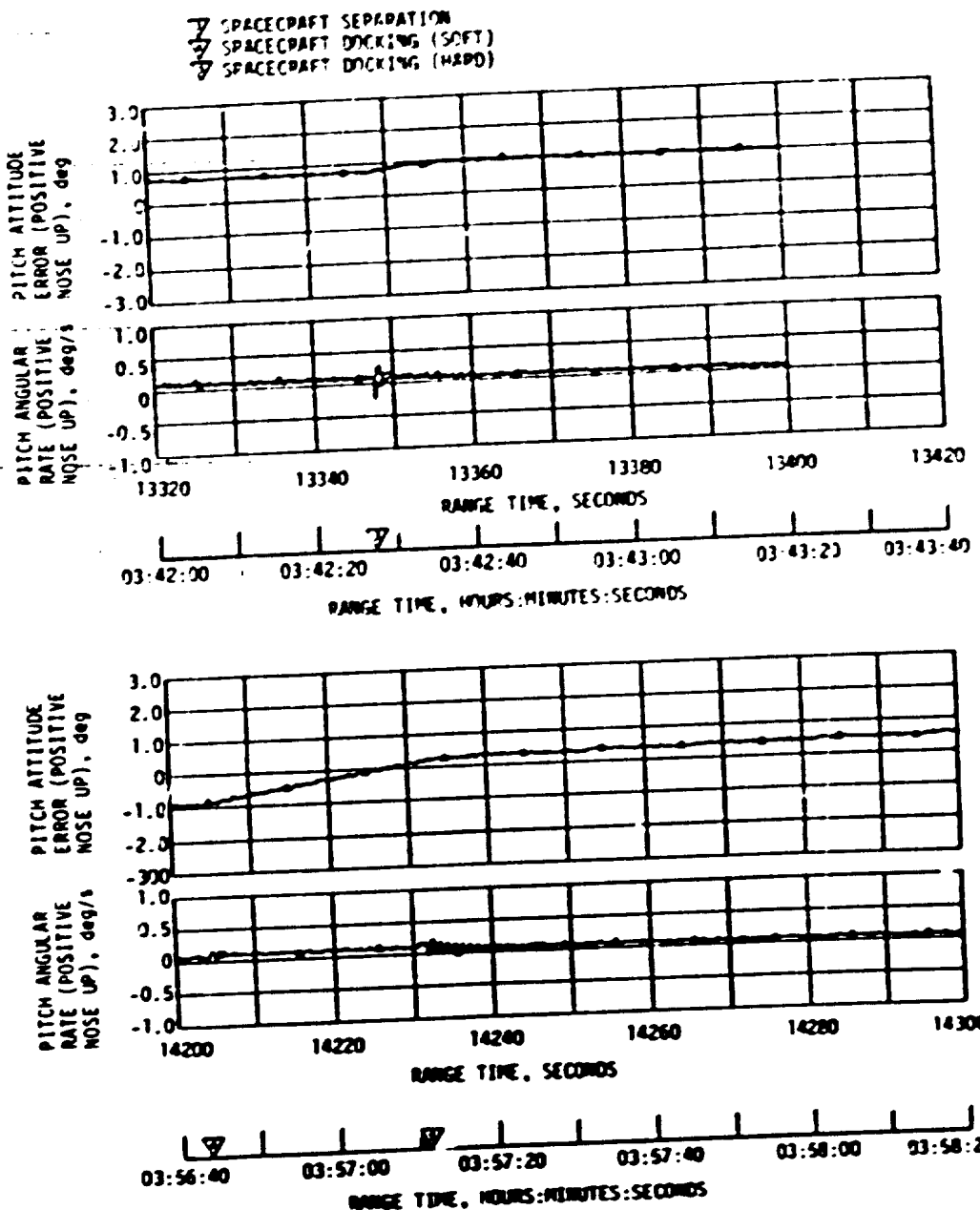


Figure 10-11. Pitch Plane Dynamics During Translunar Coast (Sheet 2 of 6)

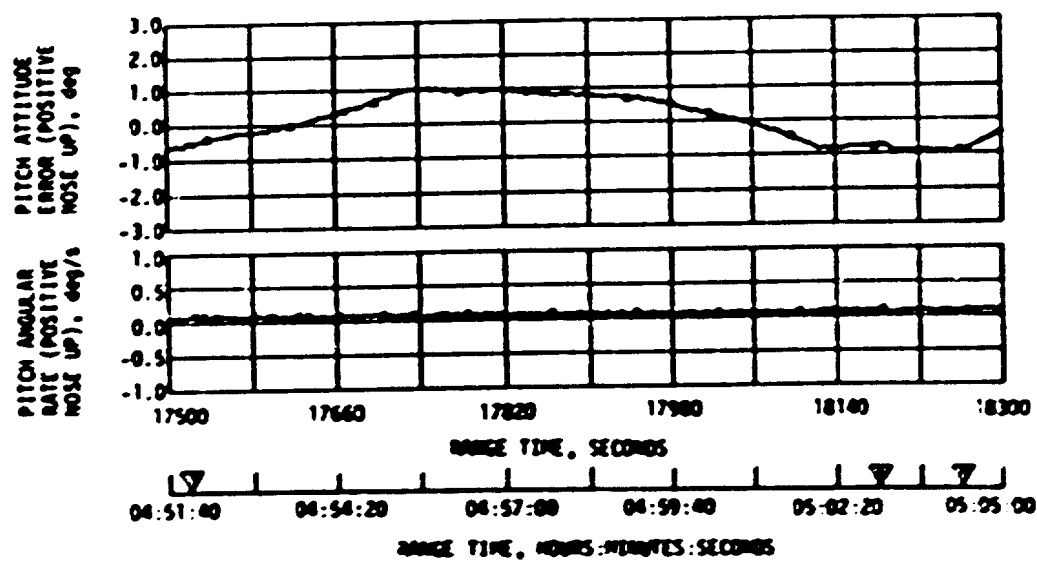
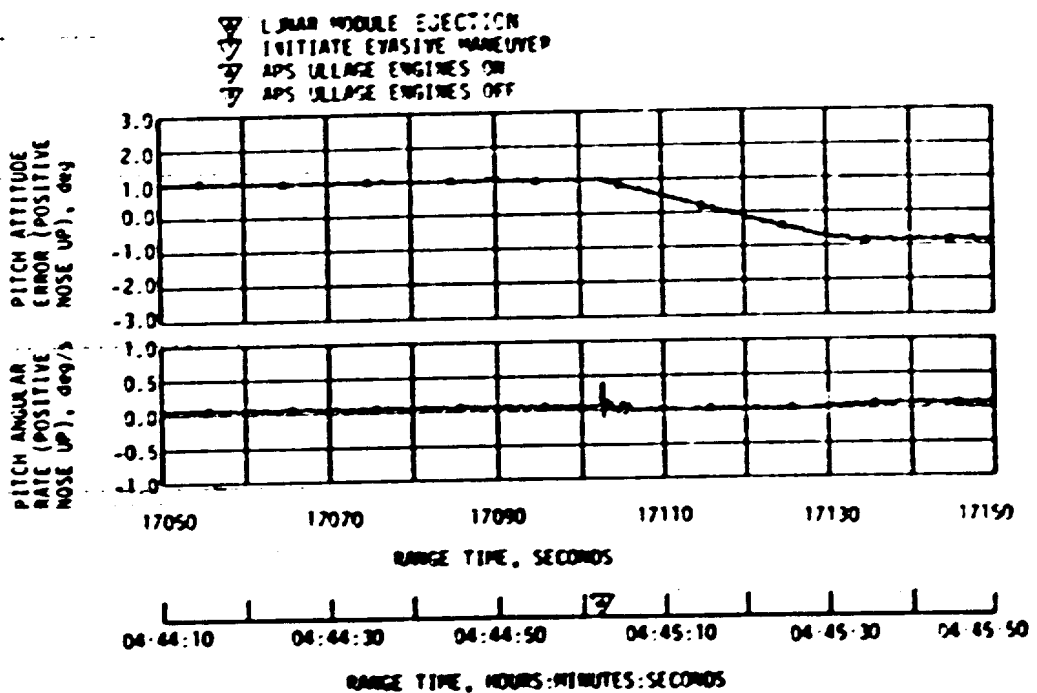


Figure 10-11. Pitch Plane Dynamics During Translunar Coast (Sheet 3 of 6)

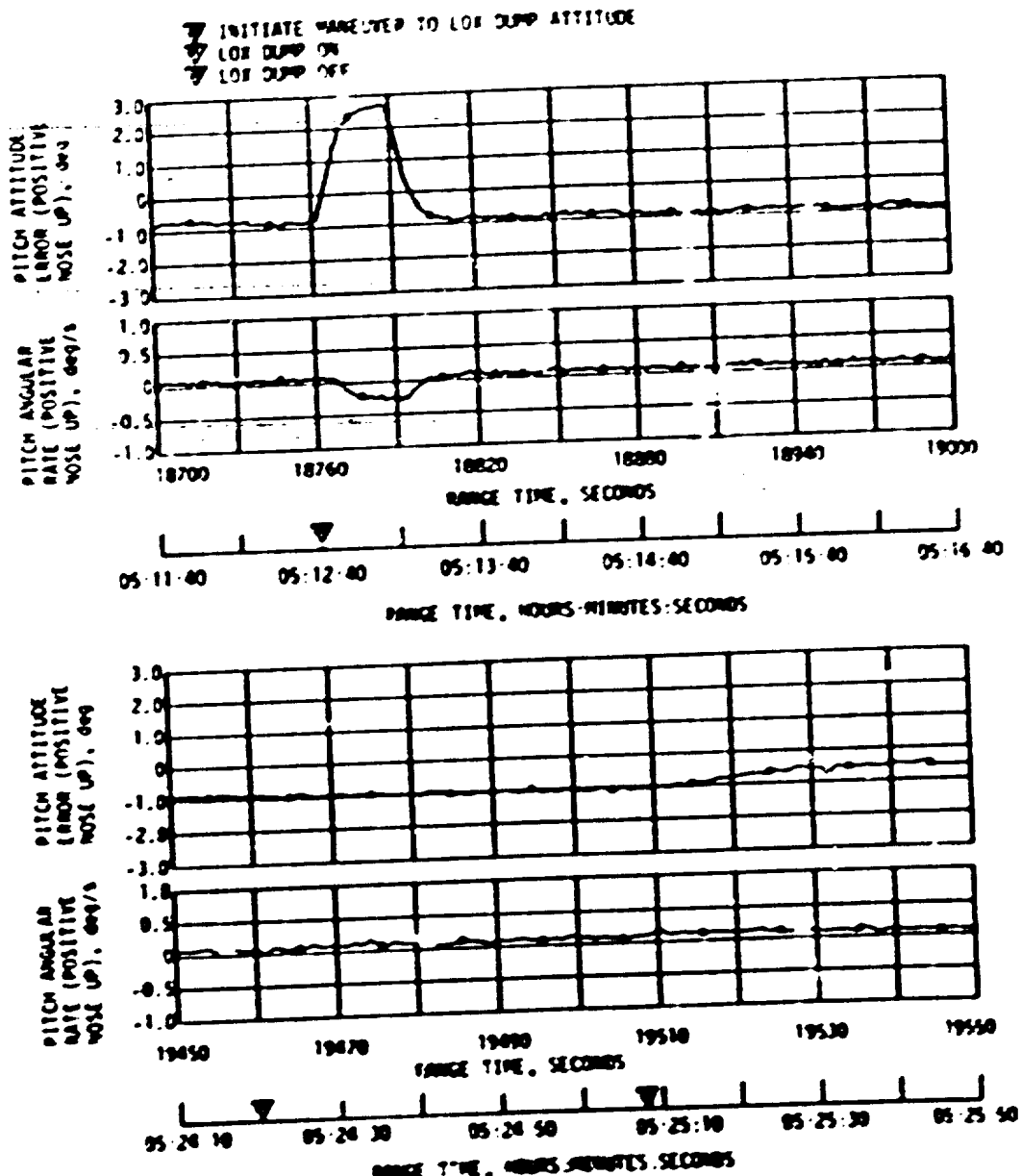


Figure 10-11. Pitch Plane Dynamics During Translunar Coast (Sheet 4 of 6)

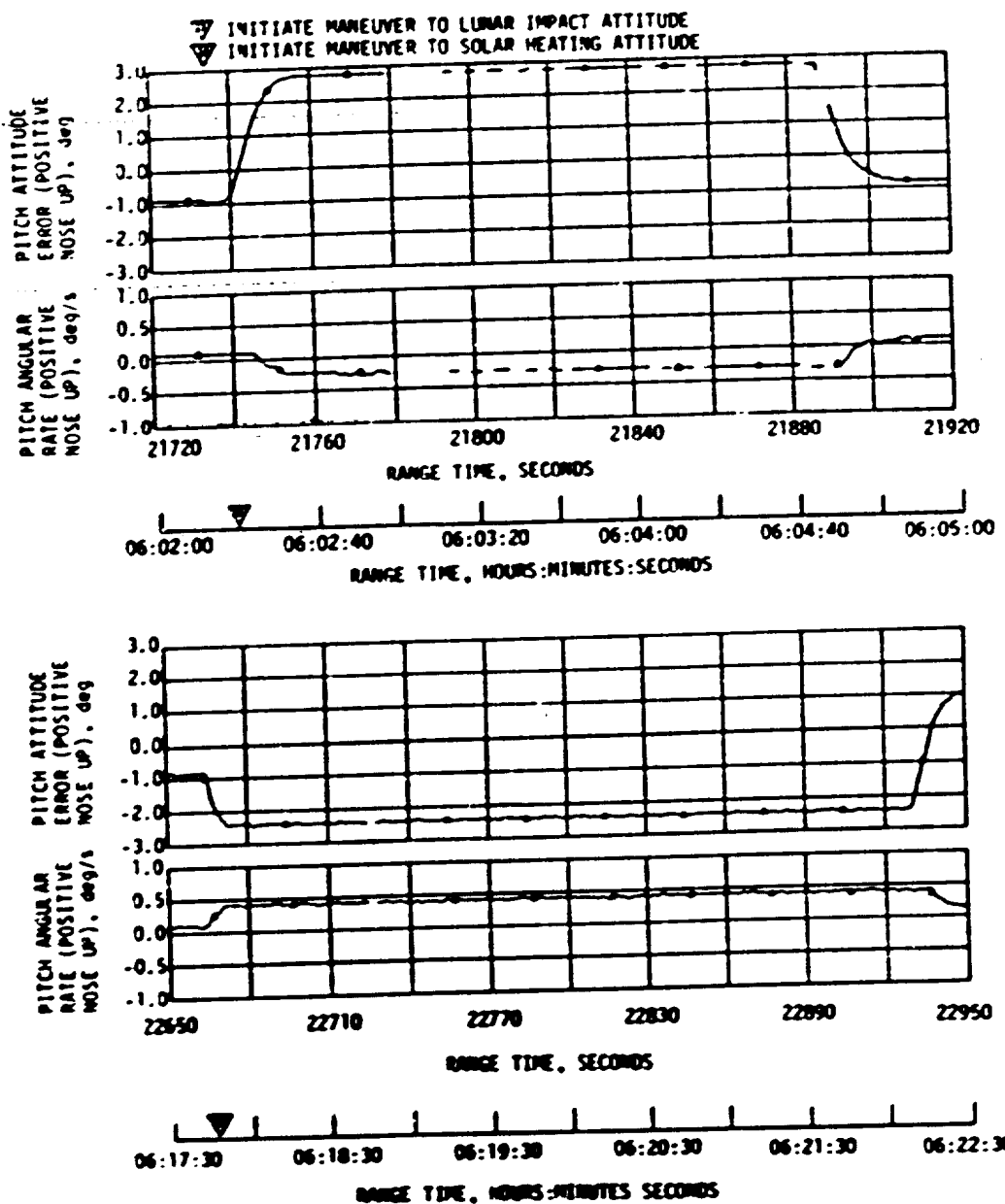


Figure 10-11. Pitch Plane Dynamics During Translunar Coast (Sheet 5 of 6)

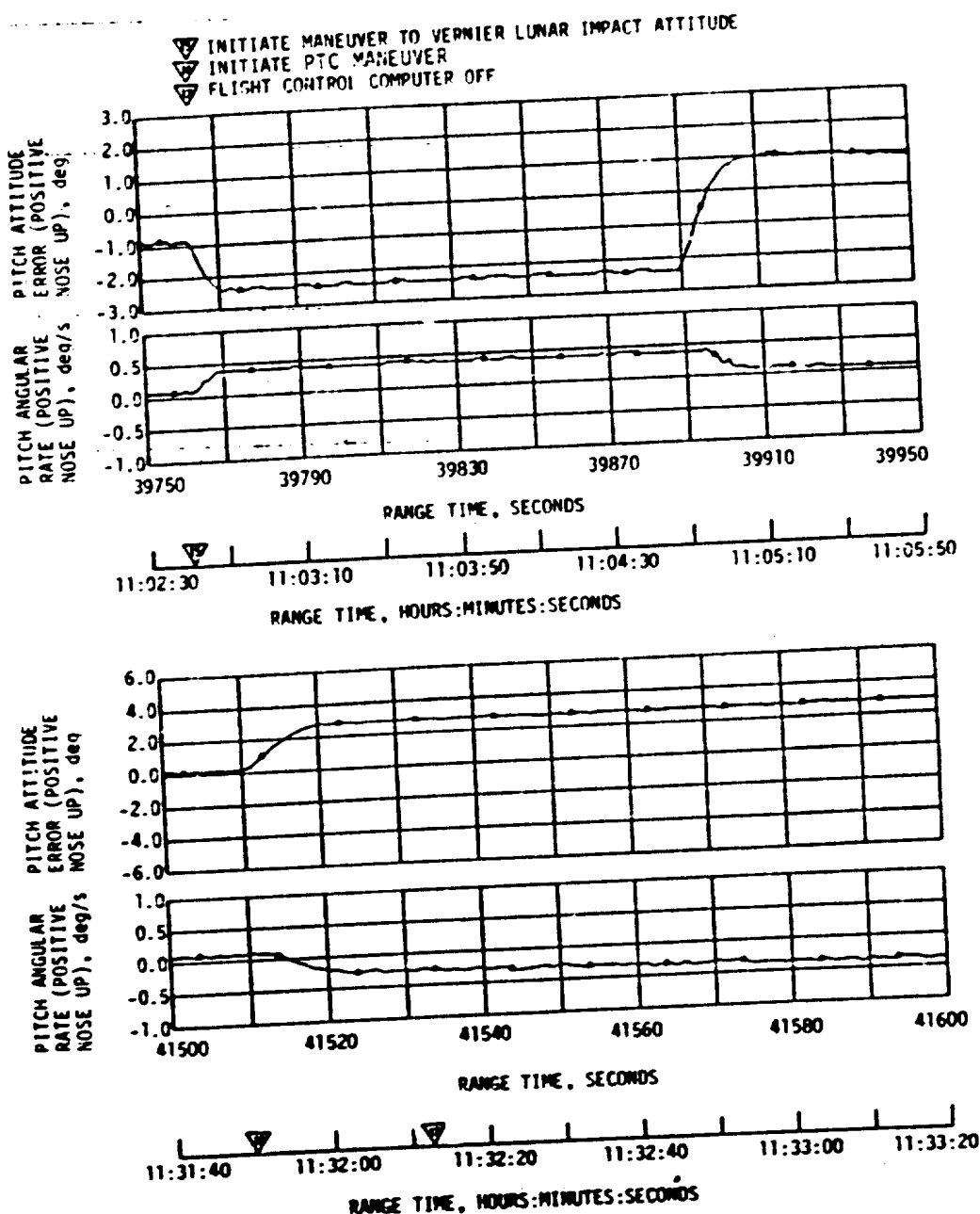


Figure 10-11. Pitch Plane Dynamics During Translunar Coast (Sheet 6 of 6)

to 190.0 degrees and yaw from -40 to -19 degrees referenced to the in-plane local horizontal. LOX dump occurred at 19,460 seconds (04:24:20) and lasted for 48 seconds.

At 21,735 seconds (06:02:15) a ground command was received to perform a maneuver to the desired attitude for the APS ullage burn for lunar target impact. This was also a two-axis maneuver and resulted in a pitch maneuver change from 190.0 to 248.0 degrees and a yaw attitude maneuver change from -19.0 to -23.0 degrees referenced to the in-plane local horizontal. At 22,200 seconds (06:10:00) the APS ullage engines were commanded on for 98 seconds to provide delta velocity for lunar target impact.

At 22,664 seconds (06:17:44) a ground command was received to perform a maneuver to the solar heating attitude to assure proper solar heating conditions. This was a single-axis pitch maneuver and resulted in a pitch maneuver change from -248.0 to 161.0 degrees referenced to the in-plane local horizontal.

At 39,760 seconds (11:02:40) a ground command was received to perform a maneuver to the desired attitude for the second lunar impact APS ullage burn. This maneuver was a two-axis maneuver and resulted in a pitch maneuver change from 161.0 to 121.0 degrees and a yaw attitude maneuver change from -23.0 to -11 degrees referenced to the in-plane local horizontal. At 40,500 seconds (11:15:00) the APS ullage engines were commanded on for 102 seconds to provide delta velocity for a more accurate lunar target impact.

The command to initiate the PTC maneuver was received at 41,510 seconds (11:31:50). This maneuver consisted of commanding the vehicle +31 degrees in the pitch, yaw and roll axis. After vehicle angular rates of approximately -0.3 degree/second pitch, -0.3 degree/second yaw, and 0.6 degree/second roll were established, a ground command was received (Flight Control Computer Power Off B) at 41,532.5 (11:32:12.5) to inhibit the IU Flight Control Computer leaving the vehicle in a three-axis tumble mode.

APS propellant consumption for attitude control and propellant settling prior to the APS burn for lunar target impact was lower than the mean predicted requirements. The total propellant (fuel and oxidizer) used prior to the first ullage burn for lunar target impact delta velocity was 51.8 kilograms (114.2 lbm) and 52.9 kilograms (116.7 lbm) for Modules 1 and 2, respectively. This was approximately 35 percent of the total available propellant in each module (approximately 147 kilograms [330 lbm]). APS propellant consumption is tabulated in Section 7, Table 7-4.

10.5 INSTRUMENT UNIT CONTROL COMPONENTS EVALUATION

The control subsystem performed properly throughout the AS-512 mission. All ST-124M Stabilized Platform Subsystem (SPS) factors remained within previously experienced limits. The equipment temperatures increased as expected when the water sublimator operation was inhibited (Section 14.4.1).

10.5.1 Gimbal Angle Resolvers

Proper vehicle attitude was indicated by the gimbal angle resolvers until the PTC maneuver was initiated at approximately 41,500 seconds. As on AS-511 the positive yaw gimbal mechanical stop was contacted for short periods of time. This was expected. No vehicle perturbation or hardware failure was evident as a result of the contacts.

10.5.2 ST-124M Power Supplies

All power parameters were within specification limits. Deviation from nominal occurred while the water sublimator operation was inhibited. The 4.8 KHz voltage increased while the 400 Hz voltage decreased, but in each case no specification limit was exceeded.

10.6 SEPARATION

10.6.1 S-IC/S-II Separation

The AS-512 S-IC/S-II stages separated as planned with no known anomalies. Clearance distance between the stages was approximately 2.4 meters (eight feet) more than required at S-II Engine Start Command (ESC) as shown in Figure 10-12. Separation distance was approximately 15.2 meters (50 feet) at J-2 engines main propellant ignition.

During the first portion of separation period (160 to 166 seconds), the maximum roll attitude and angular rate were approximately -2.7 degrees and +2.5 degrees per second, respectively. Maximum pitch and yaw attitude and -0.7 degrees, respectively. Corresponding rates at this time were -0.2 and -0.1 degrees per second.

Second Plane Separation

Second plane separation was performed as planned. No significant transients in vehicle attitudes or rates were identified that would have caused this separation to be other than nominal.

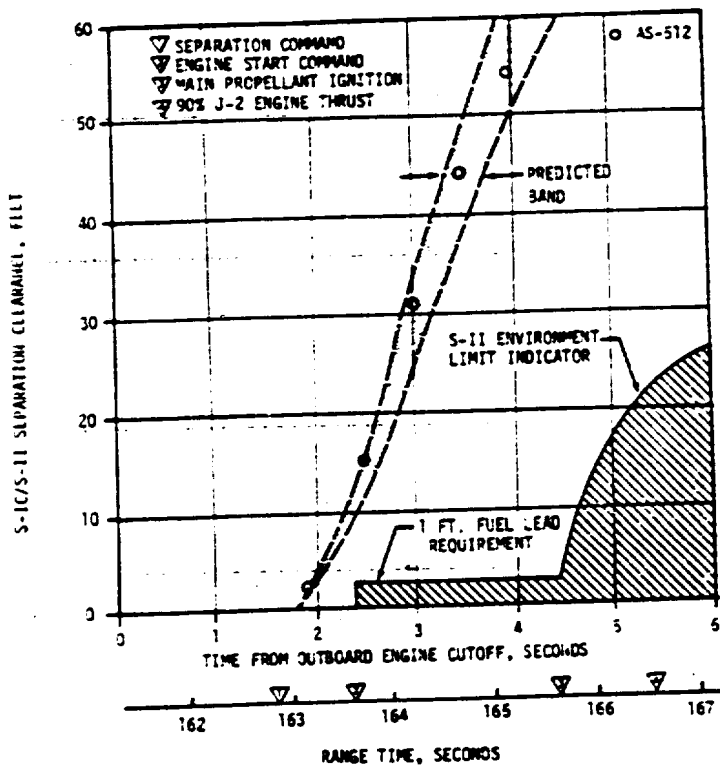


Figure 10-12. AS-512 S-IC/S-II Separation Distance

10.6.3 S-II/S-IVB Separation

Nominal accelerations were observed on the flight vehicle during the S-II/S-IVB separation. Vehicle dynamics were as predicted and well within staging limits.

10.6.4 CSM Separation

At 12,810 seconds (03:33:30) a maneuver to the TD&E attitude was initiated to assure proper lighting and communication conditions for spacecraft separation, docking, and lunar module ejection. The vehicle was commanded to pitch 120 degrees, yaw 40 degrees, and roll -180 degrees. This attitude was held inertially until the beginning of the evasive maneuver. The vehicle motion during the maneuver was close to predicted with maximum vehicle rates of 0.75 deg/sec, 0.95 deg/sec, and -0.80 deg/sec in the pitch, yaw, and roll axes, respectively.

Transients due to spacecraft separation at approximately 13,348 seconds (03:42:28) appeared nominal. Separation disturbances caused five APS Module 1 pitch firings within 10 seconds following separation. A negative roll disturbance was controlled by 6 roll firings within 15 seconds following separation.

All attitude errors remained within the 1 degree deadband during the separation process.

SECTION 11

ELECTRICAL NETWORKS AND EMERGENCY DETECTION SYSTEM

11.1 SUMMARY

The AS-512 launch vehicle electrical systems and Emergency Detection System (EDS) performed satisfactorily throughout the required period of flight. However, the temperature of the S-IVB Aft Battery No. 1, Unit No. 1, increased significantly above the nominal control limit (90°F) at approximately 9 hours due to malfunction of the primary heater control system. Operation of the Aft Battery NO. 1 remained nominal as did operation of all other batteries, power supplies, inverters, Exploding Bridge Wire (EBW) firing units, and switch selectors.

11.2 S-IC STAGE ELECTRICAL SYSTEM

The S-IC stage electrical system performance was satisfactory. Battery voltages were within performance limits of 26.5 to 32.0 V during powered flight. The battery currents were near predicted and below the maximum limits of 50 amperes for each battery. Battery power consumption was within the rated capacity of each battery, as shown in Table 11-1, but exceeded predictions due to range safety system loads during the launch delay.

Table 11-1. S-IC Stage Battery Power Consumption

BATTERY	RATED CAPACITY (AMP-HR)	POWER CONSUMPTION*	
		AMP-HR	PERCENT OF CAPACITY
Operational	8.33	2.51	30.1
Instrumentation	8.33	3.70	44.4

*Battery power consumptions were calculated from the initial power transfer (T-50 seconds) until S-IC/S-II separation and include energy used during the first countdown sequence prior to the hold including range safety consumption.

The two measuring power supplies were within the required 5 ± 0.05 V limit during power flight. All switch selector channels functioned as commanded by the Instrument Unit (IU) and were within required time limits.

The separation and retrorocket EBW firing units were armed and triggered as programmed. Charging time and voltage characteristics were within performance limits.

The range safety command system EBW firing units were in the required state-of-readiness for vehicle destruct, had it been necessary.

11.3 S-II STAGE ELECTRICAL SYSTEM

The S-II stage electrical system performed satisfactorily. All battery and bus voltages remained within specified limits through the prelaunch and flight periods. Bus currents also remained within predicted limits. Main bus current averaged 30 amperes during S-IC boost and varied from 45 to 50 amperes during S-II boost. Instrumentation bus current averaged 22 amperes during S-IC and S-II boost. Recirculation bus current averaged 87 amperes during S-IC boost. Ignition bus current averaged 30 amperes during the S-II ignition sequence.

The first countdown sequence produced an additional battery load prior to Terminal Countdown Sequencer (TCS) cutoff. The additional time on internal power was 20 seconds which resulted in an additional drain of 0.16 ampere-hours for the Main Battery, 0.13 ampere-hours for Instrumentation Battery and 0.48 ampere-hours for the combination of Recirculation and Ignition batteries. The ignition voltage drop anomaly which occurred during AS-511 did not reappear on this flight.

Battery power consumption was within the rated capacity of each battery, as shown in Table 11-2.

Table 11-2. S-II Stage Battery Power Consumption

BATTERY	RATED CAPACITY (AMP-HR)	POWER CONSUMPTION	
		AMP-HR	PERCENT OF CAPACITY
Main	35	13.99	39.7
Instrumentation	35	10.56	30.1
Recirculation #1	30	12.70	42.4
Recirculation #2	30	12.75	42.5

*Battery power consumptions were calculated from activation until S-II/S-IVB separation and include 6.5 to 6.9 amp-hrs consumed during the battery activation procedures as well as energy used during the first countdown sequence prior to the hold including range safety consumption.

There was no indication in flight of a performance degradation occurrence with the countdown long term open circuit voltage decay of forward battery No. 2 reported in Section 3.2.3.

All switch selector channels functioned as commanded by the IU and were within acceptable limits. The LH₂ recirculation pump inverters performed satisfactorily.

Performance of the EBW circuitry for the separation systems was satisfactory. The charge and discharge responses were within predicted time and voltage limits. The range safety command system EBW firing units were in the required state-of-readiness for vehicle destruct, had it been necessary.

11.4 S-IVB STAGE ELECTRICAL SYSTEM

11.4.1 Summary

The S-IVB stage electrical system performance was satisfactory. The battery voltages and currents remained within the normal range beyond their mission requirements. Battery temperatures were normal except for the temperature of the Aft Battery No. 1, Unit No. 1 which increased significantly above the cutoff limit of the primary heater control system at approximately 9 hours. Battery voltage and current plots are shown in Figures 11-1 through 11-4 and battery power consumption and capacity for each battery are shown in Table 11-3. There was no recurrence of forward Battery No. 2 early depletion that occurred during AS-510 and AS-511.

The three 5 V and seven 20 V excitation modules all performed within acceptable limits. The LOX and LH₂ chilldown inverters performed satisfactorily.

All switch selector channels functional properly and all outputs were issued within required time limits.

Performance of the EBW circuitry for the separation system was satisfactory. The charge and discharge responses of the firing units were within predicted time and voltage limits. The command destruct firing units were in the required state-of-readiness for vehicle destruct, had it been necessary.

11.4.2 S-IVB Aft Battery No. 1, Unit No. 1, Temperature Increase

The temperature of the S-IVB Aft Battery No. 1, Unit No. 1, increased significantly above the nominal cutoff limit (90°F) of the primary heater control system at approximately 9.0 hours (see Figure 11-5). The temperature of Unit No. 1 continued to increase until the high temperature backup thermostat deenergized the heater at approximately 120°F (see Figure 11-6). The temperature then decayed to approximately 87°F at which point the heater was energized. Since the high temperature thermostat has a small temperature deadband and the heater did not cycle around the high temperature thermostat control point, temperature control of Unit No. 1

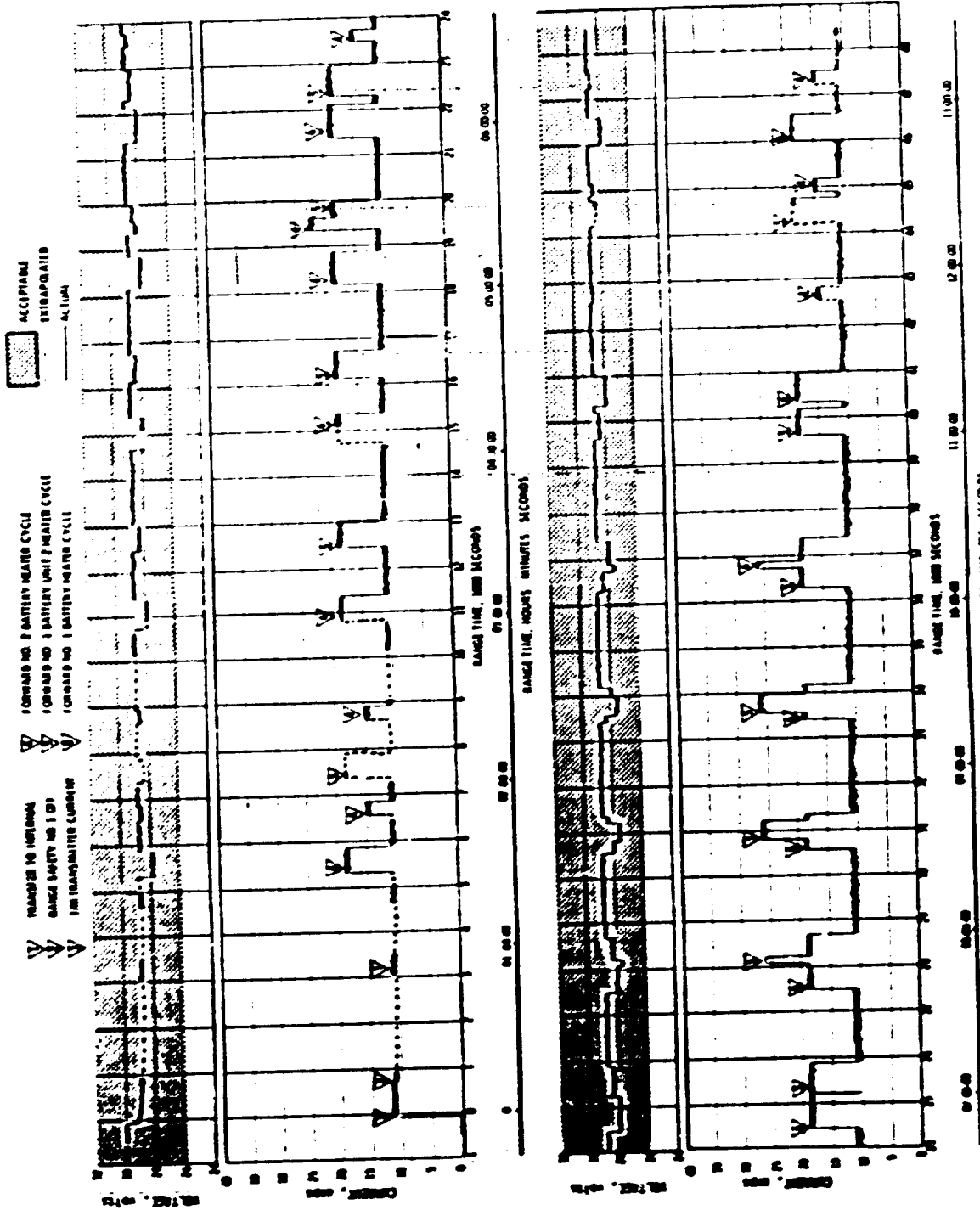


Figure 11-1. SILVER stage forward No. 1 Battery Voltage and Current

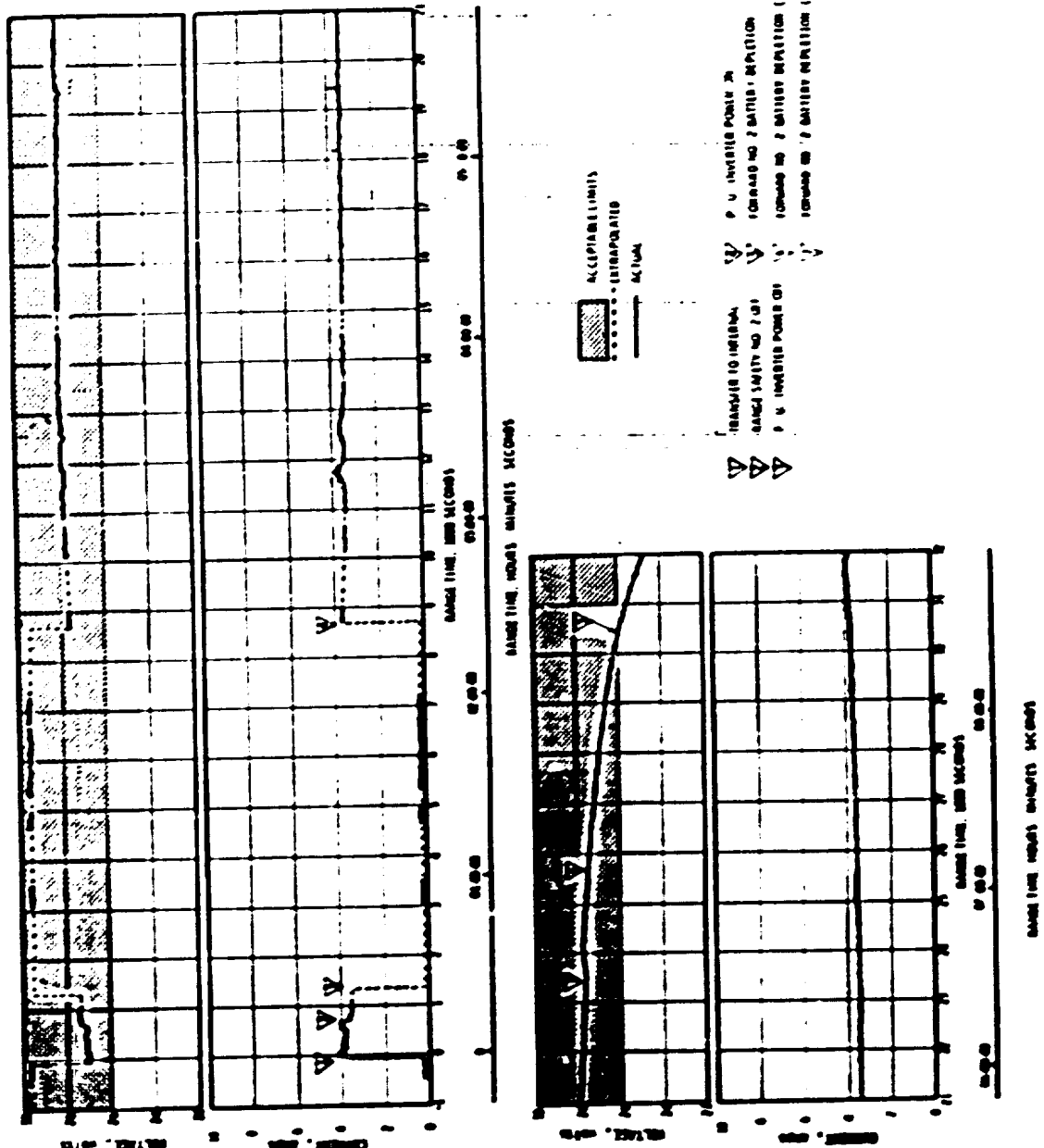


Figure 11-2. S-IVB Stage Forward No. 2 Battery Voltage and Current

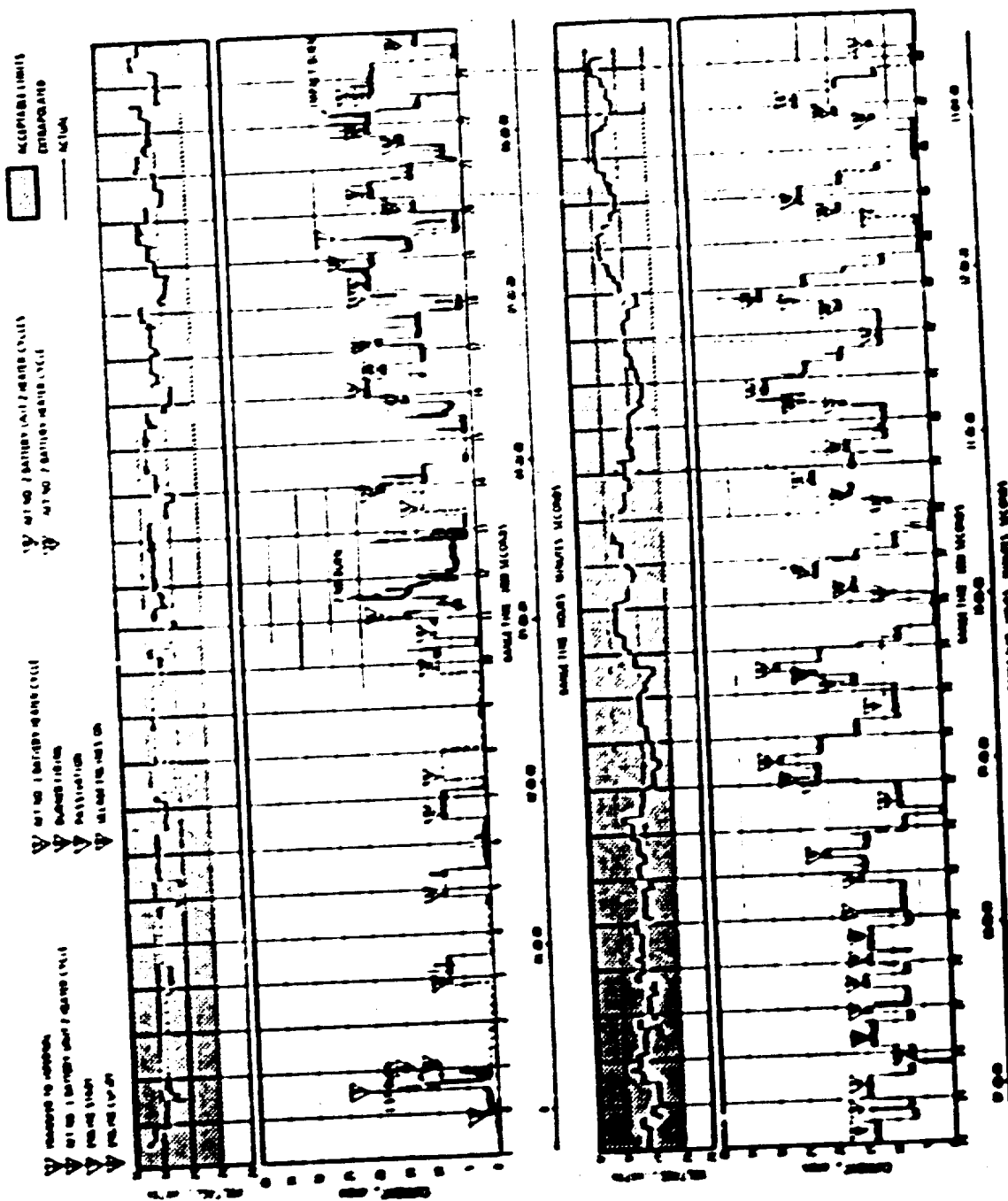


figure 11-3. 3-18 stage at No. 1 battery Voltage and Current

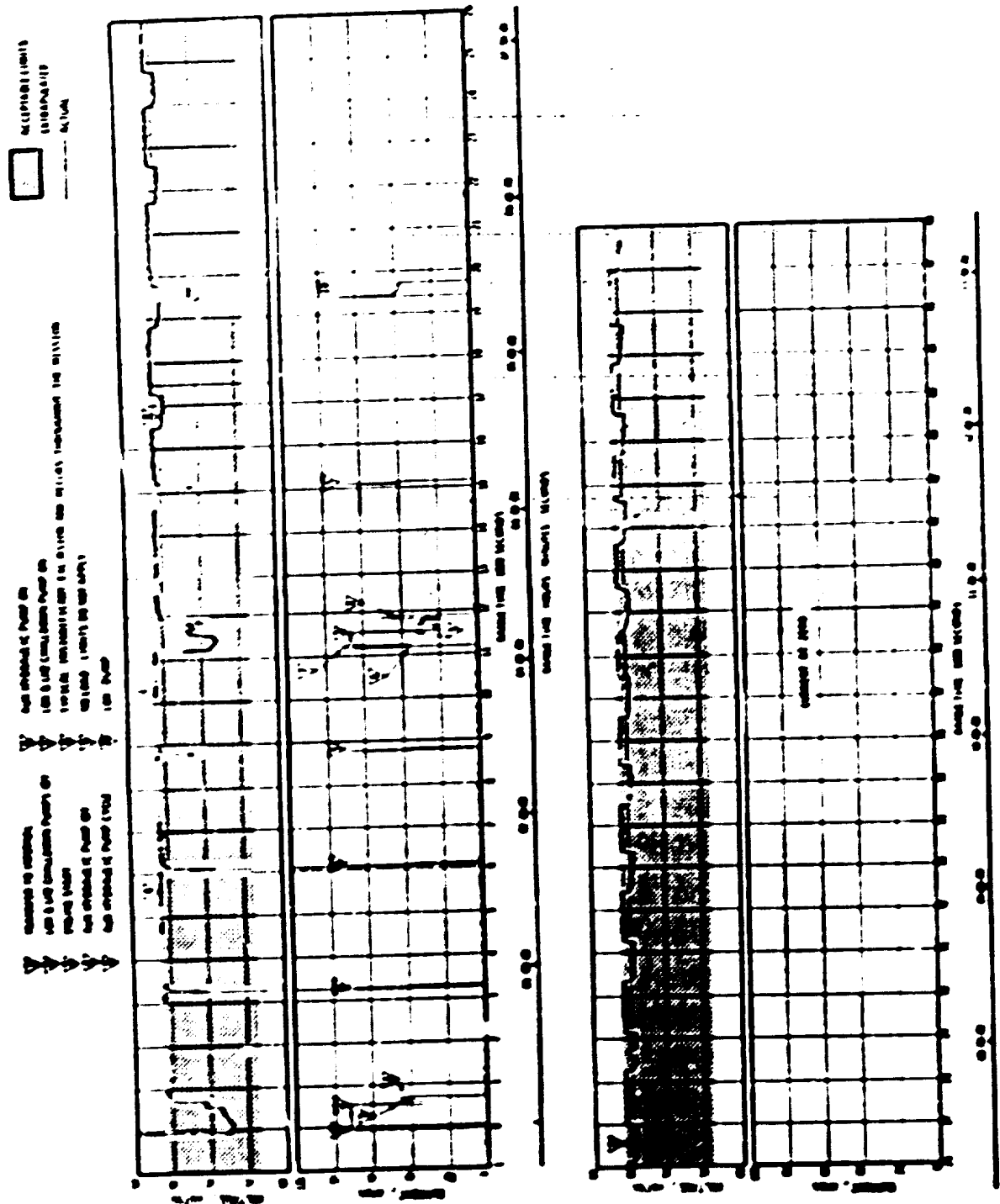


Figure 11-4. Sine Stage Att No. 2 Battery Voltage and Current

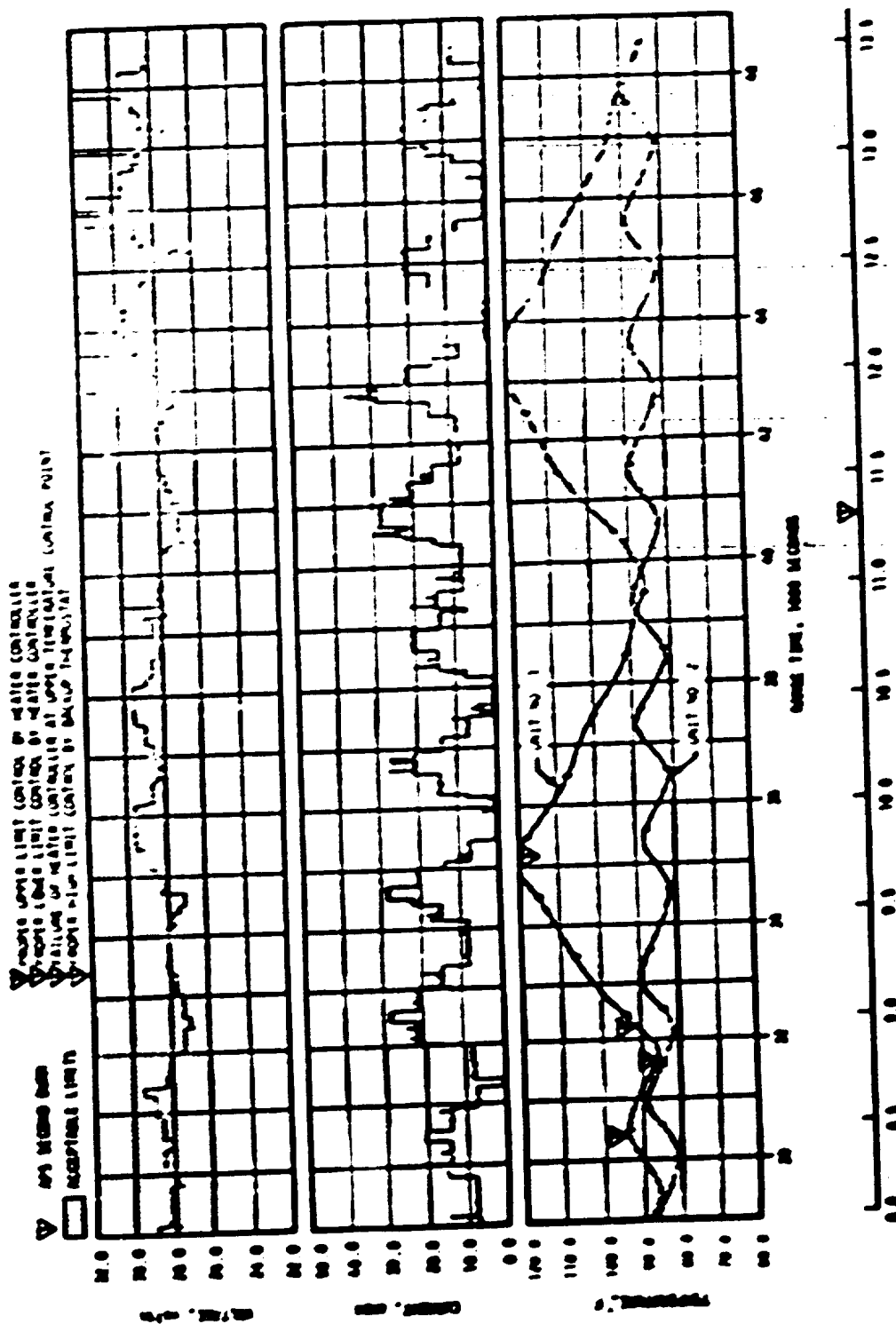


Figure 11-6. S-1VA A/C Battery No. 1 Data

Table 11-3. S-IVB Stage Battery Power Consumption

BATTERY	RATED CAPACITY (AMP-HR)	POWER CONSUMPTION	
		AMP-HR	PERCENT OF CAPACITY
Forward No. 1	227.5	200.12 ^a	87.36
Forward No. 2	14.6	26.77 ^{bc}	182.32
Aft No. 1	227.5	139.45 ^a	61.30
Aft No. 2	66.5	37.47 ^a	56.35

^aFrom battery activation until end of data (at 48,625 seconds).

^bFrom battery activation until battery voltage decayed below 26.0 volts (at 30,412 seconds).

apparently had reverted back to the heater controller (primary system). Subsequently, the heater controller again failed to turn the heater off at 90°F and the temperature again increased. This temperature sequence was repeated until termination of S-IVB data. Battery output voltage, current and the temperature of Aft Battery No. 1, Unit No. 2 remained nominal during this increased temperature cycling.

Evaluation of data indicates that the heater power transistor experienced thermal runaway whenever energized by the heater controller. This failure condition was apparently self-correcting when heater power was interrupted by the high temperature thermostat. Therefore, in the failure mode, the heater was energized normally by the heater controller and deenergized by the backup high temperature thermostat. The most likely failure mode for this anomaly has been established as a thermal runaway of the power transistor. Laboratory thermal runaway tests have simulated the flight failure. Past history has indicated poor installation of transistor heat sink would cause thermal runaway. Inspection of heat sink installation has been initiated to assure proper heat sink mounting fastener torque. Further corrective action is not considered necessary due to the presence of a backup control provided by the thermostat. This item is considered closed.

11.5 INSTRUMENT UNIT ELECTRICAL SYSTEM

The IU electrical system functioned normally. All battery voltages remained within performance limits of 26 to 30 V. The battery temperature and current during power flight were nominal. Temperature increases were experienced during the inhibiting of the Thermal Conditioning System (TCS) water valve in a closed position at 20,998 seconds (reference paragraph 14.4.1) as expected. Battery voltages, currents and temperatures are shown in Figures 11-7 through 11-10. Battery power consumption and capacity for each battery are shown in Table 11-4.

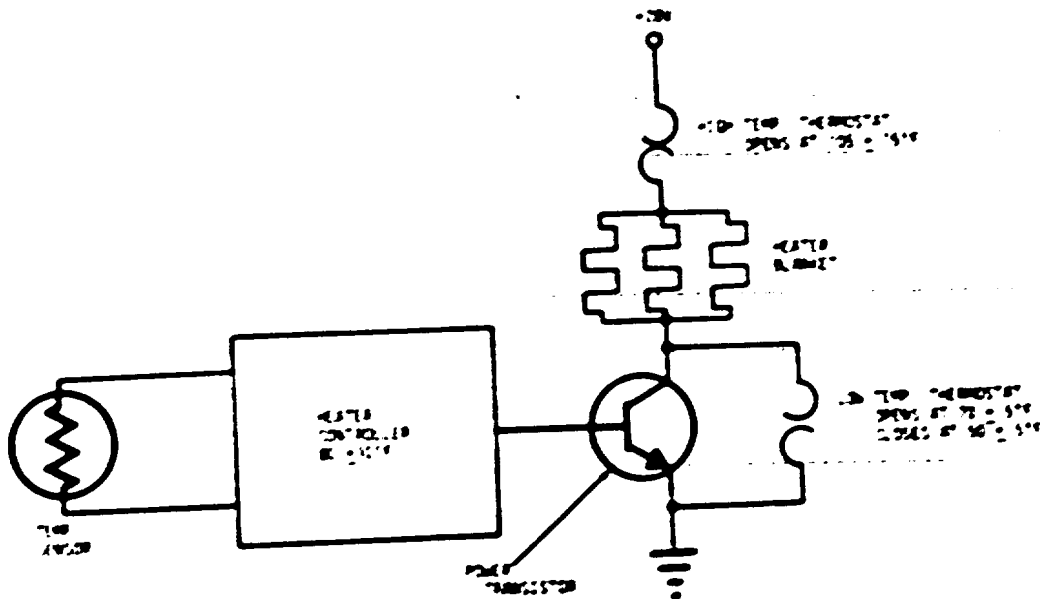


Figure 11-6. S-118 Aft Battery No. 1 Unit No. 1 Heater Control Circuit

Table 11-4. IU Battery Power Consumption

BATTERY	RATED CAPACITY (AMP-HR)	POWER CONSUMPTION	
		AMP-HR	PERCENT OF CAPACITY
6010	350	255.0*	73%
6020	350	365.4**	104**
6030	350	329.0*	93%
6040	350	387.5***	111***

*Actual usage was computed from final power transfer to 49,620 seconds (13 hours 47 minutes).

**The CES transponder, powered by the 6020 battery, was operating at S-118/IU lunar impact which occurred at 313,181 seconds (86:59:41). Power consumption until S-118/IU lunar impact was calculated based on nominal operation.

***from final power transfer until battery voltage decayed below 26.0 volts at 45,000 seconds (12.5 hours).

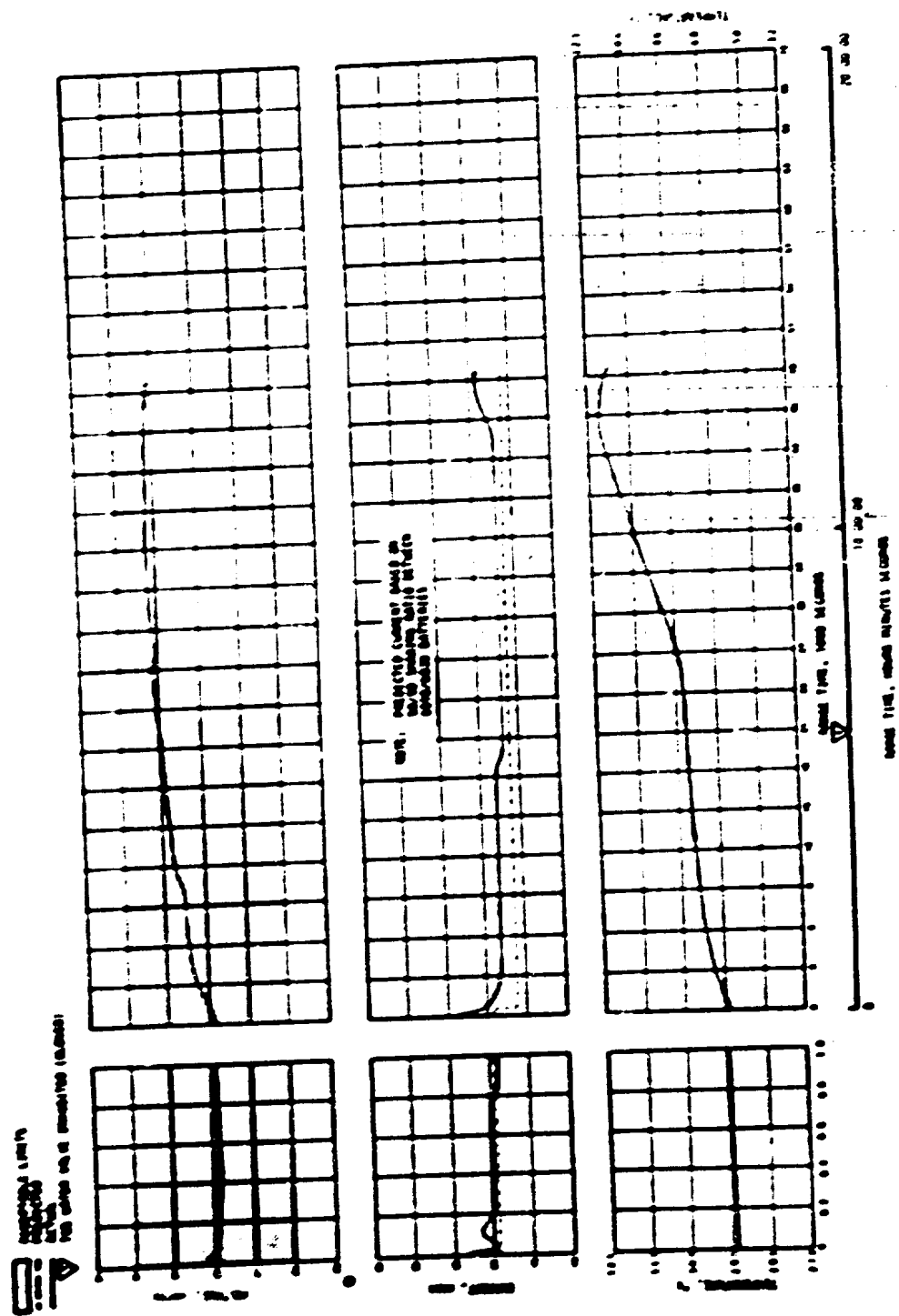


Figure 11-7. IU 6D10 Battery Parameters

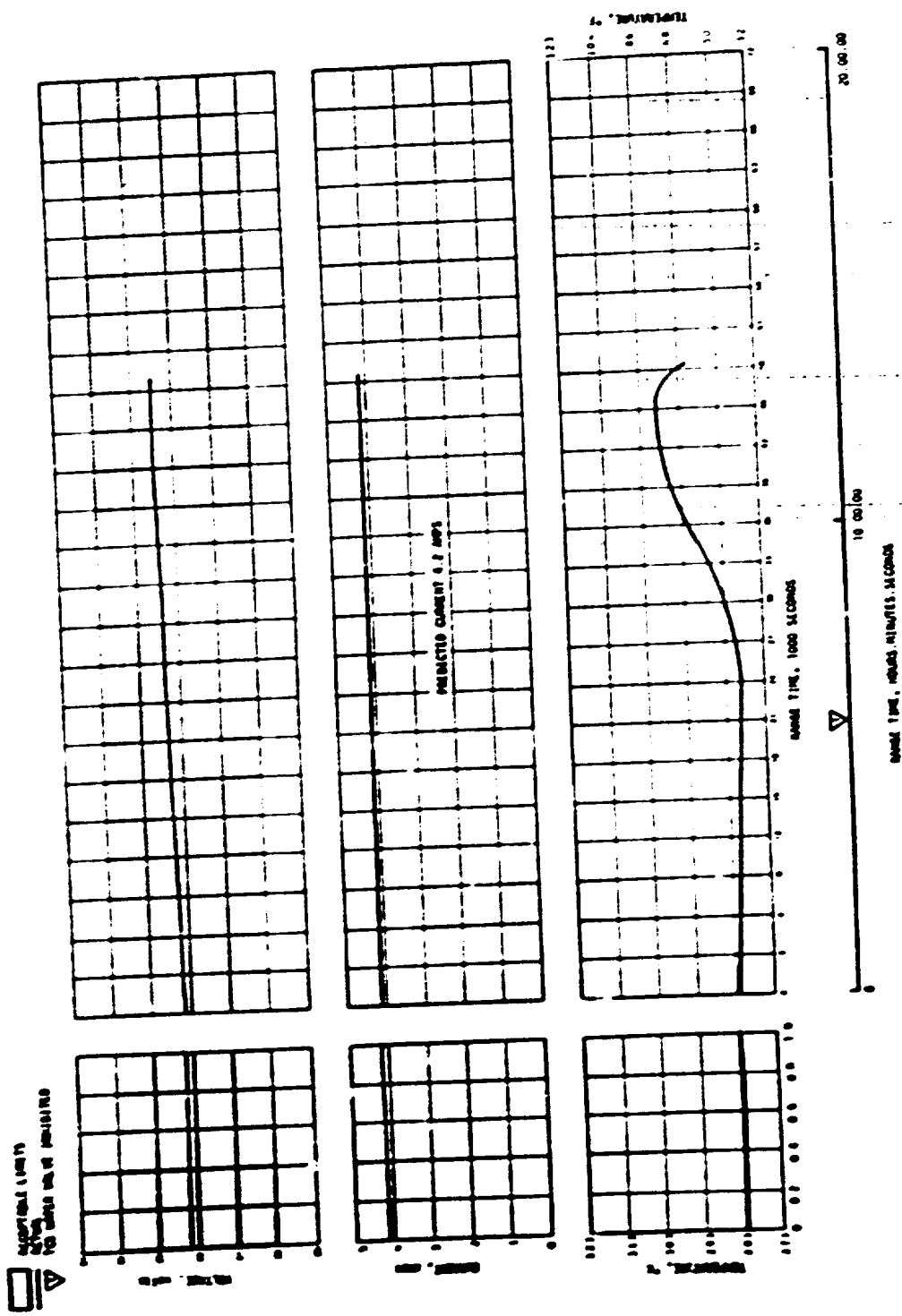


Figure 11-8. TIU 6020 Battery Parameters

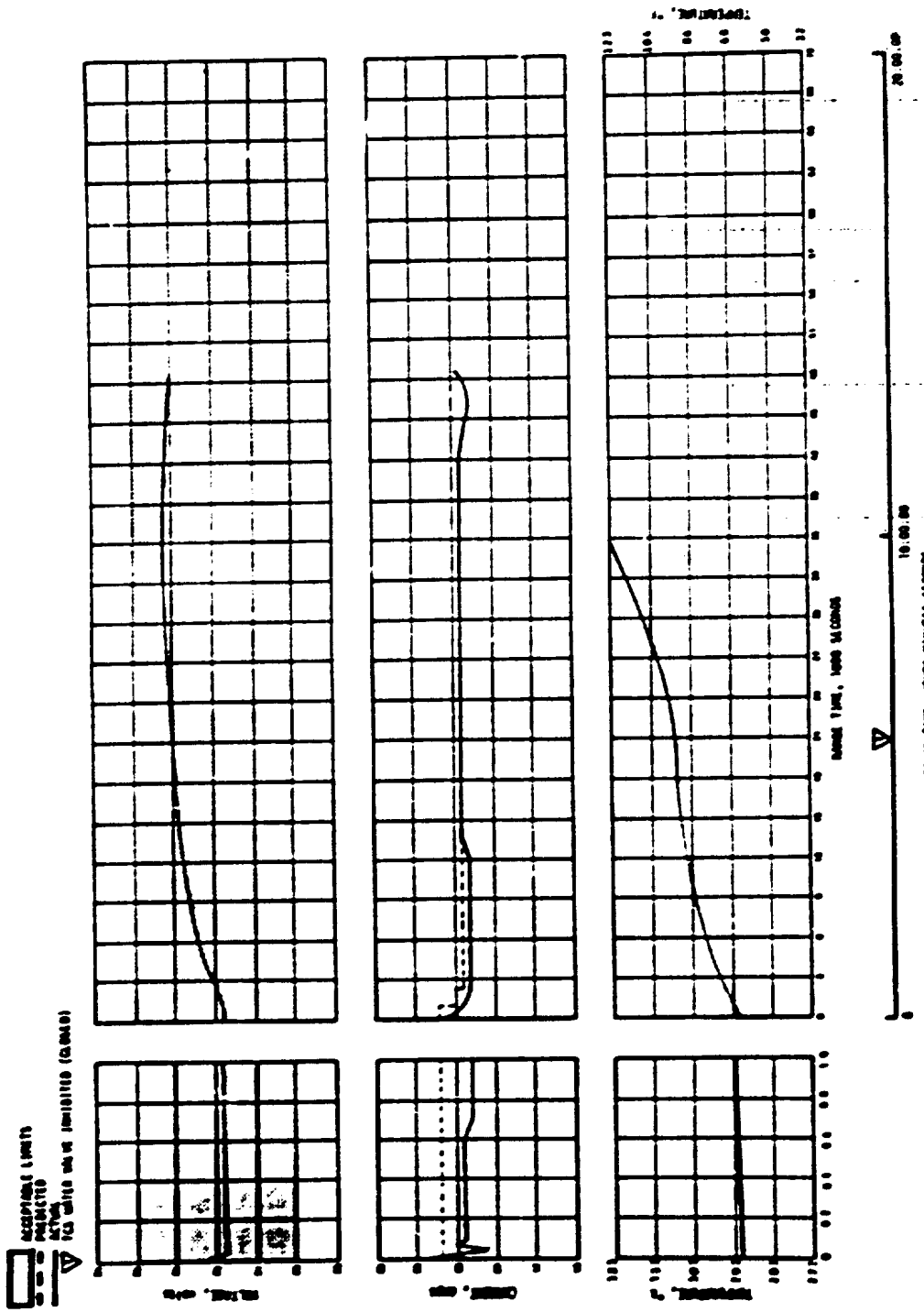


Figure 11-9. 6D30 Battery Parameters

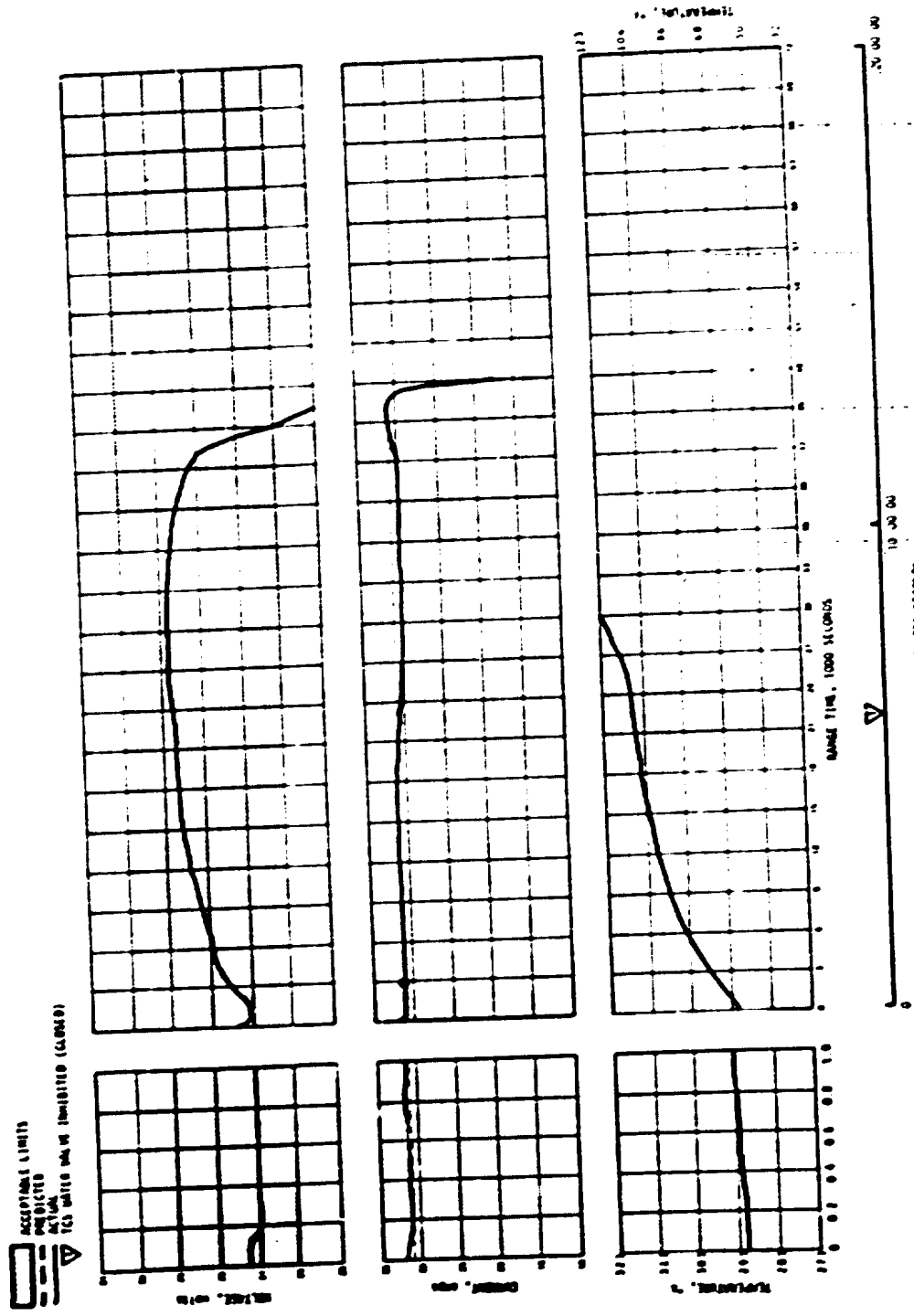


Figure 11-10. TU 6D40 Battery Parameters

The current sharing of the 6D10 and 6D30 batteries, to provide redundant power to the ST-124, was satisfactory throughout the flight. Current sharing reached a maximum of 23 amperes (6D10) and 26 amperes (6D30) compared to an average of 20 amperes (6D10) and 24 amperes (6D30) during S-IC burn (see Figures 11-7 and 11-9).

The 56 volt power supply maintained an output voltage of 56.2 to 56.6 V which is well within the required tolerance of 56 \pm 2.5 volts.

The 5 volt measuring power supply performed nominally, maintaining a constant voltage within specified tolerances.

The switch selector, electrical distributors and network cabling performed nominally.

11.6 SATURN V EMERGENCY DETECTION SYSTEM (EDS)

The performance of the AS-512 EDS was normal and no abort limits were exceeded. All switch selector events associated with EDS for which data are available were issued at the nominal times. The discrete indications for EDS events also functioned normally. The performance of all thrust OK pressure switches and associated voting logic, which monitors engine status, was nominal insofar as EDS operation was concerned. S-IVB tank ullage pressures remained below the abort limits. EDS displays to the crew were normal.

The maximum dynamic pressure difference sensed by the Q-ball was 1.2 psid at 88.0 seconds. This pressure was only 37.5 percent of the EDS abort limit of 3.2 psid.

As noted in Section 10, none of the rate gyros gave any indication of angular overrate in the pitch, yaw, or roll axis. The maximum angular rates were well below the abort limits.

SECTION 12

VEHICLE PRESSURE ENVIRONMENT

12.1 SUMMARY

The S-IC base pressure environments were consistent with trends and magnitudes observed on previous flights. The S-II base pressure environments were consistent with trends seen on previous flights, although the magnitudes were higher than seen on previous flights. The pressure environment during S-IC/S-II separation was well below maximum allowable values.

12.2 BASE PRESSURES

12.2.1 S-IC Base Pressures

The S-IC base heat shield was instrumented with two differential (internal minus external) pressure transducers. The data recorded by both instruments, D046-106 and D047-106, are in good agreement with previous flight data in both trends and magnitudes. A maximum differential pressure of 0.12 psi occurred at an altitude of 6.0 n mi.

12.2.2 S-II Base Pressures

Figure 12-1 shows the AS-512 post-flight heat shield forward face pressure data. The heat shield forward face pressure transducer (D150-206) provided no useful data during S-II mainstage. Post-flight analysis, using semi-empirical correlations based on 1/25 scale model hot flow test results, indicated that the S-II-12 heat shield forward face pressures were within the previous flight data band.

The thrust cone post flight reconstruction is shown in Figure 12-2. The thrust cone pressure transducer (D187-206) provided no useful data during S-II mainstage. Post-flight analysis based on the semi-empirical correlations mentioned above indicates higher thrust cone pressures, prior to interstage separation, than previous flight data.

The heat shield aft face pressures, shown in Figure 12-3, were higher than those seen on previous flights.

The higher pressures in the S-II-12 base region as indicated by post-flight analysis and measured flight data, are attributed to further inboard deflections of the engines than on previous flights. Effective with AS-510, the S-II engine precent angle was reduced from 1.8° to 0.6°. Since base pressures result from reverse flow of the engine exhaust gases, a further inboard deflection would

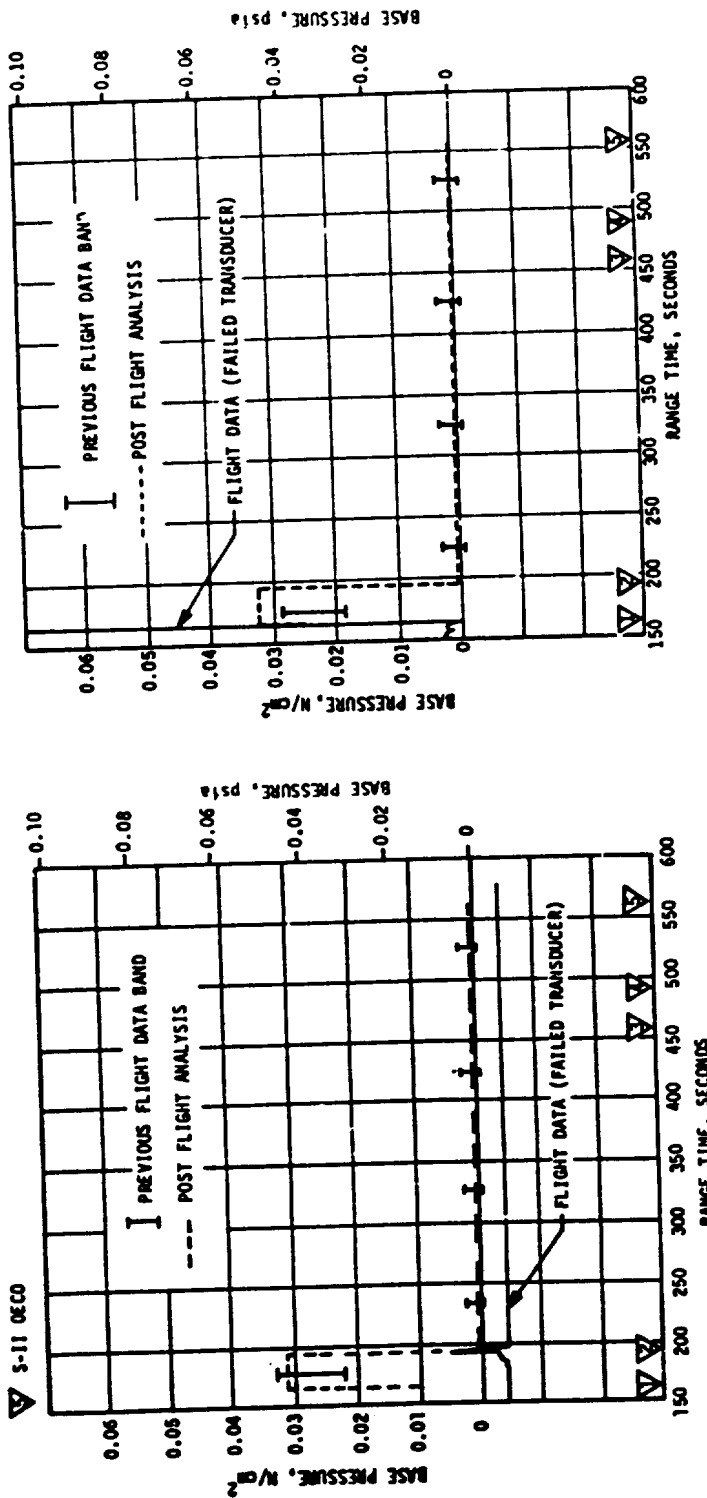
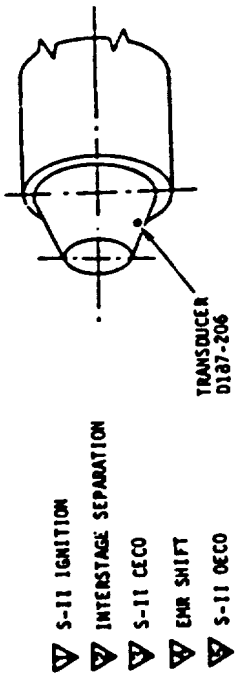


Figure 12-1. S-II Heat Shield Forward Face Pressure
Figure 12-2. S-II Thrust Cone Pressure

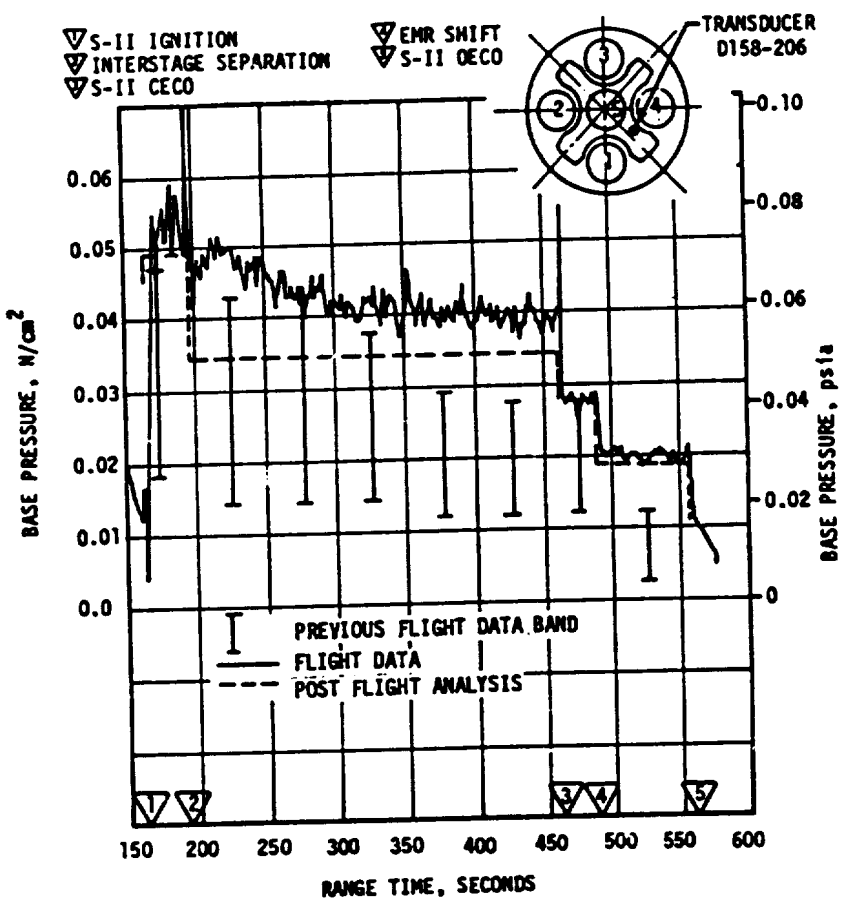


Figure 12-3. S-II Heat Shield Aft Face Pressure

cause higher pressures in the base region.

12.3 S-IC/S-II SEPARATION PRESSURES

Details of the S-IC/S-II separation are presented in Section 10.6. At main propellant ignition, the separation distance was over 50 feet, and over 100 feet at 90% thrust; consequently the pressure environment during S-IC/S-II separation was well below maximum allowable values.

SECTION 13

VEHICLE THERMAL ENVIRONMENT

13.1 SUMMARY

The AS-512 S-IC base region thermal environments exhibited trends and magnitudes similar to those seen on previous flights, except that the ambient temperature under engine No. 1 cocoon showed an unexpected rise that peaked at about 50 seconds.

The base thermal environments on the S-II stage were consistent with the trends and magnitudes seen on previous flights and were well below design limits.

Aerodynamic heating environments and S-IVB base thermal environments were not measured on AS-512.

13.2 S-IC BASE HEATING

Thermal environments in the base region of the S-IC stage were recorded by two total calorimeters, C0026-106 and C0149-106, and two gas temperature probes, C0050-106 and C0052-106, which were located on the aft heat shield. The sensing surfaces of the total calorimeters were mounted flush with the aft shield surface. The base gas temperature sensing surfaces were mounted at distances aft of the heat shield surface of 0.25 inch (C0050-106) and 2.50 inches (C0052-106). In general, the AS-512 data was in good agreement with previous flight data in both trends and magnitudes. Typical base thermal data, total heating rates recorded by C0026-106, are presented in Figure 13-1 and compared to data from the AS-511 flight. The maximum recorded total heating rate was approximately 17 Btu/ft²-s and occurred at an altitude of 11.5 n mi.

The ambient temperature measurement (C242-101) under Engine No. 1 cocoon showed an unexpected rise starting soon after liftoff and peaking at about 50 seconds (see Figure 13-2). Following the peak, the temperature returned to a normal level at about 100 seconds, and remained similar to cocoon temperature levels for the other engines. The peak temperature at 50 seconds was approximately 13°C above the upper band experienced during previous flights.

There are two possible causes for this anomaly:

1. The first possibility is that hot gas from the Gas Generator (GG) may have leaked through the GG drain port. This port is plugged in flight and opened only during ground operations. Leakage past the plug has occurred in the past during low pressure ground checkout. The temperature sensor is located in

the vicinity of the GG drain port and a leak of about 0.003 lb/sec would propagate enough hot gas under the cocoon to cause such a temperature rise. A leak of such small magnitude would tend to be self-sealing due to the deposition of hydrocarbon solids from the fuel-rich GG combustion gases. This could explain why the temperature reading returned to the normal level.

2. The second possibility is a temporary loss of cocoon insulation integrity (possible loose combustion drain access cover) which later corrected itself, allowing the instrument to return to the normal temperature level. The temperature rise was coincident with the normal rise in base heating rate which peaks at about 50 seconds as shown in Figure 13-1. A loss of cocoon insulation integrity would show up in a temperature rise. However, the loss of cocoon insulation integrity would have to have been temporary because the temperature rise did not recur when the base heating rate peaked the second time at about 110 seconds (a normal occurrence). Base heating rates and temperatures do not show any unusual excursions during S-IC flight, indicating normal gas flow in the base region.

Special attention will be given during prelaunch operations to inspection of the GG plug and cocoon access covers.

13.3 S-II BASE HEATING

Figure 13-3 shows the AS-512 flight heat shield aft face total heat rate history. The flight data falls well within the data band of previous flights except at Center Engine Cutoff (CECO) when the heating rates were equal to the previously recorded peak value of 3.2 Btu/ft²-s.

The AS-512 flight and the post-flight analytical value of the gas recovery temperature probe indicated output are shown in Figure 13-4. The corresponding data band of the AS-503 through AS-511 flights is included for comparison.

Figure 13-5 shows the AS-512 flight and post-flight analytical values of the radiometer indicated radiative heat flux to the heat shield aft surface. Also shown is the post-flight analytical value of the actual incident radiative heat flux at the same location. The discrepancy between the radiometer indicated value and the incident heat flux is due to the heating of the radiometer quartz window by convection and long-wave plume radiation. Consequently, the radiometer sensor receives additional heat from the quartz window by radiation and convection across the air gap between the window and the sensor. This explains the apparently slow radiometer response at engine start, CECO, Engine Mixture Ratio (EMR) shift and at engine cut-off. Figure 13-5 shows that the actual incident radiative heat flux prior to CECO is about 30% less than the radiometer indicated value. The post-flight analytical history of the radiometer output is in good agreement with the flight radiometer output history.

There were no structural temperature measurements on the base heat shield and only three thrust cone forward surface temperature measurements in the entire base region. In order to evaluate the structural temperatures experienced on the aft surface of the heat shield, a maximum post-flight predicted temperature was determined for the aft surface using maximum post-flight predicted base heating rates for the AS-512 flight. The predicted maximum post-flight temperature was 794°K (969°F) and compares favorably with maximum post-flight temperatures predicted for previous flights, and was well below the maximum design temperatures of 1066°K (1460°F) for no engine out and 1175°K (1550°F) for one control engine out. The effectiveness of the heat shield and flexible curtains as a thermal protection system was again demonstrated on this flight as on previous flights by the relatively low temperatures recorded on the thrust cone forward surface. The maximum measured temperature on AS-512 by any of the three thrust cone forward surface temperature measurements was 260°K (9°F), which also compares favorably with data recorded on previous flights. The measured temperatures were well below design values.

13.4 VEHICLE AEROHEATING THERMAL ENVIRONMENT

Aerodynamic heating environments were not measured on the AS-512 S-IC stage. Due to the similarity in the trajectory, the aerodynamic heating environments are believed to be approximately the same as previous flight environments. Because of the nighttime launch, ground optical data from Melbourne Beach and Ponce de Leon cameras do not have sufficient clarity to define the flow separation point on the S-IC stage, but it is expected that the data would be similar to previous flights.

13.5 S-IC/S-II SEPARATION THERMAL ENVIRONMENT

Since the AS-512 S-IC/S-II separation was normal, the heat input to the S-IC LOX tank dome is assumed to be near nominal.

There were no environmental measurements in this area on the flight vehicle but nothing has been observed in related flight data to indicate anything other than a normal environment.

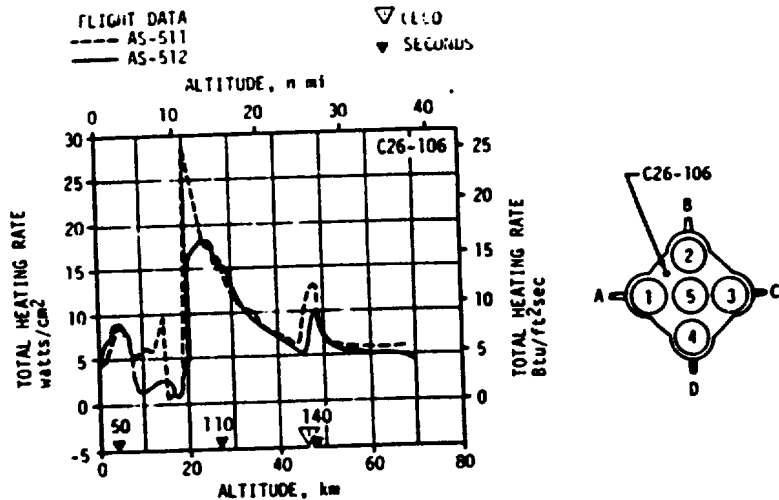


Figure 13-1. S-IC Base Region Total Heating Rate

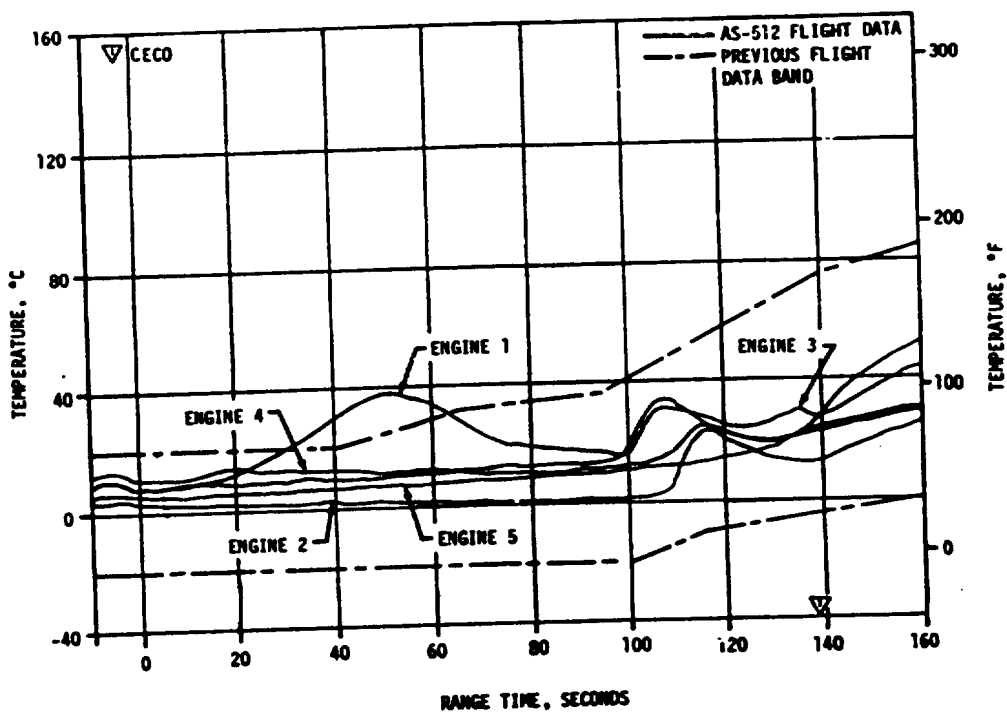


Figure 13-2. S-IC Ambient Gas Temperature Under Engine Cocoon

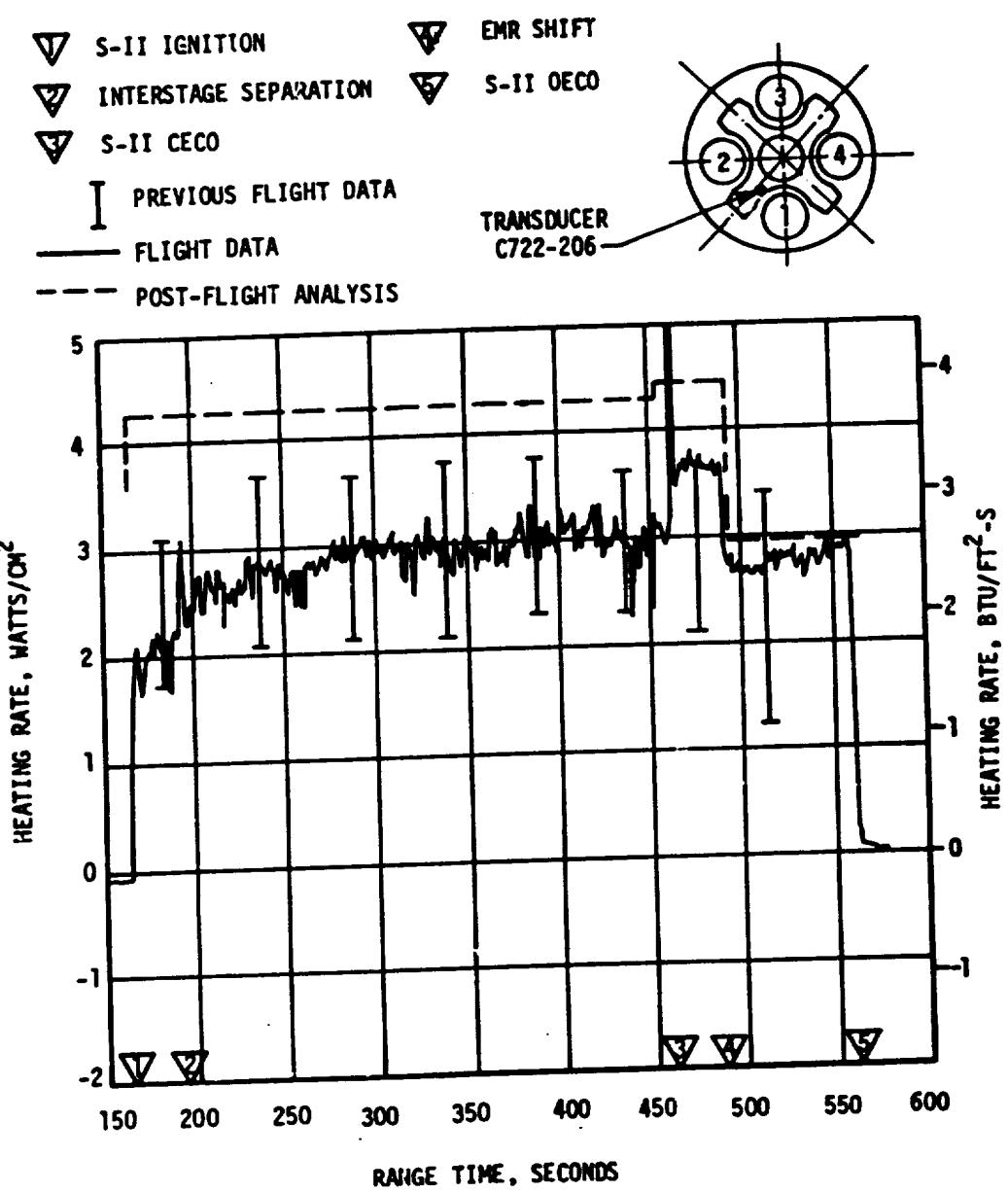


Figure 13-3. S-II Heat Shield Aft Heat Rate

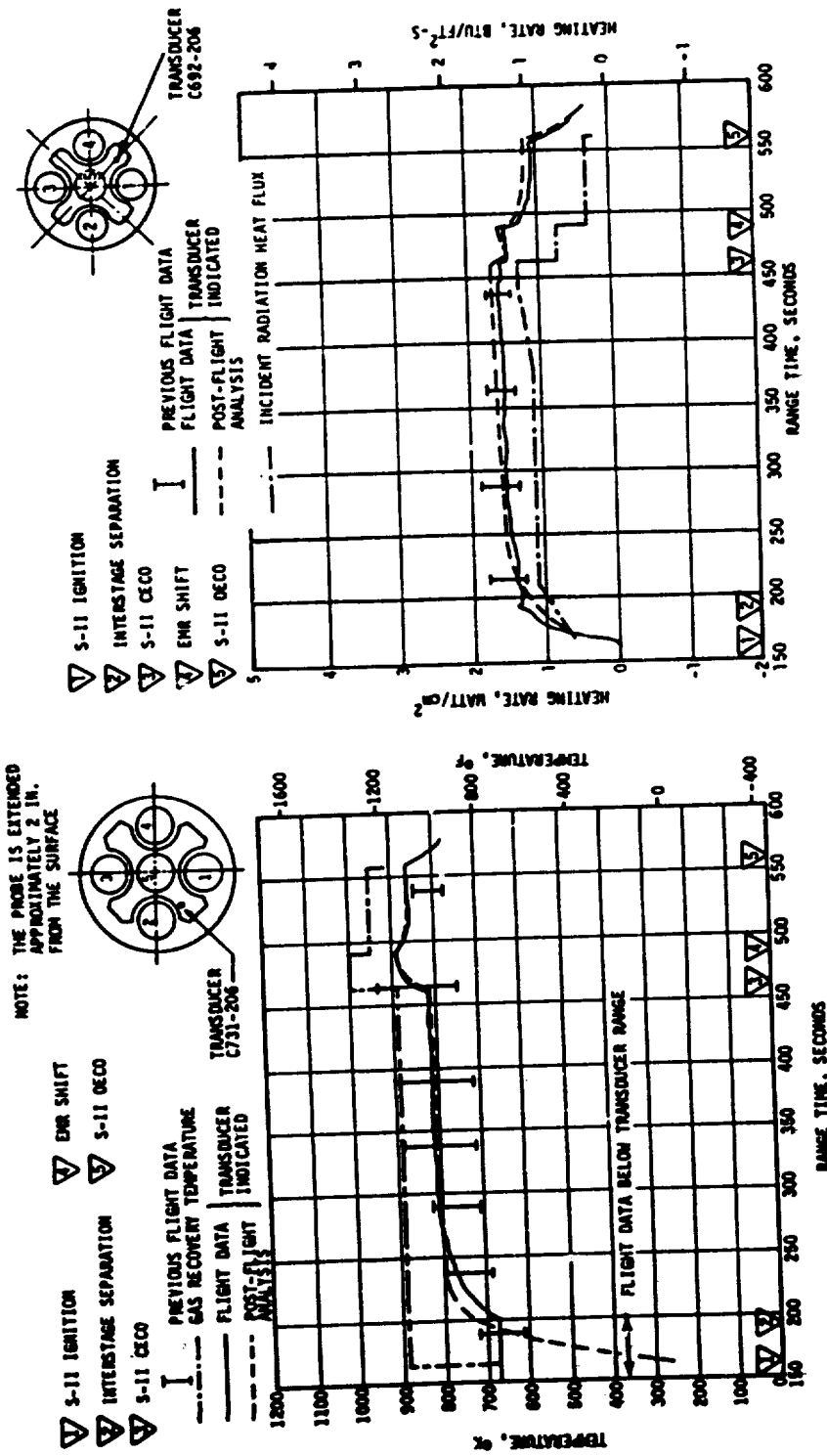


Figure 13-4. S-II Heat Shield Recovery Temperature Figure 13-4.

119

SECTION 14

ENVIRONMENTAL CONTROL SYSTEM

14.1 SUMMARY

The S-IC stage forward compartment thermal environment was adequately maintained although the temperature was lower than experienced during previous flights. The S-IC stage aft compartment environmental conditioning system performed satisfactorily.

The S-II stage engine compartment conditioning system maintained the ambient temperature and thrust cone surface temperatures within design ranges throughout the launch countdown. No equipment container temperature measurements were taken; however, since the external temperatures were satisfactory and there were no problems with the equipment in the containers, the thermal control system apparently performed adequately.

The IU stage Environmental Control System (ECS) exhibited satisfactory performance for the duration of the IU mission. Coolant temperatures, pressures, and flowrates were continuously maintained within the required ranges and design limits. At 20,998 seconds the water valve logic was purposefully inhibited (with the valve closed). Subsequent temperature increases were as predicted for this condition.

14.2 S-IC ENVIRONMENTAL CONTROL

The S-IC forward compartment pre-launch temperature reached a minimum of -92.2°F (C0206-120) at liftoff. This temperature was lower by approximately 11°F than experienced during previous flights but well above the established minimum design criteria. These criteria, established by analysis and test, permit a minimum temperature at liftoff of -110°F after an 8 minute S-II stage J-2 engine chilldown or -170°F after a 13 minute chilldown at the C0206-120 transducer location.

Therefore, it was concluded that the critical components that are in the compartment were well above their minimum qualification limits.

The aft compartment environmental conditioning system performed satisfactorily during countdown. After the initiation of LOX loading, the temperature in the vicinity of the battery (12K10) decreased to 65°F which is within the battery qualification limits of 35°F to 95°F. The temperature increased to 78°F at liftoff.

Just prior to liftoff, the other aft compartment temperatures ranged from 77°F at measurement C0203-115 location to 86.9°F at measurement C0205-115 location. During flight, the lowest temperature recorded was 63.5°F at measurement C0203-115.

14.3 S-II ENVIRONMENTAL CONTROL

The engine compartment conditioning system maintained the ambient temperature and thrust cone surface temperatures within design ranges throughout the launch countdown. The system also maintained an inert atmosphere within the compartment as evidenced by the absence of H₂ or O₂ indications on the hazardous gas monitor.

No equipment container temperature measurements were taken. However, since the ambient measurements external to the containers were satisfactory and there were no problems with the equipment in the containers, it is assumed that the thermal control system performed adequately.

14.4 IU ENVIRONMENTAL CONTROL

14.4.1 Thermal Conditioning System (TCS)

The IU TCS performance was satisfactory throughout the IU mission. The temperature of the coolant as supplied to the IU thermal conditioning panels, S-IVB TCS, and IU internally cooled components was continuously maintained within the required limits of 45° to 68°F until approximately 23,500 seconds, as shown in Figure 14-1. The coolant temperature exceeded the monitored temperature band (50° to 60°F) of measurement C15-601 due to the planned inhibition (valve closed) of the water valve. Sublimator performance during ascent is presented in Figure 14-2. The water valve opened initially at approximately 180 seconds as commanded, allowing water to flow to the sublimator. Significant cooling by the sublimator was evident at approximately 530 seconds at which time the temperature of the coolant began to rapidly decrease. At the first thermal switch sampling, (480 seconds) the coolant temperature was above the thermal switch activation point; hence the water valve remained open. At the second thermal switch sampling (780 seconds), the coolant temperature was below the actuation point, and the water valve closed.

Sublimator cooling was nominal as evidenced by normal coolant temperature (C15-601) cycling through approximately 21,000 seconds. Following water valve closure at 19,060 seconds the water line pressure indication, measurement D43-601, leveled off at about 1.4 psia rather than continuously decreasing to zero as is normally expected during the sublimator drying out cycle. The indicated pressure remained at this level until about 27,000 seconds, at which time the indicated pressure did begin a gradual decrease to zero (Figure 14-1). This same general condition has occurred on a number of previous missions and is due to either water

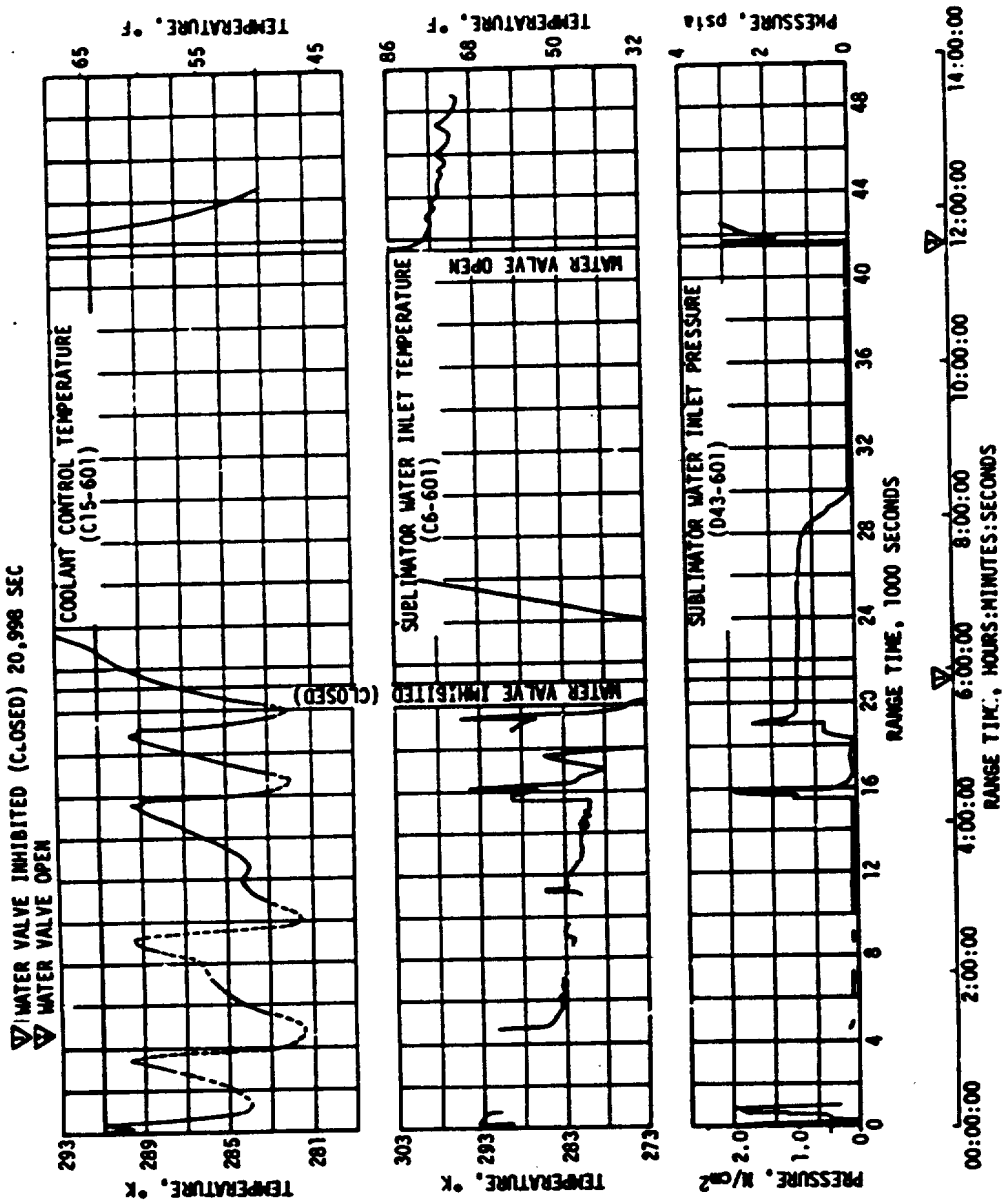


Figure 14-1. IU TCS Coolant Control Parameters

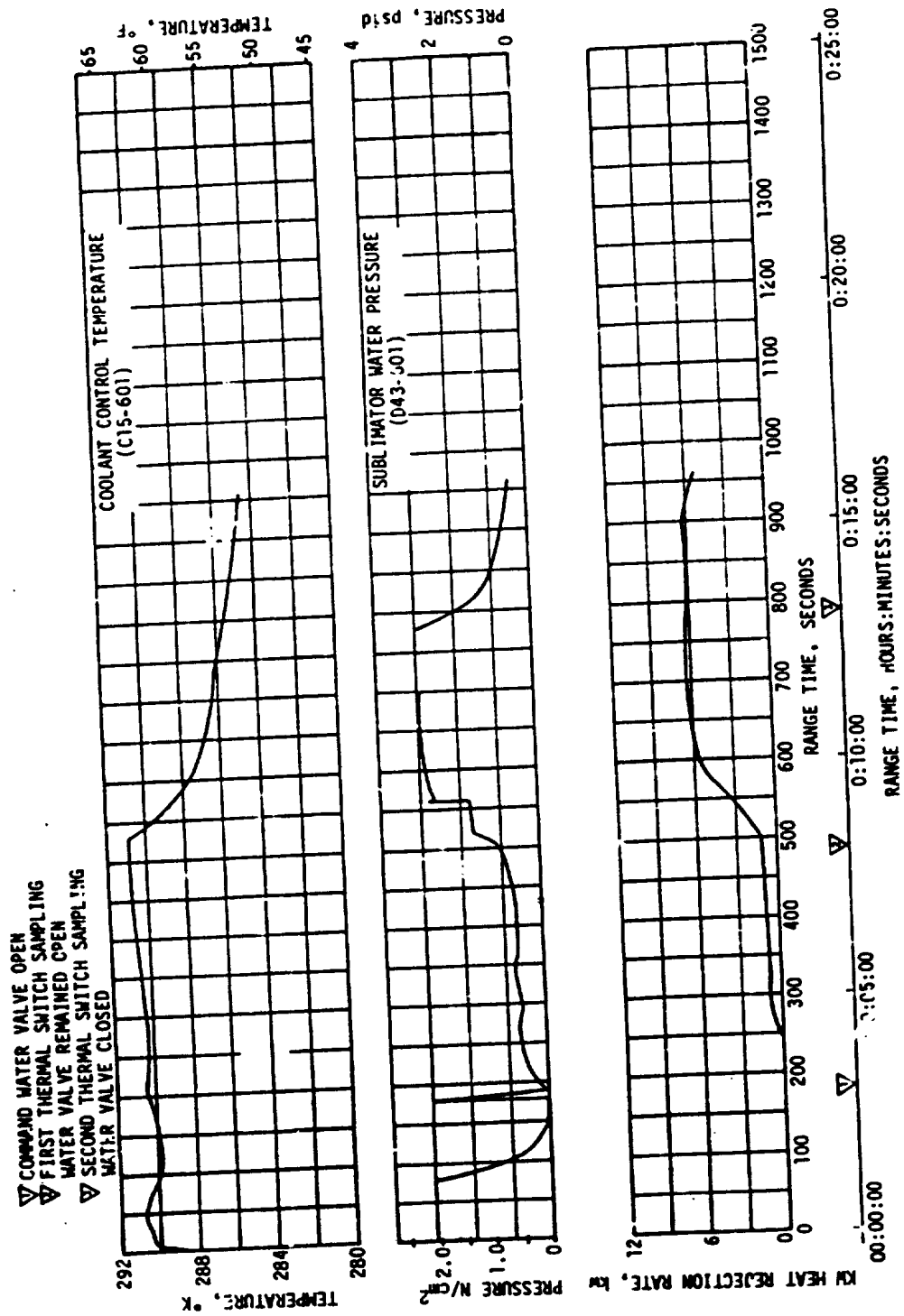


Figure 14-2: IU Sublimator Performance During Ascent

freeze-up in the pressure pick up line, or icing at the pressure transducer resulting in the diaphragm of the transducer locking in a fixed position. The latter condition is thought to be the case, though in either event system performance is unaffected, and the true pressure in the water supply line decays nominally.

At 20,998 seconds, the Launch Vehicle Digital Computer (LVDC) logic controlling water valve operation was inhibited by ground command with the valve closed. The purpose of this event was to eliminate sublimator venting during the lunar impact course correction and tracking period between APS-1 and APS-2 burns. (It had been conjectured from previous mission performance that water vapor venting from the sublimator contributed significantly to unplanned velocity changes, causing degradation in lunar impact accuracy.) The water valve remained closed and the sublimator was inoperative until the valve inhibition was removed by ground command at 41,553 seconds, after the FCC was shutdown. Within this period of no active cooling, component and coolant fluid temperatures increased at rates within the conservative predictions. When the valve opened the sublimator quickly achieved a high level of heat rejection as evidenced by the rapid decrease in component temperatures (Figure 14-3). Within twenty minutes after sublimator restart coolant temperatures had returned to normal operating ranges. The water valve, however, was allowed to remain in the open position. All component temperatures remained within their expected ranges for the duration of the IU mission except for the period of time the water valve was commanded closed. The sublimator restarted in a timely fashion, with a high level of heat dissipation as expected.

The TCS hydraulic performance was nominal as seen in Figure 14-4. The TCS sphere pressure decay was nominal as shown by Figure 14-5 and there was no evidence of any excess GN₂ usage or leakage as was experienced on AS-511.

14.4.2 Gas Bearing System Performance

The Gas Bearing System (GBS) performance was nominal throughout the IU mission. Figure 14-6 shows ST-124 platform pressure differential (D11-603) and platform internal ambient pressure (D12-603).

The GBS GN₂ supply sphere pressure decay was as expected for the nominal case as shown in Figure 14-7.

An attempt was made to evaluate the effects of residual IU venting during the period between APS-1 and APS-2 burns while the TCS water valve was commanded closed (water sublimator eliminated as a source of S-IVB/IU thrust). Platform GBS venting and the corresponding APS activity have been analyzed with regard to trajectory perturbations. Details of this analysis are presented in Section 17.3.

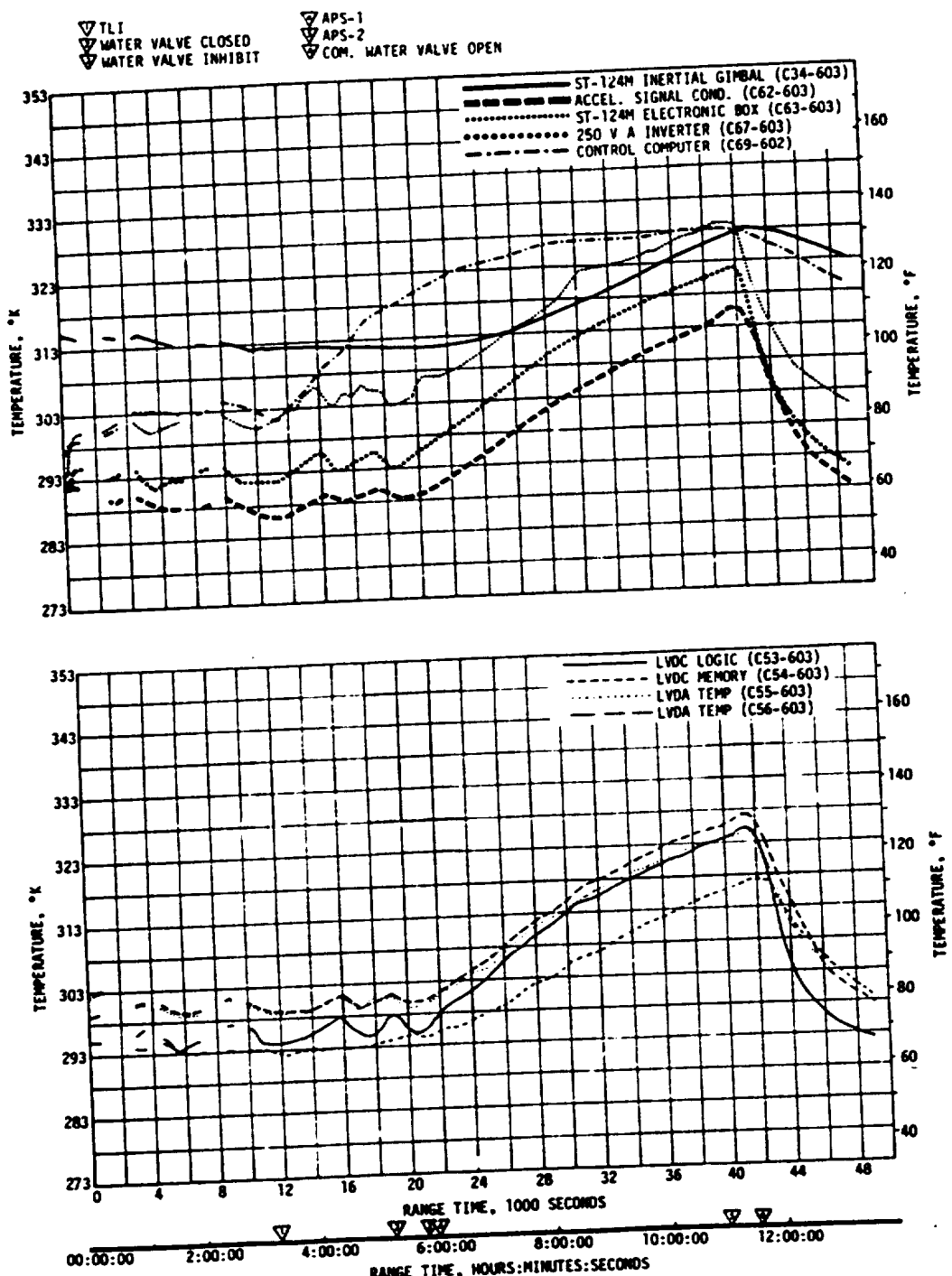


Figure 14-3. Selected IU Component Temperatures

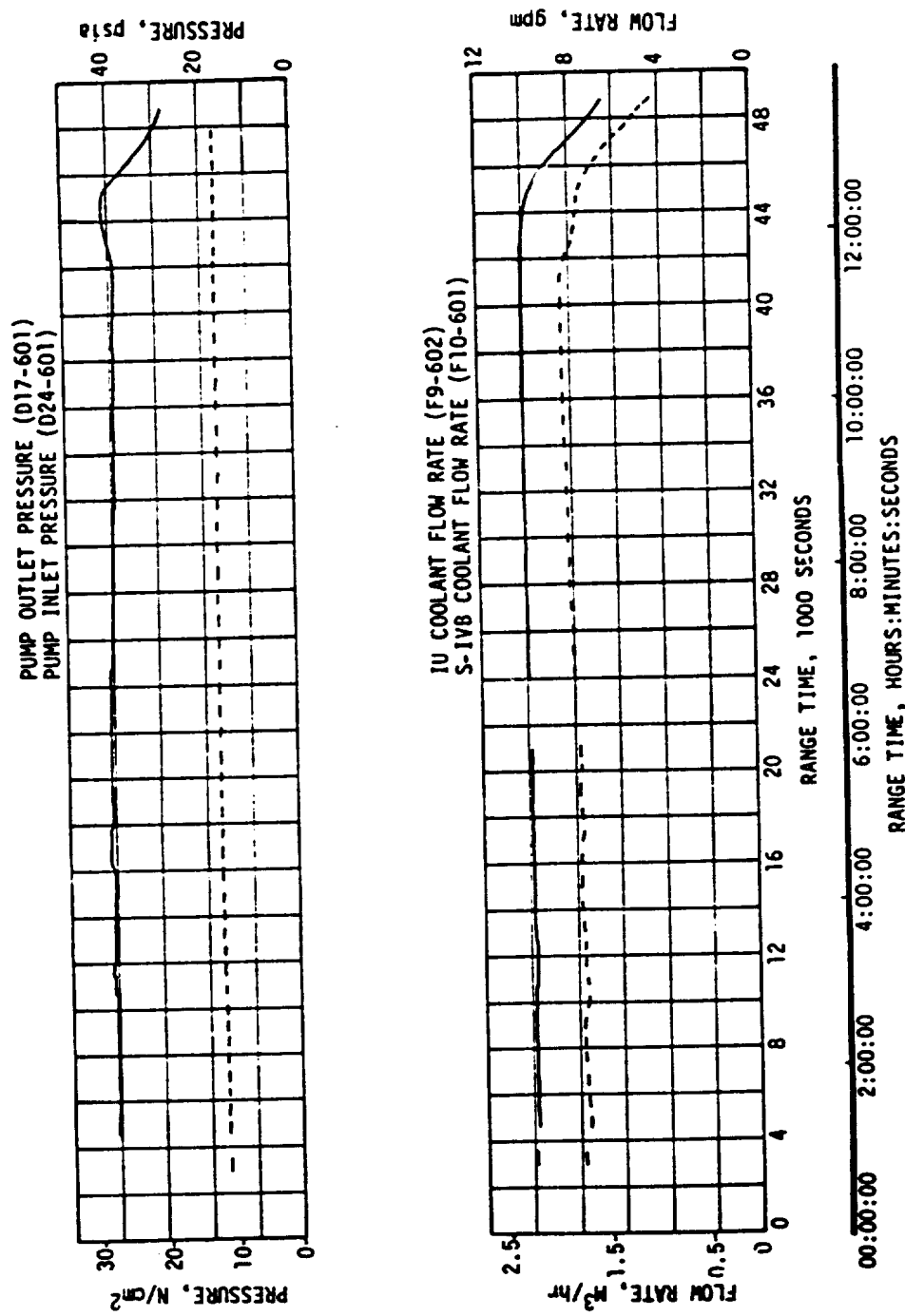


Figure 14-4. IU TCS Hydraulic Performance

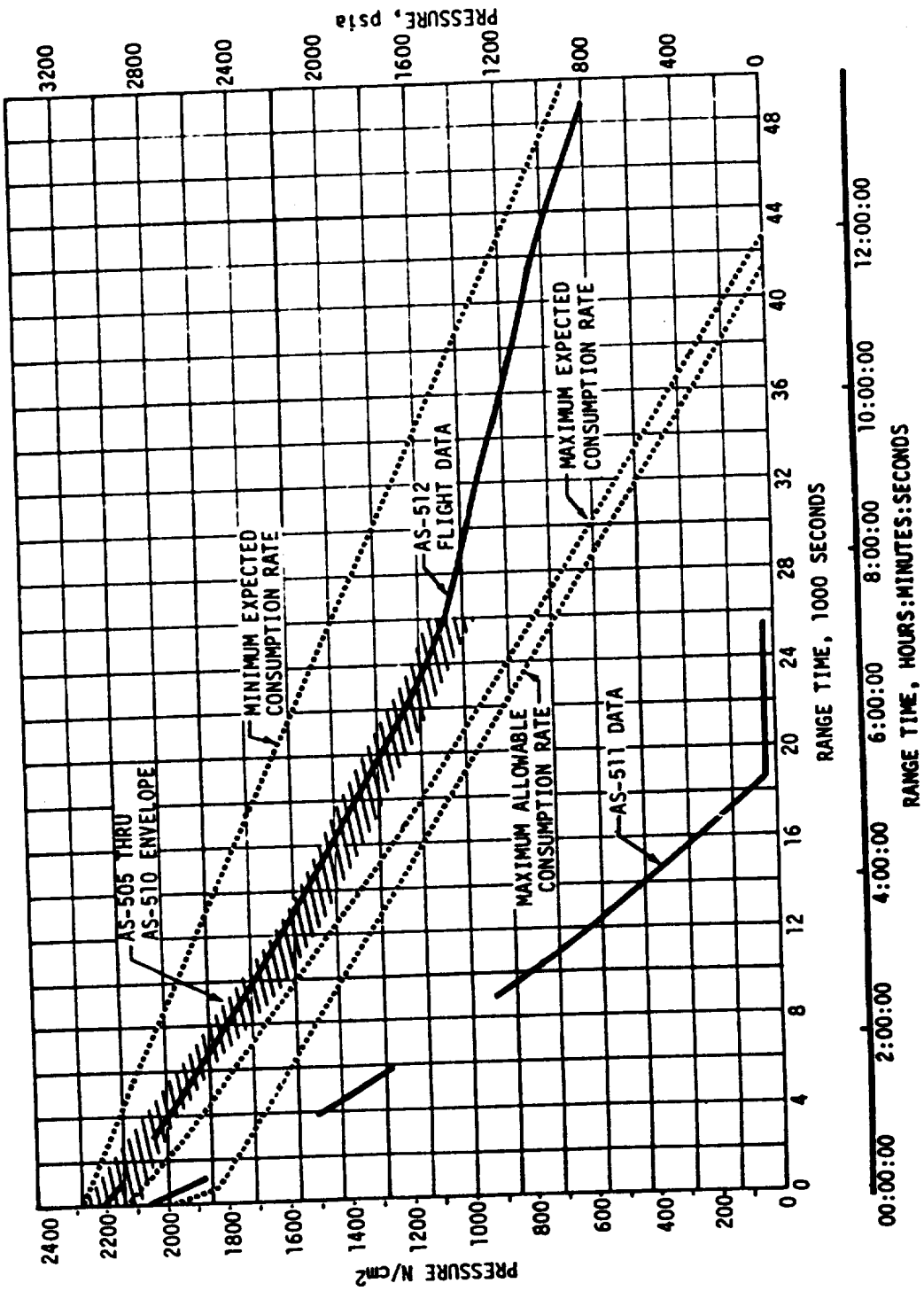


Figure 14-5. IU TCS Sphere Pressure

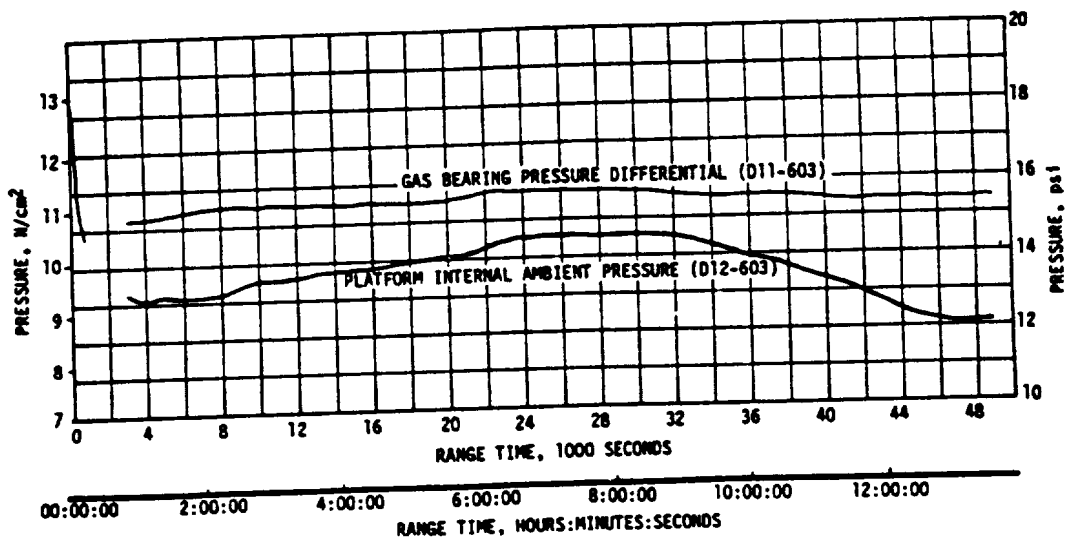


Figure 14-6. IU Inertial Platform GN₂ Pressure

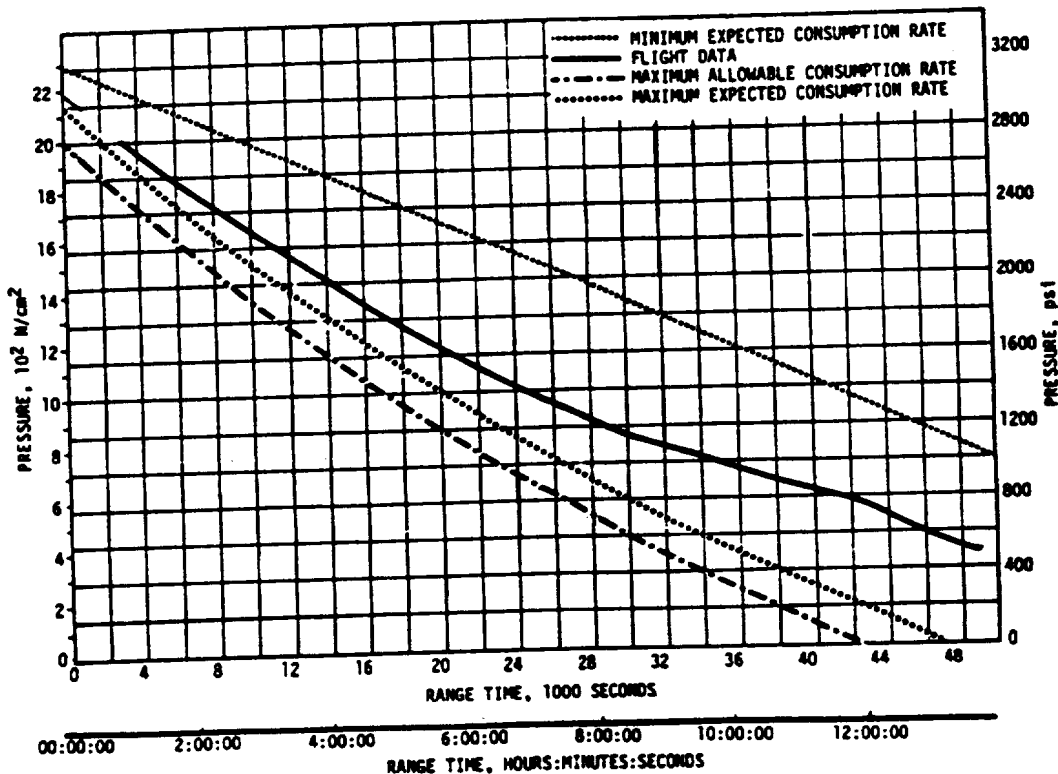


Figure 14-7. IU GBS GN₂ Sphere Pressures

SECTION 15

DATA SYSTEMS

15.1 SUMMARY

All data systems performed satisfactorily throughout the flight. Flight measurements from onboard telemetry were 99.8 percent reliable.

Telemetry performance was normal except for noted problems. Radio Frequency (RF) propagation was satisfactory, though the usual interference due to flame effects and staging were experienced. Usable Very High Frequency (VHF) data were received until 36,555 seconds (10:09:15). The Secure Range Safety Command Systems (SRSCS) on the S-IC, S-II, and S-IVB stages were ready to perform their functions properly, on command, if flight conditions during launch phase had required destruct. The system properly safed the S-IVB destruct system on a command transmitted from Bermuda (BDA) at 723.1 seconds. The performance of the Command and Communications System (CCS) was satisfactory from liftoff through lunar impact at 313,181 seconds (86:59:41). Madrid (MADX) and Goldstone (GDS) were receiving CCS signal carrier at lunar impact. Good tracking data were received from the C-Band radar, with BDA indicating final Loss of Signal (LOS) at 48,420 seconds (13:27:00).

In general, ground engineering camera coverage was good.

15.2 VEHICLE MEASUREMENT EVALUATION

The AS-512 launch vehicle had 1353 measurements scheduled for flight; four measurements were waived prior to start of the automatic countdown sequence leaving 1349 measurements active for flight. Three measurements failed during flight, resulting in an overall measurement system reliability of 99.8 percent.

A summary of measurement reliability is presented in Table 15-1 for the total vehicle and for each stage. The waived measurements, failed measurements, partially failed measurements, and questionable measurements are listed by stage in Tables 15-2 and 15-3. None of these listed failures had any significant impact on postflight evaluation.

15.3 AIRBORNE VHF TELEMETRY SYSTEMS EVALUATION

Performance of the eight VHF telemetry links provided good data from liftoff until the vehicle exceeded each subsystem's range limitations, however, data dropouts occurred as indicated in Table 15-4.

All inflight calibrations occurred as programmed and were within specifications.

Table 15-1. AS-512 Measurement Summary

MEASUREMENT CATEGORY	S-IC STAGE	S-II STAGE	S-IVB STAGE	INSTRUMENT UNIT	TOTAL VEHICLE
Scheduled	292	552	274	235	1353
Waived	1	1	2	0	4
Failed	0	1	2	0	3
Partial Failed	3	3	0	0	6
Questionable	0	0	0	0	0
Reliability, Percent	100.0	99.9	99.3	100.0	99.8

Table 15-2. AS-512 Flight Measurements Waived Prior to Flight

MEASUREMENT NUMBER	MEASUREMENT TITLE	NATURE OF FAILURE	REMARKS
S-IC STAGE			
D119-103	Pressure, Differential, Engine Global System Filter Manifold	Transducer failure	Waiver I-8-512-1
S-II STAGE			
D011-201	E1 LOX Pump Discharge	Measurement exceeded the zero shift specification requirement. Provided acceptable data during flight.	Waiver MR12-1
S-IVB STAGE			
C0001-401	Temp-Fuel Turbine Inlet	Data came on-scale from off-scale low and wandered erratic-ally.	Waiver S12-MR-13
D0225-403	Press-Cold Helium Control Valve Inlet	Low Remote Automatic Calibration System (LRACS) failed to calibrate and the dynamic response to pressure was suppressed.	Waiver S12-MR-17

Table 15-3. AS-512 Measurement Malfunctions

MEASUREMENT NUMBER	MEASUREMENT TITLE	NATURE OF FAILURE	TIME OF FAILURE (RANGE TIME)	DURATION SATISFACTORY OPERATION	REMARKS
MEASUREMENT FAILURES, S-II STAGE					
D187-206	Thrust Cone Surface Pressure	Improper response and erratic	115 seconds	Prior to 115 seconds	Probable transducer failure
MEASUREMENT FAILURES, S-IVB STAGE					
C0002-401	Temp-Oxidizer Turbine Inlet	Unsatisfactory response to temperature changes	11,778 seconds	First burn data was good. Second burn data was good until approx. 11,778 seconds.	Probable open circuit in either the sensor or inter-connecting cable
T0002-401	Speed - Fuel Pump	No response to fuel pump operation	No response during second burn	First burn	Most likely cause was open pick up coil
PARTIAL MEASUREMENT FAILURES, S-IC STAGE					
C003-101	Temperature, Turbine Manifold	Measurement pegged off scale high	83 seconds	103 seconds	Probable transducer failure
C003-103	Temperature, Turbine Manifold	Measurement pegged off scale high	22 seconds	42 seconds	Probable transducer failure
D047-106	Pressure, Heat Shield Differential	Excessive noise	20 to 50 80 to 95 105 seconds	147 seconds	Probable cable connector problem
PARTIAL MEASUREMENT FAILURES, S-II STAGE					
D180-206	Heat Shield Forward Surface Pressure	Improper response	Approximately 163 seconds	163 seconds	Probable transducer failure
B011-204	E4 LOX Pump Discharge Pressure	Zero shift of approx. 25 PSIA	425 seconds	Prior to 425 seconds	Probable transducer failure
C063-204	E4 LOX Inlet Temperature	Large positive noise excursion	450 seconds	Prior to 450 seconds	Probable transducer failure

Data degradation and dropouts were experienced at various times during launch and earth orbit as on previous flights, due to the attenuation of RF signals. Signal attenuation was caused by S-IC stage flame effects, S-IC Center Engine Cutoff (CECO) and retro-rocket effects at S-IC/S-II separation. S-IC CECO resulted in intermittent data loss from 140.65 to 142.80. The effects at S-IC/S-II separation lasted from 162.0 to 163.5 seconds. The S-II stage second plane separation effects were apparent between 195.0 and 195.2 seconds. The maximum attenuation of the DPL signal was approximately 22 db at the Central Instrumentation Facility (CIF) and is similar to that experienced on prior flights with 8 S-IC retro-rockets.

Table 15-4. AS-512 Launch Vehicle Telemetry Links

LINK	FREQUENCY (MHZ)	MODULATION	STAGE	FLIGHT PERIOD (RANGE TIME, SEC)	PERFORMANCE SUMMARY
AF-1	256.2	FM/FM	S-IC	0 to 420.65	Satisfactory
AP-1	244.3	P W/FM	S-IC	0 to 420.65	Data Dropouts
					Range Time (sec) Duration (sec)
					140.6 2.2
BF-1	241.5	FM/FM	S-II	0 to 735	Satisfactory
BF-2	234.0	FM/FM	S-II	0 to 735	Data Dropouts
BP-1	248.6	PCM/FM	S-II	0 to 735	Range Time (sec) Duration (sec)
					162.0 1.5
					195.0 0.2
CP-1	258.5	PCM/FM	S-IVB	0 to 13,900	Satisfactory
					Data Dropouts
					Range Time (sec) Duration (sec)
					163.0 2.6
					Intermittent Data
DP-1	250.7	FM/FM	IU	0 to 36,555	Satisfactory
DP-1	245.3	PCM/FM	IU	0 to 36,555	Data Dropouts
DP-1B (CCS)	2282.5	PCM/FM	IU	0 to 49,620	Range Time (sec) Duration (sec)
					163.0 (DP-1) 1.1

The last VHF signal was 36,555 seconds (10:09:15) at Ascension Island (ACN).

The performance of S-IVB and IU VHF telemetry systems was normal during earth orbit, S-IVB second burn and final coast. A summary of available VHF telemetry coverage showing Acquisition of Signal (AOS) and LOS for each station is shown in Figure 15-1.

15.4 C-BAND RADAR SYSTEM EVALUATION

The C-Band radar performed satisfactorily during flight, although several of the ground stations experienced problems with their equipment which caused some loss of signal.

Phase front disturbances were reported at Kennedy Space Center (KSC) between 123 and 137 seconds, Grand Turk Island (GTK) between 560 and 568 seconds, Grand Bahama Island (GBI) between 340 and 357 seconds, and Patrick Air Force Base (PAFB) between 28 and 90 seconds. Phase front disturbances occur when the pointing information is erroneous as a result of sudden antenna nulls or distorted beacon returns.

Carnarvon (CRO) experienced signal fade and dropout near Point of Closest Approach (PCA) during revolution 1, due to the high elevation and attendant high azimuth rates.

The BDA FPS-16 site experienced data losses during boost (552 to 642 seconds) and during the second revolution (3330 to 3366 seconds) because the vehicle look angles during these passes were such that the FPQ-6 antenna obscured the FPS-16 antenna during these intervals.

During revolution 3, Merritt Island Launch Area (MILA) reported the tracking angles wandering over a wide area before PCA although there was no evidence of beacon malfunction and the beacon was tracked from horizon to horizon. According to the Radar Operator Log, a cold front was passing through the area at the time and the operator suspected that temperature inversions were interfering with the tracking during that time. After PCA the tracking proceeded in a normal fashion.

The BDA FPQ-6 reported weak signals and intermittent track during the period between 41,760 seconds and final LOS (48,420 seconds) while the vehicle was tumbling.

A summary of available C-Band radar coverage showing AOS and LOS for each station is shown in Figure 15-2.

15.5 SECURE RANGE SAFETY COMMAND SYSTEMS EVALUATION

Telemetered data indicated that the command antennas, receivers/decoders, Exploding Bridge Wire (EBW) networks, and destruct controllers on each powered stage functioned properly during flight. They were in the required state-of-readiness if flight conditions during the launch had required vehicle destruct. Since no arm/cutoff or destruct commands

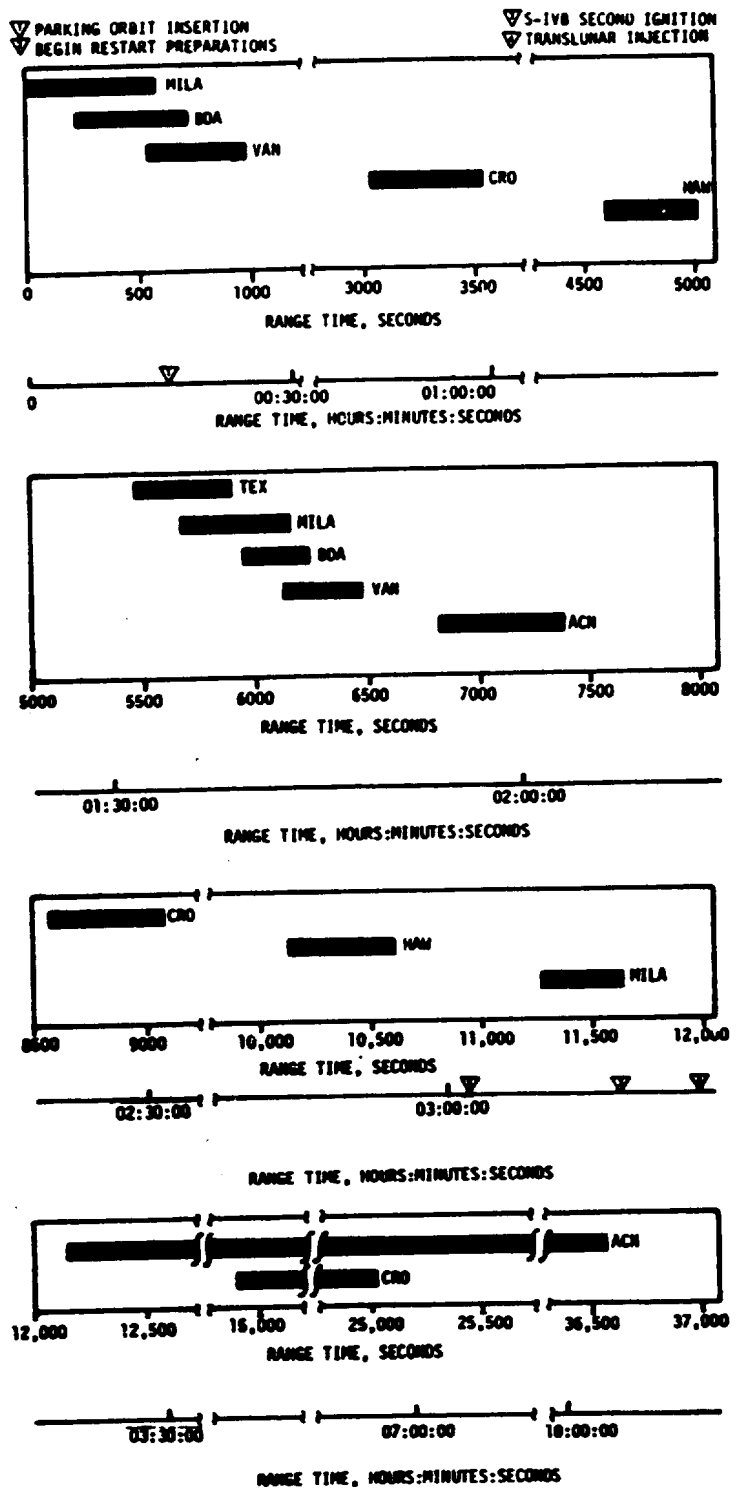


Figure 15-1. VHF Telemetry Acquisition and Loss Times

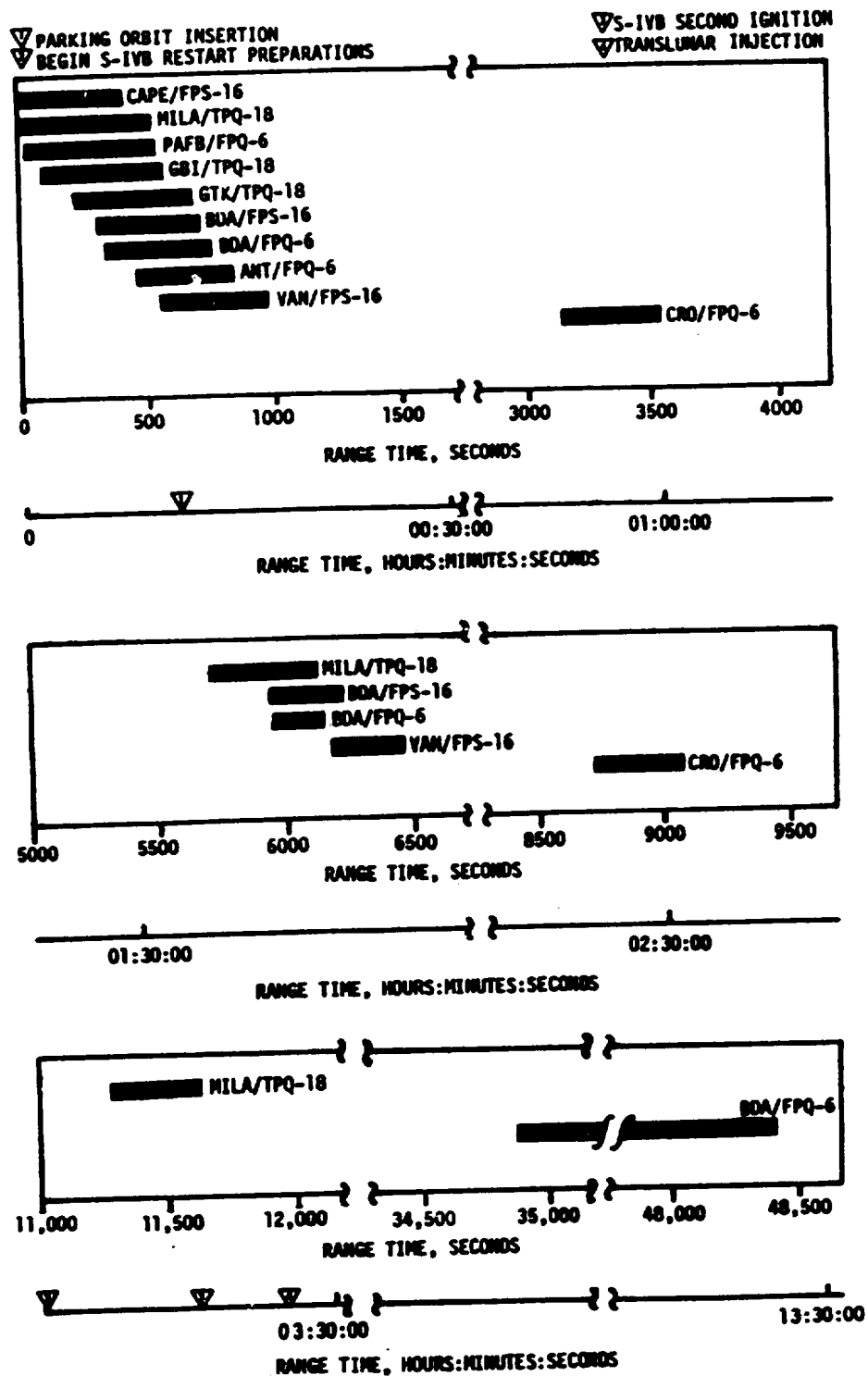


Figure 15-2. C-Band Acquisition and Loss Times

were required, all data except receiver signal strength remained unchanged during the flight. Power to the S-IVB stage range safety command systems was cutoff at 723.1 seconds by ground command, thereby deactivating (safing) the systems.

15.6 COMMAND AND COMMUNICATIONS SYSTEM EVALUATION

15.6.1 Summary of Performance

The performance of the command section of the CCS was satisfactory. No flight equipment malfunctions occurred during the flight. The phase lock periods from liftoff to Translunar Injection (TLI) for the downlink carrier are shown in Figure 15-3. Ground station coverage times from TLI through lunar impact are shown in Figure 15-4.

Nineteen commands were initiated by Mission Control Center-Houston (MCC-H) and a total of 182 words were transmitted. Two words were not received by the onboard system because the uplink signal level was below the command threshold. These words were retransmitted and accepted. One command was retransmitted when a telemetry dropout precluded verification of acceptance by the transmitting ground station. These problems resulted from signal strength fluctuations (uplink and downlink) occurring during the solar heating maneuver. A list of commands initiated by MCC-H and the number of words transmitted for each command is shown in Table 15-5.

15.6.2 Performance Analysis

The first of the three commands required to accomplish the solar heating maneuver was transmitted unsuccessfully at 22,659 seconds (6:17:39) and caused the vehicle attitude to begin moving about the pitch axis. The changing vehicle attitude resulted in uplink and downlink signal strength fluctuations from 22,665 seconds (6:17:45) to 22,860 seconds (6:21:00). As a result of uplink signal strength fluctuations, the mode word of the solar heating command initiated at 22,667 seconds (6:17:47) was not received onboard. The uplink received signal strength was down to -117 dbm and the 70 KHz subcarrier lost lock for 0.1 second at the time of word transmission. The mode word was retransmitted and accepted.

The solar heating command initiated at 22,677 seconds (6:17:57) was accepted onboard on the first transmission except for the third data word which was accepted on the first retransmission. At the time this word was first transmitted, the onboard receiver signal strength had dropped to approximately 5 to 7 db below command threshold. The command threshold measured at KSC was from -103 to -105 dbm. The momentary low signal strength levels are attributed to antenna nulls.

Single word dumps were initiated at 22,749 seconds (6:19:09). Sixteen words were accepted by the vehicle. At the time the sixteenth word was transmitted, the ground station lost telemetry lock for 0.25 second and therefore did not detect the Address Verification Pulse (AVP) and Computer Release Pulse (CRP) from the vehicle. Therefore, the

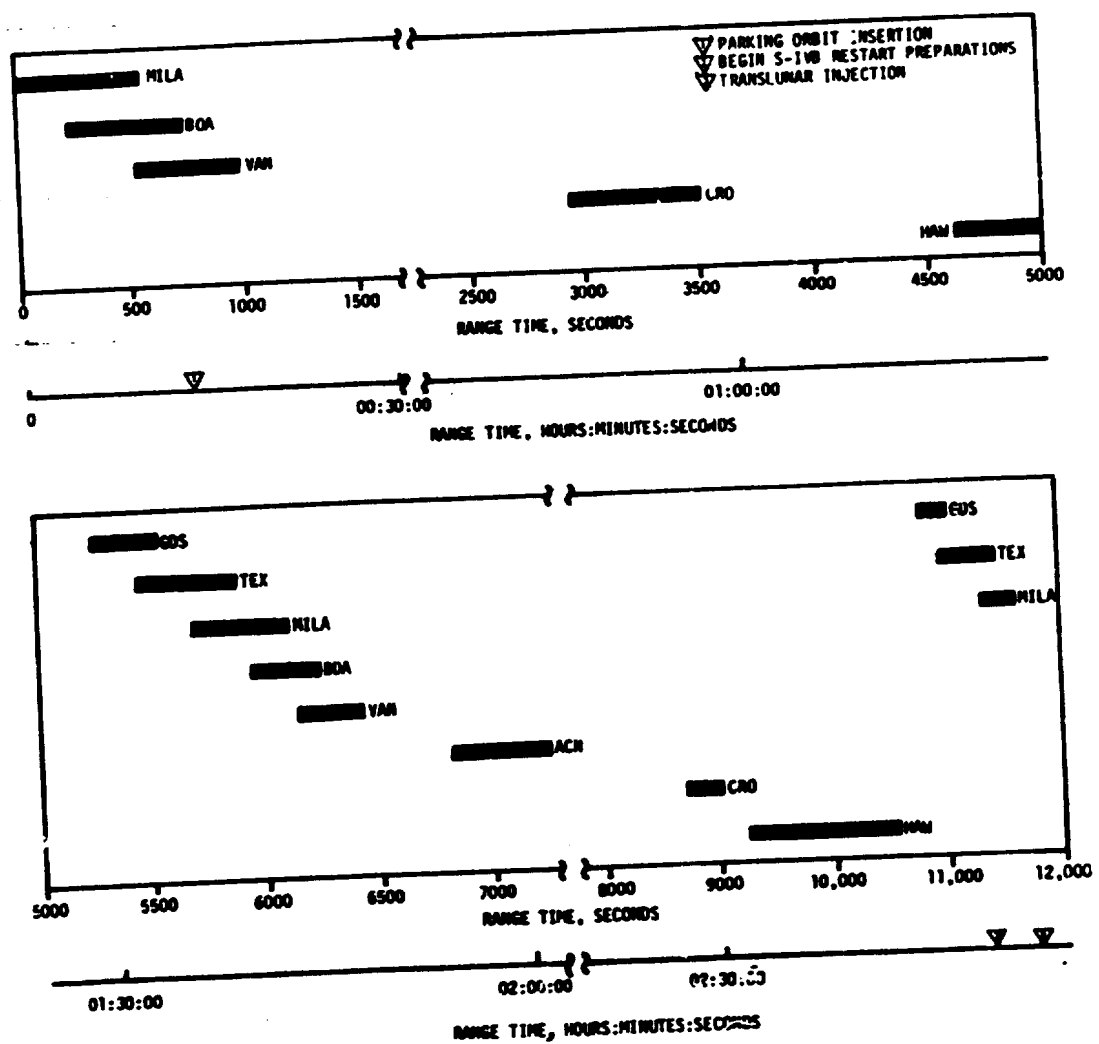


Figure 15-3. CCS Downlink Phase Lock Times (Liftoff to TLI)

▼ TRANSLUNAR INJECTION
▼ LUNAR IMPACT

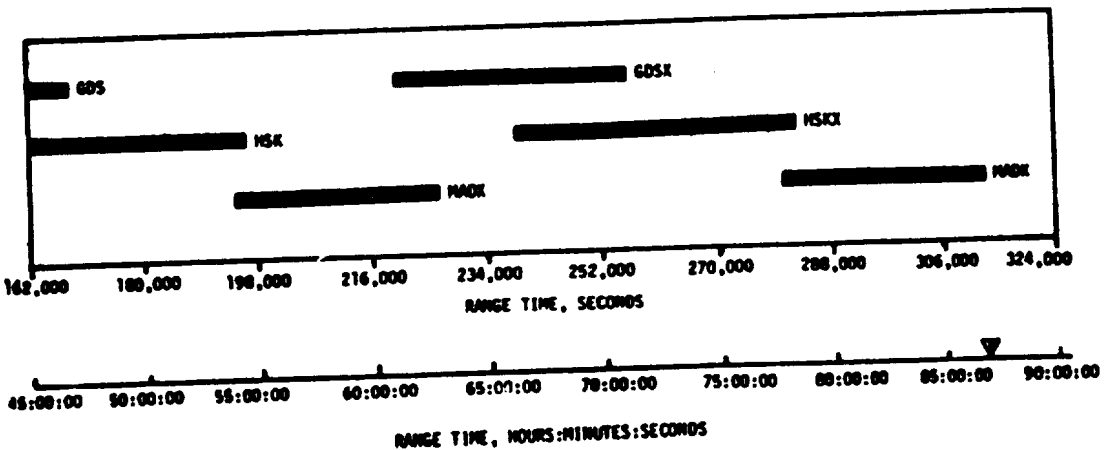
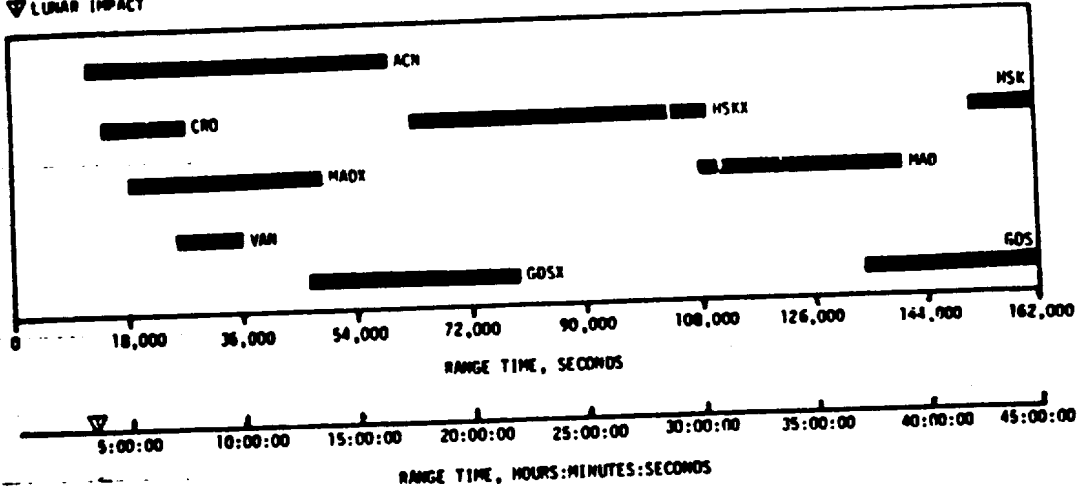


Figure 15-4. CCS Coverage (TLI to Lunar Impact)

Table 15-5. Command and Communication System Command History, AS-512

RANGE TIME SECONDS	RANGE TIME HRS:MIN:SEC	TRANS. STATION	COMMANDS	NO. OF WORDS TRANS.	REMARKS
17,519	4:51:59	ACN	Evasive Yaw Maneuver	1	Accepted
18,179	5:02:59	ACN	TBB Initiate	1	Accepted
20,998	5:49:58	MAD	Water Valve Logic Inhibit	1	Accepted
21,734	6:02:14	MAD	S-IVB/IU Lunar Impact - APS #1	3	Accepted
21,745	6:02:25	MAD	S-IVB/IU Lunar Impact - APS #1	8	Accepted
22,100	6:08:20	MAD	Single Word Dump (Group of 7)	28	Accepted
22,659	6:17:39	MAD	Solar Heating Maneuver	8	Accepted*
22,667	6:17:47	MAD	Solar Heating Maneuver	9	Accepted*
22,677	6:17:57	MAD	Solar Heating Maneuver	9	Accepted**
22,749	6:19:09	MAD	Single Word Dump (Group of 7)	19	Accepted
22,818	6:20:18	MAD	Terminate	1	Accepted
22,828	6:20:28	MAD	Single Word Dump (Group of 7)	28	Accepted
39,754	11:02:34	MAD	S-IVB/IU Lunar Impact - APS #2	8	Accepted
39,766	11:02:46	MAD	S-IVB/IU Lunar Impact - APS #2	8	Accepted
39,861	11:04:21	MAD	Single Word Dump (Group of 7)	28	Accepted
41,501	11:31:41	MAD	3-Axis Tumble Initiate	8	Accepted
41,518	11:31:58	MAD	FCC Power Off A	3	Accepted
41,529	11:32:09	MAD	FCC Power Off B	3	Accepted
41,553	11:32:33	MAD	Open Water Valve	3	Accepted

*Mode word not received on first transmission, accepted first retransmission.

**Third data word not received on first transmission, accepted first retransmission.

***All 16 words of commands accepted, however, ground station telemetry lost lock and did not receive verification pulses for the last data word, so it was retransmitted 3 times.

ground station retransmitted the word 8 times. After each retransmission the Launch Vehicle Digital Computer (LVDC) sent down an error message stating that the word received was out of sequence since it was expecting the seventeenth word. A terminate command was transmitted at 22,818 seconds (6:20:18) to clear the onboard command circuitry and at the complete single word dump command was successfully retransmitted at 22,828 seconds (6:20:28).

15.7 GROUND ENGINEERING CAMERAS

In general, ground camera coverage was good. Thirty-three items were received from KSC and evaluated. One item did not provide coverage of the entire event due to a film jam, and one did not have timing. The vehicle vertical motion data is not reducible due to timing loss.

The night launch had no effect on the camera coverage during prelaunch operations and during liftoff. Although, as expected, the tracking coverage was not nearly as clear as experienced during daylight launches.

SECTION 16

MASS CHARACTERISTICS

16.1 SUMMARY

Total vehicle mass, determined from post-flight analysis, was within 0.68 percent of predicted from ground ignition through S-IVB stage final shutdown. This small variation indicates that hardware weights, propellant loads, and propellant utilization were close to predicted values during flight.

16.2 MASS EVALUATION

Post-flight mass characteristics are compared with final predicted mass characteristics (MSFC Memorandum S&E-ASTN-SAE-72-87) and the operational trajectory (MSFC Memorandum S&E-AERO-MFT-200-72).

The post-flight mass characteristics were determined from an analysis of all available actual and reconstructed data from S-IC ignition through S-IVB second burn cutoff. Dry weights of the launch vehicle are based on actual stage weighings and evaluation of the weight and balance log books (MSFC Form 998). Propellant loading and utilization was evaluated from propulsion system performance reconstructions. Spacecraft data were obtained from the Manned Spacecraft Center (MSC).

Dry weights of the inert stages and the loaded spacecraft were all within 0.9 percent of predicted, which was well within acceptable limits.

During S-IC burn phase, the total vehicle mass was less than predicted by 470 kilograms (1036 lbm) (0.02 percent) at ignition, and less than predicted by 2878 kilograms (6344 lbm) (0.34 percent) at S-IC/S-II separation. This difference is the net of a larger than predicted LOX loading, and a less than predicted upper stage mass, S-IC fuel loading, and residuals on board at separation. S-IC burn phase total vehicle mass is shown in Tables 16-1 and 16-2.

During S-II burn phase, the total vehicle mass was less than predicted by 740 kilograms (1630 lbm) (0.11 percent) at ignition, and greater than predicted by 47 kilograms (103 lbm) (0.02 percent) at S-II/S-IVB separation. This deviation is the result of a lower than predicted S-II LOX load and a higher than predicted upper stage mass. Total vehicle mass for the S-II burn phase is shown in Tables 16-3 and 16-4.

Total vehicle mass during both S-IVB burn phases, as shown in Tables 16-5 through 16-8, was within 0.68 percent of the predicted values. A difference of 57 kilograms (125 lbm) (0.03 percent) greater than predicted at first burn ignition was due to S-IVB dry weight, LOX and APS loading. The mass at completion of first burn was 956 kilograms (2108 lbm) (0.68 percent) higher than predicted and was due primarily to the higher than predicted velocity at S-II stage cutoff. The high velocity at S-II cutoff resulted in a shorter than predicted burn time of the S-IVB stage to reach the desired trajectory end conditions and consequently more propellants were onboard at this time than predicted. A longer than predicted S-IVB second burn was required because of the mass of the extra propellants onboard. Even with the longer burn, the residual propellants were 226 kilograms (498 lbm) (0.35 percent) more than predicted but well within typical dispersions.

A summary of mass utilization and loss, both actual and predicted, from S-IC stage ignition through spacecraft separation is presented in Table 16-9. A comparison of actual and predicted mass, center of gravity, and moment of inertia is shown in Table 16-10.

Table 16-1. Total Vehicle Mass - S-IC Burn Phase - Kilograms

EVENTS	GROUND IGNITION			MOLDDOWN ARM RELEASE			CENTER ENGINE CUTOFF			OUTBOARD ENGINE CUTOFF		
	PRED	ACT	PRED	PRED	ACT	PRED	PRED	ACT	PRED	ACT	PRED	ACT
	RANGE TIME - SEC	-6.57	-6.55	0.24	0.24	139.12	139.30	161.67	161.23	161.00	160.99	160.83
DRY STAGE	130461.	130462.	130461.	130342.	130441.	130342.	130341.	130342.	130342.	130342.	130342.	130342.
LOX IN TANK	1480715.	1452255.	14649551.	14647435.	151313.	150859.	150859.	150859.	150859.	150859.	150859.	150859.
LOX BELOW TANK	21112.	21126.	210871.	210886.	210555.	210221.	2058.	2058.	2058.	2058.	2058.	2058.
LOX ULLAGE GAS	194.	191.	240.	221.	3058.	3179.	3247.	3247.	3247.	3247.	3247.	3247.
FUEL IN TANK	646374.	645190.	636180.	633521.	79271.	76625.	7625.	7625.	7625.	7625.	7625.	7625.
FUEL BELOW TANK	43117.	43118.	6000.	6000.	60C1.	60C1.	5952.	5952.	5952.	5952.	5952.	5952.
FUEL ULLAGE GAS	29.	30.	29.	34.	210.	213.	235.	235.	235.	235.	235.	235.
N2 PURGE GAS	36.	36.	36.	36.	19.	19.	19.	19.	19.	19.	19.	19.
MEDIUM IN BOTTLE	288.	288.	288.	288.	107.	105.	82.	82.	82.	82.	82.	82.
FROST	635.	635.	635.	635.	340.	340.	340.	340.	340.	340.	340.	340.
RETROROCKET PROP	1326.	1026.	1026.	1026.	1026.	1026.	1026.	1026.	1026.	1026.	1026.	1026.
OTHER	239.	239.	239.	239.	239.	239.	239.	239.	239.	239.	239.	239.
TOTAL STAGE	2285410.	2285680.	2246541.	224664.	403884.	398652.	166110.	166110.	166110.	166110.	166110.	166110.
TOTAL S-IC/S-11 1S	45531.	45224.	4531.	45224.	4531.	45224.	4531.	4531.	4531.	4531.	4531.	4531.
TOTAL S-111 STAGE	493318.	492557.	493318.	492557.	493096.	492335.	493096.	493096.	493096.	493096.	493096.	493096.
TOT S-111/S-IVB 1S	3637.	3637.	3637.	3637.	3637.	3637.	3637.	3637.	3637.	3637.	3637.	3637.
TOTAL S-111/S-IVB STAGE	120627.	120695.	120627.	120695.	120536.	120536.	120536.	120536.	120536.	120536.	120536.	120536.
TOTAL INSTRU UNIT	2046.	2027.	2046.	2027.	2046.	2027.	2046.	2027.	2046.	2027.	2027.	2027.
TOTAL SPACECRAFT	52759.	52738.	52738.	52738.	52738.	52738.	52738.	52738.	52738.	52738.	52738.	52738.
TOTAL UPPERSTAGE	676919.	676180.	676919.	676180.	676607.	675868.	676607.	676607.	676607.	676607.	676607.	676607.
TOTAL VEHICLE	2962330.	2961860.	2923460.	2917844.	1080492.	1074520.	842718.	840016.	840016.	840016.	840016.	840016.

Table 16-2. Total Vehicle Mass - S-IC Burn Phase - Pounds

EVENTS	GROUND IGNITION,		MOLDDOWN, AER RELEASE		CENTER ENGINE CUTOFF		OUTBOARD ENGINE CUTOFF		S-IC/S-II SEPARATION	
	PRED	ACT	PRED	ACT	PRED	ACT	PRED	ACT	PRED	ACT
RANGE TIME--SEC	-6.57	-6.55	0.24	0.24	139.32	139.30	161.67	161.23	163.63	163.39
DRY STAGE	287574.	287574.	267356.	267356.	287574.	287574.	287574.	287574.	287574.	287574.
LOX IN TANK	32644.59.	32579.3.	319104.8.	319104.8.	355635.	369850.	3597.	3597.	1441.	1441.
LOX BELOW TANK	469466.	46575.	-5219.	48250.	48183.	46214.	36622.	36622.	50334.	50334.
LOX ULLAGE GAS	427.	421.	933.	499.	6742.	7008.	7159.	7159.	7193.	7193.
FUEL IN TANK	1425012.	1422620.	1427336.	1395673.	17763.	168929.	160111.	15357.	15047.	15047.
FUEL BELOW TANK	9518.	5221.	13225.	13231.	13228.	13231.	13145.	13145.	13145.	13145.
FUEL ULLAGE GAS	64.	56.	56.	75.	463.	469.	518.	520.	521.	521.
N2 PURGE GAS	83.	53.	30.	90.	43.	43.	43.	43.	43.	43.
HELIM IN BOTTLE	635.	636.	636.	627.	236.	232.	182.	176.	176.	172.
FROST	1403.	1413.	1403.	1403.	750.	750.	750.	750.	750.	750.
RETROCKET PROP	2264.	2254.	2254.	2264.	2264.	2264.	2264.	2264.	2264.	2264.
OTHER	928.	328.	328.	528.	528.	528.	528.	528.	528.	528.
TOTAL STAGE	303868.	3019632.	4952776.	4942024.	890413.	878877.	366211.	361633.	357806.	351091.
TOTAL S-IC/S-II IS	9993.	5975.	9750.	9750.	9940.	9975.	9990.	9975.	9990.	9975.
TOTAL S-II STAGE	1087530.	1095322.	1097593.	1085902.	1087092.	1085414.	1085414.	1087092.	1087092.	1087092.
TOT S-II/S-IVB IS	8019.	3219.	8019.	8019.	8019.	8019.	8019.	8019.	8019.	8019.
TOTAL S-IVB STAGE	265939.	265937.	265938.	266097.	265738.	265397.	265397.	265397.	265397.	265397.
TOTAL INSTRU UNIT	4511.	4272.	4511.	4470.	4511.	4470.	4511.	4511.	4511.	4511.
TOTAL SPACECRAFT	116314.	116314.	116314.	116314.	116314.	116314.	116314.	116314.	116314.	116314.
TOTAL UPPER STAGE	149352.	1497742.	1492352.	1490722.	1491664.	1490034.	1491664.	1490034.	1491664.	1491664.
TOTAL VEHICLE	6530023.	6525724.	6445229.	6432746.	2362078.	2368912.	1857276.	1857276.	1849470.	1849470.

Table 16-3. Total Vehicle Mass - S-II, Burn Phase - Kilograms

EVENTS	S-IC IGNITION		S-II IGNITION		S-II MAINTAINSTAGE		S-II/EVACUEE CUTOFF		S-II/S-IVB SEPARATION	
	PRED	ACT	PRED	ACT	PRED	ACT	PRED	ACT	PRED	ACT
RANGE TIME--SEC	-6.57	-6.55	165.38	164.59	166.88	165.33	560.11	559.86	561.14	560.61
S-IC/S-II SMALL IS	616.	616.	0.	0.	0.	0.	0.	0.	0.	0.
S-IC/S-II LARGE IS	3914.	3908.	3914.	3908.	3914.	3908.	3908.	3908.	3908.	3908.
S-IC/S-II PROPELLANT	0.	0.	0.	0.	0.	0.	0.	0.	0.	0.
TOTAL S-IC/S-II IS	4531.	4524.	3914.	3908.	3914.	3908.	3908.	3908.	3908.	3908.
DRY STAGE	36477.	36479.	36477.	36479.	36477.	36479.	36477.	36479.	36477.	36479.
LOX IN TANK	38290.	38213.	38290.	38213.	38246.	38246.	38246.	38246.	635.	534.
LOX BELOW TANK	737.	737.	737.	737.	800.	800.	800.	800.	767.	787.
LOX ULLAGE GAS	137.	137.	137.	137.	139.	139.	139.	139.	1832.	1837.
FUEL IN TANK	72674.	72674.	72668.	72668.	72455.	72455.	72455.	72455.	1248.	1244.
FUEL BELOW TANK	104.	104.	110.	110.	127.	127.	127.	127.	123.	123.
FUEL ULLAGE GAS	17.	17.	17.	17.	18.	18.	18.	18.	757.	759.
INSULATION PURGE GAS	17.	17.	0.	0.	0.	0.	0.	0.		
FROST	204.	204.	0.	0.	0.	0.	0.	0.		
START TANK	13.	13.	13.	13.	2.	2.	2.	2.		
OTHER	34.	34.	34.	34.	34.	34.	34.	34.		
TOTAL S-II STAGE	493318.	492557.	493096.	492335.	492502.	491711.	491947.	491900.	41802.	41791.
TOT S-II/S-IVB IS	3631.	3637.	3637.	3637.	3637.	3637.	3637.	3637.	3637.	3637.
TOTAL S-II STAGE	120637.	120695.	120536.	120604.	120536.	120604.	120536.	120536.	120534.	120602.
TOTAL IU	206.	2027.	2046.	2027.	2046.	2027.	2046.	2027.	2046.	2027.
TOTAL SPACECRAFT	52759.	52738.	52759.	52738.	52759.	52738.	52759.	52738.	48601.	48609.
TOTAL UPPER STAGE	179070.	179098.	178979.	179007.	178979.	179007.	178979.	179007.	174819.	174876.
TOTAL VEHICLE	676919.	676180.	675991.	675291.	675396.	674658.	674658.	674658.	216621.	216668.

Table 16-4. Total Vehicle Mass - S-II Burn Phase - Pounds

EVENTS		S-IC IGNITION		S-II IGNITION		S-II MAINSTAGE		S-II ENGINE CUTOFF		S-II/SIVB SEPARATION	
PRED	ACT	PRED	ACT	PRED	ACT	PRED	ACT	PRED	ACT	PRED	ACT
RANGE TIME SEC	-6.57	-6.57	165.39	164.59	166.88	166.38	561.13	559.66	561.14	560.61	
S-IC/S-II SMALL IS	1359.	0.	0.	0.	0.	0.	0.	0.	0.	0.	
S-IC/S-II LARGE IS	9631.	9616.	9631.	9616.	9631.	9616.	0.	0.	0.	0.	
S-IC/S-II PROPELLANT	0.	0.	0.	0.	0.	0.	0.	0.	0.	0.	
TOTAL S-IC/S-II IS	9990.	9975.	8631.	8616.	8631.	8616.	65.5.	65.5.	65.5.	65.5.	
DRY STAGE	80420.	90423.	80420.	80423.	80420.	80423.	80420.	80423.	80420.	80423.	80423.
LOX IN TANK	844150.	842469.	844150.	842469.	843149.	843149.	1401.	1401.	1401.	1401.	1422.
LOX BE-CA TANK	1625.	1625.	1624.	1624.	1764.	1764.	1736.	1736.	1736.	1736.	1736.
LOX ULLAGE GAS	302.	302.	302.	302.	307.	307.	4040.	4040.	4040.	4051.	4051.
FUEL IN TANK	160220.	160220.	160220.	160220.	159736.	159736.	2658.	2658.	2752.	2752.	2676.
FUEL BELT TANK	231.	231.	244.	244.	282.	282.	272.	272.	272.	272.	272.
FUEL ULLAGE GAS	38.	38.	38.	38.	41.	41.	1668.	1668.	1668.	1668.	1674.
INSULATION PURGE GAS	38.	38.	0.	0.	0.	0.	0.	0.	0.	0.	0.
FROST	450.	450.	0.	0.	0.	0.	0.	0.	0.	0.	0.
START TANK	30.	30.	30.	30.	5.	5.	5.	5.	5.	5.	5.
OTHER	76.	76.	76.	76.	76.	76.	76.	76.	76.	76.	76.
TOTAL S-II STAGE	1037580.	1035902.	1097092.	1085414.	1085762.	1085762.	92478.	92478.	92158.	92158.	92158.
TOT S-II/SIVB IS	8019.	8019.	8019.	8019.	8019.	8019.	8019.	8019.	8019.	8019.	8019.
TOT S-II/SIVB STAGE	265938.	266017.	265738.	265887.	265756.	265937.	265738.	265887.	265738.	265887.	265887.
TOTAL S-II STAGE	4911.	4410.	4511.	4470.	4511.	4470.	4511.	4511.	4511.	4511.	4511.
TOTAL SPACECRAFT	116314.	116269.	116314.	116269.	116314.	116269.	116314.	116269.	116314.	116269.	116269.
TOTAL LOWER STAGE	394782.	394845.	394582.	394645.	394582.	394645.	385415.	385415.	385415.	385415.	385415.
TOTAL VEHICLE	1492351.	1490722.	1490305.	1433675.	1433995.	1437350.	47793.	47793.	47793.	47793.	47793.

Table 16-5. Total Vehicle Mass - S-IVB First Burn Phase - Kilograms

EVENTS	S-IC IGNITION			S-IVB IGNITION			S-IVB ULLAGE			S-IVB ENGINE CUTOFF			S-IVB END DECAY		
	PRED	ACT	PRED	ACT	PRED	ACT	PRED	ACT	PRED	ACT	PRED	ACT	PRED	ACT	
RANGE TIME--SEC	-6.57	-6.55	964.24	963.83	565.74	565.22	736.74	732.65	707.33	702.90					
DRY STAGE	11333.	11327.	11339.	11334.	11349.	11324.	11248.	11273.	11243.	11273.					
LOX IN TANK	88548.	88572.	88534.	88572.	88411.	88443.	62549.	63344.	62523.	63316.					
LOX BELOW TANK	166.	166.	166.	166.	166.	166.	190.	180.	180.	180.					
LOX ULLAGE GAS	11.	13.	15.	13.	13.	19.	14.	98.	98.	70.					
FUEL IN TANK	19822.	19826.	19817.	19819.	19789.	19773.	14626.	14624.	14618.	14792.					
FUEL BELOW TANK	21.	19.	26.	23.	26.	23.	23.	23.	23.	23.					
FUEL ULLAGE GAS	15.	17.	15.	18.	18.	16.	18.	18.	18.	18.					
ULLAGE ROCKET PROP	53.	53.	9.	9.	285.	301.	235.	331.	283.	298.					
APS PROPELLANT	285.	301.	285.	301.	203.	202.	203.	201.	184.	179.					
HELIUM IN BOTTLES	204.	202.	45.	45.	45.	45.	45.	45.	45.	45.					
FROST	136.	136.	2.	2.	2.	0.	0.	0.	3.	3.					
START TANK GAS	2.	2.	25.	25.	25.	25.	25.	25.	25.	25.					
OTHER	25.	25.													
TOTAL S-IVB STAGE	120627.	120694.	120469.	120336.	120333.	120363.	89326.	90293.	89290.	90457.					
TOTAL IU	2046.	2027.	2046.	2027.	2049.	2027.	2046.	2027.	2046.	2027.					
TOTAL SPACECRAFT	46601.	46609.	46601.	46609.	43501.	43509.	48601.	48601.	48609.	48609.					
TOTAL UPPER STAGE	90647.	50636.	50647.	50636.	50647.	50636.	50647.	50636.	50647.	50636.					
TOTAL VEHICLE	17127.	171331.	171116.	171113.	170541.	171113.	171113.	171113.	171113.	171113.					

Table 16-6. Total Vehicle Mass - S-IVB First Burn Phase - Pounds Mass

EVENTS	S-IC IGNITION		S-IVB IGNITION		S-IVB MAINSTAGE		S-IVB ENGINE CUTOFF		S-IVB E-N2 DECAY	
	PRED	ACT	PRED	ACT	PRED	ACT	PRED	ACT	PRED	ACT
RANGE TIME-SEC	-6.57	-6.55	564.24	563.93	566.14	560.22	736.74	736.65	737.23	736.93
DRY STAGE	24985.	25040.	24934.	24989.	24934.	24989.	24985.	24985.	24747.	24747.
LOX IN TANK	195217.	195269.	195227.	195261.	194914.	194935.	197676.	197676.	197659.	197659.
LOX BELOW TANK	367.	367.	367.	367.	397.	397.	397.	397.	397.	397.
LOX ULLAGE GAS	25.	30.	34.	36.	43.	32.	217.	217.	217.	217.
FUEL IN TANK	43702.	43710.	43690.	43692.	43536.	43594.	32249.	32249.	32227.	32227.
FUEL BELOW TANK	45.	42.	58.	52.	58.	52.	59.	59.	58.	52.
FUEL ULLAGE GAS	35.	38.	35.	40.	35.	41.	122.	122.	123.	123.
ULLAGE ROCKET PROP	116.	117.	22.	22.	630.	664.	664.	664.	657.	657.
APS PROPELLANT	630.	664.	630.	664.	630.	664.	645.	645.	626.	626.
METHANE IN BOTTLES	450.	447.	449.	447.	448.	448.	445.	445.	435.	435.
FROST	300.	300.	130.	130.	130.	130.	130.	130.	130.	130.
START TANK GAS	5.	5.	5.	5.	1.	1.	7.	7.	7.	7.
OTHER	56.	57.	56.	57.	56.	57.	56.	57.	56.	57.
TOTAL S-IVB STAGE	265936.	266086.	265593.	265737.	265232.	265337.	195936.	195934.	195252.	195252.
TOTAL IU	4511.	4470.	4511.	4470.	4511.	4470.	4511.	4511.	4511.	4511.
TOTAL SPACECRAFT	107147.	107145.	107147.	107145.	107147.	107147.	107147.	107147.	107147.	107147.
TOTAL UPPERSTAGE	111638.	111635.	111638.	111635.	111632.	111632.	111638.	111638.	111638.	111638.
TOTAL VEHICLE	377596.	377721.	377248.	377312.	376860.	376992.	305945.	310511.	303913.	303913.

Table 16-7. Total Vehicle Mass - S-IVB Second Burn Phase - Kilograms

EVENTS	S-IVB 15.111CN		S-IVB MAIN STAGE		S-IVB ENGINE CUT-OFF		S-IVB END DECAY		SPACECRAFT SEPARATION	
	PRED	ACT	PRED	ACT	PRED	ACT	PRED	ACT	PRED	ACT
	RANGE TIME - SEC	1555.54	115556.65	11561.04	11559.1J	11905.54	11907.64	11905.79	11907.9J	10.00
DRY STAGE	11243.	11275.	11249.	11273.	11249.	11273.	11248.	11273.	11248.	11273.
LOX IN TANK	62493.	63291.	62367.	63155.	1549.	1760.	1521.	1733.	144.	1723.
LOX BELOW TANK	157.	166.	180.	180.	180.	190.	180.	180.	166.	171.
LOX ULLAGE GAS	124.	110.	124.	111.	199.	155.	203.	161.	213.	213.
FUEL IN TANK	13-83.	13606.	13414.	13520.	529.	769.	518.	779.	542.	776.
FUEL BELOW TANK	26	23	26	23	26.	23.	26.	23.	23.	21.
FUEL ULLAGE GAS	144.	178.	149.	179.	277.	273.	274.	273.	147.	1274.
APS PROPELLANT	236.	234.	236.	234.	234.	234.	224.	224.	210.	473.
HELIO ^W IN BOTTLES	164.	164.	168.	168.	168.	168.	168.	168.	148.	148.
FROST	45.	45.	45.	45.	45.	45.	45.	45.	45.	45.
START TANK GAS	2.	2.	0.	0.	0.	3.	3.	3.	3.	3.
OTHER	25.	25.	25.	25.	25.	25.	25.	25.	25.	25.
TOTAL S-IVB STAGE	89154.	89113.	87991.	88613.	16927.	15014.	14741.	15017.	14641.	2027.
TOTAL IU	2346.	2027.	2046.	2027.	2046.	2027.	2046.	2027.	2046.	2027.
TOTAL SPACECRAFT	49631.	48609.	43601.	48631.	48639.	48631.	48649.	48631.	48631.	48631.
TOTAL UPStAGE	936-7.	50636.	50647.	50636.	50647.	50636.	50647.	50636.	50636.	2612.
TOTAL VEHICLE	13667.	139753.	138638.	139589.	63474.	65711.	65438.	65664.	16223.	17396.

Table 16-8. Total Vehicle Mass - S-IVB Second Burn Phase - Pounds Mass

EVENTS	S-IVB IGNITION		S-IVB MAX STAGE		S-IVB FLUID CUTOFF		S-IVB END DECAY		SPACESHIFT SEPARATION	
	PRED	ACT	PRED	ACT	PRED	ACT	PRED	ACT	PRED	ACT
	RANGE TIME-SEC	11558.5*	11556.63	11561.04	11559.03	11935.54	11937.64	11935.77	11937.73	0.00 17102.33
DRY STAGE	26799.	24854.	24799.	26954.	24776.	24654.	26777.	24956.	24799.	24554.
LOX IN TANK	137774.	139511.	137497.	139234.	3-17.	3-32.	3-22.	3-22.	3179.	3259.
LOX BELOW TANK	368.	368.	397.	397.	397.	397.	397.	397.	367.	367.
LOX ULLAGE GAS	274.	244.	274.	245.	438.	438.	438.	438.	471.	371.
FUEL IN TANK	29692.	29998.	29584.	29584.	2643.	2643.	2646.	2646.	4659.	4676.
FUEL BELOW TANK	58.	52.	58.	52.	52.	52.	52.	52.	52.	42.
FUEL ULLAGE GAS	328.	394.	328.	395.	662.	662.	664.	664.	250.	250.
APS PROPELLANT	521.	516.	521.	516.	521.	521.	525.	525.	454.	454.
HELIUM IN BOTTLES	370.	363.	370.	370.	362.	362.	351.	351.	231.	231.
FROST	100.	150.	100.	130.	126.	126.	126.	126.	120.	120.
START TANK GAS	5.	5.	1.	1.	7.	7.	7.	7.	7.	7.
OTHER	96.	97.	96.	97.	56.	57.	59.	59.	56.	57.
TOTAL S-IVB STAGE	194347.	196462.	193987.	196020.	32097.	32097.	32654.	32654.	31211.	31337.
TOTAL IU	4511.	4470.	4511.	47070.	4314.	4314.	4211.	4211.	4511.	4470.
TOTAL SPACECRAFT	107147.	107165.	107147.	107165.	107147.	107147.	107165.	107165.	1363.	14.
TOTAL UPPER STAGE	111658.	111655.	111658.	111655.	111655.	111655.	111653.	111653.	5952.	5952.
TOTAL VEHICLE	308005.	308097.	305645.	307655.	2-3-7.	1-3-7.	1-2-7.	1-2-7.	37122.	37337.

Table 16-9. Flight Sequence Mass Summary

MASS HISTORY	PREDICTED		ACTUAL	
	KG	LBS	KG	LBS
S-IC STAGE TOTAL	2285410.	5038463.	2283679.	5039362.
S-IC/S-II IS TOTAL	4531.	9990.	4524.	9975.
S-II STAGE TOTAL	493318.	1087583.	492557.	1085902.
S-II/S-IVB IS TOTAL	3637.	8019.	3637.	8019.
S-IVB STAGE TOTAL	120627.	265939.	120695.	266087.
INSTRUMENT UNIT	2046.	4511.	2027.	4470.
SPACECRAFT TOTAL	52759.	116314.	52739.	116269.
1ST FLT STG AT IGN THRUST BUILDUP	2962329.	6530820.	2961859.	6529784.
	-38859.	-85691.	-44015.	-97037.
1ST FLT STG AT FDIR FROST	2923460.	6445128.	2917843.	6432746.
MAINSTAGE	-294.	-650.	-294.	-650.
N2 PURGE GAS	-953.	-2101.	-997.	-2198.
THRUST DECAY-IE	-189.	-418.	-189.	-418.
ENG EXPENDED PROP	-17.	-38.	-17.	-38.
S-II ISUL PURGE	-204.	-450.	-204.	-450.
S-II FRCST	-90.	-200.	-90.	-200.
S-IVB FRCST	0.	0.	0.	0.
THRUST DECAY-DE				
1ST FLT STG AT DECO THRUST DECAY-DE	842718.	1857876.	840016.	1851919.
S-IC/S-II ULL RKT	-3812.	-8405.	-3988.	-8793.
	0.	0.	0.	0.
1ST FLT STG AT SEP STG AT SEPARATION	838905.	1849470.	836027.	1843126.
S-IC/S-II SMALL IS	-162298.	-357806.	-160159.	-353091.
S-IC/S-II ULL RKT	-616.	-1359.	-616.	-1359.
	0.	0.	0.	0.
2ND FLT STG AT SSC	675991.	1490306.	675251.	1488675.
FUEL LEAD	0.	0.	0.	0.
S-IC/S-II ULL RKT	0.	0.	0.	0.
2ND FLT STG AT IGN THRUST BUILDUP START TANK	675991.	1490305.	675251.	1488675.
S-IC/S-II ULL RKT	-582.	-1285.	-582.	-1284.
	-11.	-25.	-11.	-25.
	0.	0.	0.	0.
2ND FLT STG AT MS MAINSTAGE	675396.	1488995.	674557.	1467366.
LES	-490501.	-993185.	-449797.	-991633.
S-IC/S-II LARGE IS	-4159.	-9167.	-4129.	-9104.
TD 6 ENG PROP	-3914.	-8631.	-3908.	-8616.
	-93.	-118.	-44.	-97.
2ND FLT STG AT COS THRUST DECAY	216768.	477893.	216778.	477915.
S-IVB ULL RKT PROP	-145.	-320.	-108.	-238.
	-2.	-5.	-2.	-5.
2ND FLT STG AT SEP STG AT SEPARATION	216621.	477568.	216668.	477671.
S-II/S-IVB IS DRY	-41302.	-92158.	-41791.	-92135.
S-II/S-IVB PROP	-3156.	-6959.	-3154.	-6955.
S-IVB AFT FRAME	-480.	-1060.	-482.	-1064.
S-IVB ULL RKT PROP	-21.	-48.	21.	-48.
S-IVB DET PKG	-1.	-3.	-1.	-3.
	-1.	-3.	-1.	-3.
3RD FLT STG AT SSC	171157.	377337.	171214.	377463.

Table 16-9. Flight Sequence Mass Summary (Continued)

MASS HISTORY	PREDICTED		ACTUAL	
	KG	LB	KG	LB
3RD FLT STG 1ST SSC ULLAGE ROCKET PROP FUEL LEAD	171157.	377337.	171214.	377453.
	-39.	-85.	-39.	-85.
	-0.	-1.	-1.	-1.
3RD FLT STG 1ST IGN ULLAGE ROCKET PROP START TANK THRUST BUILDUP	171116.	377248.	171173.	377372.
	-9.	-22.	-9.	-22.
	-1.	-4.	-1.	-4.
	-163.	-361.	-160.	-354.
3RD FLT STG 1ST VS ULLAGE ROCKET CASE MAINSTAGE APS	170941.	376860.	171000.	376922.
	-61.	-135.	-61.	-135.
	-30901.	-65127.	-30006.	-65152.
	-1.	-4.	-3.	-7.
3RD FLT STG 1ST COS THRUST DECAY	139976.	302594.	140930.	310592.
	-38.	-84.	-36.	-90.
3RD FLT STG 1ST ETO ENGINE PROP FUEL TANK LOSS LOX TANK LOSS APS START TANK C2/H2 BURNER	139937.	308510.	140893.	310613.
	-18.	-40.	-18.	-40.
	-1045.	-2305.	-1041.	-2297.
	-5.	-11.	0.	0.
	-47.	-105.	-63.	-141.
	-0.	-2.	-0.	-2.
	-7.	-16.	-7.	-15.
3RD FLT STG 2ND SSC FUEL LEAD	138832.	306029.	139761.	308122.
	-11.	-24.	-11.	-25.
3RD FLT STG 2ND IGN START TANK THRUST BUILDUP	138801.	306005.	139750.	308097.
	-1.	-4.	-1.	-4.
	-161.	-356.	-198.	-433.
3D FLT STG 2ND VS MAINSTAGE APS	138638.	305649.	139549.	307553.
	-73161.	-161293.	-73828.	-152764.
	-1.	-4.	-4.	-11.
3RD FLT STG 2ND COS THRUST DECAY	65474.	144347.	65711.	144369.
	-36.	-79.	-42.	-90.
3RD FLT STG 2ND ETO JETTISON SLA CSM S-IVB STAGE LOSS	65438.	144267.	65664.	144763.
	-1170.	-2581.	-1170.	-2581.
	-30367.	-66949.	-30364.	-66942.
	-338.	-745.	-314.	-693.
STR TRANS/DOCK CSM	33562.	73992.	33814.	74549.
	30367.	66949.	30364.	66942.
END TRANS/DOCK CSM LM S-IVB STAGE LOSS	63929.	140941.	64179.	141491.
	-30367.	-66949.	-30364.	-66942.
	-16436.	-36237.	-16448.	-36267.
	-295.	-652.	-272.	-622.
LAU VEH AT S/C SEP S/C NOT SEPARATED IU	16829.	37132.	17094.	37557.
	-625.	-1380.	-625.	-1380.
	-2046.	-4511.	-2027.	-4471.
S-IVB STAGE	-14157.	-31211.	-14441.	-31637.

Table 16-10. Mass Characteristics Comparison

EVENT	MASS	LONGITUDINAL C.G. IX STA. 1			RADIAL C.G.			ROLL MOMENT OF INERTIA			PITCH MOMENT OF INERTIA			YAW MOMENT OF INERTIA		
		KILO POUNDS	O/C METERS INCHES	DEV. INCHES	METERS INCHES	DELTA	INCHES	DELTIA	X10-6	KG-M2	O/U DEV.	X10-6	KG-M2	O/U DEV.	X10-6	KG-M2
S-1C STAGE DRY	PRED	13044.1 28757.4	9.314 366.7	0.000 0.000	0.0651 2.5632	0.0000 0.0003	0.0651 2.5632	0.0000 0.0003	2.562 0.001	16.418 -0.007	0.000 0.000	16.418 -0.007	16.418 -0.007	0.000 0.000	16.418 -0.007	16.418 -0.007
S-1C/S-1I INSTRUMENT	PRED	130342.0 99900.0	9.314 1644.1	-0.037 0.000	0.000 0.000	0.000 0.000	0.000 0.000	0.000 0.000	0.000 0.000	16.418 -0.007	0.000 0.000	16.418 -0.007	16.418 -0.007	0.000 0.000	16.418 -0.007	16.418 -0.007
S-1I STAGE TOTAL	ACTUAL	287356.0 99750.0	9.314 1644.1	-0.037 0.000	0.000 0.000	0.000 0.000	0.000 0.000	0.000 0.000	0.000 0.000	16.418 -0.007	0.000 0.000	16.418 -0.007	16.418 -0.007	0.000 0.000	16.418 -0.007	16.418 -0.007
S-1I/S-1V5 INSTRUMENT	PRED	80420.0 80423.0	41.760 1885.6	0.000 0.000	0.000 0.000	0.000 0.000	0.000 0.000	0.000 0.000	0.000 0.000	16.418 -0.007	0.000 0.000	16.418 -0.007	16.418 -0.007	0.000 0.000	16.418 -0.007	16.418 -0.007
S-1V5 STAGE DRY	PRED	36478.0 8019.0	47.954 2615.2	0.000 0.000	0.000 0.000	0.000 0.000	0.000 0.000	0.000 0.000	0.000 0.000	16.418 -0.007	0.000 0.000	16.418 -0.007	16.418 -0.007	0.000 0.000	16.418 -0.007	16.418 -0.007
S-1V5 STAGE TOTAL	ACTUAL	36479.0 8019.0	47.954 2615.2	0.000 0.000	0.000 0.000	0.000 0.000	0.000 0.000	0.000 0.000	0.000 0.000	16.418 -0.007	0.000 0.000	16.418 -0.007	16.418 -0.007	0.000 0.000	16.418 -0.007	16.418 -0.007
S-1V6 STAGE DRY	PRED	3637.0 8019.0	66.426 2615.2	0.000 0.000	0.000 0.000	0.000 0.000	0.000 0.000	0.000 0.000	0.000 0.000	16.418 -0.007	0.000 0.000	16.418 -0.007	16.418 -0.007	0.000 0.000	16.418 -0.007	16.418 -0.007
S-1V6 STAGE TOTAL	ACTUAL	3637.0 8019.0	66.426 2615.2	0.000 0.000	0.000 0.000	0.000 0.000	0.000 0.000	0.000 0.000	0.000 0.000	16.418 -0.007	0.000 0.000	16.418 -0.007	16.418 -0.007	0.000 0.000	16.418 -0.007	16.418 -0.007
VEHICLE UNIT	PRED	2495.0 4511.0	72.527 2855.4	0.000 0.000	0.000 0.000	0.000 0.000	0.000 0.000	0.000 0.000	0.000 0.000	16.418 -0.007	0.000 0.000	16.418 -0.007	16.418 -0.007	0.000 0.000	16.418 -0.007	16.418 -0.007
SPACECRAFT TOTAL	ACTUAL	2028.0 4470.0	72.527 2855.4	0.000 0.000	0.000 0.000	0.000 0.000	0.000 0.000	0.000 0.000	0.000 0.000	16.418 -0.007	0.000 0.000	16.418 -0.007	16.418 -0.007	0.000 0.000	16.418 -0.007	16.418 -0.007
ACTUAL	2028.0 4470.0	72.527 2855.4	0.000 0.000	0.000 0.000	0.000 0.000	0.000 0.000	0.000 0.000	0.000 0.000	0.000 0.000	16.418 -0.007	0.000 0.000	16.418 -0.007	16.418 -0.007	0.000 0.000	16.418 -0.007	16.418 -0.007
SPAC	PRED	52759.0 116314.0	91.450 3600.4	0.000 0.000	0.000 0.000	0.000 0.000	0.000 0.000	0.000 0.000	0.000 0.000	16.418 -0.007	0.000 0.000	16.418 -0.007	16.418 -0.007	0.000 0.000	16.418 -0.007	16.418 -0.007
SPACECRAFT TOTAL	ACTUAL	52735.0 116269.0	91.437 3599.9	-0.032 -0.030	0.000 0.000	0.4193 0.0103	0.0000 0.0003	0.0000 0.0003	0.0000 0.0003	16.418 -0.007	0.000 0.000	16.418 -0.007	16.418 -0.007	0.000 0.000	16.418 -0.007	16.418 -0.007

Table 16-10. Mass Characteristics Comparison (Continued)

EVENT	MASS	LONGITUDINAL		ROLL MOMENT OF INERTIA		PITCH MOMENT OF INERTIA		YAW MOMENT OF INERTIA	
		C.G. IN INCHES	C.G. C.G. IN INCHES	WEIERS DEVI.	KG-N2 DELTA X10-6	D/C DELTA X10-6	KG-N2 DELTA X10-6	D/C DELTA X10-6	KG-N2 DELTA X10-6
PRED	2962430.	30.472	30.472	0.0007	3.635	9.99325	9.98371	-----	-----
1ST FLIGHT STAGE AT IGNITION	KILO POUNDS	6530822.	1199.6	0.0008	-----	-----	-----	-----	-----
2961860.	30.474	30.474	0.0007	3.635	9.99325	9.98371	9.99321	-0.004	-----
ACTUAL	6529783.	-0.01	1199.7	0.0007	3.632	9.99325	9.98321	9.99321	-0.004
2963461.	30.474	30.474	0.0007	3.632	9.99325	9.98321	9.99321	-0.004	-----
PRED	6445128.	1197.6	1197.6	0.0008	3.635	9.99372	9.98374	-----	-----
1ST FLIGHT STAGE AT HOLDDOWN ARV RELEASE	2917844.	30.419	30.419	0.0008	3.635	9.99372	9.98374	9.99373	-0.004
ACTUAL	6432145.	-0.18	1197.6	0.0008	3.632	9.99367	9.98373	9.99369	-0.004
842718.	45.783	45.783	0.0016	3.654	9.99372	9.98374	9.99374	-0.004	-----
1ST FLIGHT STAGE AT OUTBOARD ENGINE CUTOFF SIGNAL	PRED	1857875.	1821.7	0.0008	3.635	9.99372	9.98374	9.99374	-0.004
940016.	46.371	46.371	0.0016	3.654	9.99372	9.98374	9.99374	-0.004	-----
ACTUAL	1851910.	-0.31	1845.3	0.0016	3.635	9.99372	9.98374	9.99374	-0.004
838905.	46.945	46.945	0.0016	3.654	9.99372	9.98374	9.99374	-0.004	-----
PRED	1849470.	1849.2	1849.2	0.0016	3.654	9.99372	9.98374	9.99374	-0.004
1ST FLIGHT STAGE AT SEPARATION	836027.	47.045	47.045	0.0016	3.654	9.99372	9.98374	9.99374	-0.004
ACTUAL	1843125.	-0.33	1852.2	0.0016	3.654	9.99372	9.98374	9.99374	-0.004
675991.	55.935	55.935	0.0139	3.979	1.43101	1.40113	-----	-----	-----
2ND FLIGHT STAGE AT START SEQUENCE COMMAND	PRED	1490336.	2202.2	0.0267	3.979	1.43101	1.40113	-----	-----
675252.	55.942	55.942	0.0139	3.979	1.43101	1.40113	-----	-----	-----
ACTUAL	1498676.	-0.10	2202.4	0.023	3.9757	1.43095	1.40107	-0.002	1.43097
673397.	55.936	55.936	0.0139	3.979	1.43101	1.40113	-----	-----	-----
PRED	1488955.	2232.2	2232.2	0.0267	3.979	1.43101	1.40113	-----	-----
2ND FLIGHT STAGE AT MAINSTAGE	674658.	52.943	52.943	0.0139	3.979	1.43101	1.40113	-----	-----
ACTUAL	1487396.	-0.10	2202.4	0.023	3.9757	1.43095	1.40107	-0.002	1.43097
216707.	71.413	71.413	0.0553	0.951	1.43093	1.40105	-----	-----	-----
PRED	477893.	2811.6	2811.6	0.0553	0.951	1.43093	1.40105	-----	-----
2ND FLIGHT STAGE AT CUTOFF SIGNAL	216779.	71.420	71.420	0.0553	0.951	1.43093	1.40105	-0.002	1.43097
ACTUAL	477915.	0.00	2911.8	0.019	2.2535	2.2222	2.1922	4.5378	-0.002

Table 16-10. Mass Characteristics Comparison (Continued)

EVENT	MASS KILO POUNDS	LONGITUDINAL C.G. (X STA.)			RADIAL C.G.			ADL MOMENT OF INERTIA K2-V2			FLYING MOMENT OF INERTIA K3-V3		
		O/O DEV.	METERS INCHES	DELTA	METERS INCHES	DELTA	ALO-V	ALO-V	DE-V	ALO-V	DE-V	ALO-V	DE-V
PRED	216621. 477568.	71.632 2812.3			0.0566 2.2318		0.880 —		45.252 —		5.333 —		
2ND FLIGHT STAGE AT SEPARATION	216668. 477671.	71.433 0.02	2812.3	0.03	0.0572 2.2339	0.0065 0.020	0.206 0.861	0.03 3.03	45.342 45.342	0.036 0.036	5.036 5.036	0.033 0.033	
PRED	171157. 377337.	77.296 3043.1			0.0380 1.4968		0.206 —		13.943 —		2.344 —		
3RD FLIGHT STAGE AT 1ST START SEQ- UENCE COMMAND	171214. 377463.	77.295 0.03	3043.1	-0.05	0.0383 1.4950	0.0022 0.0022	0.207 0.237	0.13 0.13	13.955 13.955	0.036 0.036	2.345 2.345	0.031 0.031	
PRED	171117. 377248.	77.297 3043.2			0.0383 1.4968		0.206 —		13.943 —		2.342 —		
3RD FLIGHT STAGE AT 1ST IGNITION	171173. 377372.	77.296 0.03	3043.1	-0.05	0.0380 1.4990	0.0022 0.0022	0.207 0.207	0.13 0.13	13.953 13.953	0.035 0.035	2.343 2.343	0.035 0.035	
PRED	170941. 376860.	77.298 3043.2			0.0382 1.4965		0.206 —		13.945 —		2.342 —		
3RD FLIGHT STAGE AT 1ST MAINSTAGE	171101. 376992.	77.298 0.03	3043.2	-0.02	0.0380 1.4990	-0.0001 -0.0001	0.207 0.207	0.13 0.13	13.942 13.942	0.035 0.035	2.342 2.342	0.035 0.035	
PRED	139976. 308594.	78.210 3079.1			0.0663 1.6264		0.205 —		13.162 —		2.348 —		
3RD FLIGHT STAGE AT 1ST CUTOFF SIG- NAL	140934. 310698.	78.173 0.68	3077.6	-1.48	0.0659 1.6094	-0.0001 -0.0111	0.206 0.206	0.12 0.12	13.163 13.163	0.031 0.031	2.349 2.349	0.031 0.031	
PRED	139938. 308510.	78.212 3079.2			0.0663 1.6264		0.205 —		13.161 —		2.347 —		
3RD FLIGHT STAGE AT 1ST END THRUST DECAY, START COAST	140894. 310618.	78.174 0.68	3077.7	-1.50	0.0659 1.6094	-0.0004 -0.0111	0.206 0.206	0.12 0.12	13.164 13.164	0.031 0.031	2.346 2.346	0.031 0.031	
PRED	139813. 306029.	78.222 3079.6			0.0664 1.6268		0.205 —		13.161 —		2.343 —		
3RD FLIGHT STAGE AT 2ND START SEQ- UENCE COMMAND	139762. 338122.	78.185 0.68	3078.1	-1.48	0.0659 1.6094	-0.0004 -0.0111	0.205 0.205	0.02 0.02	13.137 13.137	0.021 0.021	2.341 2.341	0.021 0.021	

Table 16-10. Mass Characteristics Comparison (Continued)

EVENT	MASS	LONGITUDINAL		ROLL MOMENT		PITCH MOMENT		YAW MOMENT	
		C.G.	IX STA.1	C.G.	OF INERTIA	OF INERTIA	OF INERTIA	G/O	G/O
	KILO POUNDS	O/J DEV.	METERS INCHES	DEVI TETERS INCHES DELTA	KG-M2 INCHES MELIA	KG-M2 INCHES MELIA	KG-M2 INCHES MELIA	AJG-O DEV.	AJG-O DEV.
	13630.0		73.215		0.0466		0.205	13.100	13.096
	3060.0		3079.5		1.8234		-----	-----	-----
3RD FLIGHT STAGE AT 2ND IGNITION	PRED								
	13975.0		79.181	-0.037	0.0461	0.0034	-----	-----	-----
	30339.0	J.66	3079.3	-1.63	1.9117	-0.0171	0.205	13.143	13.137
	ACTUAL								
	136537.0		78.224		0.0466		0.205	13.056	13.093
	305643.0		3079.7		1.8259		-----	-----	-----
3RD FLIGHT STAGE AT 2ND MAIN STAGE	PRED								
	13549.0		79.186	-0.038	0.0461	0.0034	-----	-----	-----
	30762.0	J.06	3074.2	-1.55	1.9117	-0.0171	0.205	13.143	13.136
	ACTUAL								
	65475.0		86.051		0.0962		0.204	5.233	5.229
	144345.0		3087.8		3.7908		-----	-----	-----
3RD FLIGHT STAGE AT 2ND CUTOFF	PRED								
	65711.0		85.993	-0.058	0.0957	-0.0445	-----	-----	-----
	30635.5	-2.03	3085.1	2.03	3.7693	-0.3217	0.204	0.03	0.299
	SIGNAL								
	654968.0	0.36	3085.9		3.7787	0.204	0.03	0.302	0.313
	ACTUAL	144968.0							
	65438.0		86.062		0.0962		0.204	5.223	5.219
	144265.0		3088.2		3.8005		-----	-----	-----
3RD FLIGHT STAGE PRED									
	65664.0		86.304	-0.056	0.0959	-0.0445	-----	-----	-----
	3085.9	-2.02	3085.9	2.02	3.7787	-0.3217	0.204	0.03	0.299
	AT 2ND END OF STAGE								
	654764.0	0.35	3085.9		3.7787	0.204	0.03	0.302	0.313
	ACTUAL	144764.0							
	33561.0		79.202		0.0935		0.145	1.669	1.664
	73990.0		3118.2		3.6948		-----	-----	-----
CSM SEPARATED	PRED								
	33514.0		79.127	-0.075	0.0928	-0.0407	-----	-----	-----
	74548.0	0.75	3115.2	-2.96	3.6540	-0.3207	0.146	-0.63	1.693
	ACTUAL								
	63529.0		85.557		0.1156		-----	-----	-----
	140939.0		3368.3		4.5550		0.195	4.632	4.627
CSM DOCKED	PRED								
	64179.0		85.489	-0.067	0.1160	0.0303	-----	-----	-----
	141430.0	0.39	3165.7	-2.65	4.5702	0.3152	0.195	-0.60	4.693
	ACTUAL								
	16828.0		73.906		0.1653		0.111	0.605	0.602
	37130.0		2905.7		6.5386		-----	-----	-----
SPACECRAFT SEPARATED	PRED								
	17094.0		73.719	-0.086	0.1605	-0.3047	-----	-----	-----
	37646.0	1.58	2802.3	-3.43	6.3227	-0.1059	0.111	-0.62	0.636
	ACTUAL								

SECTION 17

LUNAR IMPACT

17.1 SUMMARY

The Apollo 17 S-IVB/IU lunar impact mission objectives were to impact the stage within 350 km of the target, determine the impact time within 1 second, and determine the impact point within 5 km. The first two objectives have been met. Further analysis is required to satisfy the third objective. Based on analysis to date, the S-IVB/IU impacted the moon December 10, 1972, 20:32:40.99 UT (313,180.99 seconds after range zero) at 4.33 degrees south latitude and 12.37 degrees west longitude. This location is 155 km (84 n miles) from the target of 7 degrees south latitude and 8 degrees west longitude.

The velocity of the S-IVB/IU at impact relative to the lunar surface was 2,544 m/s (8,346 ft/s). The incoming heading angle was 83.0 degrees west of north and the angle relative to the local vertical was 35.0 degrees. The total mass impacting the moon was approximately 13,931 kg (approximately 30,712 lbm).

Real-time targeting activities modified the planned first Auxiliary Propulsion System (APS) lunar impact burn attitude to reduce the burn duration. A second APS burn was performed to complete vehicle targeting.

17.2 TRANSLUNAR COAST MANEUVERS

Following Command and Service Module (CSM)/Launch Vehicle (LV) separation at 13,348 seconds (3:42:28); the CSM was docked with the Lunar Module (LM) at 14,231 seconds (3:57:11). The CSM/LM was then ejected from the S-IVB/IU at 17,102 seconds (4:45:02). After CSM/LM ejection, the S-IVB/IU was maneuvered to the inertially-fixed attitude required for the APS evasive burn. Timebase 8 was initiated as planned at 18,180 seconds (5:03:00). The APS ullage engines were ignited 1 second later and burned for 80 seconds. Table 17-1 shows that the actual evasive velocity change was close to nominal.

Following the maneuver to the Continuous Vent System (CVS) and LOX dump attitude, the initial lunar targeting velocity changes were accomplished by a 300-second CVS vent starting 1,000 seconds after T_g and a 48-second LOX dump starting 1,280 seconds after T_g. Table 17-1 shows that the CVS vent and LOX dump were near nominal.

The Lunar Impact Team (LIT) at the Huntsville Operation Support Center (HOSC) decided in real-time to shorten the first APS lunar impact burn (APS-1) duration by selecting a more efficient attitude. This change

Table 17-1. Translunar Coast Maneuvers

PARAMETER	ACTUAL	NOMINAL	ACT-NOM
TIMEBASE 8 INITIATION			
UT Time 7 Dec., hr:min:sec	10:36:00	10:36:00	0
Range Time, hr:min:sec (sec)	5:03:00 (18,180)	5:03:00 (18,180)	(0)
APS EVASIVE BURN			
Initiation, sec from T ₈	1	1	0
Duration, sec	80	80	0
Velocity Increment, m/s (ft/s)	2.90 (9.51)	3.01 (9.88)	-0.11 (-0.37)
Pitch Attitude*, deg, inertial	-101.95	-104.93	2.98
Yaw Attitude*, deg, inertial	-38.42	-40.00	1.28
CVS VENT			
Initiation, sec from T ₈	1,000	1,000	0
Duration, sec	300	300	0
Velocity Increment, m/s (ft/s)	0.49 (1.61)	0.40 (1.31)	0.09 (0.30)
Pitch Attitude*, deg, inertial	-98.65	-95.87	-2.78
Yaw Attitude*, deg, inertial	-17.87	-18.62	0.75
LOX DUMP			
Initiation, sec from T ₈	1,200	1,200	0
Duration, sec	48	48	0
Velocity Increment, m/s (ft/s)	9.10 (29.06)	9.21 (30.22)	-0.11 (-0.36)
Pitch Attitude*, deg, inertial	-94.01	-96.25	2.24
Yaw Attitude*, deg, inertial	-16.60	-18.62	2.02
APS FIRST LUNAR IMPACT BURN			
Initiation, sec from T ₈	4,020	4,020	0
Duration, sec	98	98	0
Velocity Increment, m/s (ft/s)	4.07 (13.35)	4.02 (13.19)	0.05 (0.16)
Pitch Attitude*, deg, inertial	-41.71	-43.75	2.04
Yaw Attitude*, deg, inertial	-20.14	-22.66	2.51
APS SECOND LUNAR IMPACT BURN			
Initiation, sec from T ₈	22,320	22,320	0
Duration, sec	102	102	0
Velocity Increment, m/s (ft/s)	4.29 (14.07)	4.30 (14.11)	-0.01 (0.04)
Pitch Attitude*, deg, inertial	176.21	175.10	1.11
Yaw Attitude*, deg, inertial	-9.11	-10.88	1.77

*Attitudes are the velocity increment direction.

NOTE: Nominals are preflight predicted except that the nominals for both APS lunar impact burns were determined by the LIT in real-time.

conserved propellant for a second APS lunar targeting burn. The commands for this maneuver were sent from the Mission Control Center at Houston (MCC-H) by the Booster Systems Engineer (BSE) to the S-IVB/IU. The actual APS-1 occurred as planned 4,020 seconds after T_g and was close to the (real-time) nominal. The nominal values for APS-1 shown in Figure 17-1 were selected in real-time and differ from the preflight nominals of 190 seconds burn time, 8.13 m/s (26.67 ft/s) velocity change, -101.75 degrees inertial pitch, and -18.55 degrees inertial yaw.

Following the APS-1 burn, an attitude maneuver was accomplished to prevent excessive solar heating of the IU while the Thermal Control System (TCS) water valve operation was inhibited. Although the IU's thermal control system water valve was closed prior to APS-1 to minimize non-gravitational perturbations, MCC-H reported difficulty in the post APS-1 orbit determination due to venting disturbances. Therefore, the planned contingency delay of 1 hour for targeting the second APS impact burn (APS-2) was incorporated.

Upon completion of the post APS-1 orbit determination, MCC-H reported the S-IVB/IU would impact the moon at 9.64 degrees south latitude and 15.29 degrees east longitude, 678 +300 km from the target. The LIT decided an APS-2 burn was required and selected the nominal conditions shown in Table 17-1. At 22,320 seconds after T_g, the APS-2 maneuver was performed. The actual maneuver as shown in Table 17-1 was close to nominal. After APS-2, the three-axis passive thermal control (PTC) maneuver was initiated at 41,503 seconds (11:31:43) range time and the flight control computer was turned off.

Figure 17-1 presents line-of-sight range rate residuals from the Ascension Unified S-Band (USB) tracking station and depicts graphically the major S-IVB/IU velocity changes and the PTC tumbling. Residuals are obtained by differencing observed range-rate data with calculated range-rate data (observed minus calculated). The calculated range-rate data are developed from a sophisticated orbital model which is statistically fitted to portions of the observed data. Figure 17-2 verifies the reconstruction of the maneuvers presented in Table 17-1 by showing the residuals resulting from the same Ascension tracking data but with the reconstructed maneuvers modeled. However, the low-level perturbations occurring during this time period and discussed in Section 17.3 are not included in the preliminary model shown in Figure 17-2.

17.3 TRAJECTORY PERTURBATIONS

17.3.1 Introduction

Postflight analyses on recent Apollo/Saturn missions have shown small non-gravitational acceleration effects in the S-IVB/IU translunar trajectory. Such accelerations have been expected since both S-IVB and the IU stage systems vent during normal operation. These small vehicle accelerations were of no concern until AS-508 when Lunar impact became a mission objective. Since the accuracy of the S-IVB/IU's tracking data allows the determination

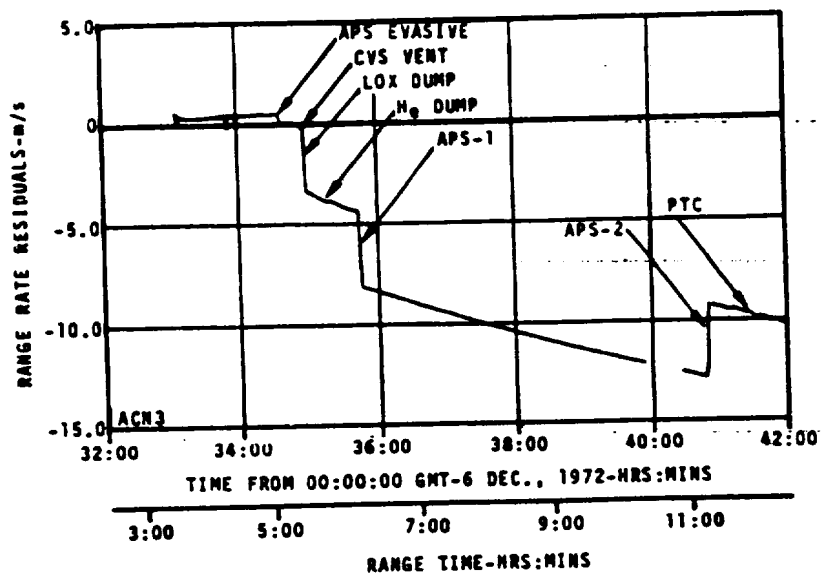


Figure 17-1. Translunar Coast Maneuvers Overview

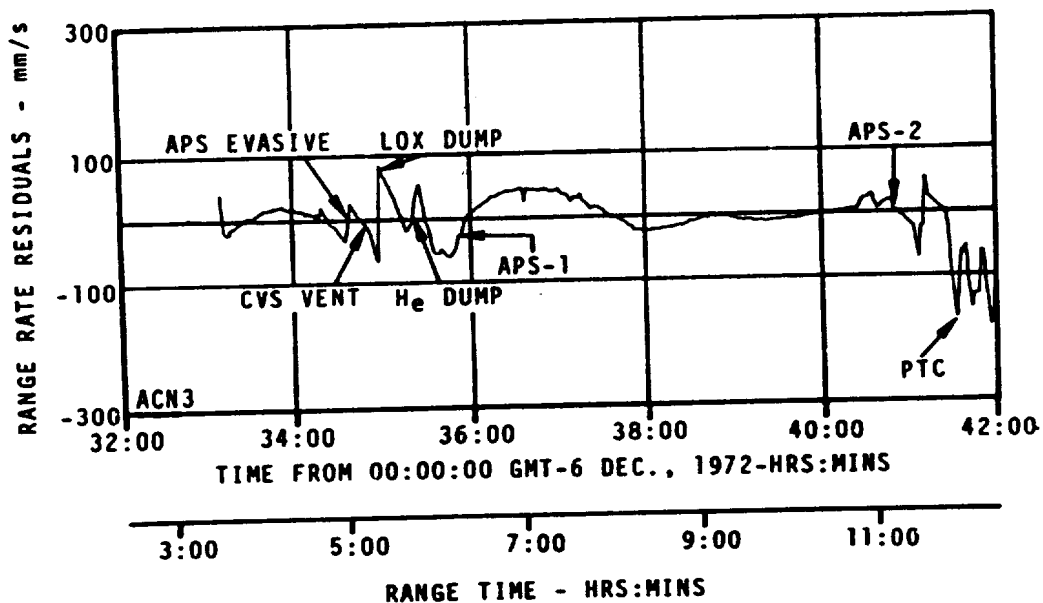


Figure 17-2. Modeled Translunar Coast Maneuvers

of these accelerations, attempts have been made to improve lunar impact targeting operations and impact location determinations. Also, attempts to identify the causes of these trajectory perturbations have been made. The identified causes, although incomplete, are reported herein since this is the last flight with a lunar impact objective.

17.3.2 Trajectory Effects

AS-508 range rate tracking data showed a shift at .70,150 sec (19:29:10) that was interpreted as a velocity decrease of 2 to 3 m/s during a 60 second period. The velocity change, fortunately, moved the predicted lunar impact point approximately 5 degrees in latitude or 150 km closer to the target.

AS-509 used a Passive Thermal Control (PTC) maneuver to average solar heating rates and translational velocity changes due to non-gravitational forces acting on the vehicle. The PTC maneuver was initiated by ground command and established vehicle pitch and yaw rates of 0.3 deg/s. The Flight Control Computer was then inhibited leaving the S-IVB/IU in a "Barbecue" or tumble mode until lunar impact.

No translational velocity perturbations following PTC were identified on this flight.

AS-510 range rate residuals give evidence of a significant velocity change following LOX dump. In addition, the data shows that velocity changes due to non-gravitational forces occurred in six steps between 25,200 and 36,001 seconds (period between APS-1 and APS-2 burns). The changes slowed the S-IVB/IU and perturbed the lunar impact point to the east. The velocity steps also caused difficulty in obtaining an accurate state vector on which to base the APS-2 burn. Following the APS-2 burn and "roll-only" PTC maneuvers, a small unbalanced force perturbed the early period of the post APS-2 trajectory. This perturbation increased the velocity of the S-IVB/IU and perturbed the lunar impact trajectory to the west. The vehicle tumble frequency increased about 50% following APS-2 until lunar impact (approximately 69.5 hours). The complexity of the angular motion also increased.

AS-511 did not perform an APS-2 burn because of suspected early depletion of the APS Helium supply. Therefore, a 3-axis PTC maneuver was performed at 21,306 sec (approximately 6 hours) and the FCC was turned off. The PTC tumble rate started at approximately 5.2 cycles per hour (cpch) and increased 100% in approximately 10 hours. During the next 10 hours the tumble rate gradually decreased by 10%.

AS-512 postflight analysis has shown that non-gravitational accelerations were acting over part of the trajectory from translunar injection (TLI) to impact. From TLI to PTC initiation these perturbations produced accelerations on the order of 0.1 mm/s^2 . After the PTC three-axis tumble was initiated, trajectory perturbing accelerations on the

order of 0.04 mm/s^2 continued to act for at least 18 hours. Figure 17-3 shows range-rate residuals produced by fitting a gravity only trajectory to the last 46 hours of tracking data. The deviations in residuals at the beginning of this time span indicate that non-gravitational accelerations acted on the S-IVB/IU.

The residuals in Figure 17-4 show the results of incorporating a preliminary model of a small constant non-gravitational acceleration acting after APS-2. The improvement in the residuals confirms the presence of perturbing influences acting on the vehicle. The observation of the effects of perturbing influences confirm real-time reports from MCC-H. The actual magnitude, direction, and duration of these perturbing accelerations have not been determined.

17.3.3 Perturbing Mechanisms

The velocity change observed on AS-508 at 70,150 sec correlates with loss of attitude control inputs to the APS system and resulting unplanned APS firing in pitch, yaw, and roll. This loss of attitude control resulted from the 6D10 battery, which supplies power to the Launch Vehicle Digital Computer (LVDC), depleting at 68,948 seconds. It is quite possible that the full-on yaw/roll APS control engines provided the translational velocity change seen in the trajectory data. Therefore, all subsequent flights were planned to incorporate (1) a passive thermal control (PTC) maneuver after the APS-2 lunar impact burn in an effort to average out thrust disturbances and (2) turn off the Flight Control Computer (FCC) after PTC to eliminate unplanned APS activities.

The PTC maneuver was performed on AS-509 as planned and the FCC turned off. The high tumble rate resulting from the PTC maneuver modulated the range rate tracking data and caused difficulty in determining the lunar impact point. No trajectory perturbations following the PTC maneuver were identified on this flight.

On the AS-510 flight a velocity change following LOX dump correlates with the inadvertent ambient helium dump through the J-2 engine. The velocity steps that occurred on AS-510 between APS-1 and APS-2 burns correlate with the times of the IU TCS sublimator cycling and the subsequent APS reaction firings to maintain the vehicle attitude. In addition to shifting the projected lunar impact point, these velocity steps caused difficulty in obtaining an accurate state vector on which to base the APS-2 burn. Following the APS-2 burn at 36,001 seconds the S-IVB/IU stage performed a "roll-only" PTC maneuver and the FCC was turned off. Since the IU TCS sublimator continues operation for several thousand seconds after APS-2 it probably accounts in part for the small non-gravitational force that perturbed the early portion of the post APS-2 trajectory. Also, the venting of the IU's gas bearing system for several thousand seconds after APS-2 may account for part of the perturbing

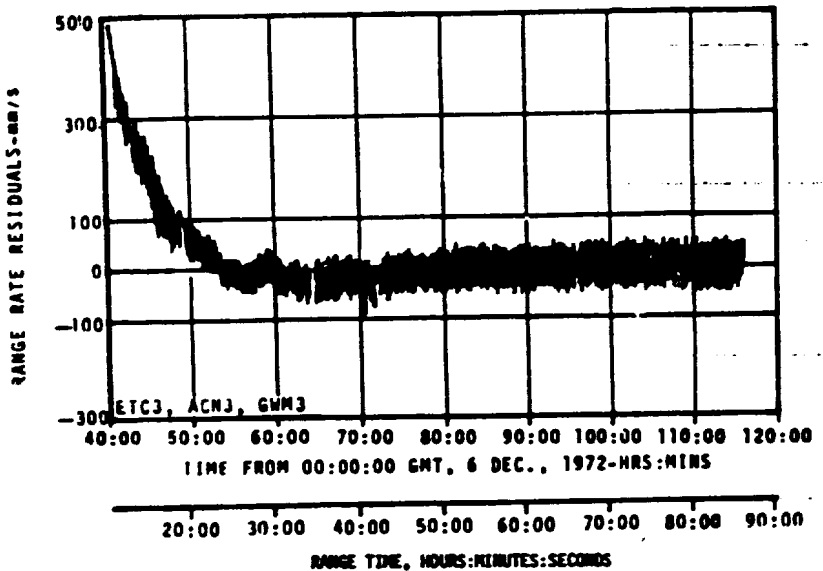


Figure 17-3. Gravity-Only Lunar Impact Trajectory Residuals

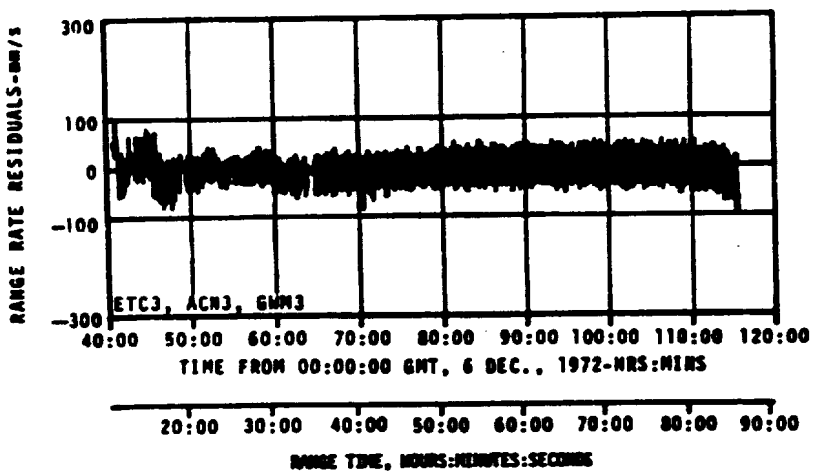


Figure 17-4. Lunar Impact Trajectory Residuals with Perturbing Influences Modeled

force. Since the APS system no longer maintains attitude control, these forces would also produce an unbalanced moment which would perturb and greatly complicate the roll motion.

The doubling of the tumble rate seen on AS-511 during the early post APS burn period correlates with the period of relief venting from the AF, Module No. 2. This venting continued until the APS He supply bottle pressure depleted to the lock-up pressure of the relief valve at a calculated range time of 15 to 16 hours.

The AS-512 accelerations during the period from translunar injection to PTC initiation were on the order of 0.1 mm/s^2 . Since the IU TCS sublimator water valve was turned off during this period, these perturbations may in part be due to the IU gas bearing system venting and associated APS attitude control firings. Calculations yield approximately 0.02 mm/s^2 theoretical acceleration from this source.

After the AS-512 APS-2 burn was completed, trajectory perturbing accelerations discussed previously continued to act for at least 18 hours. The preliminary model of this acceleration was obtained by letting the Lunar Impact Determination program solve for an average acceleration over this 18-hour period. The preliminary model gave an average acceleration of 0.04 mm/s^2 , resulting in a possible 2.8 m/s post APS-2 total velocity change. The observation of the post APS-2 effects of perturbing influences confirm real-time reports from MCC-H. The actual magnitude, direction, and duration of these perturbing accelerations have not been determined.

Since the TCS water valve is commanded on after APS-2, possible AS-512 post APS-2 perturbation sources may be the IU's sublimator venting as well as the gas bearing system. Considerable subliming should take place to dissipate the increased system temperatures.

Eventually, the battery voltage should decrease, the water valve stay open and continuous subliming take place until the coolant pump ceases to circulate fluid. Therefore, the sublimator should have a limited lifetime and, coupled with limited gas bearing subsystem venting, may cause the observed perturbations for the time period shown.

A small additional vent of 0.09 N due to the S-IVB LOX chilldown pump purge has been identified. This purge force is expected to act continuously until lunar impact and therefore, does not correlate with the 18-hour perturbation period identified in Figure 17-3.

17.3.4 Tentative Conclusions

Onboard gaseous venting sources have been identified that account in part for observed perturbations of the S-IVB/IU stage's translunar trajectory. These sources are the IU TCS sublimator water vapor and the stable platform gas bearing system GN_2 venting. However, the IU TCS sublimator was not a venting source on AS-511 or on the early part of Translunar Coast (TLC) on AS-512. Due to a leak in the TCS GN_2 storage sphere,

AS-511 lost sublimator water pressure at about 18,000 seconds effective for the remainder of the lunar trajectory. On AS-512 the sublimator water valve was turned off in the period from the APS-1 burn to the APS-2 burn in order to eliminate the sublimator as a venting source.

After the PTC maneuver the FCC is turned off thereby deactivating the APS. However, tracking data show that the stage is still subject to low order translational perturbations and to changes in the stage tumble rate. The result of the translational perturbations is to shift the final impact point on the lunar surface. Further study would be necessary to show correlation of the observed perturbations with the known disturbing forces. However, analysis has shown that a fixed thrust aligned with the vehicle longitudinal centerline will result in a net translational movement, even though the vehicle is in a three axis tumble mode. Therefore, it is possible for the observed vehicle perturbations to be caused by the type of venting sources that have been identified on the S-IVB/IU stage to date.

17.4 TRAJECTORY EVALUATION

Table 17-2 presents the actual and nominal geocentric orbital parameters of the S-IVB/IU trajectory at 17:03:00, December 7, 1972, (soon after the APS-2 burn). The orbital elements are osculating and expressed in the true-of-date epoch.

Table 17-2. Trajectory Parameters After APS-2 Burn

PARAMETER	ACTUAL	NOMINAL	ACT-NOM
Inclination, deg	28.424	28.512	-0.088
Argument of Perifocus, deg	154.915	154.981	-0.066
Right Ascension of Node, deg	-15.551	-15.764	0.213
Semi-major Axis, km	218,497	218,978	-481
Eccentricity	0.970396	0.970648	-0.000152
True Anomaly, deg	154.730	154.771	-0.041

Figure 17-5 presents range-rate residuals showing the first 24 hours of PTC tumble. This plot was made continuous by combining residual plots from four range-rate trackers (Madrid USB, Goldstone DSN, Tidbinbilla DSN, and Bermuda USB). The initial tumble rate of 5.2 cph (0.52 degrees per second) is close to the commanded pitch, yaw, and roll rates. Following PTC, a 14- to 16-hour period occurs during which the tumble changes from a "three-axis" rotation to a "spin/precession" rotation.

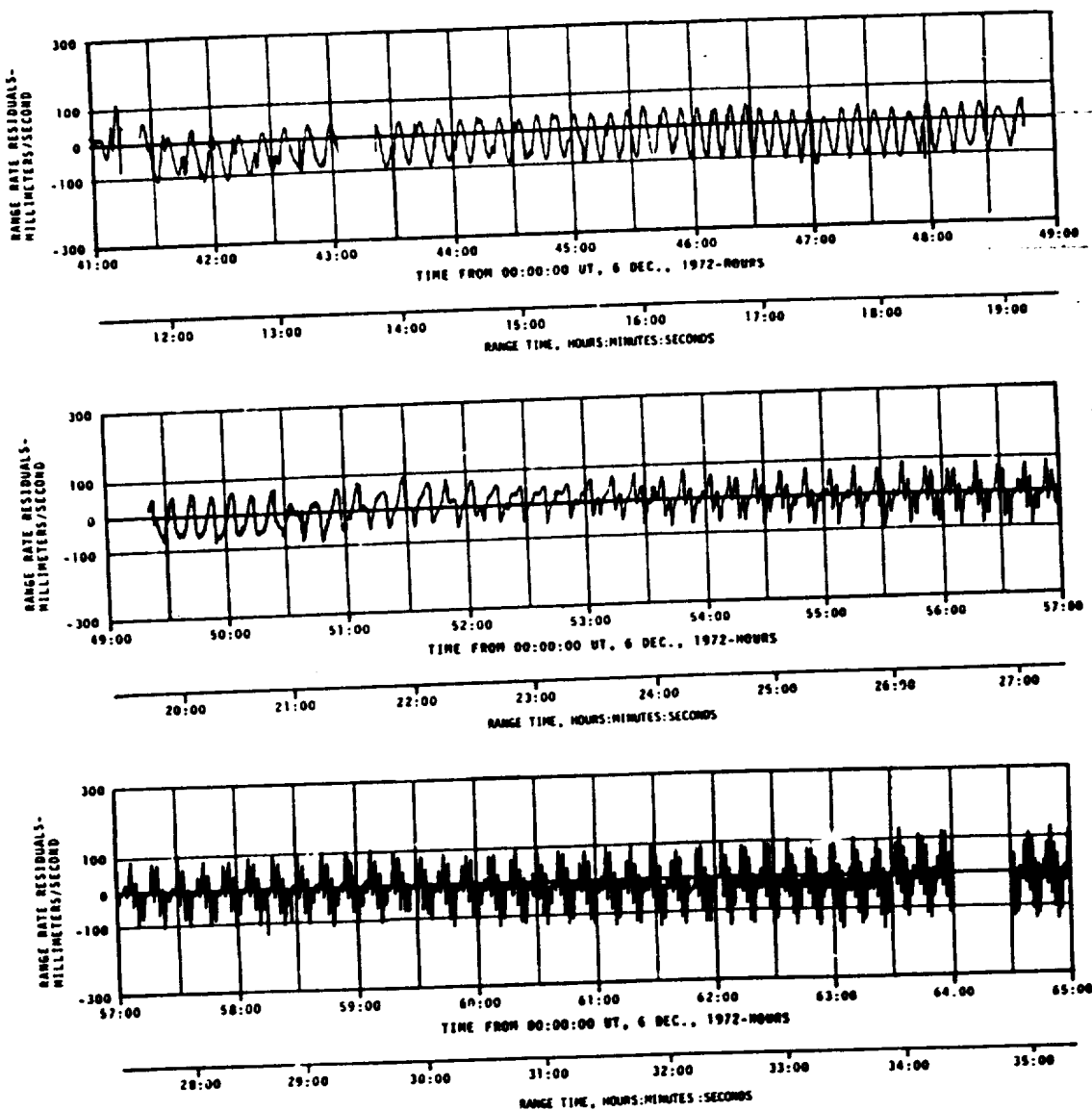


Figure 17-5. Early PTC Tumble Residuals

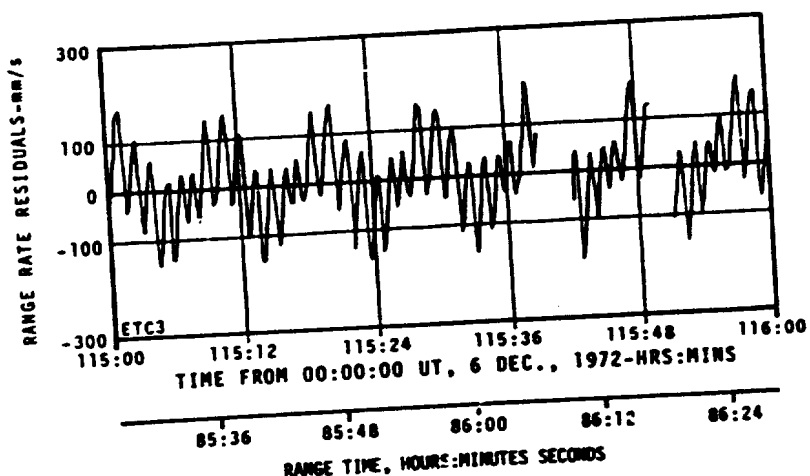
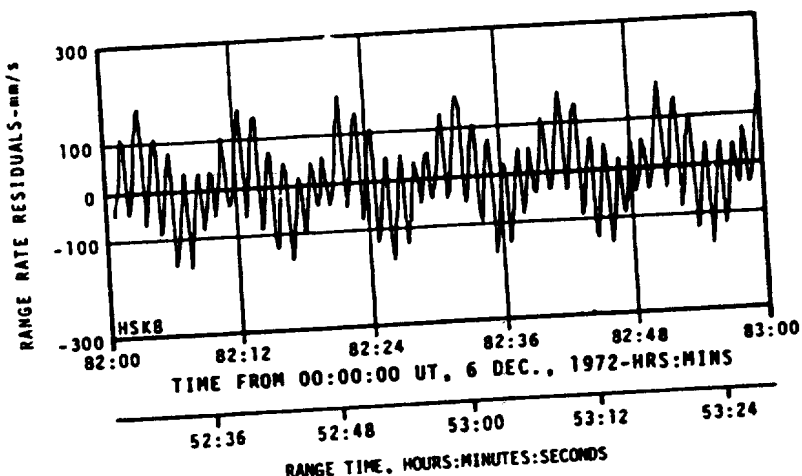
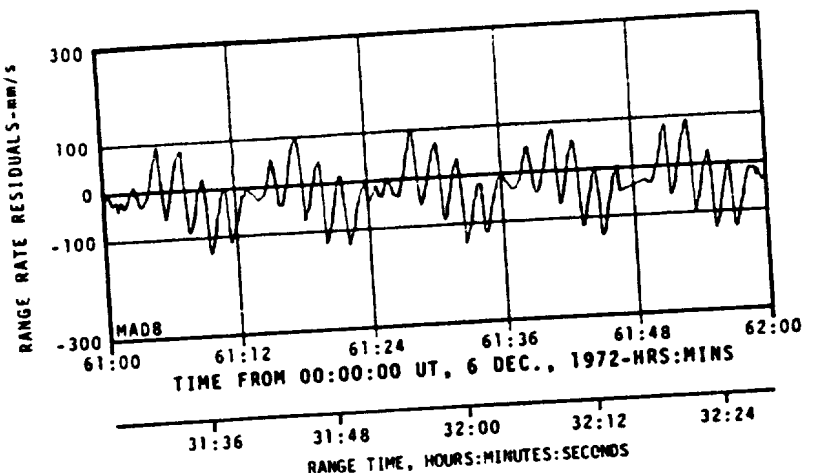


Figure 17-6. Late PTC Tumble Residuals

Table 17-3. Lunar Impact Conditions

PARAMETER AT IMPACT	ACTUAL	NOMINAL	ACT-NOM
Stage Mass, kg (lbm)	~13,931 (~30,712)	13,931 (30,712)	~0 (0)
Velocity Relative to Surface, m/s (ft/s)	2,544 (8,346)	2,545 (8,350)	-1 (-4)
Impact Angle Measured from Vertical, deg	35.0	37.8	-2.8
Incoming Heading Angle Measured from North to West, deg	83.0	82.0	1.0
Selenographic Latitude, deg	-4.33	-7.00	2.67
Selenographic Longitude, deg	-12.37	-8.00	-4.37
Impact Time, UT 10 Dec.	20:32:40.99	20:15:49.35	00:16:52.64
Distance to Target, km (n mi)	155 (84)	0 (0)	155 (84)
Distance to Apollo 12 Seismometer, km (n mi)	337 (182)	481 (260)	-144 (-78)
Distance to Apollo 14 Seismometer, km (n mi)	156 (84)	303 (164)	-147 (-80)
Distance to Apollo 15 Seismometer, km (n mi)	1,035 (559)	1,060 (572)	-25 (-13)
Distance to Apollo 16 Seismometer, km (n mi)	851 (460)	709 (383)	142 (77)

Figure 17-6 shows Madrid USB, Canberra USB, and Greenbelt USB range-rate residuals 20 hours, 41 hours, and 74 hours after PTC initiation, respectively. At 20 hours after PTC initiation, the S-IVB/IU had a spin rate around the longitudinal axis of 14.5 cph (1.45 degrees per second) and a precession rate of 5 cph (0.5 degree per second). During the next 55.5 hours to impact, the nature of the tumble changed little. The spin rate increased to 21 cph (2.1 degrees per second) and the precession rate increased to 6.5 cph (0.65 degrees per second).

17.5 IMPACT CONDITIONS

Figure 17-7 presents the lunar landmarks of scientific interest relative to the S-IVB/IU impact. Analysis to date indicates the S-IVB/IU impacted the moon at 4.33 degrees south latitude and 12.37 degrees west longitude at 20:32:40.99 UT on December 10, 1972, (313,180.99 seconds range time). Impact conditions and miss distances are presented in Table 17-3. The distance from the impact to the target is 155 km (84 n miles) which is within the 350-kilometer mission objective. The distance to Apollo 12 seismometer is 337 km (182 n miles); the distance to the Apollo 14 seismometer is 156 km (84 n miles); the distance to the Apollo 15 seismometer is 1,035 km (559 n miles); and the distance to the Apollo 16 seismometer is 851 km (460 n miles). The impact time presented in Table 17-3 is derived from the loss of signal times shown in Table 17-4 and has an accuracy one order of magnitude smaller than the mission objective of 1 second.

17.6 TRACKING DATA

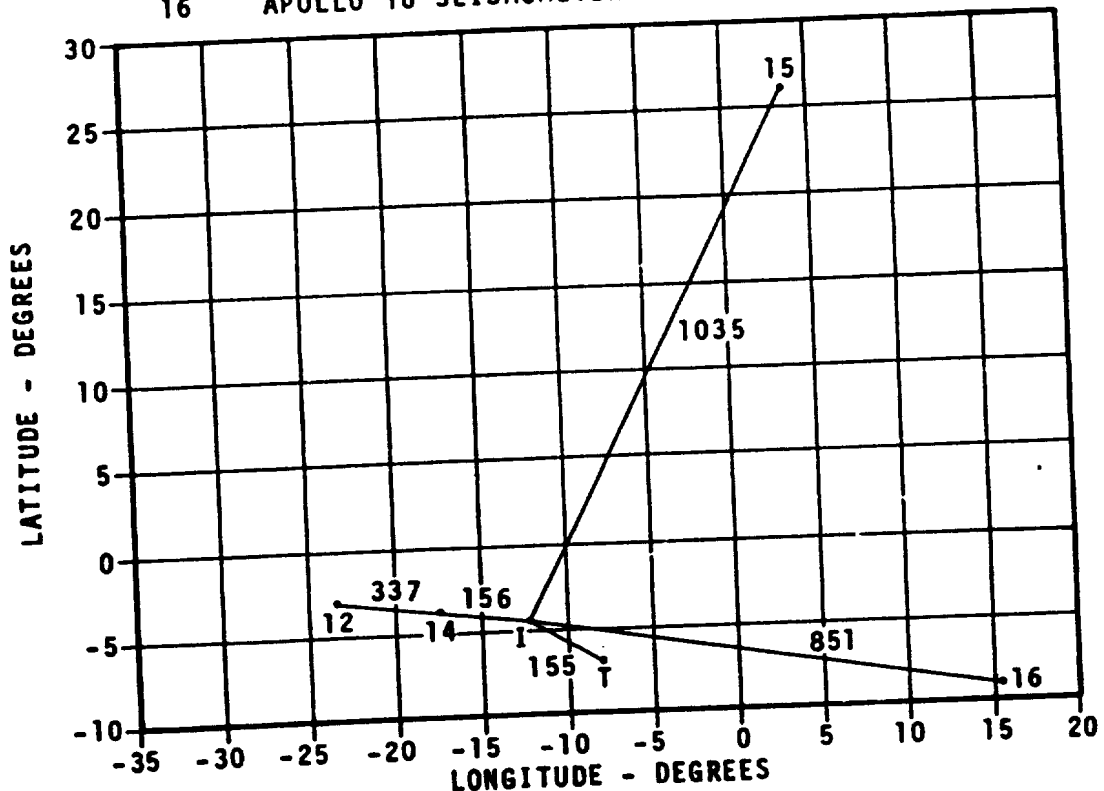
Figure 17-8 shows the tracking data available for the trajectory determination. Good quality C-band and S-band data were received over nearly 87 hours of flight to lunar impact. Table 17-5 shows the tracking site locations and configurations.

Table 17-4. Lunar Impact Times

TRACKING STATION	RECORDED TIME ON DECEMBER 10, 1972 (UT-HR:MIN:SEC)	LIGHT TIME DELAY (SEC)	CORRECTED TIME ON DECEMBER 10, 1972 (UT-HR:MIN:SEC)
Herritt Island	20:32:42.28	1.297	20:32:40.98
Madrid	42.30	1.300	41.00
Goldstone	42.30	1.307	40.99
Bermuda	42.25	1.296	40.95
Ascension	42.30	1.290	41.01
Range Time, sec	313,180.99	Average	20:32:40.99

APOLLO 17 LUNAR LANDMARKS

POINT	DESCRIPTION	LAT-DEG	LONG-DEG
I	IMPACT (TRACKING)	-4.33	-12.37
T	TARGET	-7.00	-8.00
12	APOLLO 12 SEISMOMETER	-3.04	-23.42
14	APOLLO 14 SEISMOMETER	-3.67	-17.47
15	APOLLO 15 SEISMOMETER	26.07	3.65
16	APOLLO 16 SEISMOMETER	-8.97	15.51



NOTE: DISTANCES FROM IMPACT POINT IN KILOMETERS

Figure 17-7. Lunar Landmarks

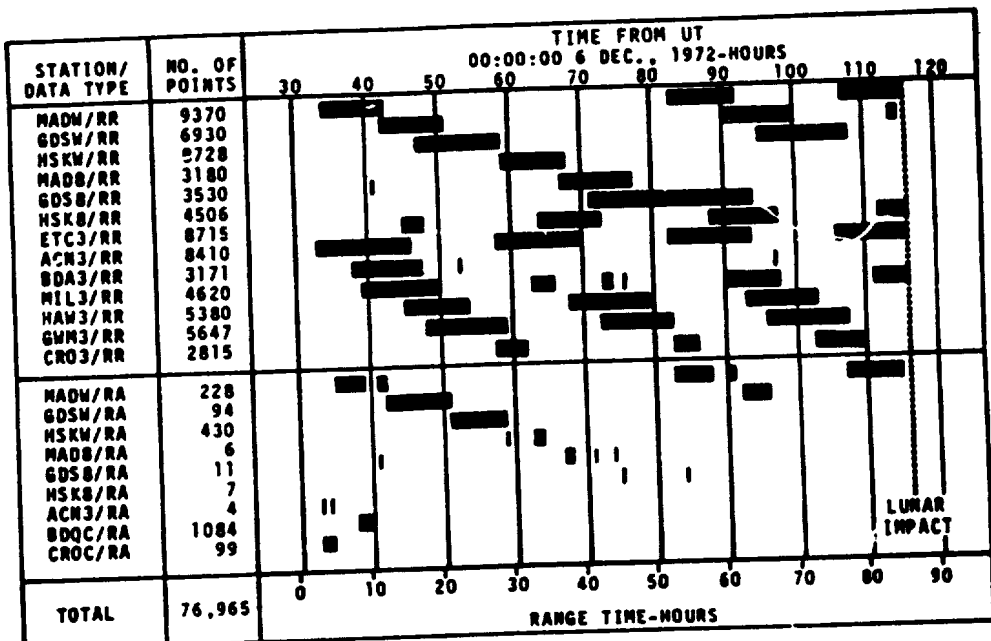


Figure 17-8. Tracking Data Availability

Table 17-5. S-IVB/IU Tracking Stations

STATION LOCATION	CONFIGURATION	ABBREVIATION
Madrid, Spain	DSN 85' S-Band	MADW
Madrid, Spain	STDN 85' S-Band	MADB
Ascension Island	STDN 30' S-Band	ACN3
Bermuda Island	STDN 30' S-Band	BDA3
Merritt Island, Florida	STDN 30' S-Band	MIL3
Greenbelt, Maryland	STDN 30' S-Band	ETC3
Goldstone, California	DSN 85' S-Band	GDSW
Goldstone, California	STDN 85' S-Band	GDSB
Kauai, Hawaii	STDN 30' S-Band	HAW3
Guam Island	STDN 30' S-Band	GWM3
Carnarvon, Australia	STDN 30' S-Band	CRO3
Tidbinbilla, Australia	DSN 85' S-Band	HSKW
Canberra, Australia	STDN 85' S-Band	HSKB
Bermuda Island	FPQ-6 C-Band	BDOC
Carnarvon, Australia	FPQ-6 C-Band	CROG

SECTION 18

SPACECRAFT SUMMARY

Apollo 17 was launched at 00:33:00 EST on December 7, 1972, from Complex 39A at the Kennedy Space Center. The spacecraft was manned by Captain Eugene A. Cernan, Commander; Commander Ronald E. Evans, Command Module Pilot; and Dr. Harrison H. Schmitt, Lunar Module Pilot. The launch was delayed 2 hours and 40 minutes because of a failure in the launch vehicle ground support equipment automatic sequencing circuitry.

The spacecraft/S-IVB/IU combination was inserted into an earth parking orbit of 90.3 miles by 90.0 miles for systems checkout and preparation for the translunar injection maneuver. In accordance with pre-flight targeting objectives, the translunar injection maneuver shortened the translunar coast period by 2 hours and 40 minutes to compensate for the launch delay so that the lunar landing could be made with the same lighting conditions as originally planned. After spacecraft separation, transposition, docking, and lunar module ejection, the evasive maneuver was performed and the S-IVB/IU was subsequently targeted for lunar impact. The S-IVB/IU impacted the lunar surface about 84 miles from the preplanned point, and the impact was recorded by the Apollo 12, 14, 15, and 16 lunar surface seismometers.

One spacecraft midcourse correction of 10.5 ft/sec was performed during the translunar coast phase to achieve the desired altitude of closest approach to the lunar surface. The crew performed a heat flow and convection demonstration and an Apollo light flash investigation during the translunar coast period. Also, the crew transferred to the lunar module twice and found all systems to be operating properly.

The scientific instrument module door was jettisoned about 4 1/2 hours prior to lunar orbit insertion. The docked spacecraft was inserted into a 170-by-52.6-mile lunar orbit following a service propulsion firing of 393 seconds. The first descent orbit insertion maneuver at 90 1/2 hours lowered the spacecraft orbit to 59 by 14.5 miles.

The crew entered the lunar module at 105 1/4 hours to prepare for descent to the lunar surface. After powering up the lunar module and undocking, the second lunar module descent orbit insertion maneuver was performed using the lunar module reaction control system to adjust the orbital conditions. The powered descent proceeded normally and the spacecraft was landed within 200 meters of the preferred landing point at 110:21:57. About 120 seconds of hover time remained at touchdown. The best estimate of the landing point is 30 degrees 45 minutes 25.9 seconds east longitude and 20 degrees 9 minutes 41 seconds north latitude on the 1:25,000-scale Lunar Topographic Photomap of

Taurus Littrow, First Edition, September, 1972.

The first extravehicular activity began at 114:22 (HR:MIN). Lunar Roving Vehicle (LRV) offloading and equipment unstowage proceeded normally, and television coverage was initiated about 1 1/4 hours into the extravehicular activity. The lunar surface experiment package was deployed approximately 185 meters northwest of the lunar module. Prior to leaving the LM site, the right rear fender extension was accidentally broken off and emergency repairs were made. The lunar surface experiment package deployment, deep core drilling, and neutron probe emplacement were accomplished. Two geologic units were sampled, two seismic explosive packages were deployed and seven traverse gravimeter measurements were taken during the traverse. The samples collected weighed about 25 pounds.

The second extravehicular activity began at 137:55. The traverse was conducted with real-time modifications to station stop times because of geologic interests. At station 4, the crew discovered the first evidence of possible volcanic activity on the lunar surface in the form of orange soil. Five surface samples and a double core sample were taken at this site. Three seismic explosive packages were deployed, seven traverse gravimeter measurements were taken, and all observations were documented photographically. The time of the second extravehicular activity was 7 hours 37 minutes with 77 pounds of samples gathered.

The third extravehicular activity began at 160:53. Specific sampling objectives were accomplished at stations 6 and 7 among some 3 to 4 m boulders. Again, seven traverse gravimeter measurements were made. The surface electrical properties experiment was terminated because the receiver temperature was approaching the point of affecting the data tape; therefore, the tape was removed at Station 9.

The crew entered and repressurized the spacecraft after 7 hours and 15 minutes of lunar surface activity. Samples amounting to about 155 pounds were obtained on the third extravehicular activity for a grand total of 257 pounds for the mission. The total distance traveled with the LRV during the three extravehicular activities was about 36 kilometers.

In addition to the panoramic camera, the mapping camera, and the laser altimeter carried on previous missions, three new scientific instrument module experiments rounded out the Apollo 17 complement of orbital science equipment. An ultraviolet spectrometer measured lunar atmospheric density and composition, an infrared radiometer mapped the thermal characteristics of the moon, and a lunar sounder acquired data

on subsurface structure.

Lunar ascent was initiated at 185:21:37 and was followed by a normal rendezvous and docking. After transferring samples and equipment from the ascent stage to the command module, the ascent stage was jettisoned for the deorbit firing and lunar impact. The preliminary coordinates of the ascent stage impact were 19.99 degrees north and 30.51 degrees east, about 0.7 mile from the planned target.

Transearth injection was initiated at about 234 hours with a service propulsion system firing of 144.9 seconds. A 1 hour and 6 minute transearth extravehicular activity was conducted by the Command Module Pilot. The film cassettes were retrieved from the scientific instrument module cameras and lunar sounder and the scientific equipment bay was visually inspected.

Entry and landing were normal. The spacecraft landed at 0 degrees 43 minutes 12 seconds south latitude and 156 degrees 12 minutes 36 seconds west longitude, as determined by the onboard computer. Total time for the Apollo 17 mission was 301 hours, 51 minutes, and 59 seconds.

SECTION 19

MSFC INFLIGHT DEMONSTRATION

19.1 SUMMARY

A Heat Flow and Convection Demonstration was performed during Apollo 17 translunar coast. The data obtained apparently were satisfactory although analysis is in progress. There were no reported problems with the experimental apparatus.

19.2 HEAT FLOW AND CONVECTION DEMONSTRATION

A Heat Flow and Convection Demonstration, similar to the one on Apollo 14, was performed on Apollo 17 translunar coast. The three related experiments comprising the demonstration were convection in a liquid caused by surface tension gradients, heat flow and convection in a confined gas at low g force (approximately 10^{-9} g due to Command Service Module drift in roll), and heat flow and convection in a confined liquid at low g force. The purpose of these experiments was to determine the type and magnitude of fluid convection encountered in a near weightless environment. Although normal convection is suppressed at near weightlessness, some fluid flow will occur due to acceleration impulses, surface tension gradients, and expansion.

The information obtained from this demonstration will provide some of the data required to evaluate space manufacturing processes and other future space applications. The thermal behavior of fluids is a vital part of manufacturing processes involving liquid separation, precipitation, solidification, etc.

The experimental apparatus consisted of a package with three test configurations, each of a particular geometry and each containing a specially chosen fluid. Data was recorded by a 16 mm camera which was attached to the package.

19.2.1 Flow Pattern Experiment

The purpose of the Flow Pattern Experiment was to investigate convection in a liquid caused by surface tension gradients. The surface tension gradients are generated by heating a thin layer of liquid with a free surface. These surface tension gradients generate a cellular circulation pattern known as Bénard cells.

The experimental apparatus consisted of an open dish containing liquid Krytox oil that was uniformly heated from the bottom. The oil contained suspended aluminum flakes to permit direct observation of flow patterns. The cover of the dish was opened during the actual experiments to expose the free surface of the liquid to the spacecraft atmosphere.

Runs were made with liquid depths of two and four millimeters. In the two millimeter run, convection was evident within a few seconds after initiation of heating as compared to five minutes in an earth environment. Bénard cells were formed, but were less orderly and symmetrical than earth environment patterns. Steady state was reached in about seven minutes.

In the four-millimeter run, the Bénard cells were more regular and larger than in the two-millimeter run. Steady state had not been reached at the conclusion of the 10 minute heating period.

19.2.2 Radial Heat Flow Experiment

The purpose of this experiment was to investigate heat flow and convection in a gas at low gravity conditions.

The experimental apparatus consisted of a centrally heated closed cylinder filled with argon gas. Liquid crystal temperature sensing strips were located to measure gas temperature changes radially from the heater. These strips change color in response to temperature changes and the color changes are recorded on 16 mm color film.

The experiment was conducted as planned. The operation of all equipment and the data obtained were apparently satisfactory. Computer analyses are currently being made to evaluate the scientific performance of the experiment.

19.2.3 Lineal Heat Flow Experiment

This experiment was similar to the gas experiment described in 19.2.2, except that the fluid medium was Krytox oil and the cylinder length-to-diameter ratio was greater so that lengthwise heating was measured. Equipment operation and data obtained were apparently satisfactory. However, the results of computer analyses of the data are in progress.

SECTION 20

LUNAR ROVING VEHICLE

20.1 SUMMARY

The Lunar Roving Vehicle (LRV) satisfactorily supported the Apollo 17 Taurus-Littrow lunar surface exploration objectives. The total odometer distance traveled during the three Extra Vehicular Activities (EVA's) was 35.7 kilometers at an average velocity of 7.75 km/hr on traverses. The maximum velocity attained was 18.0 km/hr and the maximum slopes negotiated were 18 degrees up and 20 degrees down. The average LRV energy consumption rate was 1.64 amp-hours/km with a total consumed energy of 73.4 amp-hours [including 14.8 amp-hours used by Lunar Communication Relay Unit (LCRU)] out of an approximate total available energy of 242 amp-hours. The navigation system gyro drift and closure error were negligible.

Controllability was good. There were no problems with steering, braking, or obstacle negotiation. Brakes were used at least partially on all down-slopes. Driving down sun was difficult because the concealed shadows caused poor obstacle visibility.

While the LRV had no problems with the dust, stowed payload mechanical parts attached to the LRV tended to bind up. The crew described dust as being an anti-lubricant and reported that there was no EVA-4 capability in many of the stowed payload items because of dust intrusion. Large tolerance mechanical items such as locking bags on the gate and the pallet lock had problems toward the end of EVA-3. Only those items which had been protected from the dust performed without degradation.

All interfaces between crew, LRV and stowed payload were satisfactory.

The following LRV system anomalies were noted:

- a. At initial power-up, the LRV battery temperatures were higher than predicted (reference paragraph 20.12).
- b. Battery No. 2 temperature indication was off scale low at start of EVA-3 (reference paragraph 20.8.3).
- c. The right rear fender extension was broken off at the Lunar Module (LM) site on EVA-1 prior to driving to the Apollo Lunar Surface Experiments Package (ALSEP) site (reference paragraph 20.11).

20.2 DEPLOYMENT

Deployment of the LRV from the LM was completed successfully using less than 10 minutes of crew time. The operation was smooth and no problems were encountered. The landing attitude of the LM was favorable (less than 3° inclination) and did not adversely affect the operation. The chassis lock pins did not seat fully in place but the crew had no difficulty in seating the pins by using the deployment assist tool per normal procedures. LRV set up and checkout required less than 9 minutes of crew time.

20.3 LPV TO STOWED PAYLOAD INTERFACE

The interfaces between the stowed payloads and LRV were satisfactory.

20.4 LUNAR TRAFFICABILITY ENVIRONMENT

The terrain created no unusual operating problems for the LRV. Traverses are shown in Figure 20-1. In general, the lunar surface character was gently undulated, hummocky, abundantly cratered and somewhat rougher than expected.

On the basis of crew debriefings and EVA photographic coverage, it appears that the LRV was operated uphill on slopes of 18 degrees or more and downhill on slopes of 20 degrees or more. Because of its light weight and the excellent traction obtained, the general performance of the vehicle on these slopes was satisfactory. Maneuvering the vehicle on slopes consisted primarily of uphill and downhill travel and did not present any serious problems. Maximum speed reached was 18 kph down-slope. Vehicle traverse cross slope caused discomfort to the crewman on the down-slope side and was avoided whenever possible. The crew also reported that driving on the lunar surface requires a constant effort to avoid obstacles.

20.5 WHEEL SOIL INTERACTION

As on Apollo 15 and 16, the LRV made only a shallow imprint on the lunar surface. This crew observation is supported by numerous photographs obtained during the lunar surface EVA's. The depth of the wheel tracks averaged 1-1/2 cm (1/2 in) for a fully loaded LRV (vehicle, crew, payload). The LRV wheels developed excellent traction in the lunar surface material. In most cases a sharp imprint of the Chevron tread was clearly discernible, indicating that the surface soil possessed cohesion and the amount of wheel slip was minimal. The shallow wheel track indicates that good flotation was provided by the wheel design and also indicates that the primary energy losses were due to compaction and rolling resistance and that bulldozing was minimal. This observation is supported by the small error in traverse closure in the navigation system.

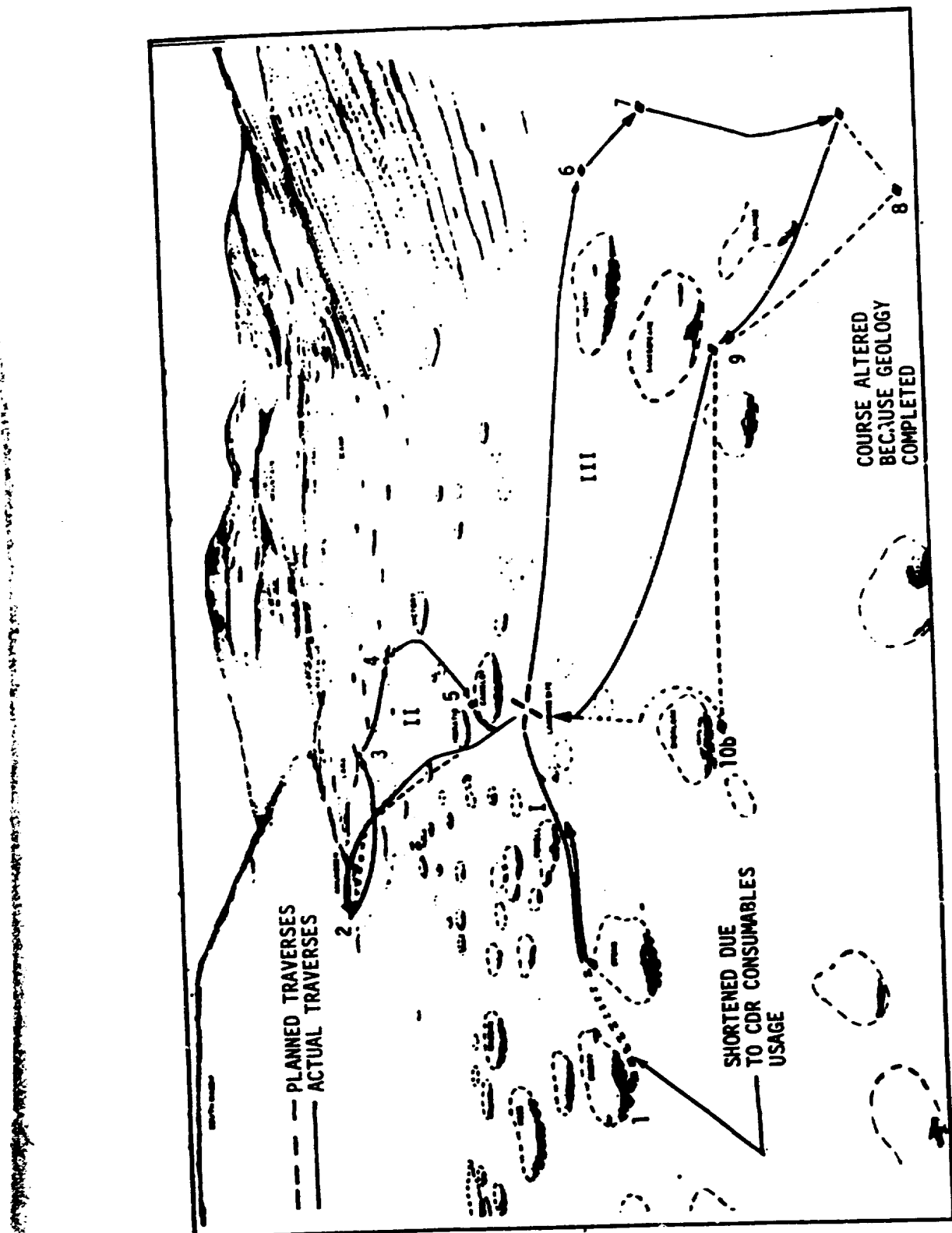


Figure 20-1. Apollo 17 LRV Traverses

20.6 LOCOMOTION PERFORMANCE

The locomotion performance of the LRV was satisfactory and met all of the demands of the Apollo 17 mission. Comparison of the LRV amp-hour integrator readings with pre-flight predictions (Figure 20-2) shows that the LRV power usage was as expected. Locomotion performance is contained in Table 20-1. As shown in Apollo Lunar EVA Summary, Table 20-2, a longer traverse and a greater distance from the LM was achieved during EVA-2 than any prior mission.

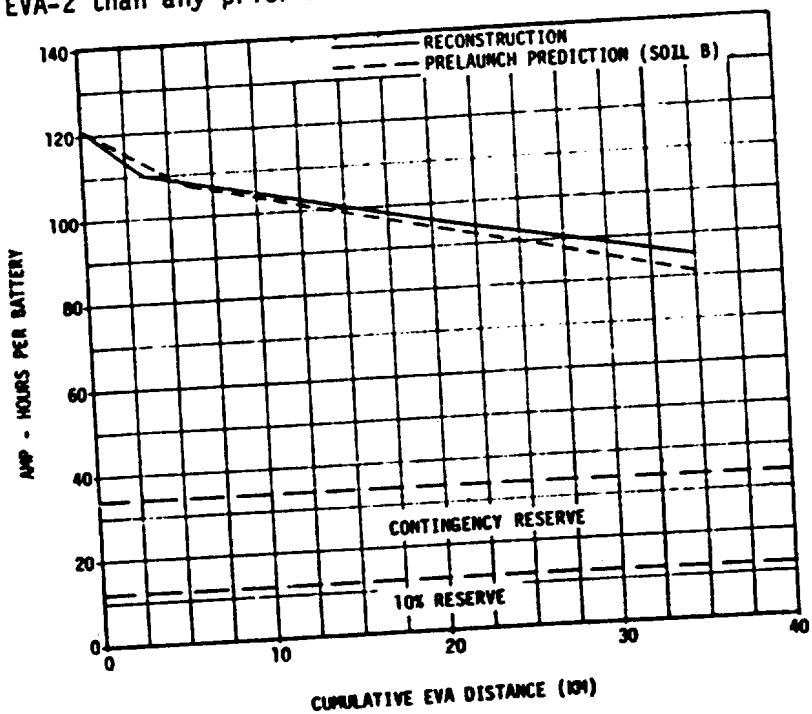


Figure 20-2. LRV Power Usage

20.7 MECHANICAL SYSTEMS

20.7.1 Harmonic Drive

The harmonic drive performed satisfactorily; no excessive power consumption or temperatures were noted nor was any mechanical malfunction apparent.

20.7.2 Wheels and Suspension

The wheels and suspension systems performed as expected. The maximum vehicle speed/obstacle size encountered was 10-12 kph over an obstacle 30 centimeters high. The vehicle scraped bottom occasionally. The left front wheel sustained a dent (about the size of a tennis ball) on the side wall but locomotion performance was not affected.

Table 20-1. Apollo 17 LRV Performance Summary

	EVA 1	EVA 2	EVA 3	TOTAL	MISSION PLANNING VALUE
Drive Time (min)	33	145	91	269	280
Map Distance (km)	2.3	19.0	11.0	32.3	32.5
Odometer Distance (Traverse) ▶	2.5	20.2	12.0	35.7	37.35
(km) Odometer Distance (Additional) ▶	0.8	0.1	.1		
Mobility Rate (kph) Traverse ▶	4.18	7.85	7.24	7.2	7.0
Average Speed (kph) Traverse ▶	4.54	8.35	7.92	7.8	8
Energy Rate amp-hr/km (LRV Only)	1.88	1.53	1.76	1.64	1.8
Amp-Hours Consumed LRV	6.2	-	-	73.4	85
Amp-Hours Consumed LMU	14.8	-	-		
Nav. Closure Error (km)	0	0	0	0	0.2
Number of Nav. Updates	0	0	0	0	3
Gyro Drift Rate (deg/hr)	<1°	<1°	<1°	<1°	1.6
Wander Factor + Slip (%) ▶	9	6	10	8.4	10.0
Max. Speed Reported (kph)	11	12 (4 to 5 up 10° slope)	12 (10 down 11°)	-	-
Max. Slope Reported (degrees)	-	10° Up 20° Down	-	-	-
▶ Odometer Distance (Traverse) - Distance actually driven from traverse starting point to end point.	▶ Odometer Distance (Additional) - Includes distance between LM and Surface Electrical Properties (SEP) or LM and ALSEP not included in traverse distance.				
▶ Mobility Rate = Map Distance / DRIVE TIME	▶ Wander Factor = $\frac{\text{Traverse Odometer} - \text{Map Distance}}{\text{Map Distance}}$				

Table 20-2. Apollo Lunar EVA Summary

	APOLLO 11	APOLLO 12	APOLLO 14	APOLLO 15	APOLLO 16	APOLLO 17
Drive Time (hr:min)	-	-	-	3:02	3:26	4:29
Map Distance (km)	-	-	-	25.3	22.0	32.3
Surface Distance Traversed (km)	0.25	2.0	3.3	27.9	26.9	35.7
EVA Duration (hr:min)	2:24	7:29	9:23	18:33	21:00	22:05
Average Speed (kph)	-	-	-	3.2	7.60	7.75
Energy Rate Amp-Hr/km (LRV Only)	-	-	-	1.9	2.1	1.6
Amp-Hours Consumed (242 Available)	-	-	-	52.0	88.7	73.4
Nav. Closure Error (km)	-	-	-	0.1	0	0
Number of Nav. Updates	-	-	-	1	0	0
Maximum Range from LM (km)	-	-	-	5.4	4.5	7.6
Longest EVA Traverse (km)	-	-	-	12.5	11.6	28.3
Rock Samples Returned (lbm)	46	75	94	170	213	257
LRV Maximum Weight (lbm)	-	-	-	1532	1549	1606.7

20.7.3 Brakes

The LRV braking capability was reported to be excellent and the vehicle came to a complete stop within one to three vehicle lengths. There was no instance of "fade" even during prolonged down-slope braking.

20.7.4 Stability

The LRV stability was satisfactory. The LRV had no tendency to roll and its response was predominantly a pitching motion. The crew felt that individual wheels became airborne occasionally, but did not cause a controllability problem. Driving cross slope was uncomfortable to the crewman on the down-slope side and was avoided whenever possible.

20.7.5 Hand Controller

The hand controller performed satisfactorily.

20.7.6 Loads

Instrumentation was not provided on the LRV to ascertain induced loads. No evidence of load problems was reported.

20.8 ELECTRICAL SYSTEMS

The LRV electrical systems satisfactorily supported the lunar surface exploration. The battery temperature anomaly had no major impact on the mission (see 20.8.3).

20.8.1 Batteries

The battery capacity was more than adequate for the mission. Amp-hour usage including LCRU, was estimated to be 73.4 out of a nominal capacity of 242 amp-hours for the two batteries.

20.8.2 Traction Drive System

The traction drive system performed satisfactorily. There were no indications of any off nominal conditions within the traction drive and all four units performed as expected. The maximum temperature reported of any traction drive unit was 270°F and occurred at Station 6 on EVA-3.

20.8.3 Distribution System

The electrical distribution system provided power to all functions as required. However, battery No. 2 temperature indication was off scale low during power-up at the beginning of EVA-3. This condition continued for the remainder of the

mission. The most probable cause was a shorted temperature sensor in the battery, which would cause the meter to read off scale low. This same condition was noted on two batteries previously tested at temperatures above the qualification level. Electrolyte leakage through the sensor bond caused by the elevated temperatures appears to have caused the short. There was no impact on the mission. Temperature monitoring was continued using Battery No. 1 as an indicator and using temperature trends established from actual data on EVA's-1 and -2. Normal performance monitoring was continued, using amp-hour integrator data.

20.8.4 Steering

The LRV steering performed satisfactorily for all three EVA's. Controllability was excellent. The Commander (CDR) reported that good vehicle maneuverability using double Ackerman steering made this the preferred mode. The CDR felt that a single steering mode (locked rear steering) would not have given the required maneuvering capability for this particular area.

The CDR also reported that he found the preferred mode was to drive over blocks and craters up to one foot in diameter and to drive through blocks and craters from 5 to 10 meters in size, rather than steer around them and put the LRV into cross slope conditions.

20.8.5 Amp-Hour Integrator

The Amp-Hour Integrator performed satisfactory throughout all three EVA-s. Amp-hour usage is shown in Figure 20-2.

20.9 CONTROL AND DISPLAY CONSOLE

The control and display console displays performed satisfactory. The only indication loss was attributed to a faulty sensor, as discussed in Section 20.8.3. There were no occurrences to suggest improper switch or circuit breaker positions.

20.10 NAVIGATION SYSTEM

The Navigation System satisfactorily supported the Apollo 17 mission. The position error was well within the mission planning value of 100 meters during all EVA's and no update was required. Table 20-1 contains a summary of navigation performance.

The LRV Vehicle Attitude Indicator pointers tended to stick throughout all three EVA's. There was no impact on the mission as the pointers worked when the crew tapped the unit. There was no recurrence of the Vehicle Attitude Indicator scale problem reported on Apollo 16, LRV-2.

20.11 CREW STATION

The crew reported no problem with the crew station. The seat belt

design functioned satisfactorily. The ground adjustments proved to be very good, with only minor adjustments required on the lunar surface. Access and stowage was adequate.

During Extravehicular Activity (EVA-1) at the LM prior to driving to ALSEP, the CDR inadvertently pulled off the right rear fender extension by catching it with the hammer carried in the right leg pocket of the Extravehicular Mobility Unit (EMU).

While still at the LM site, the CDR spent approximately 12 minutes taping the extension onto the fender. Because of the dusty surfaces, the tape did not adhere and the extension fell off returning from Station 1. In the moon's low gravity and hard vacuum, loss of the fender extension allowed dust to be thrown forward by the revolving rear wheel onto the LRV and crew. Per real time procedures established by MSC and MSFC, the crew taped together four Lunar Module (LM) maps and fastened them to the fender with two clamps from the LM (refer to Figure 20-3). Installation of this fix required approximately 7 minutes of CDR and Lunar Module Pilot (LMP) surface time at the beginning of EVA-2. This fix was adequate for the remainder of the mission.

A fender extension was also lost on Apollo 15 and 16. A fender modification was incorporated for Apollo 17 to prevent the fender extension from being dislodged from its guides. The fix would have been effective except that the force applied was so great that it fractured the guide material.

20.12 THERMAL

The thermal control system satisfactorily supported all the Apollo 17 mission lunar surface operations. At initial power-up, the LRV battery temperatures were higher than predicted and the right battery indicated 15°F higher than the left (95°F left and 110°F right actual vs. 80°F pre-mission predicted). The higher temperature was due to hot holds (orientation of LRV toward the sun instead of passive thermal control) during translunar coast. Based on the LM solar attitude during translunar coast, the LRV temperature of 95°F is reasonable at initial power-up. There was no apparent performance degradation throughout the mission due to the high battery temperatures. Battery temperatures at LRV closeout were indicated to be 139°F for Battery No. 1 and 148°F (calculated) for Battery No. 2. Predicted temperatures were 140°F and 148°F (8° included for meter bias). This meter bias was confirmed by caution and warning flag activation on EVA-2. The flag, which activates at 125°F activated when the meter indicated 132°F. All temperature values shown will be meter values and will include this bias. Because of this bias an indicated battery temperature limit of 148°F was agreed to prior to EVA-2. The amp-hour usage of both batteries followed the predicted curves throughout the mission.

The probable cause of the temperature difference between batteries at initial power-up (95°F left and 110°F right) is heat absorption by the

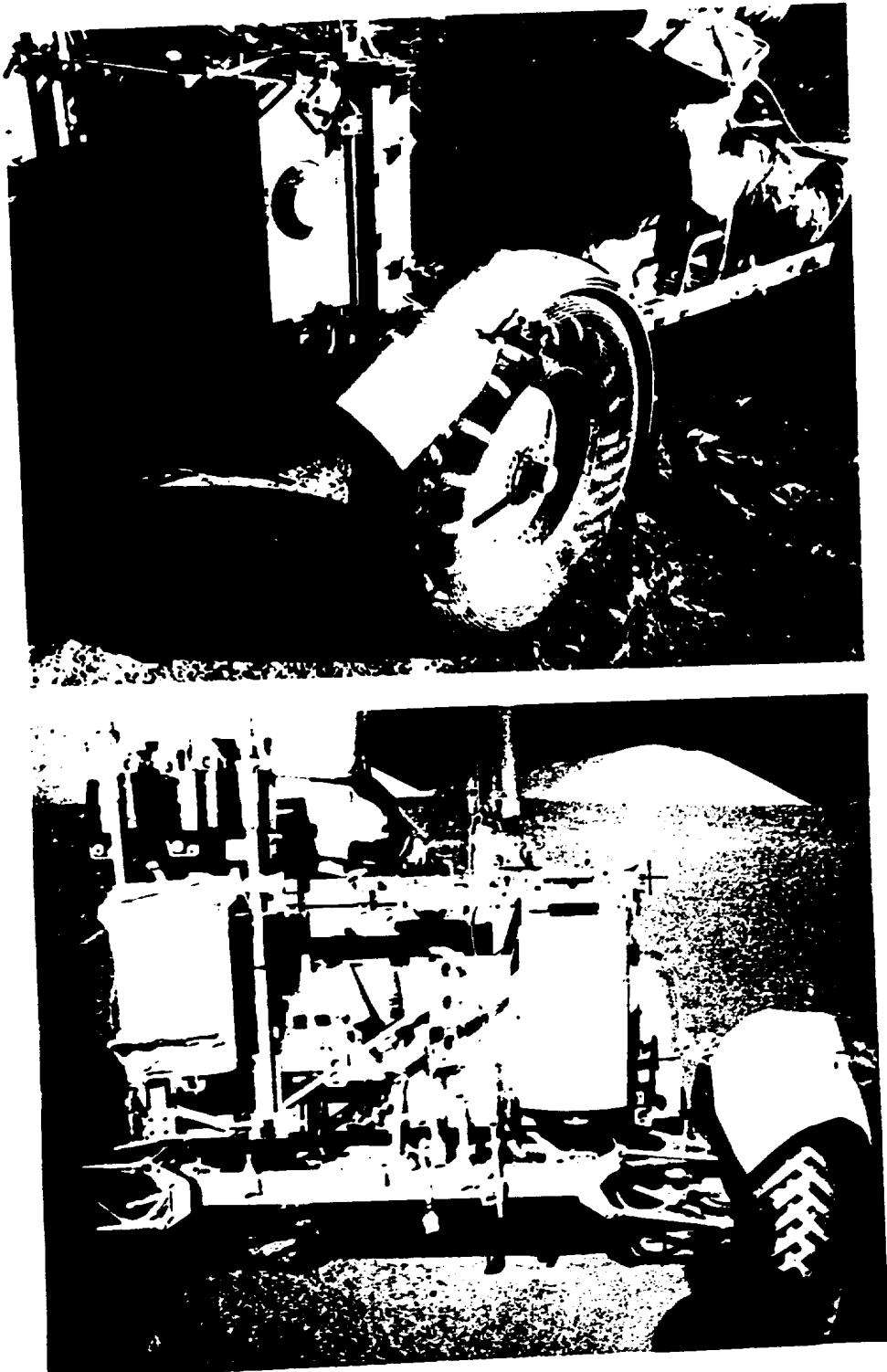


Figure 20-3. LRV Fender Fix

wax tank on the left battery. The right battery has no wax tank and it would have been unusual for both batteries to be at the same temperature above the wax tank melting point (93°F).

Revised parking constraints and careful attention to battery dusting procedures by the crew provided better cooldown than on previous missions. The CDR reported that careful dusting of the LRV battery covers at each stop, resulted in relatively dust-free radiators through all three EVA's. By keeping the covers clean, dusting of the battery mirrors was not required until the end of EVA-2. Additionally, per alternate procedures, the battery covers were opened at the ALSEP site during EVA-1 and at Station 6 during EVA-3 to maintain batteries within acceptable limits.

All LRV components remained within operational temperature limits throughout the three lunar surface EVA's. As predicted, motor temperatures were "off-scale-low" (below 200°F) throughout most of the EVA's. The maximum motor temperature of 270°F (131°C) occurred during EVA-3.

Figures 20-4 and 20-5 present the battery profiles for the three EVA's. Because of the high battery temperatures at initial power-up the LRV was parked heading up-sun for best radiation to deep space and the dust covers were opened during the ALSEP deployment period. The anticipated cooldown of 10°F (6°C)* for Battery 2, and 4°F (2°C)* for Battery No. 1 was achieved. The battery 1 and 2 temperatures, with the LRV supplying LCRU power, were 108°F (42°C) and 123°F (51°C)* at the end of EVA-1.

Adequate battery cooldown was obtained between EVA's 1 and 2. EVA-2 began with battery temperatures of 70°F (21°C)* and 92°F (33°C)*. The warning flag activated on battery 2 when the meter indicated 132°F (56°C). EVA-2 ended with temperatures of 114°F (46°C)* and 138°F (59°C)*.

EVA-3 began with a Battery No. 1 temperature of 95°F (33°C) and a non-operating temperature meter for Battery No. 2 [estimated temperature was 120°F (49°C)]. Per alternate procedures the dust covers were opened at Station 6 to maintain batteries within thermal limits. The final recorded temperature for Battery No. 1 was 139°F (59°C). A warning flag was also noted for Battery No. 1 at that time. It is estimated that the final Battery No. 2 temperature was about 148°F (64°C).

20.13 STRUCTURAL

There was no structural damage to the load bearing members of the LRV. A rear fender extension was dislodged on EVA-1 (refer to paragraph 20.11).

20.14 LUNAR ROVING VEHICLE CONFIGURATION

LRV-3 was essentially unchanged from LRV-2 which was flown on Apollo 16 other than those changes shown in Table 20-3. Refer to Saturn V Launch Vehicle Flight Evaluation Report - AS-510, Apollo 15 Mission for a basic Vehicle Description.

*Temperature as read by crew. Subsequent analysis indicated actual temperatures to be 8° lower than readouts.

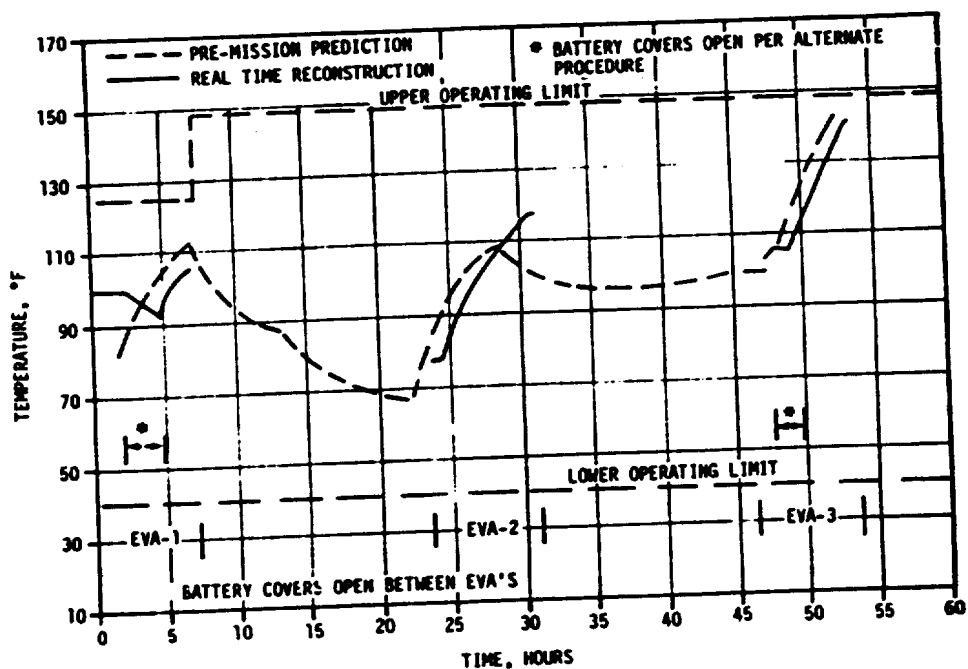


Figure 20-4. LRV Battery No. 1 (Left) Temperature

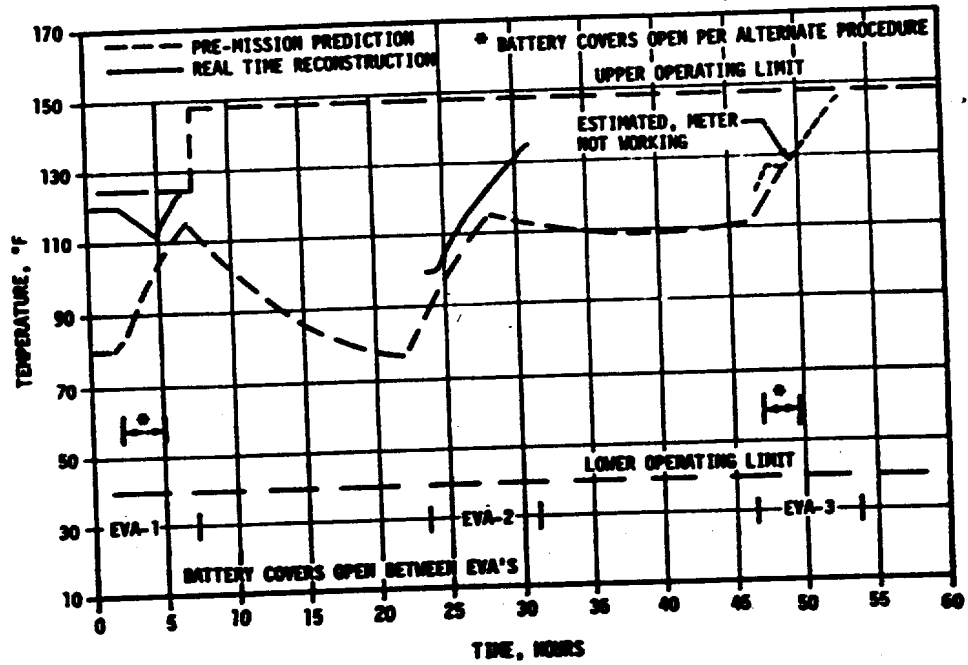


Figure 20-5. LRV Battery No. 2 (Right) Temperature

Significant configuration changes are contained in Table 20-3.

Table 20-3. LRV Significant Configuration Changes

SYSTEM	CHANGE	REASON
Payload	Add index ring for azimuth alignment dial on low gain antenna.	To provide crew with ready reference for low gain antenna azimuth pointing angle.
Payload	Install surface electrical properties (SEP) experiment signal cable (signal processing unit to SEP).	To provide vehicle location data to SEP.
Payload	Add dust cover to SEP connector.	To prevent contamination from entering receptacle.
Payload	Move Buddy/Secondary Life Support System (B/SLSS) holding strap from LMP seat back to CDR seat back.	B/SLSS moved to prevent interference with SEP.
Payload	Add decal to aft chassis locating pallet stop tether.	To provide crew with indicator of proper hole to use with stop tether.
Crew Station	Install new fender extension stops on all four fenders.	To prevent loss of fender extension during lunar operation.

APPENDIX A

ATMOSPHERE

A.1 SUMMARY

This appendix presents a summary of the atmospheric environment at launch time of the AS-512. The format of these data is similar to that presented on previous launches of Saturn vehicles to permit comparisons. Surface and upper level winds, and thermodynamic data near launch time are given.

A.2 GENERAL ATMOSPHERIC CONDITIONS AT LAUNCH TIME

During the evening launch of Apollo 17, the Cape Kennedy launch area was experiencing mild temperatures with gentle surface winds. These conditions resulted from a warm moist air mass covering most of Florida. This warm air was separated from an extremely cold air mass over the rest of the south by a cold front oriented northeast-southwest and passing through the Florida panhandle. See Figure A-1. Surface winds in the Cape Kennedy area were light and northwesterly as shown in Table A-1. Wind flow aloft is shown in Figure A-2 (500 millibar level). The maximum wind belt was located north of Florida, giving less intense wind flow aloft over the Cape Kennedy area.

A.3 SURFACE OBSERVATIONS AT LAUNCH TIME

At launch time, total sky cover was 5/10, consisting of scattered stratus-cumulus at 0.8 kilometers (2,600 ft) and scattered cirrus at 7.9 kilometers (26,000 ft). Surface ambient temperature was 294°K (70.0°F). During ascent the vehicle did pass through some thin cirrus clouds. All surface observations at launch time are summarized in Table A-1. Solar radiation data for the day of December 6, 1972, are given in Table A-2.

A.4 UPPER AIR MEASUREMENTS

Data were used from three of the upper air wind systems to compile the final meteorological tape. Table A-3 summarizes the wind data systems used. Only the Rawinsonde and the Loki Dart meteorological rocket data were used in the upper level atmospheric thermodynamic analyses.

A.4.1 Wind Speed

Wind speeds were light, being 3.6 m/s (7.0 knots) at the surface and increasing to a peak of 45.1 m/s (87.6 knots) at 12.18 kilometers (39,960 ft). The winds began decreasing above this altitude, becoming relatively

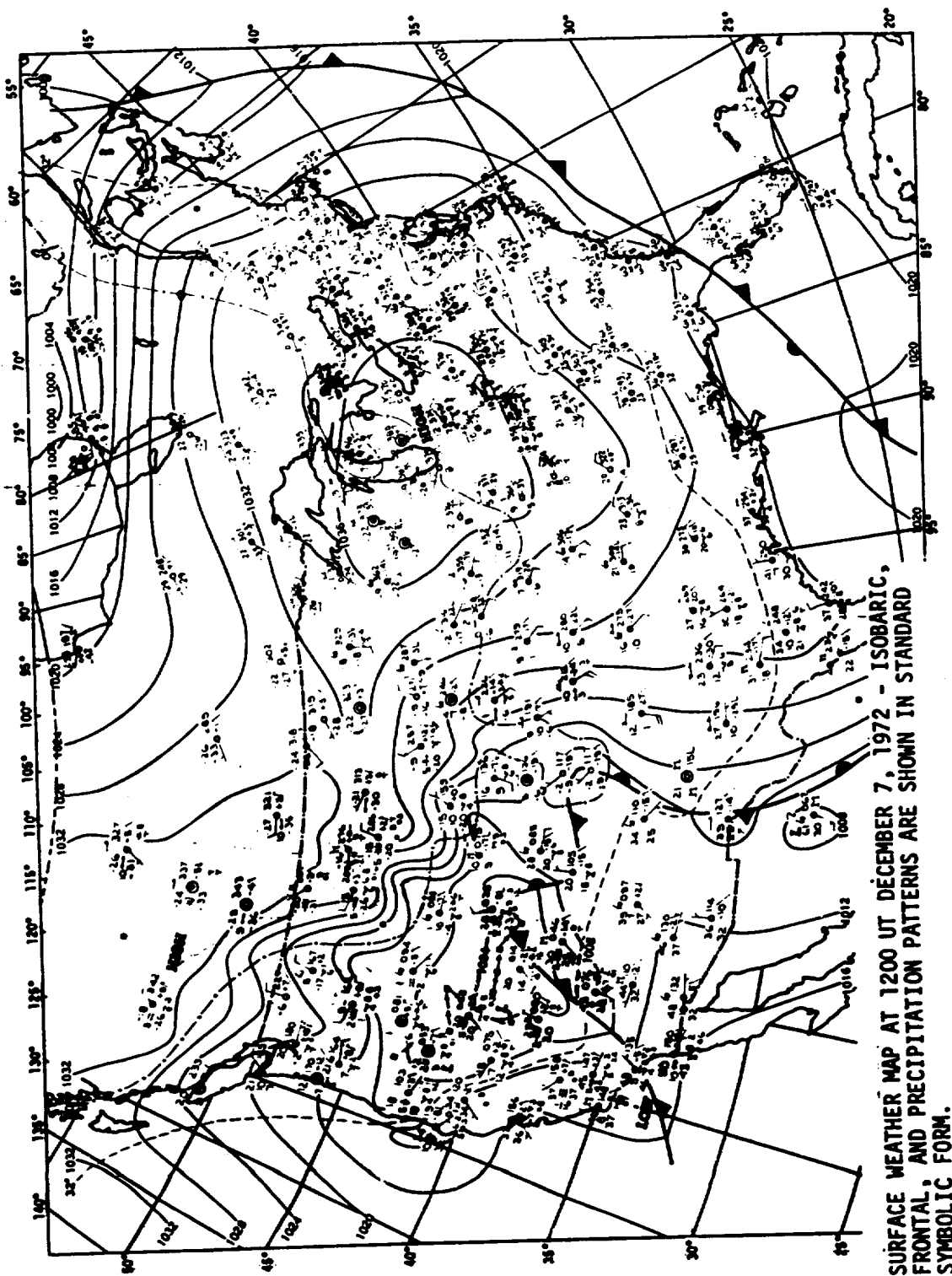


Figure A-1. Surface Weather Map Approximately 6 1/2 Hours After Launch of AS-512

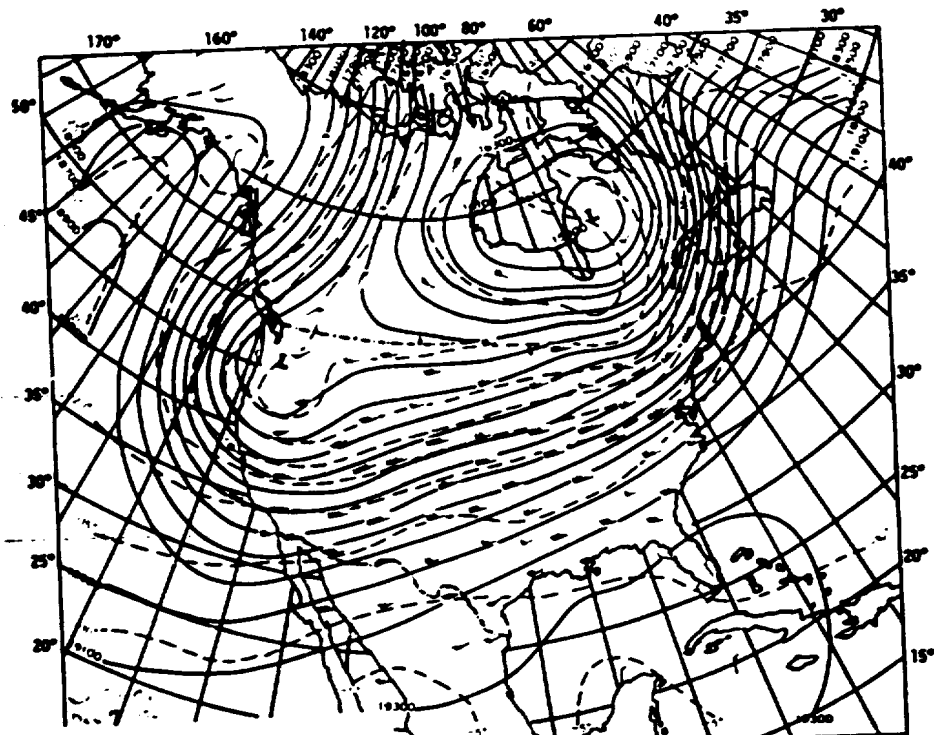
A-1. Surface Observations at AS-512 Launch Time

LOCATION	ALT. (MIL.) ¹	TEM- PERATURE °K (°F)	DEW POINT °K (°F)	VISI- BILITY IN STAT MI	CLOUD AMOUNT (TENTHS)	CLOUD TYPE	SKY COVER		WIND ²	
							HEIGHT OF BASE METERS FEET	DIR (DEG)	SPEED M/S (KNOTS)	DIR (DEG)
NASA 150 m Ground Wind Tower, Wind measured at 10 m (32.8 ft) ³	0	10.201 (14.80)	294.3 (70.0)	293.2 (68.0)	11 (7)	2	Strato- cumulus Cirrus (26 000) (2 600)	3.6 ⁴ (7.0)	300 ⁴	
Cape Kennedy Surface Measurements	10	10.200 (14.79)	295.1 (71.4)	294.9 (71.1)	--	5	--	--	2.0 ⁴ (3.9)	320 ⁴
Pad 30A Lightpole Alt 18.3 m (60.0 ft) ³	0	--	--	--	--	--	--	--	4.1 (8.0)	005
Pad 30A LUT N 161.5 m (530 ft) ³	0	--	--	--	--	--	--	--	5.4 (10.5)	335

¹ Instantaneous readings at T-0, unless otherwise noted.

³ Above natural grade.

⁴ 1 minute average about T-0.



500 MILLIBAR HEIGHT
CONTOURS AT 1200 Z

DECEMBER 7, 1972

CONTINUOUS LINES INDICATE HEIGHT CONTOURS IN
FEET ABOVE SEA LEVEL. DASHED LINES ARE ISO-
THERMS IN DEGREES CENTIGRADE. ARROWS SHOW
WIND DIRECTION AND SPEED AT THE 500 MB LEVEL.
(ARROWS SAME AS ON SURFACE MAP).

Figure A-2. 500 Millibar Map Approximately 6 1/2 Hours After
Launch of AS-512

Table A-2. Solar Radiation at AS-512 Launch Time, Launch Pad 39A

DATE	HOUR ENDING EST	TOTAL HORIZONTAL SURFACE G-CAL/CM ² -MIN	NORMAL INCIDENT G-CAL/CM ² -MIN	DIFFUSE (SKY) G-CAL/CM ² -MIN
December 6, 1972	07.00	0.00	0.00	0.00
	08.00	0.04	0.02	0.04
	09.00	0.17	0.20	0.10
	10.00	0.53	1.14	0.00
	11.00	0.63	1.32	0.00
	12.00	0.62	0.69	0.18
	13.00	0.81	0.92	0.24
	14.00	0.71	0.89	0.23
	15.00	0.32	0.51	0.31
	16.00	0.39	0.63	0.23
	17.00	0.11	0.14	0.10
	18.00	0.01	0.01	0.01
	19.00	0.00	0.00	0.00

Table A-3. Systems Used to Measure Upper Air Wind Data for AS-512

TYPE OF DATA	RELEASE TIME		PORTION OF DATA USED			
	TIME (UT)	TIME AFTER T-0 (MIN)	START		END	
			ALTITUDE M (ft)	TIME AFTER T-0 (MIN)	ALTITUDE M (ft)	TIME AFTER T-0 (MIN)
FPS-16 Jimosphere	0550	17	150 (492)	17	15 000 (4,212)	69
Rainsonde	0543	10	15 250 (50 032)	60	24 750 (81 200)	91
Int'l Dart	0815	162	58 250 (191 107)	162	25 000 (82 020)	182

light at 22.88 kilometers (75,065 ft). Above this level, winds increased to a peak of 77.0 m/s (149.7 knots) at 44.50 Km (145,996 ft) altitude as shown in Figure A-3. Maximum dynamic pressure occurred at 13.06 kilometers (42,847 ft). At max Q altitude, the wind speed and direction was 33.2 m/s (64.5 knots), from 314 degrees.

A.4.2 Wind Direction

At launch time, the surface wind direction was from 300 degrees. The wind direction varied, between southwest and northwest, with increasing altitude over the entire profile. Figure A-4 shows the complete wind direction versus altitude profile. As shown in Figure A-4, wind directions were quite variable at altitudes with low wind speeds.

A.4.3 Pitch Wind Component

The pitch wind velocity component (component parallel to the horizontal projection of the flight path) at the surface was a tailwind of 3.2 m/s (6.1 knots). The maximum tailwind, in the altitude range of 8 to 16 kilometers (26,247 to 52,493 ft), was 34.8 m/s (67.6 knots) observed at 12.18 kilometers (39,944 ft) altitude. See Figure A-5.

A.4.4 Yaw Wind Component

The yaw wind velocity component (component normal to the horizontal projection of the flight path) at the surface was a wind from the left of 1.7 m/s (3.3 knots). The peak yaw wind velocity in the high dynamic pressure region was from the left of 29.2 m/s (56.8 knots) at 11.35 kilometers (37,237 ft). See Figure A-6.

A.4.5 Component Wind Shears

The largest component wind shear ($\Delta h = 1,000$ m) in the max Q region was a pitch shear of 0.0177 sec^{-1} at 7.98 kilometers (26,164 ft). The largest yaw wind shear, at these lower levels, was 0.0148 sec^{-1} at 10.65 kilometers (34,940 ft). See Figure A-7.

A.4.6 Extreme Wind Data in the High Dynamic Region

A summary of the maximum wind speeds and wind components is given in Table A-4. A summary of the extreme wind shear values ($\Delta h = 1,000$ meters) is given in Table A-5.

A.5 THERMODYNAMIC DATA

Comparisons of the thermodynamic data taken at AS-512 launch time with the annual Patrick Reference Atmosphere, 1963 (PRA-63) for temperature, pressure, density, and Optical Index of Refraction are shown in Figures A-8 and A-9, and are discussed in the following paragraphs.

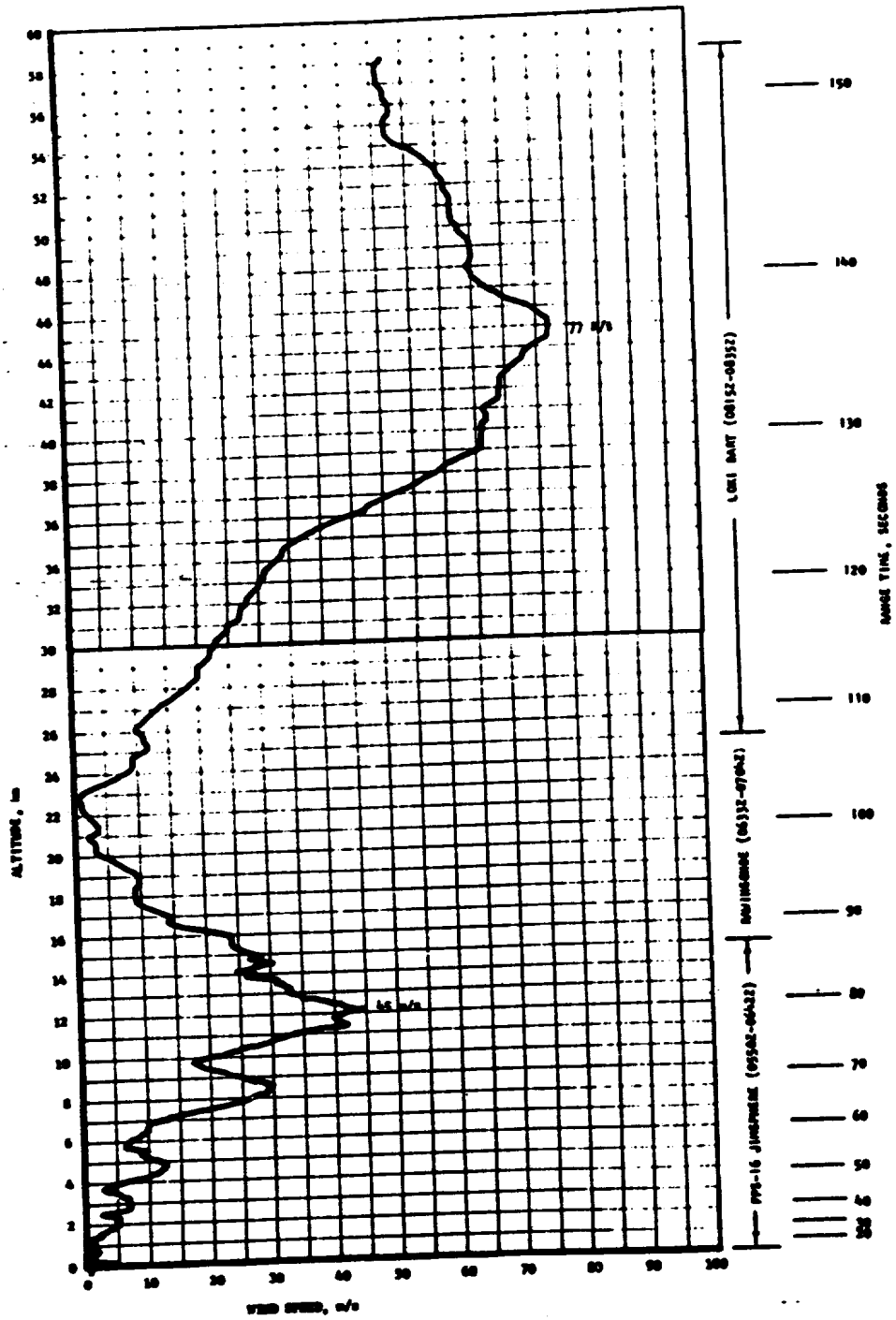


Figure A-3. Scalar Wind Speed at Launch Time of AS-512

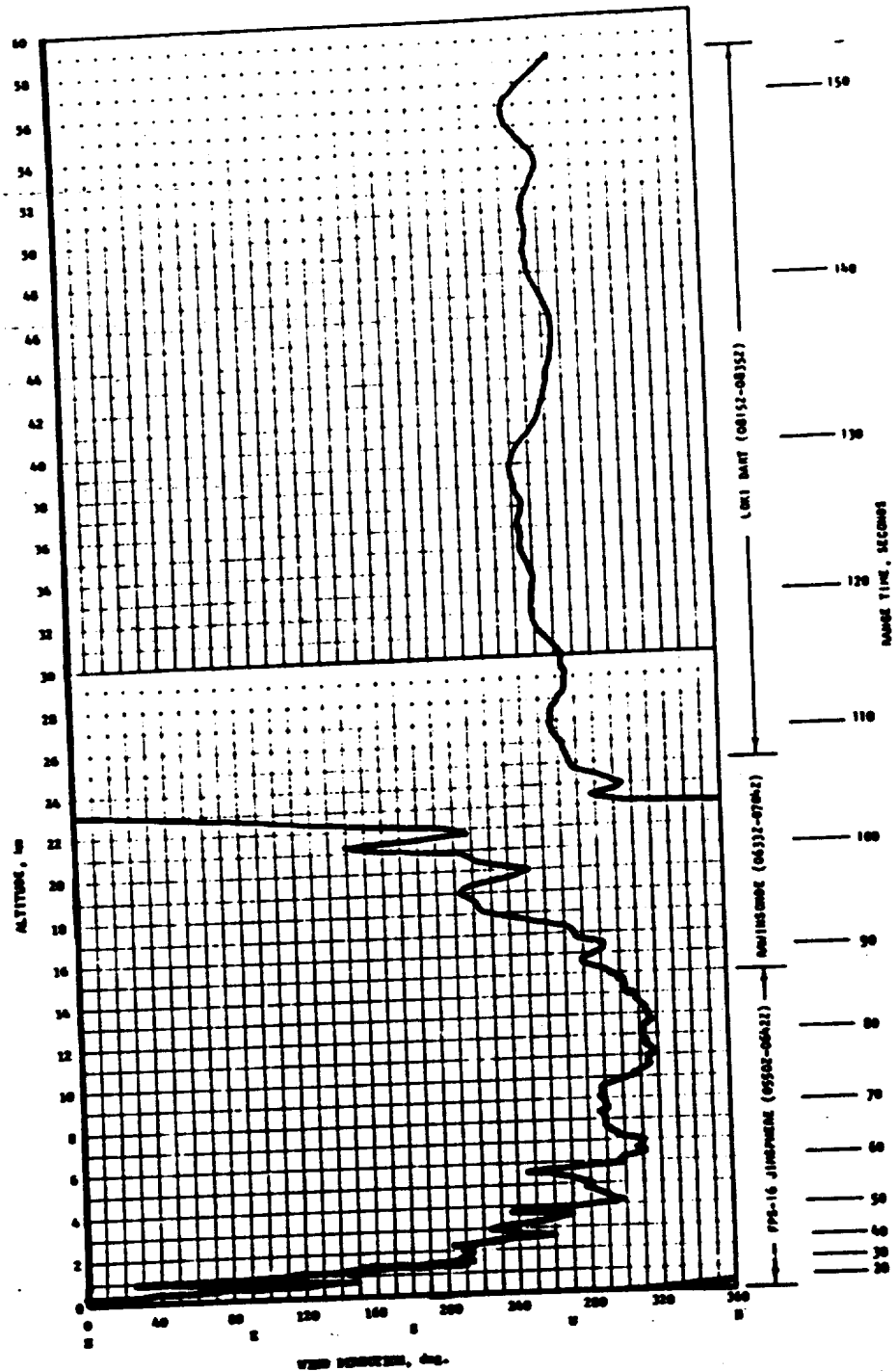


Figure A-4. Wind Direction at Launch Time of AS-512

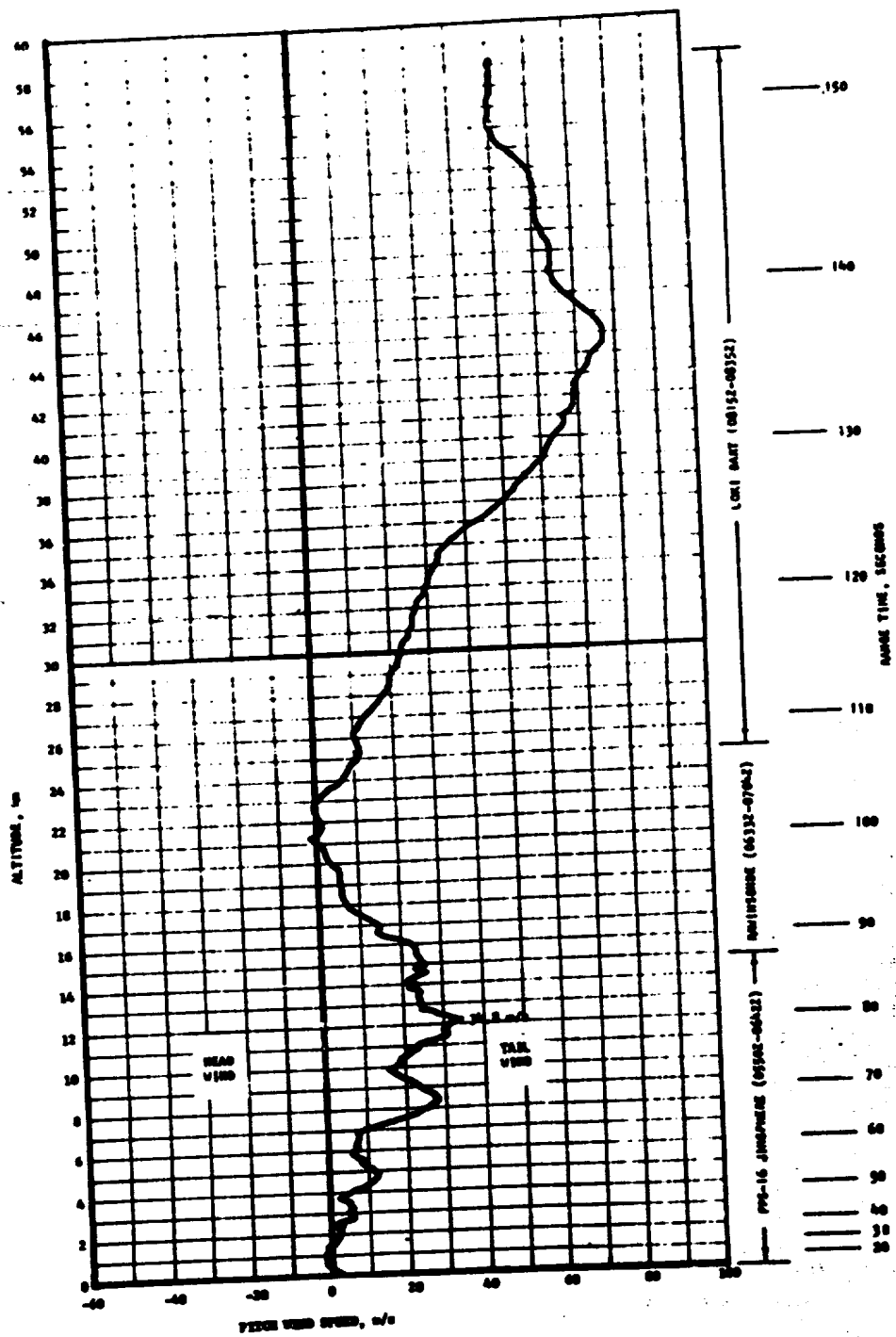


Figure A-5. Pitch Wind Velocity Component (W_x) at Launch Time of AS-512

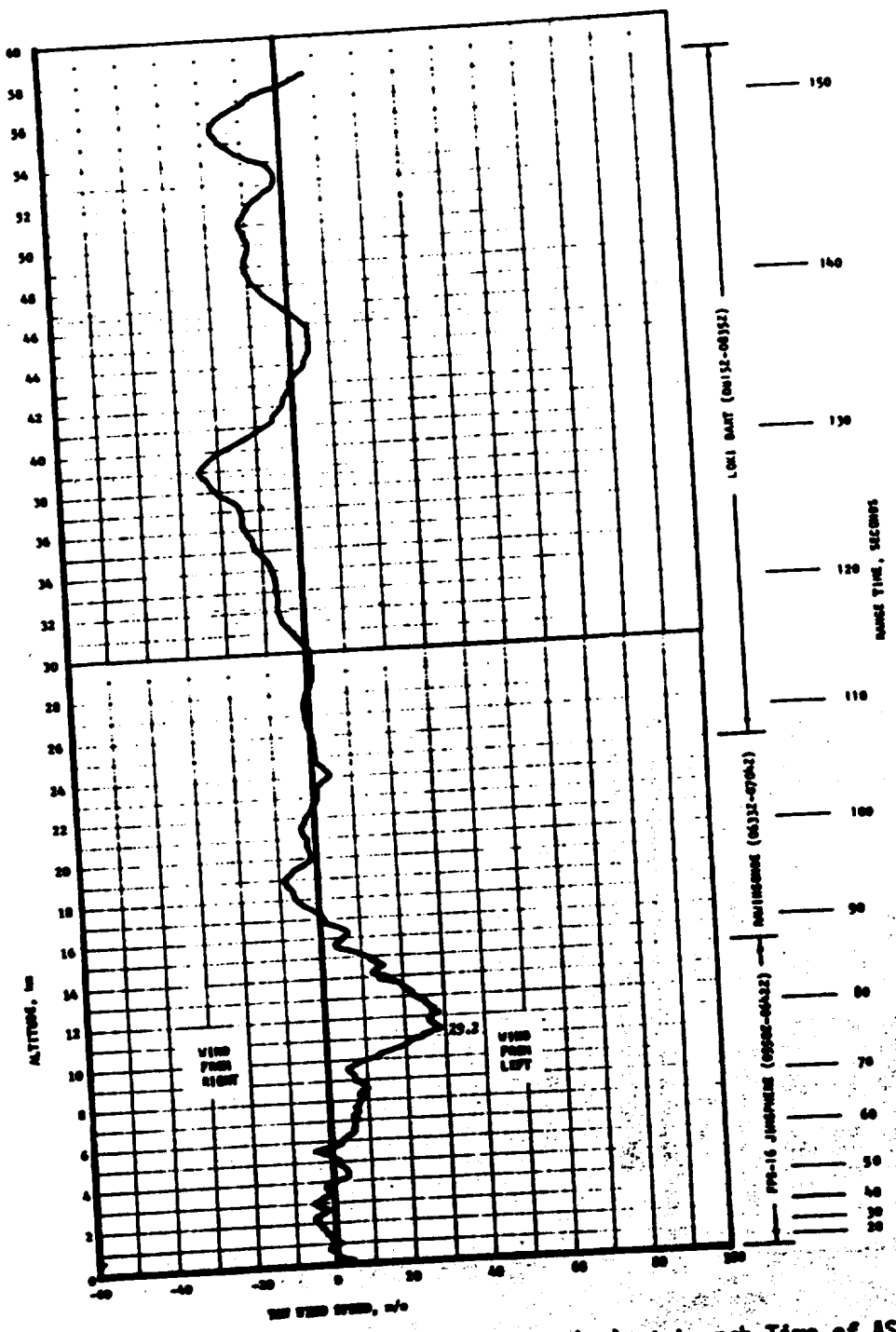


Figure A-6. Yaw Wind Velocity Component (W_z) at Launch Time of AS-512

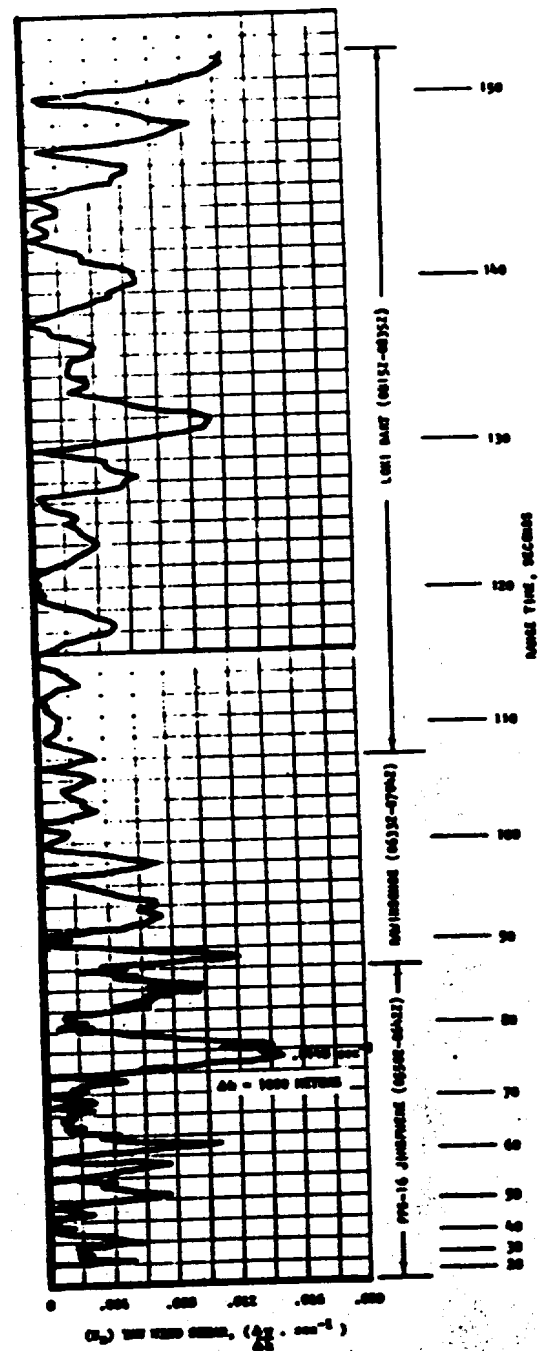
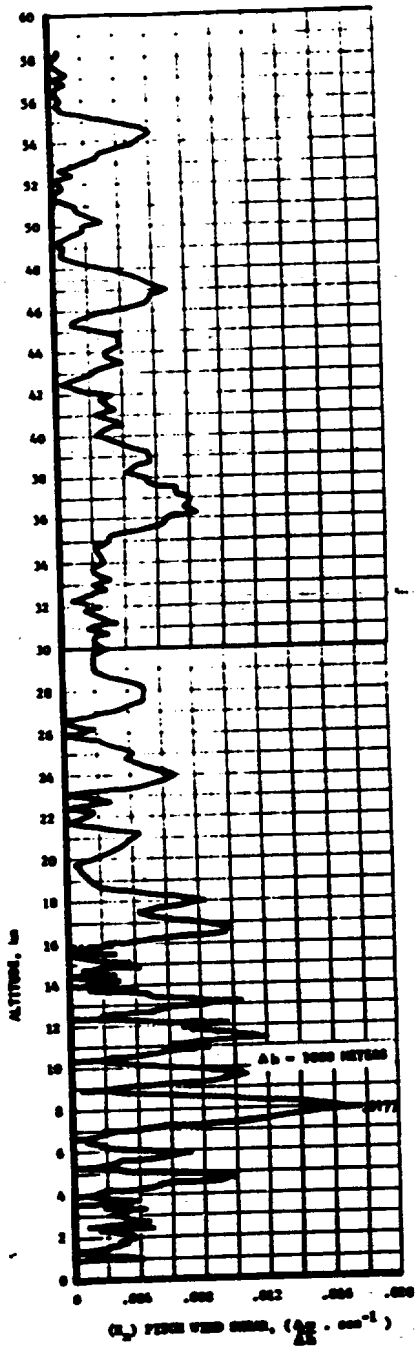


Figure A-7. Pitch (S_x) and Yaw (S_z) Component Wind Shears at Launch Time of AS-512

Table A-4. Maximum Wind Speed in High Dynamic Pressure Region for
Apollo/Saturn 501 through Apollo/Saturn 512 Vehicles

VEHICLE NUMBER	MAXIMUM WIND			MAXIMUM WIND COMPONENTS			
	SPEED M/S (KNOTS)	DIR (DEG)	ALT KM (FT)	PITCH (W _X) M/S (KNOTS)	ALT KM (FT)	YAW (W _Z) M/S (KNOTS)	ALT KM (FT)
AS-501	26.0 (50.5)	273	11.50 (37,700)	24.3 (47.2)	11.50 (37,700)	12.9 (25.1)	9.00 (29,500)
AS-502	27.1 (52.7)	255	13.00 (42,650)	27.1 (52.7)	13.00 (42,650)	12.9 (25.1)	15.75 (51,700)
AS-503	34.8 (67.6)	284	15.22 (49,900)	31.2 (60.6)	15.10 (49,500)	22.6 (43.9)	15.80 (51,800)
AS-504	76.2 (148.1)	264	11.73 (38,480)	74.5 (144.8)	11.70 (38,390)	21.7 (42.2)	11.43 (37,500)
AS-505	42.5 (82.6)	270	14.18 (46,520)	40.8 (79.3)	13.80 (45,280)	18.7 (36.3)	14.85 (48,720)
AS-506	9.6 (18.7)	297	11.40 (37,400)	7.6 (14.8)	11.18 (36,680)	7.1 (13.8)	12.05 (39,530)
AS-507	47.6 (92.5)	245	14.23 (46,670)	47.2 (91.7)	14.23 (46,670)	-19.5 (-37.9)	13.65 (44,780)
AS-508	55.6 (108.1)	252	13.58 (44,540)	55.6 (108.1)	13.58 (44,540)	15.0 (29.1)	12.98 (42,570)
AS-509	52.8 (102.6)	255	13.33 (43,720)	52.8 (102.6)	13.33 (43,720)	24.9 (48.5)	10.20 (33,460)
AS-510	18.6 (36.2)	063	13.75 (45,110)	-17.8 (-34.6)	13.73 (45,030)	7.3 (14.2)	13.43 (44,040)
AS-511	26.1 (50.7)	257	11.85 (38,880)	26.0 (50.5)	11.85 (38,880)	12.5 (24.2)	15.50 (50,850)
AS-512	45.1 (87.6)	311	12.18 (39,945)	34.8 (67.6)	12.18 (39,945)	29.2 (56.8)	11.35 (37,237)

Table A-5. Extreme Wind Shear Values in the High Dynamic Pressure Region
for Apollo/Saturn 501 through Apollo/Saturn 512 Vehicles

VEHICLE NUMBER	PITCH PLANE		YAW PLANE	
	SHEAR (SEC-1)	ALTITUDE KM (FT)	SHEAR (SEC-1)	ALTITUDE KM (FT)
AS-501	0.0066	10.00 (32 800)	0.0067	10.00 (32 800)
AS-502	0.0125	14.90 (48 900)	0.0084	13.28 (43 500)
AS-503	0.0103	16.00 (52 500)	0.0157	15.78 (51 800)
AS-504	0.0248	15.15 (49 700)	0.0254	14.68 (48 160)
AS-505	0.0203	15.30 (50 200)	0.0125	15.53 (50 950)
AS-506	0.0077	14.78 (48 490)	0.0056	10.30 (33 790)
AS-507	0.0183	14.25 (46 750)	0.0178	14.58 (47 820)
AS-508	0.0166	15.43 (50 610)	0.0178	13.98 (45 850)
AS-509	0.0201	13.33 (43 720)	0.0251	11.85 (38 880)
AS-510	0.0110	11.23 (36 830)	0.0071	14.43 (47 330)
AS-511	0.0095	13.65 (44 780)	0.0114	15.50 (50 850)
AS-512	0.0177	7.98 (26 164)	0.0148	10.65 (34 940)

A.5.1 Atmospheric Temperature

Atmospheric temperature differences were small, generally deviating less than 5 percent from the PRA-63, below 59 kilometers (193,570 ft) altitude. Temperatures did deviate to -4.82 percent of the PRA-63 value at 24.50 km (80,380 ft). Air temperatures were generally warmer than the PRA-63 from the surface through 16 kilometers (52,493 ft). Above this altitude, temperatures became cooler than the PRA-63 values through 42.0 km (137,794 ft). Above this level temperatures were again warmer than the PRA-63. See Figure A-8 for the complete profile.

A.5.2 Atmospheric Pressure

Atmospheric pressure deviations were slightly greater than the PRA-63 pressure values from the surface to 20.60 kilometers (67,584 ft) altitude. Above this level pressure became less than the PRA-63 with a peak deviation of -8.78% occurring at 42.50 kilometers (139,434 ft) altitude. See Figure A-8.

A.5.3 Atmospheric Density

Atmospheric density deviations were small, being within 4 percent of the PRA-63 below 36 kilometers (118,109 ft) altitude. The density deviation reached a maximum of 3.91 percent greater than the PRA-63 value at 17.00 kilometers (55,774 ft) as shown in Figure A-9.

A.5.4 Optical Index of Refraction

The Optical Index of Refraction at the surface was 4.7×10^{-6} units lower than the corresponding value of the PRA-63. The maximum negative deviation of -8.37×10^{-6} occurred at 250 meters (820 ft). The deviation then became less negative with altitude, and approximated the PRA-63 at high altitudes, as is shown in Figure A-9. The maximum value of the Optical Index of Refraction was 1.81×10^{-6} units greater than the PRA-63 at 5.5 kilometers (18,044 ft).

A.6 COMPARISON OF SELECTED ATMOSPHERIC DATA FOR SATURN V LAUNCHES

A summary of the atmospheric data for each Saturn V launch is shown in Table A-6.

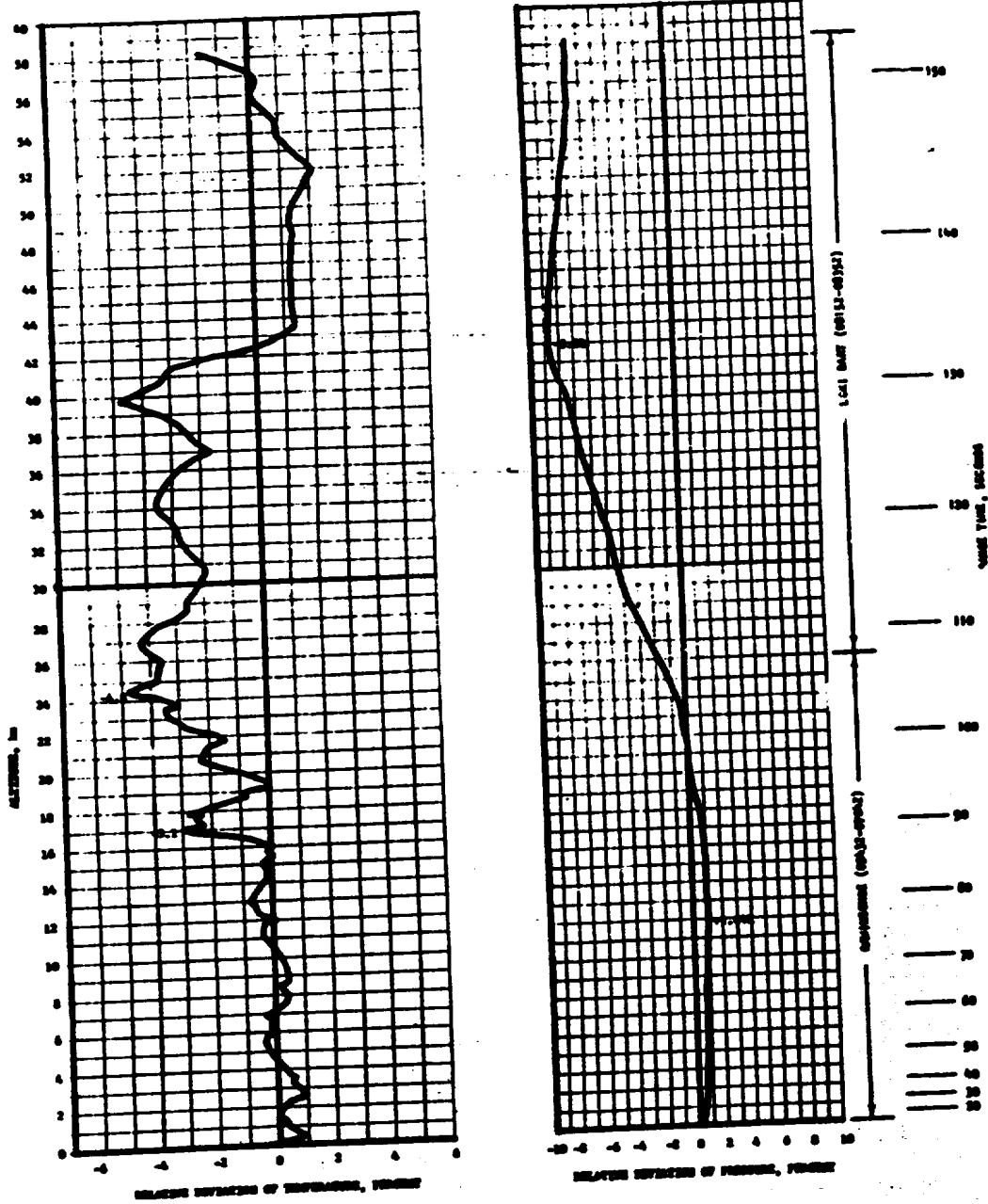


Figure A-8. Relative Deviation of Temperature and Pressure from the PRA-63 Reference Atmosphere, AS-512

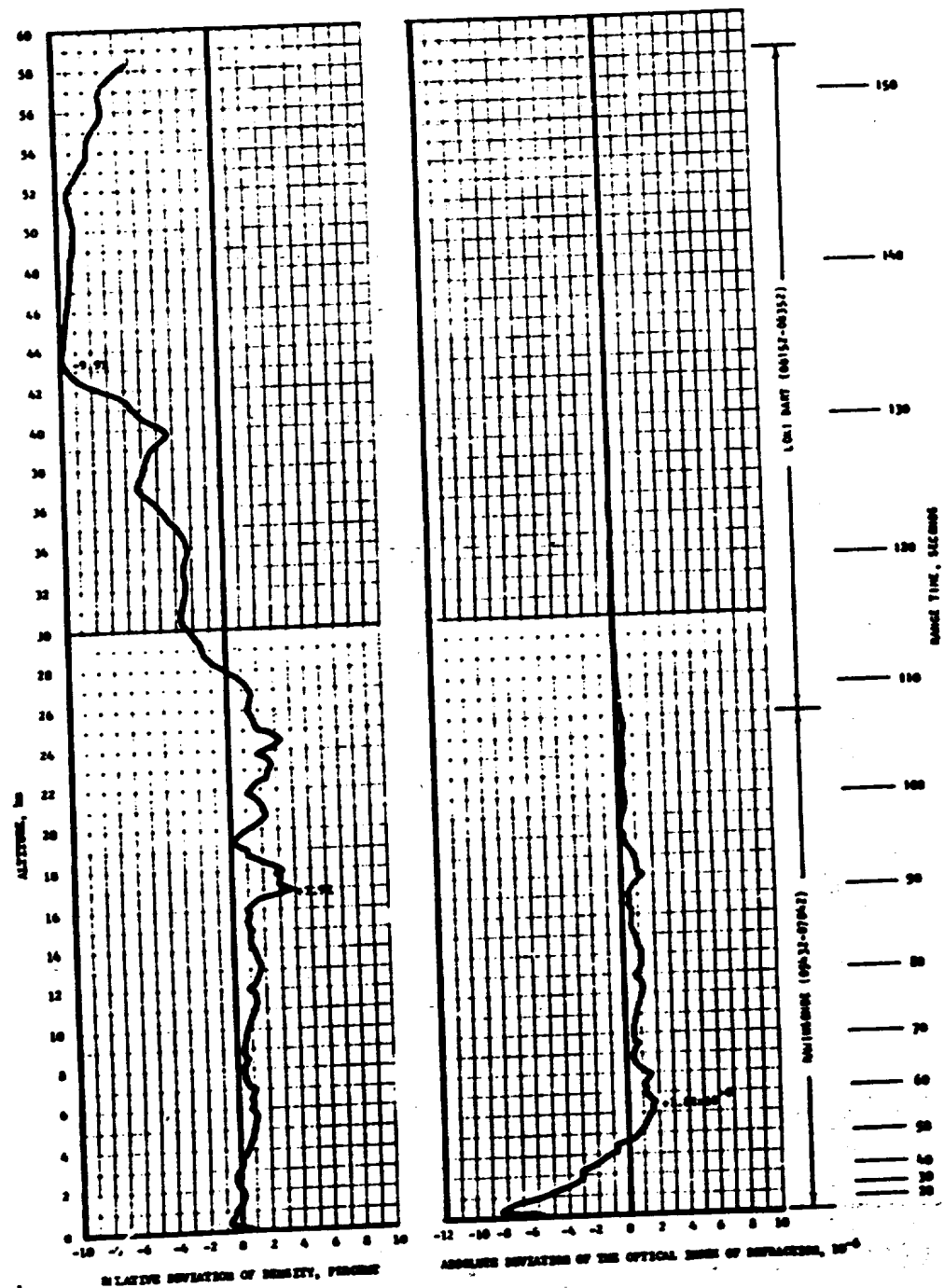


Figure A-9. Relative Deviation of Density and Absolute Deviation of the Index of Refraction From the PRA-63 Reference Atmosphere, AS-512

**Table A-6. Selected Atmospheric Observations for Apollo/Saturn 501 through
Apollo/Saturn 512 Vehicle Launches at Kennedy Space Center, Florida**

VEHICLE NUMBER	VEHICLE DATA			SURFACE DATA			INFLIGHT CONDITIONS					
	DATE	TIME NEAREST MINUTES	LAUNCH COMPLEX	PRESSURE INCHES	TEMPERA- TURE °C	RELATIVE HUMIDITY PERCENT	SPEED M/S	DIRECTION DEG	CLOUDS	MAXIMUM WIND IN 0-14 KM LAYER KM/H	SPEED M/S	DIRECTION DEG
AS-501	9 Nov 67	0700 EST	39A	10.261	17.6	95	8.20**	0700**	4/10 stratus cumulus	11.50	26.0	273
AS-502	4 Apr 68	0700 EST	39A	10.200	20.9	83	5.4**	132**	5/10 stratus cumulus, 1/10 cirrus	13.00	27.1	255
AS-503	21 Dec 68	0711 EST	39A	10.107	19.0	88	5.7**	240**	4/10 cirrus	15.22	34.8	284
AS-504	3 Mar 69	1100 EST	39A	10.095	19.6	61	6.3	160	7/10 stratus cumulus, 10/10 altostratus	11.73	76.2	264
AS-505	18 May 69	1240 EST	39B	10.190	26.7	75	9.8	142	4/10 cumulus, 2/10 altocumulus, 10/10 cirrus	14.18	42.5	270
AS-506	16 Jul 69	0932 EST	39A	10.203	23.4	73	3.3	175	1/10 cumulus, 2/10 altocumulus, 5/10 cirrus stratus	11.40	9.6	297
AS-507	16 Nov 69	1122 EST	39A	10.061	20.0	92	6.8	280	10/10 stratus cumulus with rain	14.23	47.6	245
AS-508	11 Apr 70	1413 EST	39A	10.119	24.4	67	6.3	105	4/10 altocumulus 10/10 cirrus stratus	13.58	55.6	252
AS-509	31 Jun 71	1603 EST	39A	10.102	21.7	86	5.0**	285**	17/10 cumulus 2/10 altocumulus	13.33	52.8	255
AS-510	26 Jul 71	0934 EST	39A	10.196	23.8	68	5.7**	156**	7/10 cirrus	13.75	18.6	043
AS-511	16 Apr 72	1354 EST	39A	10.183	31.2	44	6.1	260	2/10 cumulus	11.85	26.1	257
AS-512	7 Dec 72	0033 EST	39A	10.201	21.1	93	4.1	065	2/10 stratus cumulus, 1/10 cirrus	12.10	48.1	311

Elephantfoot readings from charts at T-0 (unless otherwise noted) from sensors on launch pad 39 (A & B) light pole at 18.3' (60.0 ft). Beginning with AS-50, wind measurements were required at the 161.5' (53.0 m) level from sensor charts on the LTF. These instantaneous LTF winds are given directly under the listed pad light pole winds. Heights of instruments are shown on chart. Wind speeds are about 1/4, except 1/10 instantaneous, but one minute average about 1/4.

APPENDIX B

AS-512 SIGNIFICANT CONFIGURATION CHANGES

B.1 INTRODUCTION

The AS-512, twelfth flight of the Saturn V series, was the tenth manned Apollo Saturn V vehicle. The AS-512 launch vehicle configuration was essentially the same as the AS-511 with significant exceptions shown in Tables B-1 through B-4. The Apollo 17 spacecraft structure and components were essentially unchanged from the Apollo 16 configuration. The basic launch vehicle description is presented in Appendix B of the Saturn V Launch Vehicle Flight Evaluation Report, AS-504, Apollo 9 Mission, MPR-SAT-FE-69-4.

Table B-1. S-IC Significant Configuration Changes

SYSTEM	CHANGE	REASON
Propulsion	Relocate fluid power system break points between servosetters and F-1 engines during storage.	To provide installation of engine hydraulic system pressure testing by opening plumbing connections which will not be retested at operating pressure.
Instrumentation and Communications	Replace tantalum capacitor on magnetic core register (MCR) card of PCU/BMS assembly.	Reduced possible failure mode of the MCR cards in the PCU/BMS assemblies.

Table B-2. S-II Significant Configuration Changes

SYSTEM	CHANGE	REASON
Propulsion	Installation of an improved J-2 engine redesigned Electrical Control Assembly (ECA) package incorporating new timers with redundant microcircuits. Modification of J-2 engine L12 Pump/Gas Generator Purge System to incorporate a Purge Control Valve with readjusted operating pressures, a redundant Purge Check Valve and Purge Control Valve Vent Line Orifice.	To eliminate single failure points and improve reliability. To prevent excessive loss of engine control system helium if purge control valve binds and to slow its closing.

Table B-3. S-IVB Significant Configuration Changes

SYSTEM	CHANGE	REASON
Propulsion	Installation of an improved J-2 engine redesigned Electrical Control Assembly (ECA) package incorporating new timers with redundant microcircuits. Modification of J-2 engine L12 Pump/Gas Generator Purge System to incorporate a Purge Control Valve with readjusted operating pressures, a redundant Purge Check Valve and Purge Control Valve Vent Line Orifice. Modified APS incorporating a redesigned high/low pressure transducer mounting adapter, replacement of bellhead fitting with EC adapters, replacement of Teflon "O" rings with E-dots and the addition of helium recharge system capable of supplying helium from the L12 exhaust regurgitator system.	To eliminate single failure points and improve reliability. To prevent excessive loss of engine control system helium if purge control valve binds and to slow its closing. To provide greater reliability by eliminating possible leak sources and providing its recharge system.
Electrical	Addition of control and current measurements of APS helium sphere recharge valve. Improved mechanical coupling between probe segments of the L12 PB probe. Removal of aft battery No. 2 load test circuit 20 amp motor driven switch.	To provide recharge capability for the APS. To insure proper electrical contact between PB probe segments. To eliminate a possible short circuit.

Table B-4. IU Significant Configuration Changes

SYSTEM	CHANGE	REASON
Environmental Control	Removed modulating flow control valve (MFCV), electronic Controller, F2 flowmeter and associated hardware from ICS. Only bottom thermal isolating shrouds installed on ECS panel, one located on each side of the sublimator.	MFCV subsystem is no longer required to perform an active function during either pre-launch checkout or flight operation. To provide proper sublimator vent area during flight.
Networks	Added an additional umbilical line from the +6D119 bus to the LSE. The wiring of the "S/C Separation Monitor Contacts" of relay K98 in the EDS distributor interchanged with "S/C Separation Monitor Contacts" of relay K95. Provided redundant liftoff signals via the umbilical to DIN24 or DIN7 of the LYDA/LYDC. Incorporated, "or" gating of DIN24 and DIN7 and eliminated the vertical accelerometer signal as a backup liftoff signal in the software program. Added lightning detection devices.	Provides a redundant path to energize the +6D119 bus from the ESE and decreases the possibilities of S-IC engine shutdown from the loss of this ESE connection. Makes the command system enable redundant even with the loss of +6D93 prior to issuance of the command system enable command. Eliminate single failure point which could cause early, late or erroneous time base 1 (TB-1) start times. Eliminate potential erroneous accelerometer backup signal. To establish means of determining the nature or magnitude of a lightning strike.
Instrumentation and Communications	Replaced Mallory TAM wet slug capacitors in the PCU/DDAS assembly. Changed measurement XC11-601 to XC25-602. Deleted measurements F2-601, WC3-601 and WS9-601. Added measurements: K279-602 K280-602 K281-602 K282-602 K283-602 K284-602 K285-602 P69-602 R70-602 R71-602 R72-602	Reduced possible failure mode of the MCR cards in the PCU/DDAS assemblies. To provide better fluid temperature data. Removed sublimator bypass control valve and electronic valve controller. To assign measurement numbers to IU telemetry reference voltages and sync words.
Flight Program	BOOST INITIALIZATION Starts extra accelerometer read telemetry at completion of initialization instead of T ₀ + 3. Redundant liftoff signal via discrete input 7 replaces the accelerometer backup for TB initiation. S-IVB engine cut interrupt (INT 4) is reset before enable.	To prevent extra accelerometer telemetry from interfering with liftoff check or the timer avoidance you mentioned. To process the new liftoff signals and to delete the software backup for Time Base 1. To prevent an erroneous INT 4 from being generated as it was enabled in TBS or TBS.

APPROVAL

SATURN V LAUNCH VEHICLE FLIGHT EVALUATION REPORT
AS-512, APOLLO 17 MISSION

By Saturn Flight Evaluation Working Group

The information in this report has been reviewed for security classification. Review of any information concerning Department of Defense or Atomic Energy Commission programs has been made by the MSFC Security Classification Officer. The highest classification has been determined to be unclassified.

Stanley L. Fragge

Stanley L. Fragge
Security Classification Officer

This report has been reviewed and approved for technical accuracy.

George H. McKay

George H. McKay, Jr.
Chairman, Saturn Flight Evaluation Working Group

Herman K. Weidner

Herman K. Weidner
Director, Science and Engineering

Richard G. Smith

Richard G. Smith
Saturn Program Manager

